2016-01-28

Investigating the Architecture and Vesicle Tethering Function of the Yeast Exocyst Complex: A Dissertation

Margaret R. Heider
University of Massachusetts Medical School

INVESTIGATING THE ARCHITECTURE AND VESICLE TETHERING FUNCTION OF THE YEAST EXOCYST COMPLEX

A Dissertation Presented

By

MARGARET ROSE HEIDER

Submitted to the Faculty of the
University of Massachusetts Graduate School of Biomedical Sciences, Worcester
In partial fulfillment of the requirements for the degree of

DOCTOR OF PHILOSOPHY

January 28, 2016

Biochemistry and Molecular Pharmacology

SIGNATURE PAGE

INVESTIGATING THE ARCHITECTURE AND VESICLE TETHERING FUNCTION OF THE YEAST EXOCYST COMPLEX

A Dissertation Presented By

MARGARET ROSE HEIDER

The signatures of the Dissertation Defense Committee signify completion and approval as to style and content of the Dissertation

_____
Mary Munson, Ph.D., Thesis Advisor

_____
Peter Pryciak, Ph.D., Member of Committee

_____
Nick Rhind, Ph.D., Member of Committee

_____
David Lambright, Ph.D., Member of Committee

_____
Frederick Hughson, Ph.D., Member of Committee

The signature of the Chair of the Committee signifies that the written dissertation meets the requirements of the Dissertation Committee

_____
Reid Gilmore, Ph.D. Chair of Committee

The signature of the Dean of the Graduate School of Biomedical Sciences signifies that the student has met all graduation requirements of the school.

_____
Anthony Carruthers, Ph.D.
Dean of the Graduate School of Biomedical Sciences

Biochemistry and Molecular Pharmacology Program

January 28, 2016

DEDICATION

This thesis is dedicated to the memory of my beloved aunt Mary M. (Doyle) Wilson (1966-2015). Aunt Mary was an inspiring example of perseverance, courage, and kindness despite the many challenges she faced in life. I thank God for giving us the short time we had with her and I will always try to bring positivity and humor to every situation, in her memory.

ACKNOWLEDGEMENTS

Thank you to my advisor Mary Munson for all the support and guidance she's given me over the last six years. I always felt that my ideas were heard and respected from the beginning. I want to thank you for always being open to my perspective and trusting me to take on new and challenging projects in the lab. Without the opportunities you've given me to take things in new directions, I am certain I would never have grown as much as a scientist. I am proud of all we've accomplished together and I look forward to seeing where you take the lab and these projects in the future.

Thank you to all of my fellow Munson lab members, past and present. Thank you to Francesca Morgera for being my first and biggest supporter in the lab. Even now that she's been out of the lab for a few years and living on a different continent, she continues to always believe in me and push me out of my comfort zone. I will always admire her for her ability to befriend and work with anyone. Thank you to Anne Mirza for being a constant support and true team player in the lab. She will go out of her way to help anyone and is one of the truly kindest people I've met in my time at UMass. Her help on the *NSMB* paper was truly invaluable and, despite the stress of trying to get the paper out, we had fun working together. Finally, thank you to Michelle Dubuke who has been next to me at our desks and benches for the last 6 years. We've seen it all together (good and bad) and we learned a lot from each other. I will always remember our long talks (scientific and otherwise), conference trips, and general antics in the lab. The culture of the lab has changed with each new batch of people, but we always kept it fun.

Thank you to our collaborators on the *NSMB* paper. In particular, I thank Dr. Adam Frost and Dr. Mingyu Gu for their outstanding efforts on the EM studies, excellent discussions, and patience with us as we learned about EM. Their enthusiasm and hard work made this a fun and productive collaboration. Additionally, thank you to Dr. Mike Rout, Zhanna Hakhverdyan, and Caroline Duffy for their early work on the purification method optimization, which made many experiments possible.

Thank you to my collaborators in the Gelles lab at Brandeis, particularly Jeff Gelles and Larry Friedman. Jeff and Larry listened to my pitch as a third year student to start a new, high-risk collaborative project with them and they believed in me and have shown their support and enthusiasm for my work since day one. Thank you to Larry especially for spending many hours with me in the microscope room, troubleshooting the seemingly endless technical problems associated with this project. Thank you to Dr. Ivan Correa at New England Biolabs for kindly providing us with many non-commercial SNAP substrates for these experiments and for helpful advice and discussion. Thank you to my good friends in Melissa Moore's lab for all of the help with the single molecule project particularly Eric Anderson, Joerg Braun, and Andrew Franck. Although warning me (frequently) of the challenges of single molecule work, you were all willing to help me without complaint. Thank you for making this a fun project to work on.

Thank you to all of the members of my thesis committee: Reid Gilmore, Peter Pryciak, Nick Rhind, and David Lambright. Over the years, I've found myself in all of your offices at one time or another to discuss science or career questions. These

conversations have been invaluable to me and your support at all of my committee meetings has given me confidence in my abilities as a scientist.

Thank you to everyone in the BMP Department. Everyone always says BMP is a truly unique place to work because of the friendly people and collaborative environment. I have to echo this sentiment and hope that I will be fortunate to work in a place like this again. I always looked forward to coming to work every single day, even when science wasn't going well. I have to acknowledge everyone in this department for making this such a positive place to work. I've made many friends here who I hope to keep in touch with for years to come.

I have truly wonderful family and friends who I cannot thank enough for their support during my time in graduate school. You always believed in me and encouraged me. My parents are my models for what hard work and sacrifice look like. They always taught me to have faith, work hard, and help others, and that's what I will always try to do. Finally, thank you to my husband Tom for being there with me every day through the ups and downs of graduate school. Without you and your complete and total faith in me, I might have given up a long time ago. Thank you for making me laugh and see the bright side in everything. I couldn't have done this without you.

ABSTRACT

The exocyst is an evolutionarily conserved, hetero-octameric protein complex proposed to serve as a multi-subunit tethering complex for exocytosis, although it remains poorly understood at the molecular level. The classification of the exocyst as a multisubunit tethering complex (MTC) stems from its known interacting partners, polarized localization at the plasma membrane, and structural homology to other putative MTCs. The presence of 8 subunits begs the questions: why are so many subunits required for vesicle tethering and what are the contributions of each of these subunits to the overall structure of the complex? Additionally, are subunit or subcomplex dynamics a required feature of exocyst function? We purified endogenous exocyst complexes from *Saccharomyces cerevisiae*, and showed that the purified complexes are stable and consist of all eight subunits with equal stoichiometry. This conclusion contrasts starkly with current models suggesting that the yeast exocyst tethers vesicles by transient assembly of subcomplexes at sites of exocytosis. Using a combination of biochemical and auxin-induced degradation experiments in yeast, we mapped the subunit connectivity, identified two stable four-subunit modules within the octamer, and demonstrated that several known exocyst binding partners are not necessary for exocyst assembly and stability. Furthermore, we visualized the structure of the yeast complex using negative stain electron microscopy; our results indicate that exocyst exists predominantly as an octameric complex in yeast with a stably assembled, elongated structure. This is the first complete structure of a CATCHR family MTC and it differs greatly from the EM structures available for the partial COG and Dsl1 complexes. Future work will be

necessary to determine whether exocyst conformational changes are a required feature of vesicle tethering and how such changes are regulated.

These architectural insights are now informing the design of the first *in vitro* functional assay for the exocyst complex. We developed methodology for attaching fluorescently-labeled exocyst complexes to glass slides and monitoring the capture of purified, endogenous secretory vesicles by single molecule TIRF microscopy. By this approach, we can monitor tethering events in real time and determine the required factors and kinetics of exocytic vesicle tethering.

TABLE OF CONTENTS

LIST OF FIGURES

CHAPTER I:

CHAPTER II:

CHAPTER III:

CHAPTER V:

LIST OF TABLES

LIST OF COPYRIGHTED MATERIALS

- Portions of the text for Chapter I and Figure 1.7 are published as a review in the journal *Traffic*. No permission is needed for the authors to use this material.

  Heider, M.R. and Munson, M. (2012). Exorcising the exocyst complex. Traffic 13, 898-907.

- Most of the text and figures in Chapter II (except Fig. 2.3) and portions of the text in Chapter IV, are published as a scientific article in the journal *Nature Structural and Molecular Biology*. No permission is needed for the authors to use this material.

  Heider, M.R., Gu, M., Duffy, C.M., Mirza, A.M., Marcotte, L.L., Walls, A.C., Farrall, N., Hakhverdyan, Z., Field, M.C., Rout, M.P., Frost, A., and Munson, M. (2016). Subunit connectivity, assembly determinants and architecture of the yeast exocyst complex. Nature Structural & Molecular Biology 23 (1): 59-66.

- Portions of the text and figures (Fig. 5.6 and 5.7) in Chapter V, Appendix G are published as a scientific article in the journal *Molecular Biology of the Cell*. No permission is needed for the authors to use this material.

  Morgera, F., **Sallah, M.R.,** Dubuke, M.L., Gandhi, P., Brewer, D.N., Carr, C.M., and Munson, M. (2012). Regulation of exocytosis by the exocyst subunit Sec6 and the SM protein Sec1. Molecular Biology of the Cell 23, 337–346.

- Figure 5.8 in Chapter V, Appendix H is adapted from the following publication (permission not required if properly cited):

  Songer, J.A. and Munson, M. (2009). Sec6p anchors the assembled exocyst complex at sites of secretion. Molecular Biology of the Cell 20, 973-82.

PREFACE

A version of the exocyst-specific section used in Chapter I was written by Dr. Mary Munson and me, and published as a review article in the journal *Traffic* with Dr. Mary Munson as the corresponding author.

Most of the work presented in Chapter II was performed at UMass Medical School in Dr. Mary Munson's laboratory and was published as my first-author article in the journal *Nature Structural and Molecular Biology* with Mary Munson as corresponding author. Dr. Mary Munson and I conceived the study, designed the biochemical and cell biology experiments and wrote the manuscript. I made the yeast strains (Table 5.1) and performed most of the biochemistry and cell biology experiments with assistance from Anne Mirza, Caroline Duffy, Dr. Laura Marcotte, and Alexandra Walls. Experiments included in Chapter V Appendices A-D were designed and performed by me, with assistance from Anne Mirza for the yeast EM studies, to address reviewer concerns for this publication. Dr. Mingyu Gu and Dr. Adam Frost designed, performed and analyzed the EM experiments at the University of Utah and University of California San Francisco. Early EM optimization work was done by Nicholas Farrell (University of Utah) and development of the purification method was done by Zhanna Hakhverdyan, Caroline Duffy, Dr. Michael Rout, and Dr. Mark Field at Rockefeller University. All authors contributed to discussion and approved the final manuscript.

The work presented in Chapter III is unpublished. These studies were conceived and designed by me with assistance from Dr. Jeff Gelles (Brandeis University), Dr. Larry Friedman (Brandeis University), and Dr. Mary Munson. I made the yeast strains for these

studies (Table 5.2). Most of the experiments were performed by me at UMass Medical School in Dr. Mary Munson's laboratory with the exception of Fig. 3.10, 3.11, and 3.17, which were performed by me at Brandeis University with the assistance of Dr. Larry Friedman. Data analysis for Fig. 3.10 and 3.11 was performed by Eric Anderson (laboratory of Dr. Melissa Moore, UMass Medical School). Additional technical advice and assistance was provided by Eric Anderson, Dr. Joerg Braun, and Dr. Andrew Franck (laboratory of Dr. Melissa Moore, UMass Medical School).

The work presented in Chapter V Appendix G was published in *Molecular Biology of the Cell*. Chapter V Fig. 5.6 and 5.7 were produced by me in Dr. Mary Munson's laboratory as second author on Morgera et al., 2012.

The work presented in Chapter V Appendix H (Fig. 5.9-5.14) is unpublished and was performed by me in Dr. Mary Munson's laboratory. This work was based upon the findings of Songer and Munson published in *Molecular Biology of the Cell* in 2009.

CHAPTER I: INTRODUCTION

Overview

Eukaryotic cells contain numerous different membrane-bound organelles between which various protein and lipid cargos must be specifically trafficked. Vesicles are the cargo carriers and distinct trafficking pathways exist for transporting vesicles between different pairs of compartments (Fig. 1.1). All of these pathways follow the same series of evolutionarily conserved steps, relying on several classes of proteins (to be discussed in detail below) to execute cargo delivery with a high level of efficiency and fidelity that ensures the integrity and composition of the organelles (Bonifacino and Glick, 2004). Protein and lipid cargos are sorted into a budding vesicle at the donor compartment and, once severed from the donor membrane, these vesicles are transported to the target membrane compartment. Through the combined activity of tethers, Rab GTPases, and potentially other factors, a vesicle is tethered to the target membrane. SNARE proteins on both the vesicle and target membrane, regulated by tethering factors and Sec1/Munc18 (SM) proteins, assemble into the trans-SNARE

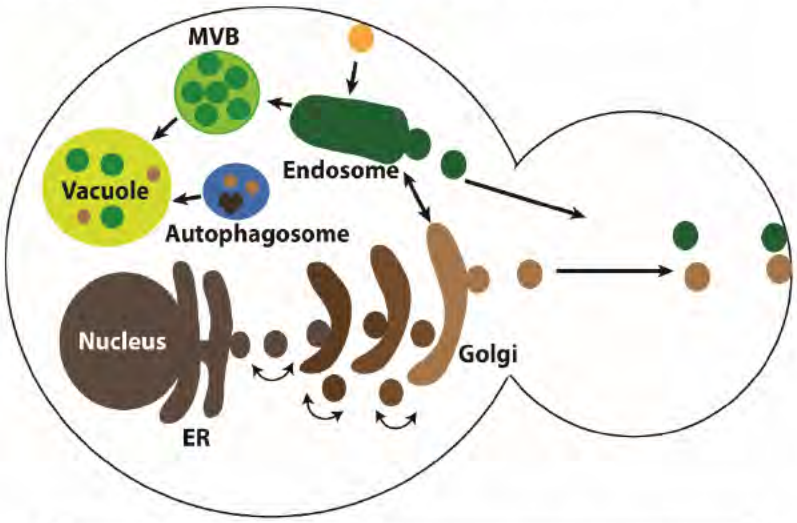

Figure 1.1 Schematic representation of vesicle trafficking pathways in *Saccharomyces cerevisiae*. ER=endoplasmic reticulum, MVB=multi-vesicular body.

complex, which directly promotes the fusion of vesicle and target membrane bilayers leading to cargo release. (Fig 1.2)

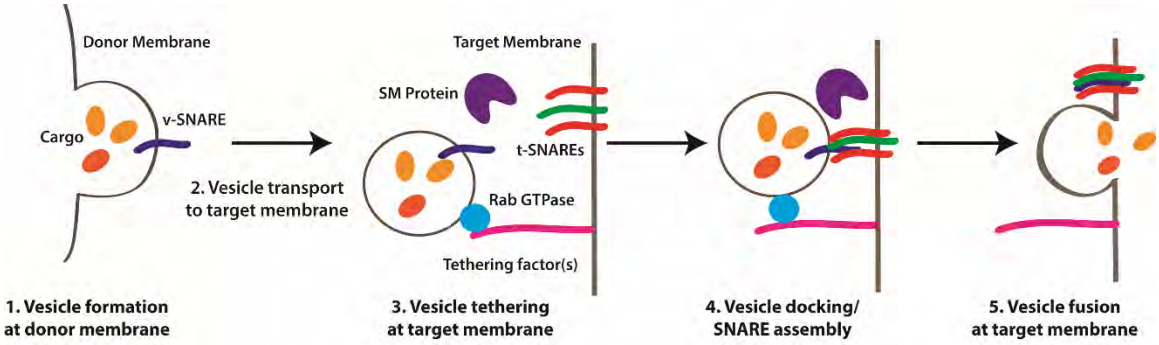

Figure 1.2: The conserved steps of vesicle trafficking. A vesicle forms at the donor compartment and is filled with specific cargos. The vesicle buds from the donor membrane and is transported to the target organelle where it is physically tethered. Following tethering, Sec1/Munc18 (SM) proteins regulate the process of SNARE complex assembly, a reaction that drives the fusion of the two bilayers and cargo release. V-SNARE=vesicle SNARE, t-SNARE=target membrane SNARE.

Small GTPases

In all trafficking pathways, small GTPases of the Ypt/Rab family are critical orchestrators of nearly every step of secretion, which will be discussed below. Ypt/Rabs are small (~200 amino acids) molecular switches that cycle between active (GTP-bound, membrane-associated) and inactive (GDP-bound, cytoplasmic) forms. In their activated form, these small GTPases interact with a diverse array of downstream effectors to coordinate vesicular trafficking (Fig 1.3). Specialized guanine nucleotide exchange factors (GEFs) serve to activate specific

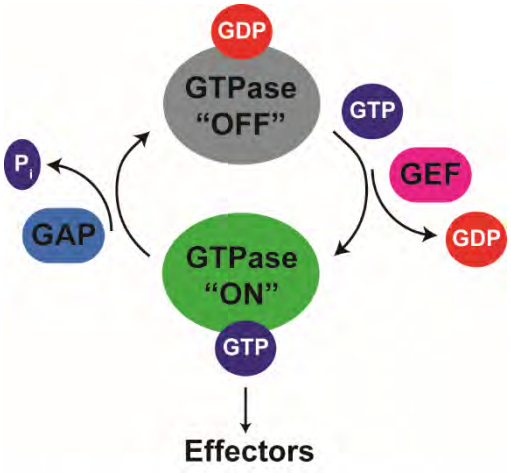

Figure 1.3: The GTPase activity cycle. Guanine nucleotide exchange factors (GEFs) stimulate dissociation of GDP so GTP can bind and activate the GTPase. GTP hydrolysis activating proteins (GAPs) promote the hydrolysis of GTP so the GTPase returns to its inactive, GDP-bound state.

Ypt/Rabs and GTP hydrolysis activating proteins (GAPs) inactivate them. Because the activity of these small GTPases can be fine-tuned and they interact with numerous downstream effectors, it is clear that eukaryotic cells can take advantage of these switches for tightly regulated processes. *S. cerevisiae* contains 11 Rab GTPases and 70 have been identified in humans so far, indicating that while we still have much to learn about the mechanism of Rab activity in yeast, a great deal of work will be required in the future to decipher the specific roles for all of these small GTPases in higher eukaryotes (Lipatova and Segev, 2014).

SNARE complexes

The soluble N-ethylmaleimide-sensitive factor attachment protein receptor (SNARE) proteins are the core machinery required for vesicle fusion with the target membrane in all intracellular trafficking pathways. SNARE proteins contributed by both the vesicle (v-SNAREs) and target membrane (t-SNAREs) assemble into a highly stable 4-helix bundle and this assembly provides the energy required to fuse the two lipid bilayers for cargo release (Jahn and Scheller, 2006). SNARE complex assembly is highly stable, thus the AAA ATPase complex NSF/α-SNAP (Sec18/Sec17 in yeast) is required after vesicle fusion for disassembly and recycling of the SNAREs for subsequent reactions (Sollner et al., 1993a; Hayashi et al., 1995; Jahn and Scheller, 2006). Additionally, since this assembly is not reversible and directly leads to membrane fusion, the timing and localization of proper SNARE complex assembly must be tightly regulated. Unique v- and t-SNAREs function in each trafficking pathway, but *in vitro* studies revealed that SNARE proteins from different pathways can assemble

promiscuously and alone are not sufficient to guarantee the specificity of vesicle delivery to the proper organelle (McNew et al., 2000; Fasshauer et al., 1999; Hohenstein and Roche, 2001; Yang et al., 1999; Izawa et al., 2012). Therefore, the combined activity of SNAREs, GTPases, SM proteins, tethers, and additional regulators (to be discussed below in relation to exocytosis) are necessary to ensure the proper spatiotemporal delivery of vesicles in the cell.

Exocytosis and its regulators

This thesis focuses on one intracellular trafficking pathway called polarized exocytosis, where vesicles budded from either the trans-Golgi network (TGN) or endosomal compartments are trafficked to a restricted region of the plasma membrane. Fusion of vesicles at the plasma membrane is required both for release of cargos to the extracellular space as well as for incorporation of lipids and proteins into the plasma membrane itself. The restricted nature of exocytic vesicle fusion promotes directional outgrowth of the membrane bilayer in these locations, which is required for many complex cellular events. This pathway has been best characterized in the budding yeast, *Saccharomyces cerevisiae*, where polarized secretion drives the growth of a budding daughter cell and separates mother and daughter cells during cytokinesis. However, this same polarized secretion pathway underlies many complex cellular processes in higher eukaryotes ranging from developmental events like neuronal growth to more specialized processes requiring localized membrane delivery like ciliogenesis, cell migration, and autophagy (Heider and Munson, 2012; Orlando and Guo, 2009). Although the

mechanistic details of exocytosis are not completely known, most of the relevant players have been identified for each step and are highly conserved from yeast to humans.

Cargos destined for the plasma membrane are recognized and concentrated in the nascent vesicle, though the molecular details of cargo sorting are much less clear for TGN to plasma membrane trafficking than other intracellular trafficking pathways. The exomer complex, which was originally identified in yeast and does not yet have a known homolog in metazoans, may be important for plasma membrane-bound cargo selection and subsequent vesicle fission from the TGN (reviewed in Paczkowski et al., 2015). A redundant pair of Ypt/Rab family GTPases, Ypt31/32 (Rab11 in mammals), are also key players at this stage (Lipatova and Segev, 2014). Ypt31/32 are localized to the TGN in their GTP-bound form and here they orchestrate both vesicle formation, through the downstream effector Sec7, and vesicle transport (Jones et al., 1999; McDonold and Fromme, 2014; Lipatova and Segev, 2014). Ypt31/32 seem to function at the beginning of a cascade of effector interactions required for the polarized transport of post-Golgi vesicles. Ypt31/32 is thought to recruit the type V myosin motor, Myo2, to vesicles as well as Sec2 (Rabin8 in mammals), the GEF for the Rab GTPase Sec4 (Rab8 in mammals) (Lipatova et al., 2008; Ortiz et al., 2002; Mizuno-Yamasaki et al., 2010; Das and Guo, 2011). During the Myo2-mediated transport of vesicles along actin to the plasma membrane, Sec2 activates Sec4, which likely exchanges places with Ypt31/32 on vesicles as both GTPases bind the same site on Myo2 and Sec4 was shown to act downstream of Ypt31/32 (Jin et al., 2011; Ortiz et al., 2002; Mizuno-Yamasaki et al., 2010). Activated Sec4 interacts with both the exocyst complex (as discussed below) and

the protein Sro7/77, interactions which are not fully understood but presumed to be important for vesicle tethering and regulation of the SNARE fusion machinery (Guo et al., 1999; Grosshans et al., 2006; Rossi et al., 2015). When a vesicle is brought within some yet unknown distance to the plasma membrane, vesicle tethering occurs, which is then followed by the assembly of the SNARE complex. The yeast exocytic SNAREs include the v-SNARE Snc1/2 (VAMP/synaptobrevin family) and the plasma membrane-associated t-SNAREs Sec9 (SNAP-25 family) and Sso1/2 (syntaxin family) (Aalto et al., 1993; Brennwald et al., 1994; Gerst et al., 1992). Assembly of Sso1/2 with Sec9 into the binary SNARE complex occurs first and then arrival of the vesicle with Snc1/2 leads to full complex assembly and vesicle fusion (Nicholson et al., 1998; Munson et al., 2000; Munson and Hughson, 2002).

Vesicle Tethering

Vesicle tethering is one of the most poorly understood steps in all vesicle trafficking pathways. This step occurs after the delivery of a vesicle at its target organelle but upstream of SNARE complex assembly and vesicle fusion (Fig. 1.2). Tethering is defined as the initial capture of a secretory vesicle at a distance from its target membrane, which may serve to stabilize the vesicle and bring it close enough to promote SNARE-mediated fusion. Due to the necessarily reversible and transient nature of vesicle tethering events, studies characterizing vesicle tethering and the factors that mediate it have been challenging.

The concept of tethering began to take shape in the mid-1990s when a series of papers came out identifying factors that Suzanne Pfeffer termed “velcro factors.”

(Pfeffer, 1996; TerBush et al., 1995; Stenmark et al., 1995). The common link between all of the factors, despite obvious structural differences, were interactions with membranes and small GTPases known to associate with membranes. Barlowe and colleagues were the first to directly demonstrate that a distinct vesicle tethering step occurs upstream of SNARE activity (Barlowe et al., 1997, Cao et al., 1998). Using an *in vitro* reconstituted ER to Golgi transport assay, they showed that an extended coiled coil yeast protein called Uso1 (p115 in mammals) was capable of physically docking vesicles at the Golgi membrane. When freely diffusing ER-derived vesicles were incubated with Uso1, COPII vesicle coat proteins, and Golgi membranes, they found that increased levels of vesicles pelleted with the Golgi membranes during ultracentrifugation rather than remaining in the supernatant (Barlowe et al., 1997). Using temperature-sensitive mutants in Golgi SNAREs that block vesicle fusion, they showed that vesicles were still tethered in the presence of Uso1, but failed to fuse with the Golgi membrane, physically distinguishing tethering from SNARE complex assembly. Additionally, Uso1's role in vesicle tethering was dependent on the Ypt/Rab GTPase Ypt1, further supporting the link between tethering and Rab GTPases (Cao et al., 1998).

Tethering factor is the generic name given to proteins and/or protein complexes that are thought to capture vesicles at the target membrane. This term encompasses two strikingly different structural classes of molecules including the homodimeric coiled coil proteins and the multi-subunit tethering complexes (MTCs). In general, most of the factors grouped under the term 'tethers' have not yet been experimentally demonstrated to perform this function (Brunet and Sacher, 2014). In the case of the homodimeric coiled

coil proteins, the group to which the previously described Uso1 belongs, there is some experimental evidence for this role (Cao et al., 1998; Drin et al., 2008; Yu and Hughson, 2010; Wong et al., 2014; Cheung et al., 2015). Their structure makes it easy to envision such a function as these proteins can extend up to 45 nm from the target membrane allowing them to capture vesicles at a distance. Furthermore, non-coiled coil domains in the middle of these extended chains are proposed to serve as hinges that allow the vesicles to be brought closer to the target membrane (Gillingham and Munro, 2003; Cheung et al., 2015). MTCs are much more complex structures containing 3-10 different subunits. Unlike the coiled coil proteins, there is little direct evidence for tethering by these complexes (as discussed further below), but an MTC is proposed to function in nearly every known vesicle trafficking pathway in the cell (Fig 1.4). In spite of their differences, all of these tethering factors have several features in common including

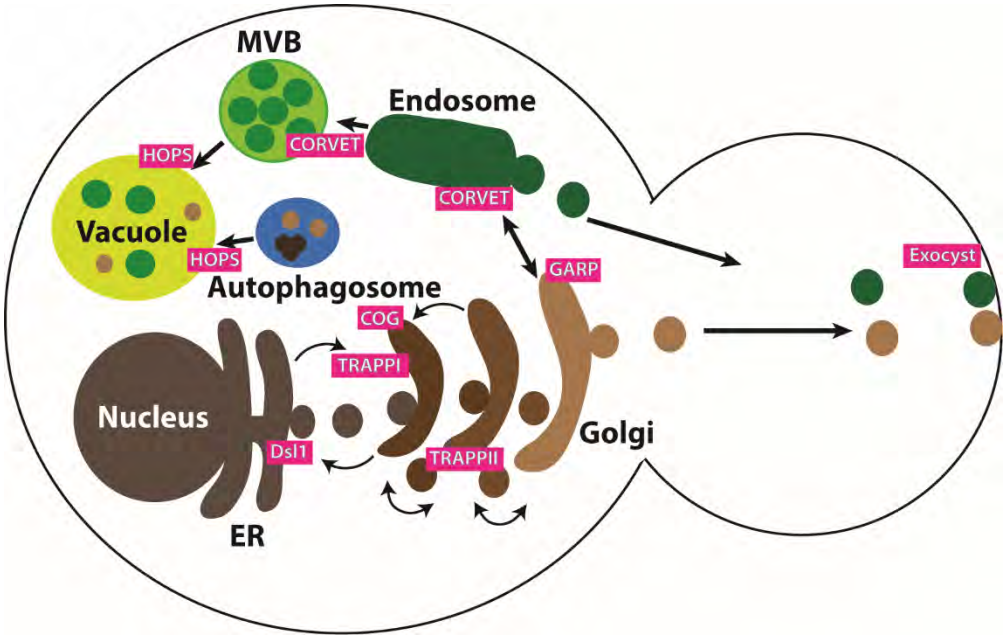

Fig 1.4: Schematic representation of vesicle trafficking pathways in *S. cerevisiae* and their MTCs. All evolutionarily conserved MTCs (pink boxes) are shown on the organelles where they localize. MTCs are required for vesicular traffic into their respective organelles.

reported interactions with Ypt/Rab GTPases, membranes, and in many cases SNARE proteins (Yu and Hughson, 2010).

It is not immediately apparent why tethering is a required step for vesicle trafficking. One hypothesis is that tethers accelerate vesicle fusion, either simply by increasing the rate of vesicle capture (facilitating the rate at which the SNAREs are brought close to each other) or by directly stimulating the assembly of SNARE complexes. SNARE-mediated vesicle fusion is always significantly slower *in vitro*, arguing that other factors are required *in vivo* to improve the efficiency of this process (Ohya et al., 2009; Stroupe et al., 2009). Furthermore, in some cases overexpression of the SNARE proteins can rescue mutations in tethering factors, suggesting that increasing the number of SNARE proteins could increase their rate of assembly, overcoming the requirement for tethers to accelerate this process (Pfeffer, 1996; Songer and Munson, 2009). A second hypothesis argues that tethers may be required for specific recognition of vesicles at the proper target organelle membrane. Both the coiled coil proteins and the MTCs have a complex array of interactions with proteins and lipids found on both vesicle and target membranes. Given that SNARE proteins are not sufficient to impart specificity, (McNew et al., 2000; Izawa et al., 2012; Fasshauer et al., 1999; Hohenstein and Roche, 2001; Yang et al., 1999; Fischer von Mollard et al., 1997; Kweon et al., 2003; Brennwald et al., 1994; Garcia et al., 1995) the tethering factors may provide additional layers of recognition to guarantee the fidelity of vesicle targeting. In support of this idea, it was recently shown that the Golgi-localized coiled coil proteins, or golgins, specifically capture certain types of vesicles based upon a poorly understood combination of unique

protein receptors and specific membrane curvature (Wong and Munro, 2014). It is possible that some or all of these reasons are correct but it will be interesting to see whether such structurally diverse classes of proteins like the coiled coil tethers and the MTCs truly serve the same tethering function and whether they function by similar mechanisms.

Multisubunit Tethering Complexes (MTCs)

Within the MTC group there is yet another structural division that separates the HOPS, CORVET, TRAPPI, TRAPPII, and TRAPPIII complexes from another group, which is collectively termed Complexes Associated with Tethering Containing Helical Rods (CATCHR). The focus of this thesis will be on the CATCHR family and one of its members, the exocyst, so the other complexes will only be briefly discussed below.

HOPS and CORVET:

Two 6-subunit MTCs called the homotypic fusion and vacuole protein sorting (HOPS) and class C core vacuole/endosome tethering (CORVET) complexes function in the endolysosomal pathway (Fig. 1.4). CORVET specifically controls homotypic endosomal fusion and all vesicle traffic into the late endosome. HOPS controls all traffic into the vacuole whether that be from multi-vesicular bodies (MVBs), AP-3 vesicles from the TGN, or autophagosomes (Balderhaar and Ungermann, 2013). These complexes are chimeras of each other, in that they share 4 core subunits and each contain 2 unique subunits of their own (Price et al., 2000; Wurmser et al., 2000; Peplowska et al., 2007; Nickerson et al., 2009). Interestingly, HOPS and CORVET are the only known MTCs to contain a built-in SM protein, the core subunit Vps33, which may facilitate binding and

regulation of SNARE proteins (Dulubova et al., 2001; Laage et al., 2001; Sato et al., 2000; Lobingier et al., 2012; Lobingier et al., 2014; Baker et al., 2015). HOPS and CORVET have not been well-characterized in metazoans, although homologues for the subunits, including additional isoforms, have been identified (Balderhaar and Ungermann, 2013)

Like other tethering factors, both HOPS and CORVET are Rab effectors (Abenza et al., 2010; Abenza et al., 2012; Brocker et al., 2012; Ostrowicz et al., 2010; Peplowska et al., 2007; Seals et al., 2000; Wurmser et al., 2000). The two unique HOPS and CORVET subunits each interact with specific activated Rab GTPases, namely Ypt7 (Rab7 in mammals) and Vps21 (Rab5 in mammals) respectively. For some time it was thought that HOPS and CORVET would tether through spatially separated Rab GTPase- and SNARE-interacting interfaces that would connect opposing membranes (Ostrowicz et al., 2010). However, the recent negative stain electron microscopy (EM) structure of the full HOPS complex revealed that the two Rab-interacting subunits on HOPS were actually located on distal sides of the complex, suggesting that HOPS tethers through recognition of Rab7 on opposing compartments (Brocker et al., 2012). This insight can likely be applied to CORVET as well, as the architecture of the complex is largely the same, with the shared subunits at the core and the unique subunits on the ends (Ostrowicz et al., 2010; Plemel et al., 2011).

Direct experimental evidence revealed roles for both HOPS and CORVET as bona fide tethers. HOPS, in particular, has been extensively studied using *in vitro* vacuole and proteo-liposome tethering and fusion assays, though there is still some debate about

the requirements for tethering and the mechanism of action for this MTC (Stroupe et al., 2009; Stroupe et al., 2012; Zucchi and Zick, 2011; Lo et al., 2011; Zick and Wickner, 2014). In general, *in vitro* fusion assays require the vacuolar SNARE proteins, SNARE disassembly machinery, Ypt7, and the HOPS complex. Interestingly, the lipid composition of the liposomes is also an important determinant, which when properly adjusted, can bypass the requirement for Ypt7, suggesting that lipid binding by HOPS may also be a redundant means by which it tethers (Mima et al., 2008; Stroupe et al., 2009). Furthermore, a recent study on the CORVET complex using vacuole-endosome clustering and fusion assays revealed that it can also tether and this function is dependent on Vps21 (Balderhaar et al., 2013).

The TRAPP complexes:

The Transport Protein Particle (TRAPP) complexes are similar to HOPS and CORVET in that they share a core set of subunits. TRAPPI contains 7 subunits and functions in ER to Golgi trafficking (Sacher et al., 1998; Sacher et al., 2001; Barrowman et al., 2010). TRAPPII contains the same core of 7 subunits and 3 additional, unique subunits for its distinct and poorly-understood role in intra-Golgi and endosome to TGN trafficking (Sacher et al., 2001; Barrowman et al., 2010). TRAPPIII is the most recently-discovered version of the complex, which contains the subunit core with an additional subunit, Gsg1, which confers a unique function for this complex in autophagy (Lynch-Day et al., 2010; Barrowman et al., 2010). A single TRAPP complex exists in metazoans and seems to play a critical role in ER-Golgi and intra-Golgi traffic as well as Golgi biogenesis (Barrowman et al., 2010). Consistent with a potential role in tethering, TRAPP

was shown to bind COPII vesicles (Sacher et al., 2001) and this function was required for COPII vesicle association with the Golgi in *in vitro* assays (Cai et al., 2007b). Extensive architectural and structural studies have made TRAPPI and TRAPPII some of the best-understood putative tethering factors (Kim et al., 2006; Cai et al., 2007; Yip et al., 2010). Although these studies presented a model for how TRAPP-mediated tethering might occur through identification of the binding surfaces for the opposing compartments, a mechanistic picture for COPII vesicle tethering has not been demonstrated experimentally (Brunet and Sacher, 2014; Kim et al., 2006; Yip et al., 201).

The TRAPP complexes are unique among tethering factors in that they function as a GEF as opposed to a Rab GTPase effector. Some of the earliest studies on TRAPPI/II revealed their role as GEF for the GTPase Ypt1, while the mammalian TRAPP complex has GEF activity toward its homolog, Rab 1 (Wang et al., 2000; Sacher et al., 2001; Yamasaki et al., 2009). TRAPPII was also proposed to function as GEF for Ypt31/32 at the TGN, but this role has been debated (Jones et al., 2000; Morozova et al., 2006; Wang et al., 2002). Structural studies on the TRAPPI complex elegantly assigned the GEF activity to a core of 4 subunits common to both TRAPPI and TRAPPII (Kim et al., 2006). However, much still remains to be understood about the role of TRAPP in activating Ypt1 (Rab1) and the timing of these events relative to vesicle delivery, the function of the coiled coil tethers at the Golgi, and recruitment of SNARE regulatory machinery (Kim et al., 2006). Given that the TRAPP complexes are not known to interact with SNAREs or SM proteins and clearly function as GEFs rather than Rab effectors, it

begs the question whether they are in fact tethers and if they function by a similar mechanism as other MTCs.

CATCHR family of tethering complexes

Four putative MTCs, namely COG, Dsl1, GARP, and exocyst, are grouped in a family termed Complexes Associated with Tethering Containing Helical Rods (CATCHR) (Yu and Hughson, 2010). Despite a low level of sequence homology among all of the subunits of this family, a striking structural similarity among these proteins has emerged that is suggestive of divergent evolution (Munson, 2009; Yu and Hughson, 2010; Koumandou et al., 2007; Munson and Novick, 2006; Whyte and Munro, 2001). The crystal structures for 12 of the 23 subunits of this family, though from different species and MTCs, all share a remarkably similar fold with contiguous helical bundles packed together into extended legs (Cavanaugh et al. 2007; Dong et al. 2005; Fukai et al. 2003; Hamburger et al. 2006; Jin et al. 2005; Moore et al. 2007; Mott et al. 2003; Ren et al. 2009; Richardson et al. 2009; Sivaram et al. 2006; Tripathi et al. 2009; Wu et al. 2005; Munson and Novick, 2006; Perez-Victoria et al., 2010; Vasan et al., 2010). Furthermore, the subunits and regions of subunits yet to be crystallized are predicted to contain the same helical fold (Croteau et al., 2009). Not surprisingly, these complexes share a number of other structural and functional features as well, which will be discussed below. It is of great interest to determine whether, given the pronounced structural similarity of the subunit building blocks, these complexes assume similar quarternary structures or whether their unique subunit composition leads to a unique structure ideally suited for their particular trafficking pathway.

COG complex:

The Conserved Oligomeric Golgi (COG) complex was identified nearly simultaneously in several different model organisms, but finally converged on the name COG when these complexes were confirmed to be the same, stable, 8-subunit entity (VanRheenen et al., 1998; Walter et al., 1998; Suvorova et al., 2001; Whyte and Munro, 2001; Ungar et al., 2002). COG localizes to the Golgi in both yeast and mammalian cells, and plays a required role in retrograde Golgi trafficking and maintenance of glycosylation enzyme homeostasis among Golgi cisternae (Miller and Ungar, 2012; Willett et al., 2013b).

COG contains 8 different subunits called Cog1-Cog8 and early electron microscopy (EM) studies suggested that these subunits are arranged into two distinct, 4-subunit lobes (Ungar et al., 2002). This model was supported by the fact that one group of subunits, Cog1-4, are known to be essential, whereas deletion of Cog5-8 has virtually no phenotype, so it was thought that these two functional units were spatially separated within the complex (Whyte and Munro, 2001; Ungar et al., 2002; Oka et al., 2005). However, extensive architectural characterization of the mammalian complex later revealed the connectivity of the subunits and that COG architecture was a bit more complex than the 2-lobe model. Instead it seems that two heterotrimers of subunits Cog2,3,4 and Cog5,6,7 are connected through the pair of subunits Cog1 and Cog 8 (Ungar et al., 2005). Furthermore, negative stain EM provided elegant support for this architecture and marked subunit positions and binding sites for key interacting partners

within the 3-dimensional structure of the Cog1-4 group bound to Cog8 (Lees et al., 2010).

COG participates in a multitude of weak interactions, which has led to the hypothesis that it may perform multiple roles at the vesicle tethering stage of Golgi trafficking. Additionally, several of the subunits appear to function as "hubs" for interactions with specific families of partners (Willett et al., 2013b). Consistent with the theme of tether-Rab GTPase interactions, COG subunits interact with the yeast Golgi Rabs Ypt1 (Rab1) and Ypt6 (Rab6), and a plethora of other Rab GTPases in mammals (summarized in Willett et al., 2013b). COG also specifically binds COPI-coated vesicles which, along with Rab interactions, may be how COG recognizes Golgi retrograde vesicles (Ram et al., 2002; Suvorova et al., 2002; Zolov et al., 2005). Interestingly, COG interacts with coiled coil tethering factors, including Uso1 (p115), suggesting that these tethers may work together to sequentially provide long-range and shorter range vesicle capture functions at the Golgi (Sohda et al., 2007; Willett et al., 2013b). Finally, the COG complex is one of the best characterized MTCs for its interactions with SNARE proteins; through these interactions, COG has been proposed to not only direct the localization of some Golgi SNAREs but also may stabilize and proofread assembled SNARE complexes (Willett et al., 2013a,b; Fotso et al., 2005; Oka et al., 2004; Shestakova et al., 2007). This function is likely coordinated with another interacting partner, the SM protein Sly1 (Laufman et al., 2009; Willett et al., 2013a).

Recent studies in mammalian cells demonstrated that targeting COG subunits to the mitochondria was sufficient to re-direct SNARE-containing, intra-Golgi vesicles as

well (Willett et al., 2013a). These studies provide strong evidence for COG as a spatial landmark for its SNARE binding partners and COPI vesicle fusion, as well as potentially serving as a scaffold for vesicle tethering activity (Willett et al., 2013a). However, given that COG's extensive network of interacting partners (including coiled coil tethering proteins) is present in the cell cytoplasm, *in vitro* reconstitution assays are required for definitively determining that COG is the tethering factor in these pathways.

Dsl1 complex:

The Dsl1 complex is the smallest CATCHR with only 3 subunits: Dsl1, Tip20, and Dsl3/Sec39, which are all encoded by essential genes (Kraynack et al., 2005; Spang et al., 2012). Dsl1 is highly conserved and plays an essential role in retrograde trafficking of COPI vesicles from the Golgi to the ER (Andag et al., 2001; Kamena and Spang, 2004; Kraynack et al., 2005; Reilly et al., 2001; Sweet and Pelham, 1993; VanRheenen et al., 2001; Zink et al., 2009). Dsl1 is known to localize to the ER through physical interactions with the SNARE proteins, which are also critical for its putative tethering function (Kraynack et al., 2005; Tripathi et al., 2009). Due to its less complex architecture, Dsl1 has been more thoroughly characterized at a structural level than other CATCHR MTCs with nearly complete crystal structures available for the subunits. These structural and biochemical studies revealed a clear model for how the subunits assemble together, with Dsl1 being the central link between Tip20 and Sec39 (Tripathi et al., 2009; Ren et al., 2009).

Despite its simpler structure, numerous known binding partners make Dsl1 the likely orchestrator of vesicle tethering, uncoating, and fusion at the ER membrane. The

central subunit, Dsl1, is proposed to capture COPI vesicles through binding directly to two subunits of the COPI coat complex (Andag et al., 2001; Andag et al., 2003; Zink et al., 2009). An additional interaction between Tip20 and the COPI coat was also identified, so it is unclear whether these subunits serve redundant roles in vesicle recognition (Diefenbacher et al., 2011). Interestingly, the Dsl1 binding sites on these COPI coat proteins overlap with coat complex interaction sites, which are required for stabilizing the coat itself, suggesting that Dsl1 binding may first tether and then destabilize the vesicle coat (Zink et al., 2009). The other potential membrane attachment point for vesicle tethering likely involves ER SNARE protein binding. The Dsl1 complex binds to the ER SNAREs Sec20 and Use1 as well as to assembled ER SNARE complexes, which may be used for anchoring the complex during tethering and for stabilizing or promoting SNARE complex assembly respectively (Ren et al., 2009). Importantly, a direct role for Dsl1 in both tethering and vesicle uncoating has yet to be tested experimentally. It is also interesting to note that, unlike most of the MTCs, no Rab GTPase is known to interact with Dsl1, though many have speculated whether a GTPase may be important during vesicle uncoating (Spang et al., 2012).

GARP complex:

Golgi-associated retrograde protein (GARP) is the four-subunit MTC localized at the TGN, which is required for retrograde trafficking between the endosome and the TGN (Bonifacino and Hierro, 2010). All four GARP subunits (Vps51, Vps52, Vps53, and Vps54) were originally identified in *S. cerevisiae* but are also required in higher eukaryotes as depletion of any of the subunits results in embryonic lethality in mice and

Arabidopsis thaliana (Conibear and Stevens 2000; Conibear and Stevens ,2003; Siniossoglou et al., 2001; Siniossoglou et al., 2002; Perez-Victoria et al. 2008; Liewen et al., 2005; Perez-Victoria et al., 2008; Schmitt-John et al., 2005; Lobstein et al., 2004; Guermonprez et al., 2008). The structures of two subunits, human Vps53 and *S. cerevisiae* Vps54, were solved by x-ray crystallography revealing the characteristic CATCHR fold of contiguous helical bundles (Perez-Victoria et al., 2010; Vasan et al., 2010); but knowledge of the overall structure of GARP has largely lagged behind the other CATCHR MTCs. Interestingly, biochemical analyses revealed an essential role for the N-termini of GARP subunits in maintaining overall complex assembly, which is another theme among CATCHR complexes that is beginning to emerge (Perez-Victoria et al., 2008; Siniossoglou et al., 2002; Quenneville et al., 2006; Perez-Victoria et al., 2010; Perez-Victoria et al., 2009; Munson and Novick, 2006; Yu and Hughson, 2010). Additionally, a recently-identified alternative version of this complex called Endosome-associated retrograde protein (EARP) complex, highlighted the role for Vps54 in TGN localization. EARP contains 3 GARP subunits with Vps54 replaced by syndetin, a modification which is sufficient to localize EARP to the recycling endosome in mammalian cells rather than the TGN and confer a unique endocytic recycling function (Schindler et al., 2015).

A number of known interacting partners are some of the few clues as to GARP function, given the lack of structural information for the complex as a whole. Vps53 and Vps54 bind endosomal retrograde vesicles destined for the TGN, but the protein or lipid contacts on these vesicles have yet to be identified (Quenneville et al., 2006; Perez-

Victoria et al., 2009; Vasan et al., 2010). As a tether, GARP must also physically interact with the TGN membrane and it does so through interactions with activated Ypt6 (Rab6) (Siniossoglou et al., 2001; Siniossoglou et al., 2002). GARP also binds another TGN-localized GTPase called Arl1, which does not seem to be required for GARP localization but rather for some unknown modulation of its function (Panic et al., 2003). Furthermore, GARP interacts with endosome-TGN pathway SNARE proteins including Tlg1, Syntaxin6, Syntaxin 16, and VAMP4 as well as assembled SNARE complexes (Perez-Victoria et al., 2009). Although the function of GARP-SNARE interactions is not well understood, depletion of GARP subunits results in mislocalization of SNAREs and reduced levels of assembled SNARE complexes suggesting a potential role in stabilizing SNARE complexes (Perez-Victoria et al., 2009). In summary, it remains to be tested whether these interactions underlie GARP's putative role as a vesicle tether or suggest additional functions. Given that depletion of a number of golgin coiled coil proteins also disrupts endosome to TGN trafficking, it is likely that there is some redundancy in tethering in this pathway and GARP may be essential for additional reasons (Reddy et al., 2006; Derby et al., 2007; Lieu et al., 2007; Lieu et al., 2010; Goud and Gleeson, 2010).

Exocyst complex

The putative CATCHR MTC for exocytosis, and focus of this dissertation, is called the exocyst complex. The composition of the exocyst is highly conserved in eukaryotic systems, with eight different subunits Sec3, Sec5, Sec6, Sec8, Sec10, Sec15, Exo70, and Exo84, each found at single copy in the complex (TerBush et al., 1995; TerBush et al., 1996; Guo et al., 1999; Hsu et al., 1996). Six of the eight subunits were

identified in the original *S. cerevisiae* screen for secretory mutants and all but *SEC3* are essential genes in yeast (Novick and Schekman, 1980; Finger et al., 1997; Haarer et al., 1996; Wiederkehr et al., 2004). Since the identification of the complex, budding yeast has proven to be a powerful tool for elucidating functional and structural information about the exocyst complex. Moreover, homologues of all the subunits exist in both unicellular and multicellular eukaryotes and the essential role for the complex in growth and development is conserved as well. Null mutants in a number of exocyst subunits result in early lethality in both mice and *Drosophila* indicating a critical role in development (Friedrich et al., 1997; Murthy et al., 2003; Murthy et al., 2005).

Exocyst assembly and architecture:

As for other members of the CATCHR family, the available crystal structures of exocyst subunits display a common motif of tandem helical bundles that form extended rod-like structures (reviewed in Munson and Novick, 2006). Biochemical studies predict that the subunits may pack together in a side-by-side manner in the assembled holocomplex (Fig. 1.5, Munson and Novick, 2006) and that the N-termini of exocyst subunits, which have not been amenable to structural characterization, are important for intra-complex stability (Dong et al., 2005; Croteau et al., 2009; Shen et al., 2013). Although the exocyst subunits share structural homology, their surfaces are characterized by unique hydrophobic and electrostatic patterns (Sivaram 2006). This diversity of

surface properties indicates unique binding interfaces and functions for the individual subunits and biochemical studies have been important in characterizing these unique binding sites and interactions (reviewed in Liu and Guo, 2012; Munson and Novick, 2006). In addition to the conserved helical bundles, several exocyst subunits contain additional functional domains. The yeast Sec3 N-terminal region contains a novel Pleckstrin Homology domain in a region demonstrated to interact with PI(4,5)P_2 and a number of small GTPases (Baek et al., 2010; Yamashita et al., 2010). Moreover, mammalian-specific domains of Sec5 and Exo84 were each crystallized in complex with the mammalian GTPase RalA, structures that were invaluable in defining the specificity of binding to the GTP-bound form of RalA (Fukai et al., 2003; Jin et al., 2005).

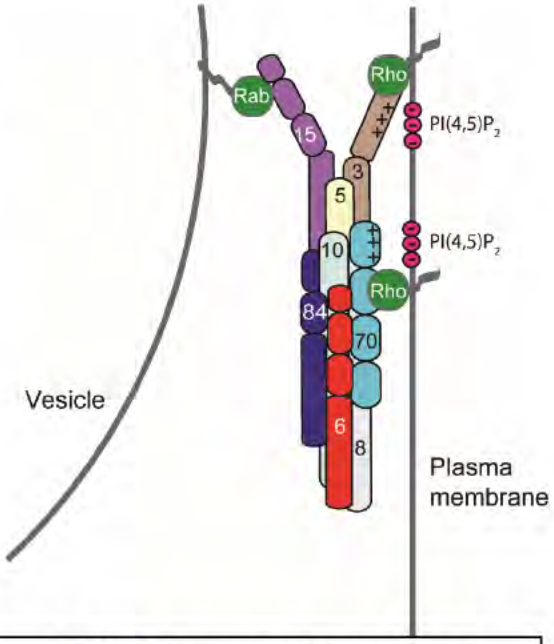

Figure 1.5 Model for exocyst architecture. Subunits are labeled by their number Sec3-Sec5-Sec6-Sec8-Sec10-Sec15-Exo70-Exo84 (3-5-6-8-10-15-70-84) and are depicted with predicted, elongated, helical bundle structures. Subunit arrangement based on available biochemical data for pairwise subunit interactions. (Modified from Munson and Novick, 2006).

A key aspect of understanding exocyst function is to determine the mechanism(s) of its assembly and disassembly of its subunits. Many questions remain unanswered, such as when, where and how many of the subunits assemble together, and if they always stay assembled. Whether the exocyst requires disassembly is unknown, although considering

the ~850 kDa size of the complex, disassembly may remove the exocyst as an obstacle for vesicle fusion and/or facilitate recycling of the complex.

Early biochemical experiments discovered that the eight unique polypeptides of the exocyst form a high molecular weight complex (TerBush et al., 1996; Guo et al., 1999b; Hsu et al., 1996; Hsu et al., 1998). Differential centrifugation, cell fractionation, and immunofluorescence experiments in both yeast and higher eukaryotes indicated that the exocyst subunits are found primarily as a single complex, with both cytosolic and plasma membrane pools (TerBush et al., 1996; Hala et al., 2008; Guo et al. 1999a; TerBush et al., 1995; Grindstaff et al., 1998; Bowser et al., 1992; Morgera et al., 2012). This observation is consistent with the localization of all of the exocyst subunits to sites of polarized secretion at the bud tip and mother-bud neck in yeast, and polarized sites of membrane expansion in plant and animal cells (Vega and Hsu, 2001; Grindstaff et al., 1998; Blankenship et al., 2007; Bryant et al., 2010). However, these results are inconsistent with the prevailing model where a subset of yeast exocyst subunits associate with secretory vesicles while others associate with the plasma membrane prior to complex assembly and vesicle tethering (Boyd et al., 2004) (Fig. 1.6a).

The existence of subcomplexes or monomeric free pools would lead to a greater array of functional possibilities and mechanisms for exocyst regulation. Although the exocyst subunits predominantly co-migrate when examined by centrifugation and gel filtration studies, the broad distributions and trailing peaks for some exocyst subunits suggested that some of the subunits may exist in free pools outside of the complex (Guo et al., 1999; Morgera et al., 2012). Localization studies in *Drosophila melanogaster*

indicate that specific exocyst subunits exhibit unique localization patterns during oogenesis, development and adulthood, suggesting that the subunits might not always function as a single entity (Murthy et al., 2005). Additionally, recent imaging studies in the growing hyphae of *Neurospora crassa* suggest that subsets of exocyst subunits associate with vesicles at the Spitzenkörper, whereas another subset localizes to the apical membrane (Riquelme et al., 2014).

Cell fractionation studies in mammalian cells provide the strongest evidence for subcomplexes. Ral GTPases function in trafficking, but are unique to metazoan systems. Activated RalA and RalB are associated with secretory vesicles (Bielinski et al., 1993) and each binds to two exocyst subunits: Sec5 and Exo84, which are predicted to be in separate subcomplexes by cell fractionation (Moskalenko et al., 2003; Moskalenko et al., 2002). Recent studies also showed that Ral GTPases interact with Exo84 and Sec5 in distinct subcellular locations (Hazelett et al., 2011; Bodemann et al., 2011). It seems likely that there would be a greater need for functional subcomplexes in mammalian systems, where different combinations of subunits could respond to a complex array of signals.

Despite a number of studies suggesting that subcomplexes of exocyst subunits exist, isolating them and defining their composition has proven challenging, possibly due to weak pairwise interactions between the subunits (Dong et al., 2005; Sivaram et al., 2006). Weak interactions are likely to be functionally important for cooperative assembly and disassembly of the complex. More sensitive quantitative techniques for detection of these subcomplexes, as well as robust activity assays, will be important for determining

their physiological relevance. Furthermore, identification of specific mutants that disrupt intra-exocyst interactions is required to tease apart the functions of individual subunits, the complex as a whole, and to understand which subunits are critical for stabilization of exocyst structure.

Very little information is available regarding the overall architecture of the exocyst complex and how the 8 subunits assemble together. Work using yeast two-hybrid analyses, immunoprecipitation, and *in vitro* binding studies with recombinant proteins identified weak pairwise binding interactions among the subunits of the exocyst (reviewed in Munson and Novick, 2006 and Liu and Guo, 2011; Katoh et al., 2015) (Fig. 1.5). Structural and biochemical studies of the holocomplex remained an outstanding challenge for the field, to achieve an understanding of how the subunits are pieced together, and details of assembly and disassembly of the complex (See Chapter 2). Moreover, it will be interesting to see if these mechanisms are conserved across all eukaryotes.

Exocyst localization and activation:

Consistent with its required role in polarized vesicle exocytosis, the exocyst is concentrated at limited regions of the plasma membrane, where it mediates the delivery of lipids and proteins necessary for polarized membrane growth. In *S. cerevisiae*, these sites are the tip of the growing bud and the mother-bud neck during cytokinesis (He and Guo, 2009). Similarly, the *Schizosaccharomyces pombe* exocyst is localized at growing cell poles and the division septum during membrane scission (Wang et al., 2002; Bendezu et al., 2012). Studies in *Drosophila* and mammalian neurons indicate that the

exocyst is found at the ends of neuronal growth cones during neurite branching, as well as at sites of synaptogenesis (Hazuka et al., 1999; Mehta et al., 2005; Lalli et al., 2005). Cell-cell contact sites in polarized epithelial cells and the leading edge of cell motility processes are also sites of exocyst concentration (reviewed in Hertzog and Chavrier, 2011 and Liu and Guo, 2012). Data is rapidly emerging about the role of the exocyst in plants, where the complex localizes to the growing ends of pollen tubes, root hair tips and the cell plate for division (Hala et al., 2008; Fendrych et al., 2010). Recently, the exocyst was shown to localize to the apical membrane and Spitzenkörper in the rapidly growing hyphal tips of *Neurospora crassa* (Riquelme et al., 2014).

How the exocyst is recruited and maintained at polarized sites is a critical question, and one that has been the focus of much effort since the complex was identified. Early studies in budding yeast implicated the exocyst subunit Sec3 as a spatial landmark for exocytosis, as the localization of Sec3-GFP appeared unaffected by disruptions of the secretory pathway, actin, and cell cycle proteins (Finger et al., 1998). Immunofluorescence of endogenous Sec3 called this result into question, however, and later reports demonstrated that Sec3 is not sufficient to target and/or retain exocyst complexes at sites of secretion (Roumanie et al., 2005; Zhang et al., 2005; Songer et al., 2009; Bendezu et al., 2012). Consistent with exocyst localization being dependent on secretion and polarized actin, live imaging and fluorescence recovery after photobleaching (FRAP) analyses suggested that six of the eight exocyst subunits arrive at polarized sites on vesicles via transport on actin cables (Boyd et al., 2004) (Fig. 1.6a). Sec3 and Exo70 were the exceptions in that Sec3-GFP seemed to localize independently

of these mechanisms and Exo70-GFP appeared to use both vesicle-independent and -dependent routes to polarized sites. The model proposed that exocyst subunits arrive on vesicles and assemble with Exo70 and Sec3 at the plasma membrane (Fig 1.6a), although it is not clear whether the rest of the subunits would arrive individually or already assembled together. Alternatively, consistent with a lack of definitive subcomplexes in yeast, the exocyst complex may arrive fully assembled on vesicles where plasma membrane binding is mediated by Sec3 and Exo70 (Fig. 1.6b). However, it has been challenging to detect a pool of exocyst complex in association with secretory vesicles, potentially due to a weak interaction or because only a small fraction requires vesicular transport to polarized sites. A third possibility is that exocyst complex is concentrated at polarized secretion sites and it participates in numerous vesicle tethering/fusion events without the need for vesicular delivery or recycling (Fig 1.6c). The data supporting each

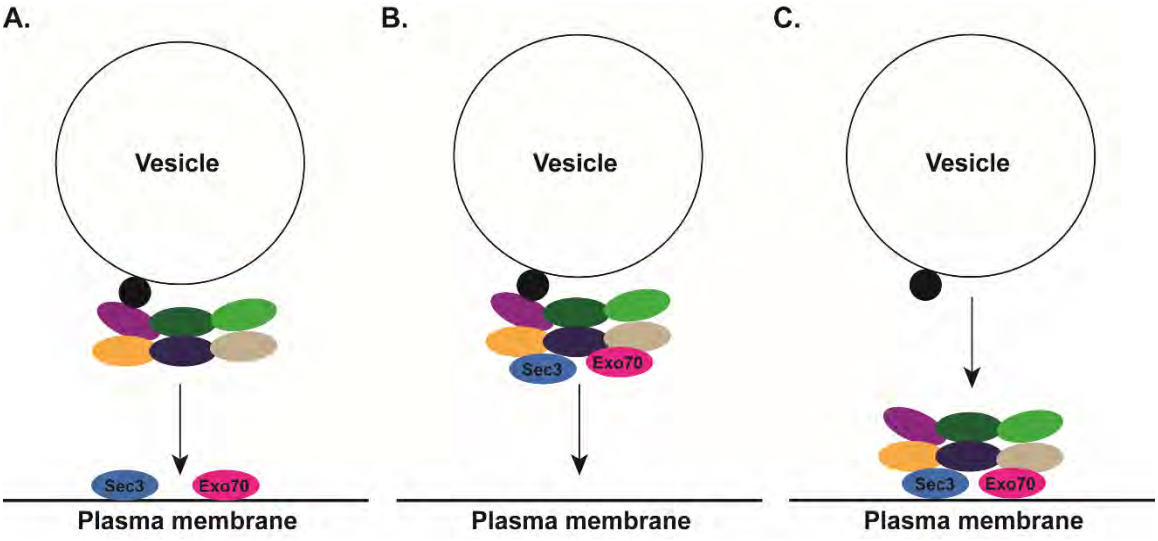

Fig 1.6: Hypothetical models for exocyst-mediated vesicle tethering in yeast. (**a**) According to the Boyd *et al.* model, a subset of exocyst subunits associates with secretory vesicles via one or more binding partners (black spheres) and assembles with Sec3 and Exo70 at the plasma membrane, effectively driving tethering. (**b**) Exocyst complexes may arrive fully assembled to the plasma membrane where Sec3 and Exo70 will mediate binding to the plasma membrane. (**c**) Exocyst complexes are anchored to polarized sites on the plasma membrane via Exo70 and Sec3 and wait for incoming vesicles to tether.

of these models remains to be reconciled and it is important to determine whether exocyst assembly/disassembly are required for the tethering and targeting of vesicles. It seems likely that exocyst disassembly or conformational changes must follow to initiate another round of vesicle fusion, but there is no direct evidence yet to suggest whether this occurs *in vivo*.

Exocyst association with the membrane, regardless of the models proposed in Fig. 1.6, depends upon the subunits Exo70 and Sec3. Both subunits are effectors for Rho GTPases, which are master cell polarity regulators that are localized to the plasma membrane and are critical in polarizing the actin cytoskeleton for vesicle delivery. The yeast Sec3 N-terminal domain interacts with Rho1, Cdc42 and PI(4,5)P_2, while Exo70 binds Rho3, Cdc42 and PI(4,5)P_2 (Baek et al., 2010; Yamashita et al., 2010; Wu and Brennwald, 2010; He et al., 2007; Adamo et al., 2001; Adamo et al., 1999; Guo et al., 2001; Zhang et al., 2001; Robinson et al., 1999). The GTPase interactions of Exo70 are conserved, as mammalian Exo70 interacts with the Rho protein TC10 (Inoue et al., 2003). Elegant genetic studies in *S. cerevisiae* revealed that exocyst interactions with Cdc42 and the other Rho GTPases serve an exocytosis-specific function separate from their role in establishing cell polarity (Adamo et al., 2001; Adamo et al., 1999). Furthermore, these studies identified partial redundancy between Exo70 and Sec3 in their interactions with the Rho GTPases, but that Exo70 is the primary effector for Cdc42 (Roumanie et al., 2005; Wu et al., 2010) consistent with Sec3 being the only non-essential exocyst subunit (Haarer et al., 1996; Finger et al., 1997; Guo et al., 2001).

Interestingly, Rho-binding defective exocyst mutants can be rescued by GTP-hydrolysis deficient versions of the Rho GTPases, suggesting that the GTPase cycle is not required for their exocytosis-specific functions (Roumanie et al., 2005). Small GTPases, such as Cdc42, function both through GTP hydrolysis and hydrolysis-independent mechanisms. Commonly, molecular recognition and timing events that require binding and release of effectors require hydrolysis of GTP; for example, the Sec4 interaction with the exocyst requires this function (see below). Hydrolysis-independent mechanisms are proposed to be allosteric regulatory events, where binding of the GTPase activates the binding partner through a conformational change (Wu et al., 2008). Since exocyst interactions with Rho appear to fit this allosteric model, it is possible that these interactions function primarily to activate the exocyst at polarized sites, potentially to accelerate SNARE complex assembly for vesicle fusion.

Because Rho GTPase interactions are not critical for polarized exocyst localization, phospholipid interactions may provide this function. *sec3ΔN* mutants crossed to *exo70* mutants defective in binding to PI(4,5)P_2 are severely growth defective or synthetically lethal in yeast, indicating possible redundant functions for these subunits in stabilizing exocyst localization through lipid binding (Zhang et al., 2008; Hutagalung et al., 2009; Pleskot et al., 2015). Furthermore, mutations in yeast *MSS4,* the kinase that produces PI(4,5)P_2, cause diffuse exocyst localization (He et al., 2007). Mammalian Exo70 is also dependent on PI(4,5)P_2 binding for localization and the residues involved in this interaction constitute the most conserved domain on the protein (Liu et al., 2007). Plant Exo70 isoforms are also predicted to bind phospholipids (Zárský et al., 2009). The

lipid binding residues in the N-terminal region of Sec3 are also highly conserved among Sec3 homologues (Baek et al., 2010). Finally, in addition to phospholipid interactions, it is likely that additional factors critical for exocyst localization remain to be identified. The yeast *sec6* mutant alleles, *sec6-49* and *sec6-54* result in mislocalization of the assembled exocyst complex (Songer and Munson, 2009). The mutations are in regions suggestive of protein-protein, rather than protein-lipid, interactions. Therefore, these mutants are proposed to be defective in binding to a protein factor that anchors the assembled complex at the plasma membrane.

Vesicle recognition and regulation by other small GTPases:

Similar to the previously discussed MTCs, the yeast exocyst subunit Sec15 interacts with the GTP-bound Rab protein Sec4 on vesicles, presumably for specific secretory vesicle recognition (Guo et al., 1999, TerBush et al., 1995, Goud et al., 1988) (Fig. 1.6). It is not yet known whether the Sec4-GTP-Sec15 interaction only facilitates exocyst interaction with vesicles or if it plays an additional role in regulating the complex. Furthermore, it is not clear whether the Sec4 interaction with exocyst is direct as previous studies relied on crosslinking/co-immunoprecipitation in yeast extract and yeast 2-hybrid assays (Guo et al., 1999). Since these early studies, the exocyst has been shown to interact with the vesicle SNARE Snc1/2, the Sec4 GEF Sec2, the cell polarity factor Sro7/77, and the type V myosin Myo2 in yeast, suggesting that vesicle binding and recognition may not be solely mediated by Sec4 (Shen et al., 2013; Medkova et al., 2006; Zhang et al., 2005; Grosshans et al., 2006; Jin et al., 2011). Vesicle binding by the

exocyst complex has been suggested to be weak or transient, thus novel approaches are required to characterize tethering activity (see Chapter 3).

Exocyst interactions with Rab GTPases are conserved in higher eukaryotes as well. In both mammals and *Drosophila,* Sec15 interacts with the Rab GTPase Rab11; this interaction appears to be important for endocytic recycling (Zhang et al., 2004; Wu et al., 2005; Jafar-Nejad et al., 2005). Additionally, interactions with Rab8 and Rab11 were later shown to function in trafficking from the Golgi and recycling endosome to the plasma membrane, as well as to the base of the primary cilium during ciliogenesis (Das and Guo, 2011). It will be interesting to determine which of these Rab GTPases function similarly to Sec4 and what role they may play in regulating exocyst activity.

The interaction of the GTPase Ral with two different exocyst subcomplexes in metazoans may be functionally important for exocyst assembly. The reduction of Ral expression results in decreased association of Sec10 with Sec6 (Moskalenko et al., 2002). Additionally, release of the Ral-exocyst interactions may be triggered by phosphorylation events (Chen et al., 2011), possibly leading to dissociation of the exocyst from vesicles or disassembly of the complex.

Exocyst functions:

Tethering:

The exocyst, like most of the other CATCHR MTCs, has numerous interactions consistent with a role in vesicle tethering at the plasma membrane, though a direct role in tethering has yet to be demonstrated experimentally. Establishing an assay for tethering

has been hindered by the challenge of purifying intact exocyst complexes and monitoring what is likely to be a transient interaction (Fosmarck et al., 2011; Donovan and Bretscher, 2015b). It is not known which of the known protein and lipid interacting partners described above might contribute to this role and how these interaction sites are spatially oriented within the exocyst complex. Additionally, it is unclear whether the 8 exocyst subunits are all required for vesicle tethering, maintaining complex assembly, or if they contribute to additional functions through the diverse array of partners identified in both yeast and metazoans (see Chapters 2 and 3).

SNARE regulation:

In addition (or alternatively) to tethering, the recognition of exocytic vesicles by the exocyst may directly ensure the fidelity of secretion by promoting specific SNARE complex assembly. For example, the yeast exocyst subunit Sec6 binds to the exocytic plasma membrane SNARE Sec9 (Sivaram et al., 2005) as well as the assembled exocytic SNARE complex (Dubuke et al., 2015). The function of this interaction is unclear but could be involved in regulation or stabilization of SNARE complex assembly, which is an emerging trend among MTCs (Sivaram et al., 2005; Dubuke et al., 2015; Hong and Lev et al., 2014). HOPS binds to SNARE complexes, promotes proper vacuolar SNARE pairing, and may protect SNARE complexes from disassembly (Starai et al., 2008; Kramer and Ungermann, 2011; Baker et al., 2015). Similarly, COG binds to SNAREs and increases the stability of intra-Golgi SNARE complexes, possibly preventing disassembly and promoting fusion. It is unclear whether COG may have an effect on the rate of SNARE complex assembly; Dsl1has a slight stimulatory effect on Golgi to ER

SNARE complex assembly *in vitro,* and GARP promotes the assembly of TGN SNARE complexes (Shestakova et al., 2007; Ren et al., 2009; Bonifacino and Hierro, 2011). As the mechanistic details for these functions are explored further, it will be interesting to discover whether all the tethering complexes function similarly in SNARE complex regulation, or if there are interesting organelle-specific (or species-specific) differences.

As described previously in relation to HOPS and COG, interplay between SM proteins and tethering complexes is an important, but poorly understood, mechanism of SNARE complex regulation. Consistent with this, we identified an interaction between the exocyst subunit Sec6 and the yeast exocytic SM protein Sec1, suggesting a potential role for the exocyst in recruiting and/or stabilizing Sec1 at sites of secretion for SNARE regulation (Morgera et al., 2012, Appendix G). Together, the exocyst and Sec1 may function to spatially and temporally control SNARE assembly. *In vitro* reconstitution of SNAREs with purified exocyst complexes, and other regulators, such as Rab and Rho GTPases, Sec1, and Sro7/77, will be necessary to determine the effect of the exocyst on SNARE assembly and membrane fusion.

Cytoskeleton interactions:

Yeast post-Golgi vesicles are transported from the trans-Golgi network to the plasma membrane along actin filaments using the type V myosin motor Myo2. The Rab GTPases Ypt31/32 and Sec4 both associate with post-Golgi vesicles and bind to Myo2, but not simultaneously, as they exchange during the progression of vesicle transport (Jin et al., 2011; Mizuno-Yamasaki et al., 2010). Due to this GTPase shuffling, it seems unlikely that Rabs would be the sole interactors maintaining the cytoskeletal connection

to the vesicle. Indeed, it was recently shown that the cargo-binding domain of Myo2 is structurally homologous to the exocyst subunits (Pashkova et al., 2006) and this domain of Myo2 directly binds to Sec15; abrogation of the Myo2-Sec15 interaction leads to growth and secretion defects in yeast (Jin et al., 2011). Immunoprecipitation of Myo2 pulls down other exocyst subunits, suggesting association with the full complex, although it is unclear whether this occurs during vesicle transport or upon arrival at sites of secretion (Jin et al., 2011). The function of this interaction may be to recruit exocyst complexes to vesicles for delivery to polarized sites or potentially for stabilizing Myo2 association with vesicles (Jin et al., 2011). However, no exocyst mutants identified to date specifically disrupt vesicle transport so more specific mutant alleles of Sec15 and Myo2 are required to tease apart the functional importance of this interaction.

In mammalian systems, vesicles are transported from the Golgi by microtubules and their associated kinesin motors to cortical actin networks at the plasma membrane (Wang and Hsu, 2006). Numerous approaches have demonstrated an interaction between the exocyst complex and microtubules; furthermore, Exo70 was shown to inhibit the polymerization of tubulin *in vitro* (Wang and Hsu, 2006). The exocyst or one or more of its subunits may play a role as adaptors in the connection of vesicles to microtubules, analogous to its proposed role in actin-based transport in yeast. Moreover, it was proposed that the exocyst may be needed to release vesicles from microtubules to the actin networks (Wang and Hsu, 2006). During cell migration, actin is remodeled to build a branched network at the leading edge of cells. Polymerization of these networks is nucleated by the Arp2/3 complex (Pollard and Borisy, 2003; Ridley et al., 2003) and

several studies indicated a distinct role for Exo70 in binding and regulating Arp2/3 activity during cell motility (Zuo et al., 2006; Liu et al., 2012). There is no mechanistic understanding yet for the role of the exocyst in these processes but, taken together, all of these interactions provide important clues that the exocyst may be involved in multiple stages of trafficking from vesicle transport up through regulating SNARE complex assembly.

Diverse cellular functions:

In contrast to the traditional view of the exocyst as a simple tether of secretory vesicles to the plasma membrane, the complex has been implicated in a great variety of cellular processes (Fig. 1.7). The common theme seems to involve exocyst-mediated localization of membrane-bound vesicles or compartments to specific target sites at the appropriate time. For example, at least three yeast exocyst subunits (Sec3, Sec5, and Sec8) have been implicated in ER inheritance, potentially by anchoring the cortical ER at the bud tip where the exocyst is localized (Wiederkehr et al., 2003). A later study also identified an interaction between yeast Sec6 and Rtn1, a protein important for ER reticulation, with Rtn1 potentially serving as an exocyst receptor on the ER (De Craene et al., 2006). Several studies implicate the exocyst in prospore membrane formation during meiosis in budding yeast (Mathieson et al., 2010; Neiman et al., 1998).

In higher eukaryotes, the exocyst subunits are expressed in all tissue types analyzed thus far (Hsu et al., 1996). Similar to the phenotype in yeast, exocyst mutants or knock-downs in more complex organisms are associated with cell growth and developmental defects, as has been shown in mouse, plant, and *Drosophila* model systems (Friedrich et al., 1997; Murthy et al., 2003; Murthy et al., 2005, Zhang et al., 2010). The function of the exocyst in growth and secretion in many cell types reflects its

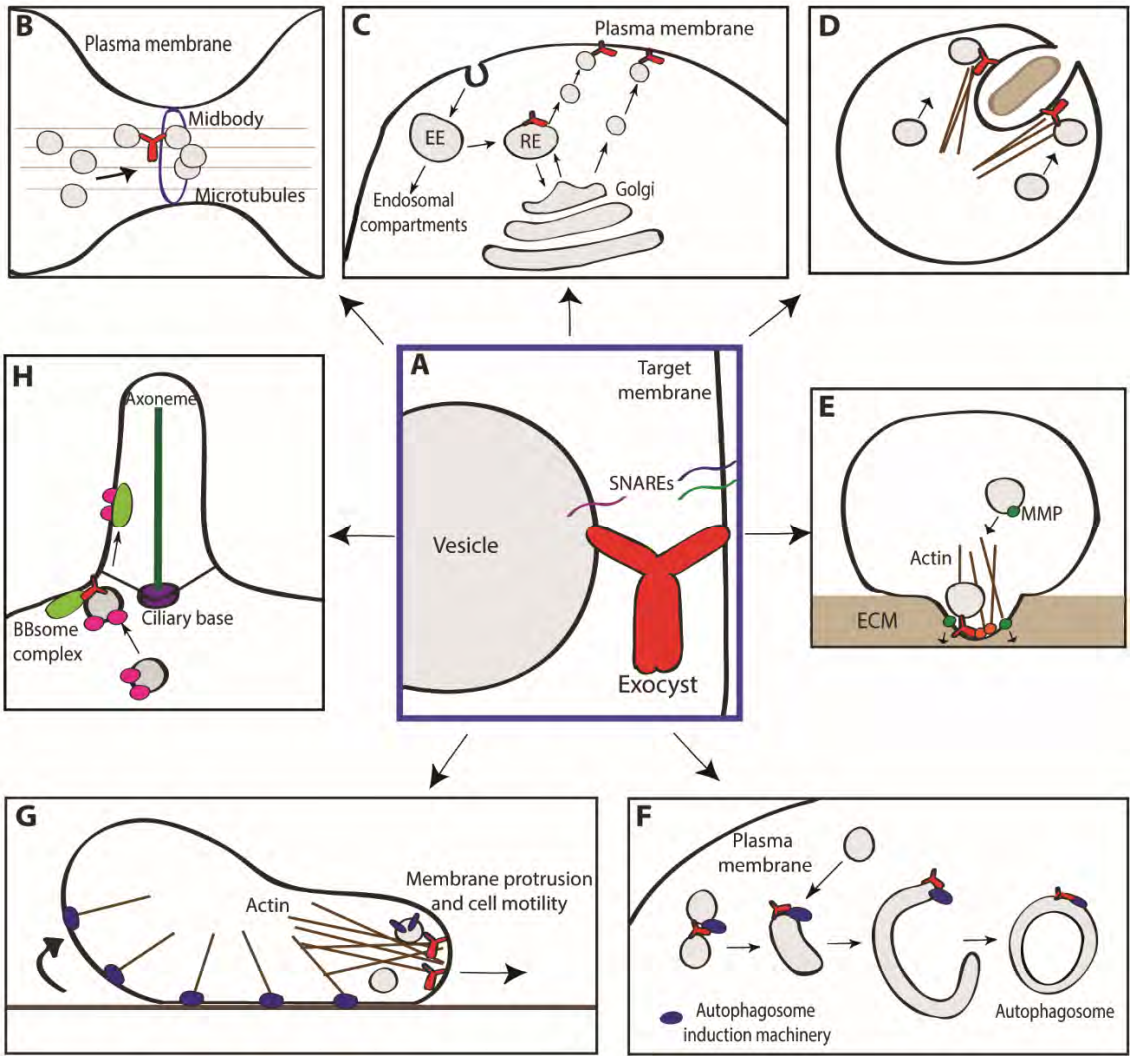

Figure 1.7 Exocyst functions in a variety of processes in single- and multi-cellular eukaryotes. (**a**) The exocyst is proposed to form an initial connection between vesicle and target membrane through interactions with proteins and lipids on both surfaces. The interactions may bring the vesicle close enough to promote SNARE complex formation and vesicle fusion and/or the exocyst may play an active role in regulating SNARE assembly. (**b**) The exocyst localizes to the site of cytokinesis to direct and tether vesicles at these sites, leading to formation of a new membrane and facilitating abscission. (**c**) During polarized secretion, the exocyst tethers both exocytic vesicles generated at the Golgi apparatus and vesicles that are being recycled to the plasma membrane from the recycling endosome (RE, recycling endosome; EE, early endosome). (**d**) An invading pathogen mediates its entry into the cell by hijacking host cell processes including the exocyst complex, to polarize the cytoskeleton and vesicle delivery for membrane ruffling and macropinocytosis. (**e**) The exocyst colocalizes with IQGAP1 (orange) in invadopodia, directing the growth of invasive processes and the delivery of matrix metalloproteinases (MMPs) that degrade the extracellular matrix (ECM). (**f**) Exo84 and a possible subcomplex of exocyst subunits interact with autophagosome induction machinery (blue), promoting the formation of the autophagosome. The exocyst may function to tether vesicles or tubules to each other leading to the production of this compartment. (**g**) The exocyst interacts with lipids and proteins to localize to the leading edge of migrating cells, promoting the outgrowth of the leading edge and delivering focal adhesion (blue) components recycled from the rear. (**h**) The exocyst directs membrane and protein delivery to the ciliary base to promote ciliogenesis and the BBsome complex shuttles proteins into the cilium beyond the diffusion barrier. (Adapted from Heider and Munson, *Traffic* 2012).

critical role in tethering and SNARE-mediated fusion of exocytic vesicles. Furthermore, as suggested by its bud neck localization in budding yeast, the exocyst also appears to direct vesicles to the midbody during cytokinesis in mammalian cells (Gromley et al, 2005; Neto et al., 2014) (Fig. 1.7b), *Drosophila* (Giansanti et al., 2015), and plants (Rybak et al., 2014) . In addition, the exocyst has been shown to be important for endocytic recycling in yeast (Jose et al., 2015; Riezman, 1985), *Drosophila* (Sommer et al., 2005) and animal cells (Fig. 1.7c) (He and Guo 2009, Wilson et al., 2005). Highly specialized secretory pathways, such as the insulin-stimulated delivery of the glucose transporter Glut4 in adipocytes, also require functional exocyst complexes (Inoue et al., 2003; Inoue et al., 2006, Sano et al., 2015).

The exocyst is required for many other types of membrane expansion, including ciliogenesis, tubulogenesis and cell migration in mammalian systems (Thapa et al., 2012; Hertzog and Chavrier, 2011; Liu and Guo, 2012; Das and Guo, 2011) (Fig. 1.7g,h). Due to its promotion of cell growth, cell migration, interactions with Ral GTPases, the exocyst

has been linked with cancer progression and metastasis (Hertzog and Chavrier, 2011; Camonis and White, 2005). In one example, the secretion of matrix metalloproteinases (MMPs) in tumor cell invadopodia requires exocyst-mediated exocytosis (Sakurai-Yageta et al., 2008; Liu et al., 2009; Ren and Guo, 2012; Yamamoto et al., 2013)(Fig. 1.7e). Furthermore, the exocyst-mediated exocytic pathway has also been shown to play a role in bacterial pathogenesis; the exocyst is co-opted by the bacteria *Salmonella* to promote its invasion of intestinal epithelial cells (Nichols and Casanova, 2010) (Fig. 1.7d). The exocyst also has roles in host survival responses in numerous species; several studies have linked exocyst function to various aspects of the innate immune response (Chien et al., 2006; Ishikawa et al., 2009; Zárský et al., 2013; Stegmann et al., 2014; Guichard et al., 2014).

Another interesting facet to exocyst function was discovered through the study of the involvement of the GTPase RalB in autophagosome biogenesis (Bodemann et al., 2011) (Fig. 1.7f). This study proposed that RalB triggers its exocyst binding partner Exo84 to serve as a platform for the assembly of the autophagy induction complex and vesicle formation machinery. A more recent study in *Arabidopsis* revealed a role for the exocyst in targeting autophagosomes to the vacuole as well (Kulich et al., 2013). It will be interesting to see whether the exocyst's role in autophagy is yet another aspect of its tethering/membrane fusion activities, or truly a novel function for some of its subunits as a scaffold for autophagy induction machinery.

In contrast to these various roles for the exocyst, several secretory processes appear not to be dependent on wild-type levels of exocyst function.

In *Schizosaccharomyces pombe* for example, severely reduced levels of Sec8 protein blocked septum cleavage with only a modest effect on cargo secretion and no significant effect on polarized growth (Wang et al., 2003). It is possible that exocyst function is rate-limiting during cytokinesis and not growth, but recent results suggested the presence of parallel actin-dependent and exocyst-dependent secretory pathways in *S. pombe* (Bendezu et al., 2011). Additionally, *Drosophila* Sec5 mutants suggested a requirement for the exocyst during neuronal development, but not for synaptic vesicle fusion (Murthy et al., 2003). This specialized system may have evolved additional mechanisms to mediate the fine-tuned release of synaptic vesicles. However, Sec8 was found on purified mammalian synaptic vesicles, so it is possible that the exocyst could be required for synaptic transmission in other animals (Takamori et al., 2006).

The exocyst complex is tied to a vast array of cellular processes and this diversity may be aided in part by the large number of subunits each with their unique surface properties and binding partners. Additionally, post-translational modifications such as phosphorylation are emerging as mechanism by which exocyst function is regulated in different cell types and situations (Luo et al., 2013; Ren and Guo, 2012; Chen et al., 2011). Alternative splicing is another means of modulating exocyst function and several Exo70 splice variants were shown to possess unique functions, particularly with regard to actin polymerization (Lu et al., 2013). In multicellular eukaryotes, some exocyst subunits contain several paralogues, which may allow for functional diversification. In plants, Exo70 is highly diversified with several dozen duplications per genome in *Arabidopsis*

thaliana and some of these paralogues are proposed to possess unique functions in certain plant cell types (Cvrčková et al., 2012; Wang et al., 2010).

Summary:

Early genetic and biochemical experiments laid the foundation for our understanding of exocyst as an essential, evolutionarily conserved factor that functions just upstream of exocytic SNARE assembly and vesicle fusion. We now know that the exocyst functions at the center of a complex network of protein and lipid interactions and its role extends far beyond basic cellular growth and secretion (Heider and Munson, 2012). However, despite nearly two decades of research in yeast and higher eukaryotic systems, these studies have yet to shed light on the specific, definitive role of the exocyst in these pathways. Structural studies are essential to making mechanistic predictions about the function of the holocomplex, the roles for each of the 8 subunits, and the requirement for dynamic assembly and disassembly of exocyst subunits (see Chapter 2). However, the size, complexity, and presumed instability of the exocyst have impeded such biochemical and structural studies over the years (TerBush et al., 2001). For similar reasons, *in vitro* activity assays have been challenging to implement; since *in vivo* disruption of the exocyst provides only limited phenotypic insight, *in vitro* studies are critical to dissecting the function of the exocyst and its partners (see Chapter 3). With recent advancements in purification and structural techniques for large protein complexes as well as quantitative, high resolution imaging techniques, we are in a fortunate position to begin answering many of these open questions about exocyst and its related MTCs.

CHAPTER II: Subunit connectivity, assembly determinants, and architecture of the yeast exocyst complex

Significant background and experimental rationale:

Similar to other tethering factors, the exocyst is a peripheral membrane protein complex that interacts with numerous GTPases, SNAREs, phospholipids, and the vesicle transport motor Myosin V (Heider and Munson, 2012; Yu and Hughson, 2010; Jin et al., 2011; Munson and Novick, 2006). The exocyst is proposed to interact with vesicles through Sec15 binding to the Rab GTPase Sec4 and Myosin V, as well as Sec6 binding the v-SNARE Snc (Guo et al., 1999; Jin et al., 2011; Shen et al., 2013). On the target membrane side, both Sec3 and Exo70 interact with Rho GTPases and PI(4,5)P_2 (Wu et al., 2008; Wu et al., 2010; He et al., 2007; Zhang et al., 2008; Baek et al., 2010), and Sec6 may interact with an as yet unidentified "anchor" factor at the plasma membrane (Songer and Munson, 2009). It is through this myriad of connections that the exocyst is predicted to selectively capture secretory vesicles and tether them to the plasma membrane. A current model for exocyst function proposes that a subcomplex of exocyst subunits in *S. cerevisiae* is carried on vesicles to another subcomplex at the plasma membrane, and that assembly of these together drives vesicle tethering (Boyd et al., 2004), although this model has not yet been validated biochemically, nor have the putative subcomplexes been identified. Whether regulated assembly of the exocyst is required for tethering and SNARE complex regulation in yeast or other organisms, and if these mechanisms differ between different species, are important unanswered questions.

Mechanistic models for exocyst function must be informed by the structural arrangement of its subunits. Crystal structures of several exocyst subunits reveal a strikingly similar motif of contiguous helical bundles that pack together into long rods,

classifying it in the evolutionarily conserved Complexes Associated with Tethering Containing Helical Rods (CATCHR) family (Yu and Hughson, 2010; Munson and Novick, 2006). Numerous pairwise subunit interactions were identified via yeast-2-hybrid assays, immunoprecipitations, and *in vitro* binding experiments using recombinant and *in vitro* translated proteins (Munson and Novick, 2006; Katoh et al., 2015). To examine the architecture and regulation of assembly of the exocyst, we developed a new robust exocyst purification method to reproducibly isolate stable exocyst complexes from *S. cerevisiae*. Using an auxin-inducible degradation system to deplete single subunits, we mapped the connectivity of the eight subunits and determined that most of the subunits are required for the association of two assembly modules within the exocyst. In contrast, depletion of known binding partners had no effect on the assembly status of the exocyst. Here we present the first structure of a fully assembled CATCHR MTC—we determined the structure of the fully assembled exocyst using negative stain electron microscopy (EM) and 2-dimensional averaging. Furthermore, we demonstrate that exocyst complexes are stoichiometric, with no detectable subcomplexes; therefore, we propose that the yeast exocyst functions predominantly as a fully assembled complex.

Results:

Purification of intact yeast exocyst complexes

Biochemical and structural studies of the intact exocyst complex were previously limited by preparations with poor yield, stability and purity (TerBush et al., 1996; TerBush et al., 1995; TerBush et al., 2001; De Craene et al., 2006; Hsu et al., 1998; Munson lab unpublished data). In order to answer critical questions regarding the architecture of the yeast exocyst complex and its putative assembly dynamics, we developed an improved protocol for isolating the entire native complex from yeast extract (Oeffinger et al., 2007; Hakhverdyan et al., 2015). In order to maintain endogenous expression levels and function, we fused C-terminal Protein-A (PrA) affinity tags onto each exocyst subunit individually by integrating DNA encoding PrA at each genomic locus, creating eight different tagged haploid *Saccharomyces cerevisiae* strains (for yeast strains used see Appendix E, Table 5.1) The C-terminal PrA tags did not confer growth defects (Fig. 2.1a), thus demonstrating that each of the tagged subunits was functional. Yeast strains were grown, harvested in log phase as frozen noodles, and lysed using a planetary ball mill grinder (see Methods). The lysate powder was resuspended in a physiological buffer, bound to rabbit IgG-conjugated magnetic beads, and eluted from the beads either by proteolytic digestion, or by denaturation using SDS loading buffer (Fig. 2.2). Exocyst subunit identities were confirmed by the molecular weight shift of the PrA tag on SDS-PAGE (Fig. 2.2), MALDI-MS, and western blot analyses.

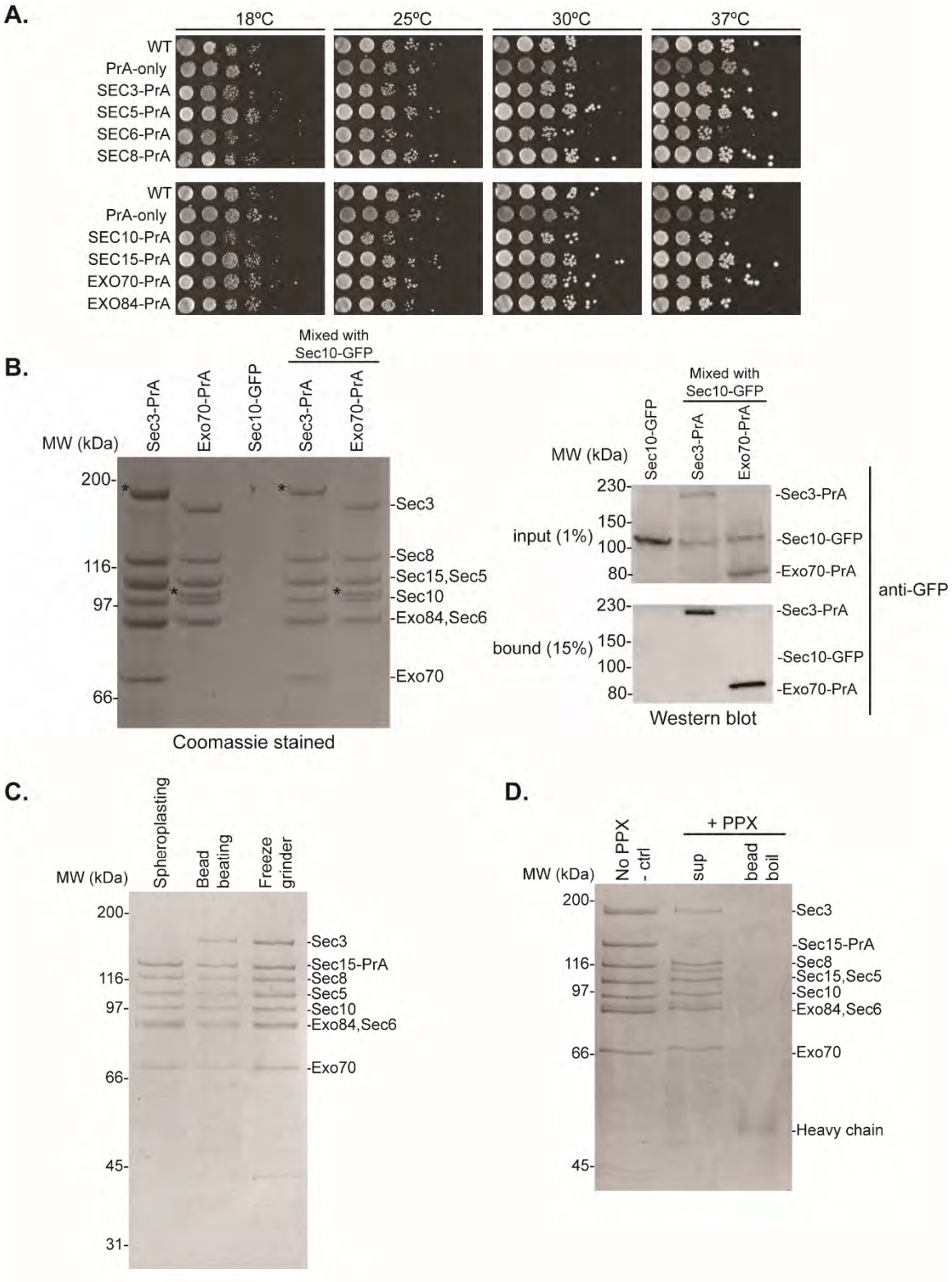
A.
18ºC
25ºC
30ºC
37ºC
WT
PrA-only
SEC3-PrA
SEC5-PrA
SEC6-PrA
SEC8-PrA
WT
PrA-only
SEC10-PrA
SEC15-PrA
EXO70-PrA
EXO84-PrA
B.
Mixed with Sec10-GFP
Sec3-PrA
Exo70-PrA
Sec10-GFP
Sec3-PrA
Exo70-PrA
MW (kDa)
200-
116-
97-
66-
-Sec3
-Sec8
-Sec15,Sec5
-Sec10
-Exo84,Sec6
-Exo70
Coomassie stained
Mixed with Sec10-GFP
Sec10-GFP
Sec3-PrA
Exo70-PrA
MW (kDa)
230-
150-
100-
80-
input (1%)
bound (15%)
-Sec3-PrA
-Sec10-GFP
-Exo70-PrA
anti-GFP
Western blot
C.
Spheroplasting
Bead beating
Freeze grinder
MW (kDa)
200-
116-
97-
66-
45-
31-
-Sec3
-Sec15-PrA
-Sec8
-Sec5
-Sec10
-Exo84,Sec6
-Exo70
D.
+ PPX
No PPX - ctrl
sup
bead boil
MW (kDa)
200-
116-
97-
66-
45-
-Sec3
-Sec15-PrA
-Sec8
-Sec15,Sec5
-Sec10
-Exo84,Sec6
-Exo70
-Heavy chain

Figure 2.1 Characterization of purified yeast exocyst complexes. (**a**) Yeast strains with C-terminally PrA-tagged exocyst subunits show normal growth compared to wild-type (WT) by serial dilution at all temperatures tested. PrA-only corresponds to yeast expressing PrA tag alone. (**b**) Lysate mixing reveals exocyst complexes are not disassembling and reassembling during purification. Sec3-PrA or Exo70-PrA lysate powders were each mixed individually with lysate powder from Sec10-GFP. Exocyst complexes were subsequently purified from the mixed lysates (after 60 min binding at 4°C in 20 mM PIPES pH 6.8, 300 mM KCl) and run on SDS-PAGE for Coomassie staining (left) and Western blot (right). GFP antibody also recognizes exocyst PrA tag. Asterisks indicate PrA-subunit on Coomassie gel. (**c**) Cryogenic ball mill grinding improves yield and complex integrity. Protein concentrations (mg/ml) were measured using BioRad protein assay and all beads were incubated with the same total protein in the same volume. Purified complexes were separated by SDS-PAGE and visualized by Coomassie staining. (**d**) Native elution from IgG-beads using a PreScission Protease site engineered between the C-terminus of each exocyst subunit and the PrA tag. Sec15-PrA tagged exocyst complexes bound to IgG-beads were incubated with PPX for 60 minutes at 4°C to elute native, intact complexes into buffer 20 mM PIPES pH 6.8, 300 mM NaCl (sup). IgG-beads were boiled in SDS/DTT loading buffer to release any undigested complexes (bead boil). Heavy chain of Rabbit IgG is indicated.

We isolated intact exocyst complexes from yeast extracts using each of the eight subunits as the PrA-tagged purification handle. The eight exocyst subunits co-purify with equal stoichiometry by both Coomassie-stained SDS-PAGE and densitometry using Krypton fluorescent protein stain (Fig. 2.2, 2.3, and Appendix 5.2), consistent with earlier reports (TerBush et al., 1996; De Craene et al., 2006). We next asked if the complexes purified by this method undergo disassembly and reassembly during the purification. When Sec10-GFP lysate was mixed with either Sec3-PrA or Exo70-PrA

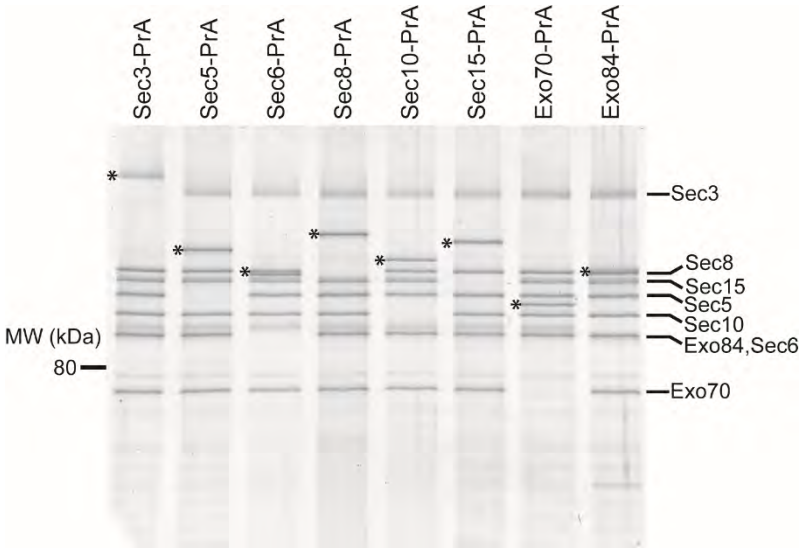

Figure 2.2 Purification of intact yeast exocyst complexes. Purified complexes were separated by SDS-PAGE and visualized by Krypton staining (Thermo Scientific). The asterisk corresponds to the PrA-tagged exocyst subunit used as purification handle (shifts the protein molecular weight by 25 kDa). Both the Sec3 and Exo84 protein bands often migrate as multiple species due to phosphorylation, which appear as slightly smeared bands on SDS-PAGE. The resuspension buffer used was 50 mM Hepes pH 7.4, 300 mM NaCl, plus protease inhibitors.

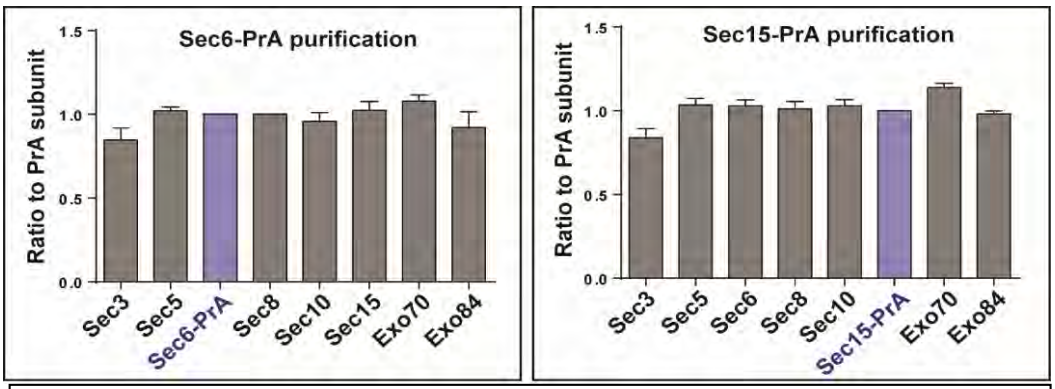

Figure 2.3 All exocyst subunits co-purify with equal stoichiometry. Exocyst complexes were purified with each subunit as PrA purification handle (two representative handles shown), run on SDS-PAGE, and stained with Krypton fluorescent protein stain. Densitometry analysis showed equal stoichiometry for all subunits with no excess of purification handle or subsets of subunits, suggesting there are no detectable free pools or subcomplexes for any subunits. Error bars indicate SEM (n=3-4 technical replicates).

lysates, and the exocyst complexes were subsequently purified, no Sec10-GFP was detected in either pull-down, indicating that no exchange or assembly of subunits occurred during the incubation (1h at 4 °C) (Fig. 2.1b), consistent with our previous studies (Songer and Munson, 2009). Therefore, the purified complexes represent the state of the endogenous complex at the time of cell lysis.

The improved yield and purity of our exocyst preparations are due to reduced proteolysis from cryogenic lysis (Fig. 2.1c) and the use of rabbit IgG-conjugated magnetic beads, which has a tight affinity for PrA (Richman et al., 1982; Oeffinger et al., 2007). Additionally, protease cleavage allowed for increased purity and native elution of untagged complexes for structural studies (Fig. 2.1d). Substoichiometric levels of co-purifying proteins were detected by mass spectrometry and krypton fluorescent protein staining, but they appear to primarily be highly expressed, non-specific contaminants or previously detected binding partners, including Rtn1 (De Craene et al., 2006).

We next tested the functionality of our exocyst preparations by western blotting for known exocyst interacting partners (Fig. 2.4). The improved yield and rapid, gentle purification procedure allowed detection of binding of Sec1, Myo2, and Snc1/2 (redundant paralogues) to the exocyst. Previous studies revealed an interaction of the exocyst subunit Sec6 with both Sec1 and Snc2 (Morgera et al., 2012; Shen et al., 2013) and Sec15 with Myo2 (Jin et al., 2011). Here, we show that these proteins can be pulled down with tagged exocyst subunits that are not their direct binding partners, suggesting that these interactions occur within the context of the assembled complex.

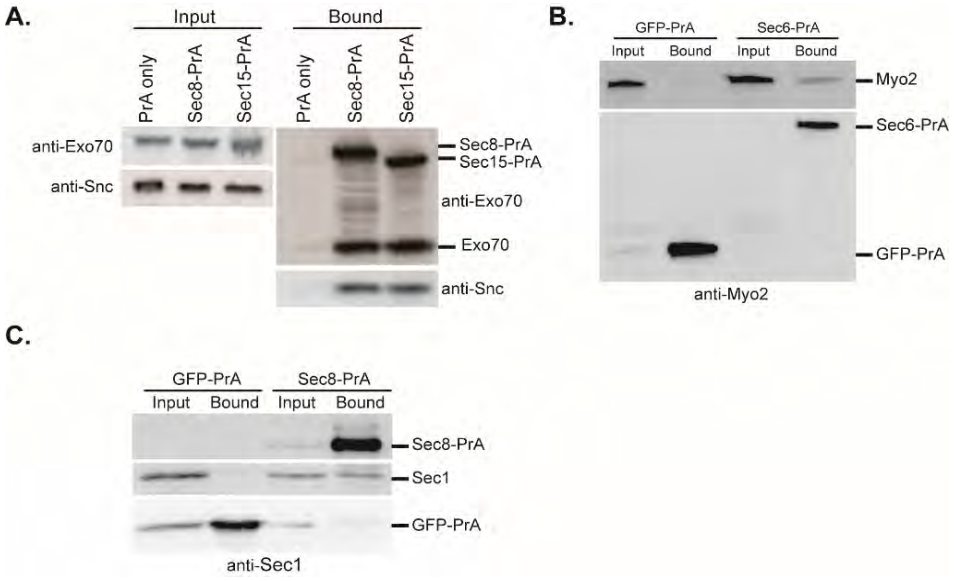

Figure 2.4 Exocyst complexes purified under physiological conditions interact with known binding partners. Exocyst complexes were purified from yeast lysate (using 50 mM Hepes pH 7.4, 150 mM NaCl as resuspension buffer), run on SDS-PAGE, and western blotted to look for co-purification of known exocyst interacting partners when compared to a negative control (PrA-expressing strain in (**a**) and GFP-PrA expressing strain in (**b**) and (**c**)). 0.5% lysate input samples were run for the Sec1 and Myo2 binding experiments and 0.4% input for the Snc binding blot. 100% of bound samples were used in all cases. (**a**) Sec8-PrA and Sec15-PrA were each used as purification handles to co- purify Snc. We blotted our pull-downs for Exo70 to show that we are pulling down assembled exocyst complexes with Sec8-PrA and Sec15-PrA. The rabbit antibody reacts with both Exo70 and the PrA tag. (**b**) Sec6-PrA was purified and Myo2 binding was detected. (**c**) Sec8-PrA was purified and Sec1 binding was detected. There was some bleed over of the GFP-PrA bound lane into the input lane of Sec8-PrA.

Using Sec15-PrA as the purification handle, we monitored exocyst integrity under a variety of pH and salt conditions (Fig. 2.5a). The presence of reducing agents had no effect on complex recovery, and the complex was stable across a range of pH solutions, in contrast to previous studies (TerBush et al., 2001). Increasing the pH above 8.5 rendered purified exocyst complexes sensitive to salt concentrations ≥300 mM. Using Tris, pH 8.5 and ≥500 mM salt, only Sec15 and Sec10 remained bound together, indicating a strong physical interaction between these two subunits, consistent with earlier studies (Guo et al., 1999a).

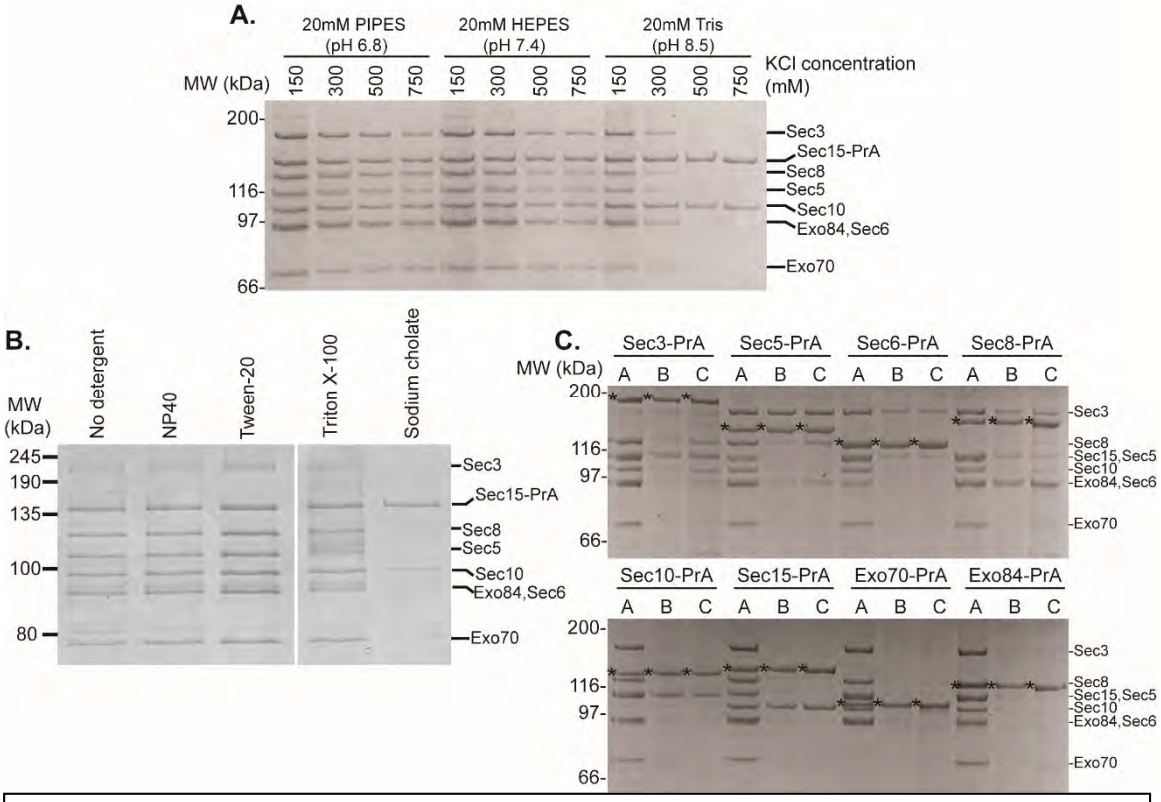

Figure 2.5 Purified exocyst complexes are stable over a wide range of conditions and are comprised of discrete pairwise interactions. (**a**) Sec15-PrA exocyst complexes were purified using buffers of different pH and KCl concentration as indicated and visualized using Coomassie-stained SDS-PAGE (**b**) Sec15-PrA exocyst complexes were purified using 50 mM Hepes pH 7.4, 300 mM NaCl buffer and various commonly used detergents at the following concentrations: 0.1% NP-40, 0.1% Tween-20, 1% Triton X-100, 20 mM Sodium cholate. (**c**) Destabilizing buffer conditions were used with each exocyst subunit as PrA purification handle in order to isolate subcomplexes and stable subunit pairs. A=20 mM PIPES pH 6.8, 300 mM KCl. B=20 mM Tris pH 8.0, 500 mM KCl. C=20 mM Tris pH 8.0, 300 mM KCl, 500 mM Urea. Asterisks correspond to the PrA-tagged subunit.

The exocyst complex peripherally associates with vesicles and the plasma membrane (Bowser et al., 1992). We therefore tested the effect of detergents, particularly whether the stoichiometry changes due to the solubilization of membrane-bound subcomplexes or disruption of intersubunit interactions. We tested several non-ionic detergents including NP-40 (Igepal), Tween-20, and Triton X-100, and none affected the overall yield of assembled exocyst or the relative stoichiometry of the subunits (Fig. 2.5b). In contrast, the exocyst was severely disrupted by sodium cholate, a strong anionic detergent. Taken together, these results indicate that varying the ionic strength of the resuspension buffer has a pronounced effect on exocyst integrity, suggesting that ionic interactions may be a major stabilizing force for intersubunit connections.

We used our pull-down assay to identify stable intracomplex interactions within the endogenous exocyst complex using partially destabilizing buffer conditions with each of the eight PrA-tagged exocyst subunits (Fig. 2.5c). Several stable subunit pairs emerged: Sec3-Sec5, Sec8-Sec6, and Sec10-Sec15. Neither Exo70 nor Exo84 bound tightly to any of the other subunits under these destabilizing conditions. Although several of these pairwise interactions had been previously identified (Guo et al., 1999a; Katoh et al., 2015; Roth et al., 1998; Wiederkehr et al., 2004), the relative stabilities of the subunit pairs compared to other intersubunit interactions were unknown.

Subunit connections and intra-complex assembly determinants

We applied a more targeted approach to answer additional architectural questions: How are these pairs of subunits assembled into the overall connectivity map of the assembled

exocyst? Which of these intersubunit interactions are functionally important for maintaining exocyst integrity? Are some subunits more important for interactions with binding partners on the plasma membrane and vesicle? We decided to selectively eliminate individual exocyst subunits to define their role in maintaining overall complex assembly. All exocyst subunits except Sec3 are encoded by essential genes and, therefore, cannot be deleted from the yeast genome (Wiederkehr et al., 2004; Haarer et al., 1996). We tested the temperature-sensitive (ts) mutants *sec3-2*, *sec5-24*, *sec6-4*, *sec8-6*, and *sec10-2* using Sec15-PrA as the purification handle and only *sec8-6* had a major effect on exocyst integrity at the restrictive temperature. These results were difficult to interpret, however, as the ts alleles vary in severity and amount of destabilization or degradation of the mutant protein. Previous studies using a similar panel of exocyst ts mutants showed greater disassembly for several of the mutants than we observed, even at the permissive temperature (TerBush et al., 1995). These differences are likely due to proteolysis of exocyst subunits during spheroplasting lysis, which destabilizes the complex (see Fig. 2.1c). To overcome these challenges, we employed an auxin-inducible degradation (AID) system to specifically remove each individual exocyst subunit.

This degron system uses the IAA17 AID sequence from *Arabidopsis thaliana*, which is fused to each exocyst subunit. When co-expressed with OsTIR1, exposure to the plant hormone auxin leads to rapid proteosomal degradation of the tagged subunit (Nishimura et al., 2009; Nishimura et al., 2014) (Fig. 2.6a). Addition of these tags to the C-terminal ends of exocyst subunits conferred no growth defects on their own, but when

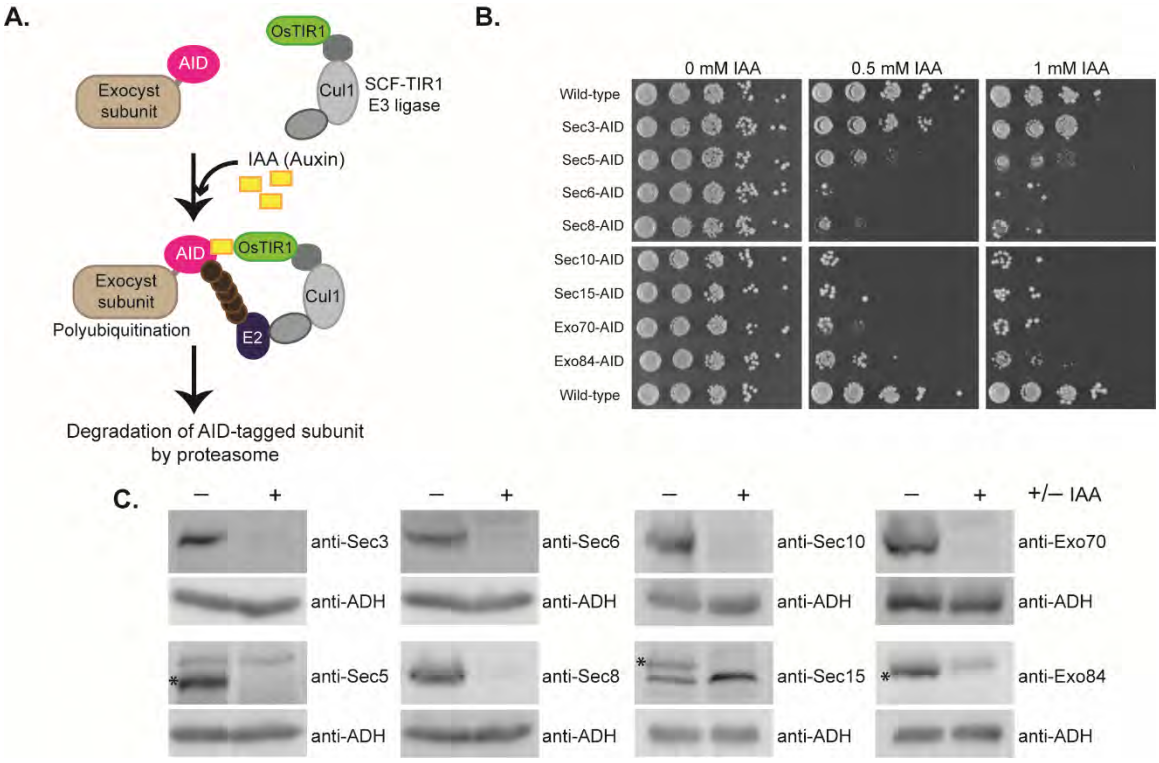

Figure 2.6 Use of the auxin-inducible degron (AID) system to selectively degrade essential exocyst proteins from yeast. (**a**) Schematic of the AID system. The auxin-inducible degron (AID) tag from *Arabidopsis thaliana* was fused to the C-terminus of exocyst subunits at their genomic locus in yeast strains constitutively expressing OsTIR1 (F-box transport inhibitor response 1) protein. Upon treatment with the natural plant hormone auxin (IAA=Indole 3-acetic acid), the SCF-OsTIR1 E3 Ubiquitin ligase complex is activated, which then recruits E2 Ubiquitin ligases for polyubiquitination of the AID-tagged protein. The AID-tagged protein is then rapidly degraded by the proteasome (Nishimura 2009, Nishimura 2014). (**b**) AID-tagged exocyst strains were tested for growth by serial dilution growth assay on YPD plates containing the indicated amount of IAA. Suppressor colonies can be seen in some dilutions. (**c**) Degradation of exocyst subunits in these strains was confirmed by western blotting lysates from NaOH/SDS lysis. (–) denotes untreated strains and (+) treated with IAA. All subunits were degraded to <10-12% of starting protein level. Asterisks indicate the AID-tagged exocyst subunit in blots where antibodies also bind non-exocyst subunits.

grown on plates containing auxin (Indole 3-acetic acid, IAA), all exocyst-AID strains were inviable except for Sec3-AID (Fig. 2.6b). We confirmed rapid and specific IAA-

induced degradation of individual exocyst subunits in liquid culture by western blot analyses of yeast lysates. Each exocyst subunit was degraded to <12% of the starting level within 60 minutes of IAA treatment (Fig. 2.6c), whereas the protein levels of the remaining subunits were mostly unchanged (Fig. 2.7).

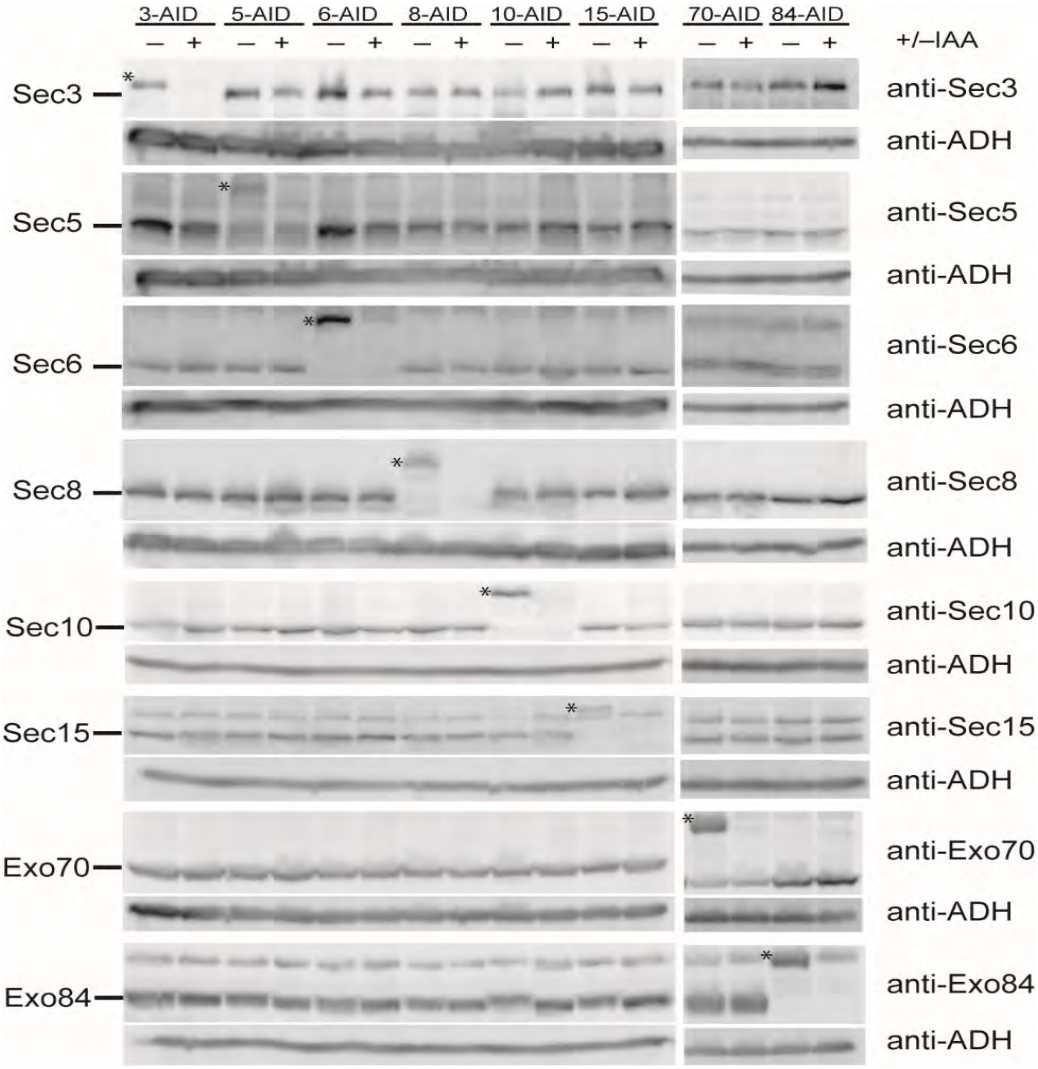

Figure 2.7 Degradation of one exocyst subunit does not affect the protein levels of the remaining exocyst subunits. Exocyst-AID strains were grown in YPD 30°C and treated with IAA for 60 minutes. Degradation of the AID-tagged exocyst subunit was confirmed by western blot of yeast lysates from NaOH/SDS lysis. The protein levels for the remaining subunits were blotted in the same strain (same column in the western blot). (–) denotes untreated and (+) treated with IAA. The positions of the untagged exocyst subunits are indicated to the left of the blots and the AID-tagged subunit is marked with (*). All lysates were blotted for ADH as a loading control.

To assess the role of each individual subunit in maintaining the assembly of the endogenous exocyst complex, we combined this AID system with our PrA-tag purification approach. Genomic C-terminal PrA tags were added to Sec8, Sec15, or Sec6 in strains already expressing an AID-tagged exocyst subunit and OsTIR1. Two different PrA-tag handles were tested for each AID-tagged subunit in order to determine the fate of each of the exocyst subunits. Most of the dual-tagged exocyst strains grew normally, but

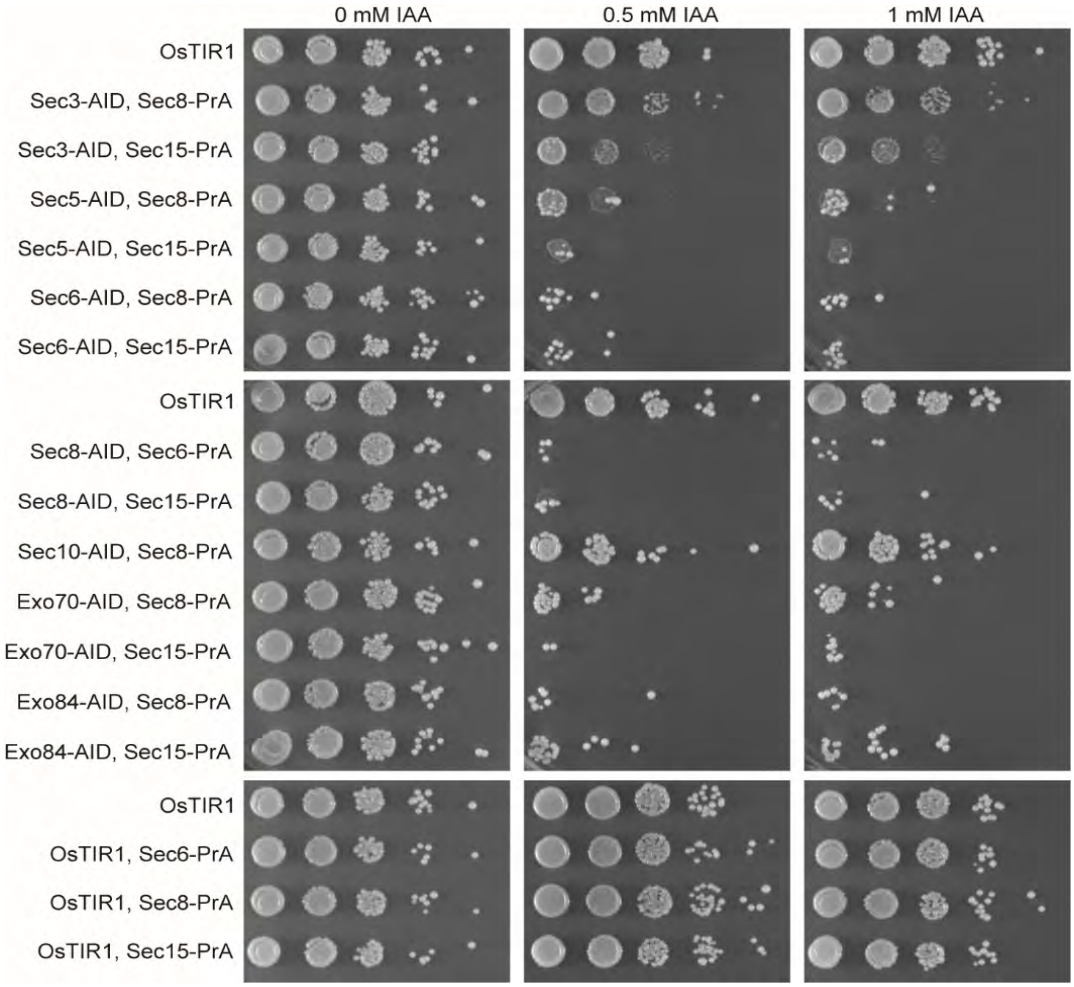

Figure 2.8 Exocyst AID/PrA strains are functional and inviable on IAA-containing YPD plates. We constructed yeast strains expressing double-tagged exocyst complexes: one subunit with a C-terminal AID-tag and another with a C-terminal PrA tag. All tags were integrated at the genomic loci under the endogenous promoter. Strains were serially diluted on standard YPD plates or YPD plates containing IAA and grown at 30°C.

were inviable on IAA plates, as expected (Fig. 2.8). Surprisingly, Sec10-AID/Sec15-PrA showed no growth defect on IAA plates and no loss of Sec10-AID in IAA-containing liquid culture; similarly, Sec15-AID was not degraded in combination with PrA-tagged exocyst subunits (Fig. 2.9). We speculate that the lack of degradation in these strains may be due to masking of the AID tag by the 25 kDa PrA tag on a neighboring exocyst subunit.

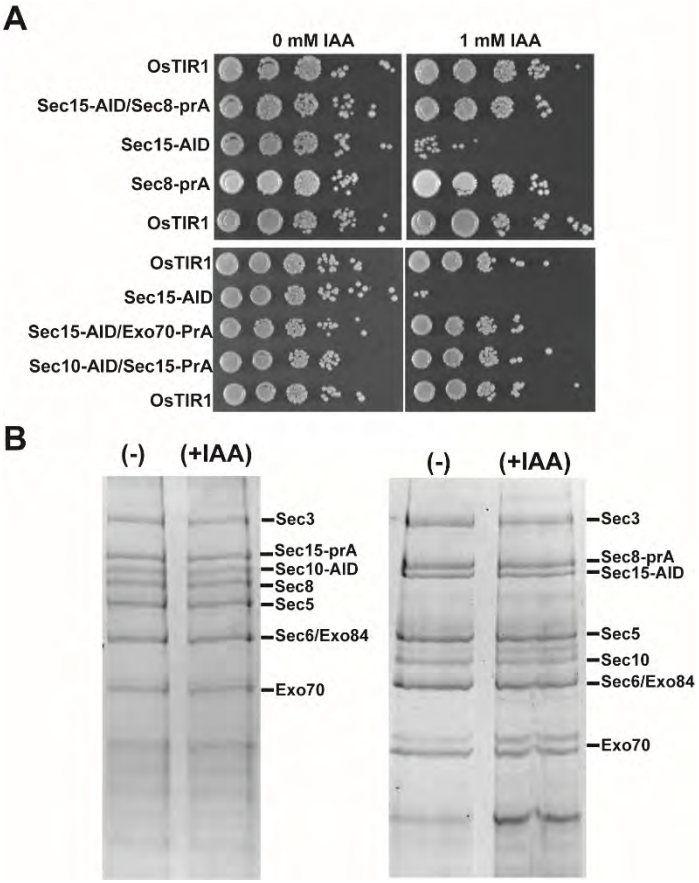

Figure 2.9 Sec15-AID and Sec10-AID did not show depletion in combination with several C-terminal Protein-A tagged exocyst subunits. (**a**) Sec15-AID was viable on IAA plates in combination with Sec8-PrA and Exo70-PrA. Sec10-AID was viable on IAA plates in combination with Sec15-PrA. Strains were serially diluted on standard YPD plates or YPD plates containing IAA and grown at 30°C. (**b**) AID strains that were viable on IAA also did not show depletion by Coomassie-stained SDS-PAGE and exocyst complexes remained fully assembled.

We purified the exocyst complex from both untreated and IAA-treated cultures for each exocyst-AID-PrA combination strain and visualized the complexes by Coomassie staining and western blots (Fig. 2.10 and Fig. 2.11). Surprisingly, the loss of Sec5, Sec6, Sec8, Sec10, Exo70, or Exo84 resulted in the exocyst complex splitting into two distinct, stable modules: Sec3–Sec5–Sec6–Sec8 (3–5–6–8) and Sec10–Sec15–Exo70–Exo84 (10–15–70–84). The results from the different combinations of AID and PrA tags are summarized in the table in Fig. 2.10, showing the

division of the exocyst structure into two modules. Loss of Sec3 had the least destabilizing effect on exocyst complex assembly. Degradation of each of the other subunits had distinct effects on its own module, depending on the strength and connectivity of its interactions with its partners, but no effect on the integrity of the opposing module.

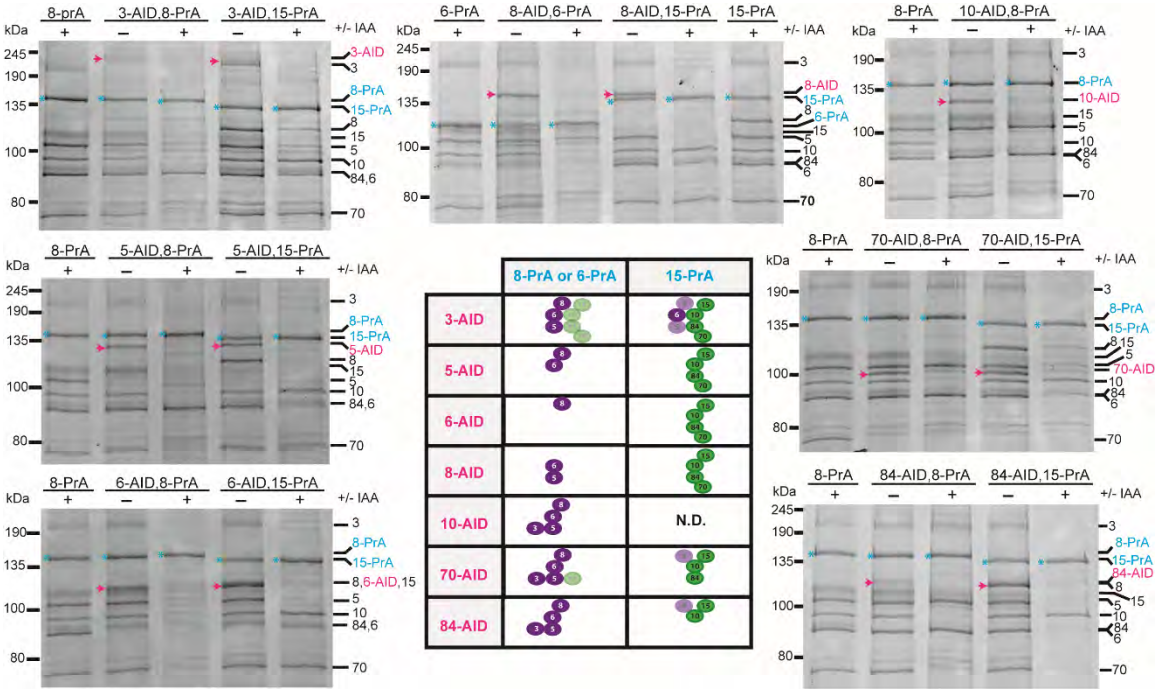

Figure 2.10 Most exocyst subunits are critical for maintaining the assembly of two 4-subunit modules within the full octameric complex. Exocyst complexes were purified using the indicated PrA purification handle (blue) from yeast strains where one AID-tagged subunit (magenta) is degraded. The resuspension buffer used was 50 mM Hepes pH 7.4, 150 mM NaCl. Purified complexes were run on SDS-PAGE and visualized with Coomassie staining. (–) denotes untreated and (+) treated with IAA. Exocyst subunits are denoted by their number (Sec3,Sec5,Sec6,Sec8,Sec10,Sec15,Exo70,Exo84 as 3,5,6,8,10,15,70,84). Degradation of 6 of the subunits tested led to the complete separation of exocyst into two 4-subunit modules: 3–5–6–8 and 10–15–70–84 with the connections depicted in the central table. Sec10-AID,Sec15-PrA was not determined (N.D.). Faded symbols represent subunits that showed partial loss from the complex.

We found that the individual assembly of each module is predominantly based on the association of three stable subunit pairs (3–5, 6–8, and 10–15), instead of requiring the cooperative assembly of all four subunits together. If exocyst assembly was cooperative, we would expect to observe complete disassembly of all four subunits from

Figure 2.11 Western blot confirms composition of exocyst subcomplexes following depletion of individual subunits. Exocyst complexes were purified using the indicated PrA purification handle (blue) from yeast strains where one AID-tagged subunit (magenta) is degraded. Purified complexes were run on SDS-PAGE and visualized by Western blotting with antibodies specific to exocyst subunits (antibody indicated in inset box for each blot). (–) denotes untreated and (+) treated with IAA for 40 minutes. Exocyst subunits are denoted by their number. Magenta asterisks indicate the AID-tagged subunit, and green asterisks indicate the subunit whose co-purification is being monitored in that particular blot. Polyclonal antibodies also recognize PrA-tagged subunits, which in all cases is the band running higher than the subunit monitored (green asterisk), with the exception of Sec3, which runs above the PrA- tagged subunit.

each module upon loss of one subunit; instead, we generally find subcomplexes containing 2-3 subunits (e.g. Sec6 and Sec5 remain bound after Sec8 is degraded). This finding is consistent with our earlier biochemistry results demonstrating that these subunit pairs are stable enough to be co-purified (Fig. 2.5c). Therefore, the most robust interactions within the complex exist between pairs of subunits and the overall assembly appears to be mediated by a network of weaker interactions. Several additional rules for exocyst assembly can be drawn from these results (Fig. 2.12). Sec8 requires Sec6 for

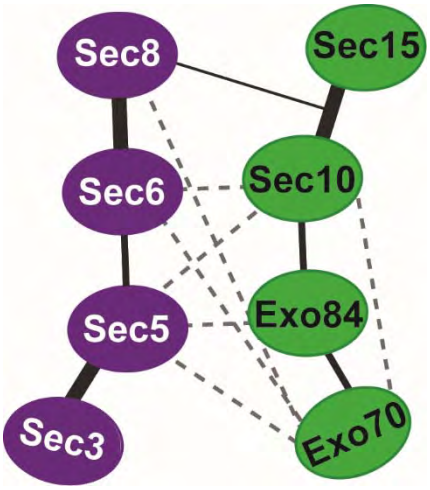

Figure 2.12 Model depicting the subunit connectivity within and between each exocyst module (green and purple). Thick lines indicate the strong pairwise connections identified in Fig. 2.5c, Fig. 2.9, and Fig. 2.10 which are required for stability of the assembled exocyst. The thin line depicts a putative connection between Sec8 and Sec10–Sec15 identified in the AID studies, but Sec8's direct binding partner within this pair is not known. Dashed lines represent interactions identified in previous *in vitro* studies using Y2H and recombinant proteins (summarized in Munson and Novick, 2006); these are consistent with several additional, weaker pairwise interactions identified here.

assembly into the complex. Sec5 is required for Sec3's assembly and for the stable interaction of Sec3 with Sec6 and Sec8. In the absence of Sec8, there was also loss of Sec3 from Sec5–Sec6, suggesting either a potential interaction between Sec3 and Sec8 or a potential conformational change that weakens Sec3's association with Sec5–Sec6. In the case of the other module, Sec10 and Sec15 are a stable pair that require Exo84 for their association with Exo70. Although we were unable to test it, we predict that degradation of Sec15 would not disrupt Sec10's connection with Exo84 and Exo70, as its only known stable exocyst partner is Sec10 (Guo et al., 1999a) (Fig. 2.5).

These studies only provide a few clues as to the interconnections between the modules. All subunits are required for the assembly of the two modules, including Exo70 and Exo84, which is perhaps surprising in light of our biochemical studies, which demonstrated that they were not tightly associated with any other subunits of the complex (Fig. 2.5). We propose that the interconnections between the modules are made up of a network of weaker subunit-subunit interactions, although we cannot rule out that the degradation of a subunit from one module may alter the structure of its respective subcomplex, making it incompatible for binding the opposing

module. Other previously identified subunit interactions may contribute to this inter-module network but their relative contributions remain to be tested (Fig. 2.12) (Munson and Novick, 2006; Katoh et al., 2015).

Exocyst binding partners have no effect on exocyst assembly

We wondered if any additional binding partners would be necessary to maintain this stable assembly. However, only substoichiometric amounts of known binding partners were detected in our exocyst preparations, suggesting that these partners do not need to remain bound to the exocyst to maintain its integrity (Fig. 2.2 and Fig. 2.4).

A major unresolved question is how the exocyst assembles *in vivo* and whether additional factors are required for regulating this assembly. Selective elimination of individual exocyst interacting partners along the late secretory pathway might identify subcomplexes, indicating a failure of the complex to fully assemble. To test this idea, we again employed our AID tag approach to deplete the master polarity regulator Cdc42 (Adamo et al., 2001), the type V myosin motor Myo2 (Jin et al., 2011), the SNARE regulator Sec1 (Hashizume et al., 2009), the v-SNARE Snc2 (Shen et al., 2013), and the Rab GTPase Sec4 (Guo et al., 1999a) (Fig. 2.13a). The functional consequences of each of these interactions are not known, and it is unclear at which stage in exocytosis these interactions occur (Morgera et al., 2012; Wu et al., 2010; Wiederkehr et al., 2004; Zhang et al., 2001).

The AID-tagged partner strains were treated with IAA for 1 hour, which is sufficient time for numerous rounds of vesicle delivery and fusion in *S. cerevisiae* (Donovan and Bretscher, 2012). Degradation of Sec1 induced a severe vesicle

accumulation phenotype, as expected (Novick and Schekman, 1979), while degradation of Myo2 and Cdc42 caused a more mild secretion defect consistent with previous reports

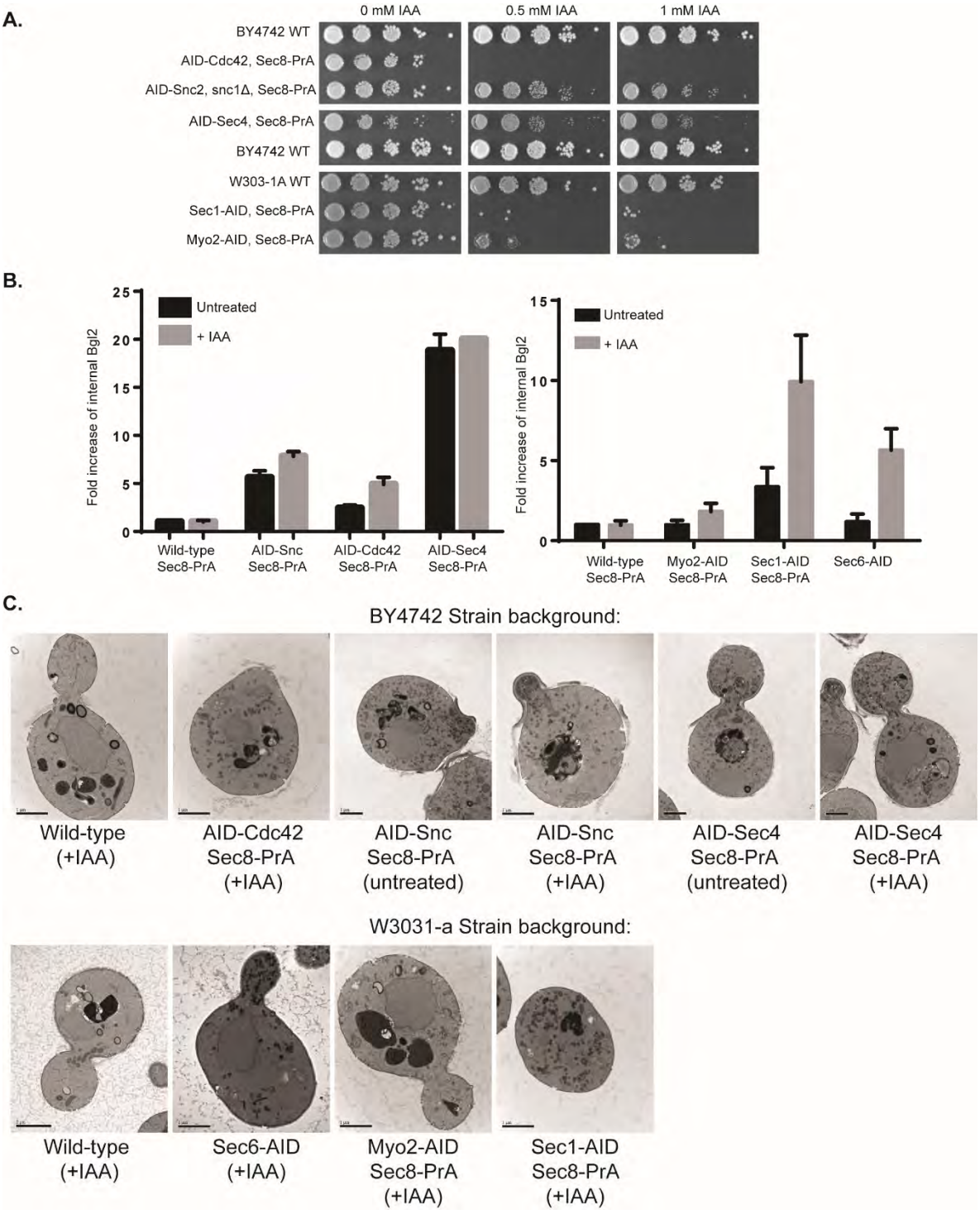

Figure 2.13 AID-tagged exocyst binding partners are functional and have varying levels of growth and secretion defects in IAA-containing media. **(a)** N-terminally AID-tagged Cdc42, Snc2, and Sec4 combined with Sec8-PrA and OsTIR1 were tested for growth on YPD and YPD-IAA plates at 30°C relative to the wild-type (WT) parent strain (BY4742). AID- Sec4/Sec8-PrA demonstrated a mild growth defect on YPD plates and in liquid culture (data not shown); this growth defect was exacerbated slightly in the presence of IAA. AID-Snc2/ *snc1*Δ/Sec8-PrA showed a slight growth defect in the presence of IAA, and AID-Cdc42/Sec8-PrA was inviable on IAA plates. Sec1-AID/Sec8-PrA and Myo2-AID/Sec8-PrA showed no growth defects when compared to their parent strain (W303-1A) but were inviable on IAA plates. (b) Graphs depict the fold increase of internal Bgl2 levels in AID-tagged partner strains over internal Bgl2 levels in the appropriate WT untreated control strain. Sec1-AID and Sec6-AID showed severe secretion defects, while Myo2-AID and AID-Cdc42 showed minor defects consistent with previous reports[43,44,48]. AID-Snc and AID-Sec4 showed severe Bgl2 accumulation even before treatment, suggesting a partial loss of function due to the AID tag. Error bars indicate SEM for n=3-4 different treated or untreated yeast cultures. (c) Thin section EM confirms the vesicle accumulation defects observed in the Bgl2 assay. AID-Cdc42 cells also showed a loss of polarity and fewer budding cells. Scale bar=1 μm.

(Fig. 2.13b,c) (Adamo et al., 2001; Govindan et al., 1995). N-terminal AID-tagging Snc and Sec4 resulted in severe vesicle accumulation even before IAA treatment, suggesting that these N-terminal tags partially impair protein function (Fig. 2.13b,c). Using a PrA tag on Sec8, we pulled out exocyst complexes after degradation of these partners (Fig.

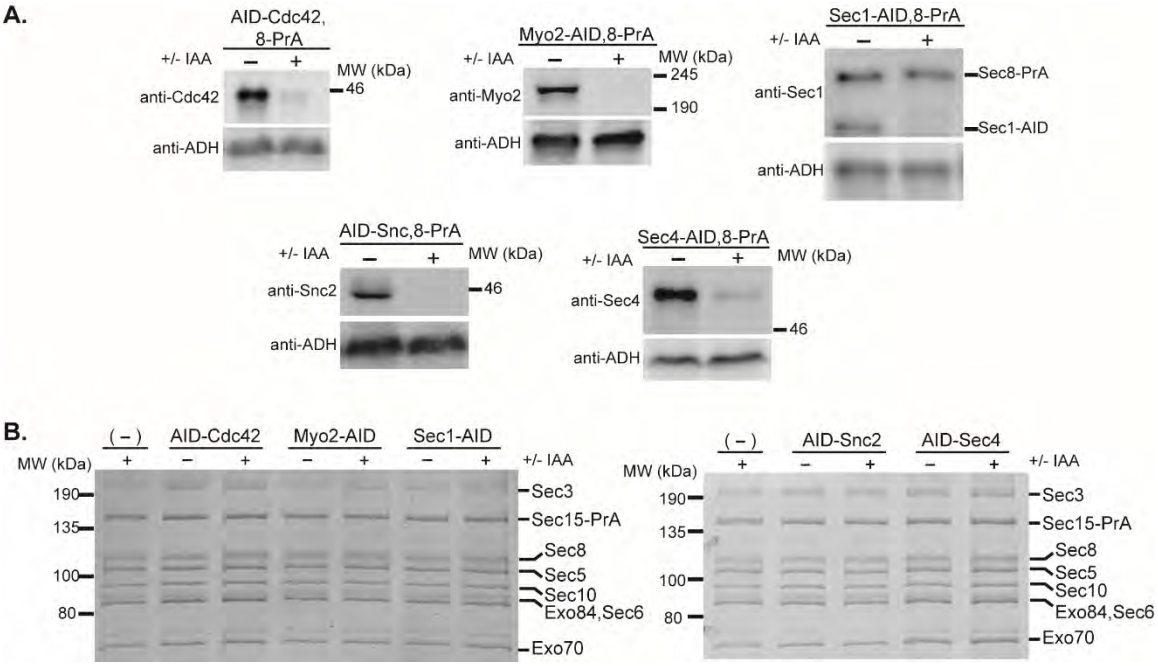

Figure 2.14 Depletion of known exocyst binding partners does not affect the assembly of exocyst complex. (a) Exocyst binding partners Cdc42, Myo2, Sec1, Snc2 (in *snc1*Δ strain background), and Sec4 were AID-tagged in strains with Sec8-PrA and constitutively expressing OsTIR1. (–) denotes untreated and (+) treated with IAA for 60 minutes. Western blots demonstrate degradation of these proteins from yeast lysate using antibodies specific to the AID-tagged protein of interest. In the Sec1 blot, the Sec1 antibody also reacts with the PrA tag on Sec8-PrA. (b) Exocyst complexes were purified using Sec8-PrA as the purification handle from untreated (–) versus IAA-treated (+) yeast lysates.

2.14). For each of the proteins tested, we observed that the exocyst complexes were fully assembled, stoichiometric, and could be recovered with the same yield. This indicates that none of these components are required for driving or stabilizing the assembly of exocyst complexes. Together with the preceding observations that the exocyst subunits copurify in stoichiometric complexes, these data support a model where the exocyst functions predominantly in a fully assembled state in actively growing cells, even under conditions where vesicles are not being transported and the exocyst is not interacting with its partners.

Visualization of exocyst structure by electron microscopy

Our new purification method for the yeast exocyst complex allowed us to obtain pure complexes for structural studies. We purified both Sec15-GFP and wild type complexes and analyzed them using negative stain EM. Raw micrographs revealed distinct particles (Fig. 2.15a) with an ellipsoid structure, approximately 25 nm in length (Fig. 2.15a). Iterative rounds of unsupervised 2D classification and class averaging revealed multiple coherent views of the exocyst complex resolved between 17 – 25 Å resolution (Fig. 2.15b,c, Fig. 2.16). However, this averaging failed to reveal a unique density attributable to GFP, precluding identification of Sec15's location within the structure. At this resolution, the orientations and overall architecture of the exocyst were indistinguishable between these biologically and technically independent datasets (Fig. 2.15c and Fig. 2.16). No apparent density or class averages were observed for smaller particles, such as subcomplexes.

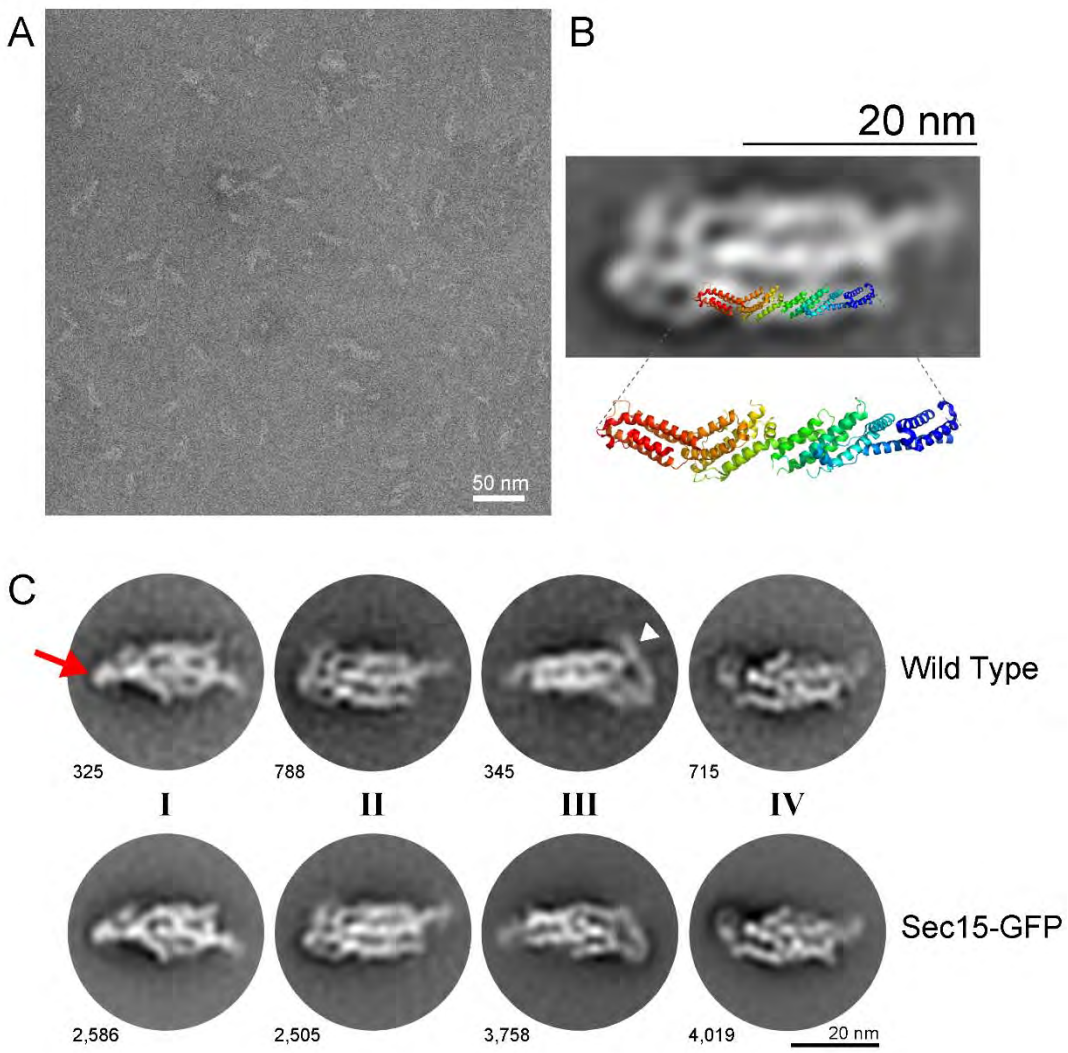

Figure 2.15 Negative stain electron microscopy of purified exocyst complexes. (a) A representative transmission electron micrograph of Sec15-GFP exocyst complexes after negative staining in uranyl acetate. Scale bar is 50 nm. (b) Representative 2D class average (Sec15-GFP) is shown, overlaid with a ribbon diagram of the structure of yeast Exo70 (residues 67-623), PDB ID 2B1E (Dong et al., 2005). The orientation and position of Exo70 were arbitrarily chosen to illustrate the similarities in the length and width of the "legs" of the complex and Exo70. (c) Highly populated 2D class averages generated by unsupervised classification for both wild type and Sec15-GFP image datasets, the number of particles per class is indicated next to each 2D average. Four apparent "faces" of the complex are labeled as I-IV. The red arrow points to the more "compact" end of the complex in class I, while the white arrowhead points to the more "open" flexible end in class III. Scale bar is 20 nm.

The 2D class averages resolve into roughly four distinct views of the complex (Fig. 2.15c and Fig. 2.16), which may represent four "faces" of the complex as it interacts with the EM grid. One end of the structure (left side of each of the 2D images; arrow)

appears to be more tightly packed and ordered than the other end, which appears to be more flexible, often containing a long looping leg wrapping around the end (right side; arrowhead). Two of the faces of the complex (I and II) appear wider and contain three to four "legs" or columns of density packed together, whereas the two slightly narrower faces (III and IV) appear to have only two to three legs each. We speculate that the more tightly packed end of the long axis of the complex may be comprised of many of the N-terminal ends of exocyst subunits, as they generally have not been amenable to biochemical studies in isolation (Croteau et al., 2009). The C-terminal ends, therefore,

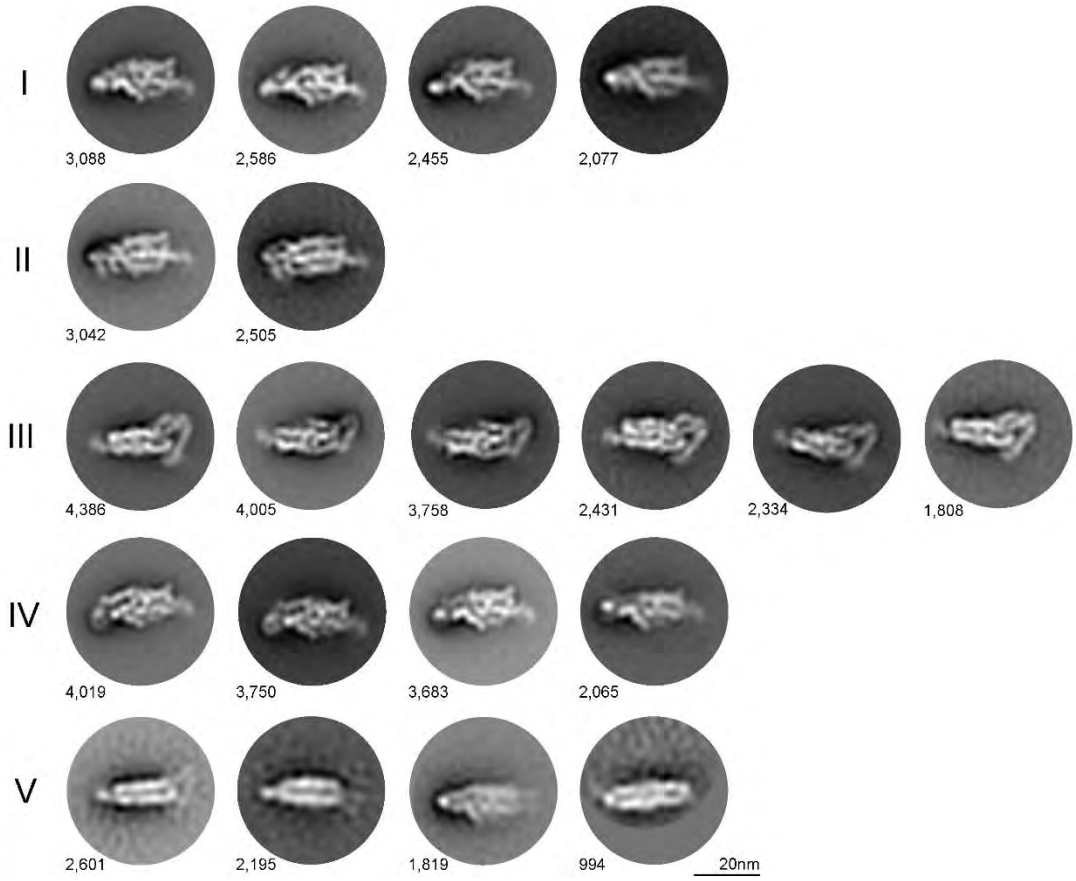

Figure 2.16 The complete class gallery of the Sec15-GFP tagged exocyst complexes. Class averages with similar orientations are shown in the same row. Each row starts with the most populated class and ends with the least populated class. The number of particles per class is shown near the lower left corners. Although the last row is labeled V as a different class from the others, we cannot rule out that these 2D averages belong to class III and the flexible ends were averaged out. Classes I-IV are equivalent to the numbered classes shown in Figure 2.15c.

would be present in the more flexible, “open” end of the structure; these regions contain many of the regions involved in binding GTPases and the plasma membrane (Wu et al., 2010; He et al., 2007; Wu et al., 2005; Dong et al., 2005). The exception is Sec3, whose membrane-interaction domain is located at its N-terminal end (Baek et al., 2010; Yamashita et al., 2010), and may therefore lie at the flexible open end of the exocyst (arrowhead), in an opposite orientation to the others.

Each of the individual legs observed in the 2D class averages of the exocyst complex are ~3 nm wide. Although the N- and C-terminal ends of the subunits cannot be unambiguously identified at this resolution, we can estimate the length of the legs in the range of ~15-35 nm, with the additional long leg at the flexible end ~25 nm longer than the others. The width and lengths of the legs are consistent with the crystal structure of nearly full-length yeast Exo70 (residues 67-623), which is ~16 nm long and ~3-3.5 nm wide (Dong et al., 2005), as shown in Fig. 2.15b, in which the crystal structure of Exo70 is superimposed onto an arbitrarily chosen leg. Exo70 is the smallest exocyst subunit (71 kDa), the others range from 84 kDa to 155 kDa. The large size of Sec3 (155 kDa, estimated extended helical bundle length of ~38 nm) also suggests that it may be the subunit that wraps around the end of the complex (Fig. 2.15c, arrowhead). The other available crystal structures (Exo84CT, Sec6CT and Sec15CT) also revealed similar CATCHR family helical bundles that are ~3 nm wide; the other subunits are predicted to have similar folds (Croteau et al., 2009; Wu et al., 2005; Dong et al., 2005; Hamburger et al., 2006; Sivaram et al., 2006). The subunits of the complex appear to lie in a roughly parallel arrangement to each other, as suggested by previous interaction studies (Munson

and Novick, 2006; Dong et al., 2005; Sivaram et al., 2006). Our interpretation of the 2D averages suggests that this structure represents a fully assembled complex with an estimated volume of ~1800-2200 nm^3. Using the volume and molecular weight of the structure of Exo70, and the assumption that all the subunits have roughly similar helical bundle structures, we calculate a comparable volume of ~1900 nm^3 for the octameric complex. Therefore, we suggest that our structure contains all eight subunits, consistent with the biochemical and AID experiments. Furthermore, we speculate that the wider faces containing 3-4 legs represent the two distinct modules identified in our AID studies, with one module as the top face, and the other as the bottom face. However, we cannot rule out that the 2D averages could actually be showing the same face in alternative conformations; higher resolution data will therefore be necessary to resolve these models.

Experimental procedures

Yeast methods. The strains used in this study are listed in Appendix table 5.1. Standard methods were used for yeast media and genetic manipulations. Cells were grown in YPD medium containing 1% Bacto-yeast extract (Fisher Scientific), 2% Bacto-peptone (Fisher Scientific), and 2% glucose (Sigma Aldrich). All protein-A (PrA) tags were integrated at the genomic loci in haploid yeast strains (BY4741 or BY4742) by integration of linear PCR products. PrA products were amplified from a plasmid (pProtAHIS5, Rout lab Rockefeller) encoding a PreScission Protease (PPX) site upstream of the PrA tag and a *S. pombe HIS5* selection marker (Oeffinger et al., 2007). Approximately 60 bp of homology to the 3' end of the coding sequence and 60 bp of homology to the 3' flanking sequence were used for homologous recombination. All exocyst PrA tags were added at the C-

terminal ends. AID tags (IAA17) and linker were amplified from BYP6740 (pMK43, Yeast Genome Resource Center (YGRC), Japan). For C-terminal AID tag strains, tags were added at the genomic locus of the strain BY25598 (YGRC), which expresses OsTIR1 under the ADH1 promoter (parent w303-1a), using linear PCR products and *kanMX* selection. N-terminal AID tags (*SNC2*, *SEC4*, and *CDC42* only) were integrated at the genomic locus of BY4742 using the pRS306 integrating plasmid (Sikorski and Hieter, 1989). Inserts were amplified by overlap extension of PCR products to generate a product consisting of ~300bp of 5' regulatory element, AID tag, linker, and homology to 5' end of the gene of interest, and this was then inserted into pRS306 using NotI and XhoI restriction sites. The plasmids were linearized using restriction enzymes specific to the 5' regulatory elements of each gene (*SNC2*: MluI, *SEC4*: BsrGI, *CDC42*: HpaI) prior to yeast transformation. For the AID-Snc2 strain, *SNC1* was deleted by replacing the genomic locus with the *kanMX* cassette. Finally, for all N-terminal AID tag strains, the OsTIR1 gene was integrated at the *MET15* locus using a *URA3* marker and *ADH1* promoter. The plasmid BYP6744 (pNHK53, YGRC) was used as template for generating the OsTIR1 PCR product and homology to the *MET15* regulatory elements was added to the ends. For serial dilution growth assays, yeast were grown in YPD to OD 1.5 and serially diluted 10-fold across YPD plates or YPD plates containing indicated concentrations of Indole-3-acetic acid, IAA (VWR). Yeast plates were incubated at 30°C for 2 days before imaging on Fujifilm LAS3000 (GE).

Exocyst protein-A purification. 2 liters of yeast cells were grown in YPD at 30°C to an OD of 1.3-1.5. Cells were washed with water, extruded through a syringe as frozen noodles into liquid nitrogen, and stored at -80°C until ready to be lysed (Oeffinger et al., 2007). Noodles were lysed in a 50 ml stainless steel Komfort jar with stainless steel ball bearings pre-chilled in liquid nitrogen using a PM100 machine (Retsch). The resulting yeast powder was stored at -80°C. 150 mg of yeast powder was added to 1.5 ml microfuge tubes prechilled in liquid nitrogen. 600 µl of resuspension buffer (50 mM Hepes pH 7.4, 150 mM NaCl unless noted otherwise in the text, with 1X cOmplete Mini EDTA-free protease inhibitor solution (Roche Life Science) was added to the tube (buffer composition dependent upon experiment and noted in the relevant figure) then vortexed and pipetted briefly to resuspend completely. Spheroplasting and bead beating lysis were performed as previously described[7] using 50 mM Hepes pH 7.4, 300 mM KCl lysis buffer. The use of NaCl versus KCl had no effect on exocyst preparations. Tubes were spun at 14,000xg for 10 minutes at 4°C and the supernatant is added to 5 µl home-made Rabbit IgG-magnetic bead slurry (Hakhverdyan et al., 2015; Oeffinger et al., 2007). Binding was done for 45 minutes at 4°C on nutating platform. The beads were washed in resuspension buffer and eluted in either 1X SDS loading buffer or by 1 h treatment with PreScission Protease (GE Healthcare) at 4°C for a native elution. Samples were run on SDS-PAGE and stained with Coomassie Blue or Krypton fluorescent protein stain (Thermo Fisher Scientific). Western blot analyses were performed using rabbit polyclonal antibodies to Sec6, Sec8, Sec10, Exo70, and Exo84 (Morgera et al., 2012; Songer and Munson, 2009). Rabbit polyclonal antibodies to Sec3, Sec15, and Sec5 and

mouse monoclonal antibodies to Cdc42 and Sec4 were gifts from P. Brennwald (University of North Carolina Chapel Hill). Rabbit polyclonal antibodies to Sec1 and Snc were gifts from C. Carr (Texas A&M University). Goat polyclonal antibody to Myo2 was a gift from L. Weisman (University of Michigan). Rabbit polyclonal antibody to ADH was purchased from Abcam (Catalog number ab20994). Mouse monoclonal antibody to GFP was purchased from Clontech (Catalog number 632380). Western blot analyses of exocyst protein levels in input versus unbound samples showed that ~60% of exocyst complexes are bound to the beads (varies slightly by bead preparation). The IgG beads are saturated in these experiments, however, as the exocyst complexes remaining in the lysates can be pulled down by sequential bead incubations. Krypton staining of the resulting gels showed no differences in stoichiometry in sequential pull-downs of either Sec5-PrA or Sec15-PrA (Appendix 5.1). Coomassie-stained gels were imaged on a LAS 4000 (GE Healthcare Life Sciences) and Krypton gels were imaged on a Typhoon FLA9000 (GE Healthcare Life Sciences). Western blots were treated with ECL and imaged on a LAS 4000.

Auxin-induced degradation of exocyst subunits and exocyst regulators. 2L of yeast cells were grown in YPD at 30°C to an OD of 1.0. Indole-3-acetic acid, or IAA, (VWR) dissolved in 100% ethanol at 500 mM was added to yeast cultures for a final concentration of 0.7 mM. The cells were allowed to grow in IAA for 45 min (with 15 minutes for post-processing) at 30°C until reaching an OD of about 1.5. The cells were then washed with water, harvested as frozen noodles, and lysed as described in

purification method. NaOH/SDS lysis was used for visualizing IAA-induced degradation in yeast lysates for Fig 2.6 and 2.7. Briefly, 2.5 OD units of yeast were incubated in 100 mM NaOH for 5 minutes, centrifuged to remove the NaOH, resuspended in SDS loading buffer with DTT, and heated at 95°C before loading onto gel for SDS-PAGE and Western blot.

Bgl2 Secretion Assay. AID strains were grown at 30°C in YPD and treated for 1 hour with 0.7 mM IAA before harvesting. Bgl2 secretion assays were performed as previously described (Adamo et al., 1999). Internal Bgl2 levels were quantified by western blots and normalized to internal ADH levels. All strains were normalized relative to internal Bgl2 levels of the appropriate untreated, wild-type strain control.

Thin-section Electron Microscopy. EM on wild-type and AID-tagged yeast strains was performed as described (Perkins et al., 2007). Briefly, yeast were grown in YPD at 30 °C and treated with 0.7 mM IAA for 1 hr. 10 OD units were harvested, fixed for 1 h at room temperature with 3% gluteraldehyde, 2.5% sucrose, 5 mM $CaCl_2$, 5 mM MgCl in 0.1 M sodium cacodylate, pH 7.4. Cells were spheroplasted using buffer containing 10% β-glucuronidase and 0.5 mg/ml zymolyase for 30 min at 30 °C, washed in 0.1 M cacodylate/1 M sorbitol, resuspended in 0.1 M sodium cacodylate, pH 6.8/1 M sorbitol, and embedded in 2% agarose. Agarose pieces were stained with 1% OsO_4, 1% potassium ferrocyanide in 0.1 M sodium cacodylate, pH 6.8 for 30 min, then washed completely and stained in 1% thiocarbohydrazide for 5 min at rt. After washing completely, samples

were treated for 5 min with 1% OsO_4/1% potassium ferrocyanide and washed again. After ethanol dehydration and embedding in Epon resin (Electron Microscopy Science), thin sections were cut at 70 nm and added to uncoated copper grids. Grids were post-stained with uranyl acetate and lead citrate. Samples were viewed on a Philips CM10 at 80kV and recorded using a Gatan Erlangshen 785 CCD Digital Camera.

Negative Stain Electron Microscopy and Image Analysis. Sec15-PrA and Sec15-GFP,Sec6-PrA complexes were purified in 20mM PIPES at pH 6.8 and 300mM KCl. The complexes were released from IgG beads after PPX cleavage to produce purified wild-type and Sec15-GFP complexes. Those complexes were absorbed to glow discharged carbon-coated copper grids and stained with 1% uranyl acetate. Micrographs of wild-type complex were collected on FEI Tecnai F20 electron microscope operated at 200kV and 20,400x nominal magnification. The defocus value ranged from 0.5 to 2.0 μm. Images were collected with a Gatan K2 summit direct detector with final pixel size 2.45 Angstroms. We semi-automatically picked 67,509 Sec15-GFP particles and 24,891 wild type particles, and gray-scale normalized with Relion-1.3 (Scheres et al., 2012). Micrographs of Sec15-GFP complex were collected on FEI Titan Krios electron microscope operated at 300kV and 29,000x nominal magnification. The defocus value ranged from 0.5-3.0 μm. Images were collected automatically using EPU (FEI) with final pixel size 2.87 Angstroms. Particles were selected manually and gray-scaled normalized with BOXER as implemented in EMAN2 (Ludtke et al., 1999). For the Sec15-GFP dataset, there were: 2,568 unique micrographs; 67,509 particles picked; and 60,751

particles survived. For the untagged wild-type dataset, there were 298 unique micrographs; 24,891 particles picked; and 17,420 particles survived. Contrast Transfer Function (CTF) estimation was performed with CTFFIND3 (Mindell et al., 2003). CTF-correction, two-dimensional classification and averaging were performed via Maximum A Posteriori refinement as implemented in RELION (Scheres et al., 2012).

CHAPTER III: A single molecule fluorescence microscopy assay to study vesicle tethering by the exocyst complex

Significant background and experimental rationale:

Tethers are one class of factors required for the proper delivery of vesicles to their target intracellular compartment. Upon vesicle arrival at the appropriate destination, tethering factors are proposed to physically capture vesicles at a distance through physical interactions with protein and/or lipid factors on the vesicle and target membranes. This activity is proposed to serve as the first vesicle recognition step but may also serve to promote SNARE-mediated fusion either by increasing v-SNARE proximity to the target membrane or by actively promoting SNARE complex assembly.

The group of molecules called tethers is subdivided into two major classes: the long coiled coil proteins and the multisubunit tethering complexes (MTCs) (Yu and Hughson, 2010). As previously described (Chapter I), there is experimental evidence for vesicle tethering by the coiled coil proteins and their extended structures seem ideally suited to this role. A recent study elegantly demonstrated using atomic force microscopy that one TGN coiled coil tether, GCC185, can extend as far as 145 nm from the Golgi and capture vesicles with a splayed, N-terminal end. After vesicle capture, this tether uses its hinge domain to collapse into the Golgi and bring vesicles closer to the TGN membrane (Cheung et al., 2015). Furthermore, recent *in vivo*, microscopy experiments suggest that a number of the coiled coil tethers each possess an intrinsic ability to recognize a specific class of vesicles, though the protein or lipid requirements for this recognition remain to be determined (Wong and Munro, 2014).

In the case of the MTCs, very little direct evidence exists to support their classification as vesicle tethers beyond inferences from *in vivo* genetic and cell biological

experiments. In exocyst temperature-sensitive mutants or AID strains, vesicle accumulation is observed (Novick and Schekman, 1980 and Fig. 2.12). However, it is not clear whether the vesicles accumulate due to the loss of tethering function or rather some other more direct role in vesicle fusion with the SNAREs. A recent study in yeast showed that re-directing exocyst complexes to the mitochondria results in re-targeting of Sec4-vesicles as well (Luo et al., 2014). However, since these experiments are performed *in vivo,* in the presence of many trafficking factors, it is difficult to determine if exocyst is directly functioning as a tether or recruiting other factors to the mitochondria to perform this role.

Given its classification as a tethering complex, it is necessary to experimentally determine whether the octameric exocyst complex is capable of vesicle tethering. Although we know that most of the subunits are required to maintain complex assembly, components that interact with both vesicular and plasma membrane factors exist within both 4-subunit modules. In the Sec3-Sec5-Sec6-Sec8 module, Sec6 interacts with the v-SNARE Snc (Shen et al., 2013) and Sec3 with plasma membrane Rho GTPases and $PI(4,5)P_2$ (Baek et al., 2010; Yamashita et al., 2010; Zhang et al., 2008). The other module containing Sec15-Sec10-Exo70-Exo84 interacts with the vesicular Rab GTPase Sec4 (Guo et al., 1999a), the Sec4 GEF Sec2 (Medkova et al., 2006), and Myo2 through Sec15 (Jin et al., 2011); Exo70 binds plasma membrane Rho GTPases and $PI(4,5)P_2$ (Wu et al., 2008; Wu et al., 2010; He et al., 2007). It is unknown whether the combined contributions of these subunits or modules are required for stable vesicle capture. It is important to determine which exocyst subunits, secretory vesicle proteins, and potentially

other accessory cytosolic factors are required for vesicle capture to occur. The optimal way to definitively determine these requirements is to develop an *in vitro* assay that is capable of monitoring vesicle tethering events. In this way, vesicle tethering can be reconstituted using a defined set of factors.

Exocyst, like other putative tethers, is thought to weakly or transiently associate with secretory vesicles in order to release a vesicle for SNARE-mediated fusion and to free exocyst for the next tethering event. Transient protein-protein interactions are prevalent in membrane trafficking pathways and others including the Cdc42 and Rho GTPase signaling pathways (Nooren and Thornton, 2003). In the case of vesicle trafficking, a long sequence of regulators hands off vesicles at each stage of the pathway until a vesicle is fused at its destination, thus weak or transient interactions are not unexpected. However, such interactions are challenging to study by traditional immunoprecipitation or pull-down approaches where weak partners may fall apart during preparation or the copy number of interacting complexes are too low for detection (Jain and Ha, 2012).

In vitro single molecule fluorescent imaging methods present a number of advantages that can overcome these challenges (Aggarwal and Ha, 2014). In this approach, which will be discussed in more detail below, one can effectively perform a pull-down assay with a bait protein immobilized on a microscope slide and watch the binding of prey proteins in real time. If the fluorescent background signal of the prey-sample solution is sufficiently low, washing out this sample is not required and transient events can be monitored as they occur, rather than requiring numerous steps before

detection. Even if the number of events is not high, all the individual binding events occurring on the slide surface are detectable, as opposed to western blot of pull-down assays, for example, where a minimal signal is required for detection. Other advantages include the small amount of required input material, the ability to determine complex stoichiometry, and the ability to quantify the kinetics and heterogeneity of events in a population that are normally averaged out in ensemble experiments.

We are developing the first *in vitro* tethering assay for the exocyst using colocalization single molecule spectroscopy (CoSMoS) (Friedman et al., 2006; Hoskins et al., 2011). In this assay, we attach fluorescently-labeled exocyst complexes to a glass slide and monitor the capture of fluorescent, endogenous secretory vesicles by colocalization on a single molecule, multi-wavelength TIRF microscope. Using the AID system and mutants in exocyst subunits or their interacting partners, we will determine the required factors for vesicle tethering. This assay will also allow us to characterize the kinetics of tethering and potential conformational changes of the exocyst complex during tethering events in real time. The insights gained from this approach and our architectural studies will also provide a foundation for understanding the enigmatic mechanism of vesicle tethering by related multi-subunit complexes that are specific to other vesicle trafficking pathways.

Premise of the assay:

Colocalization single molecule spectroscopy (CoSMoS) is a multi-wavelength single molecule fluorescence microscopy method developed by the laboratory of Jeff Gelles at Brandeis University (Friedman et al., 2006). This method has been used with

great success to visualize the activity and dynamic assembly/disassembly of macromolecular complexes by monitoring the colocalization of single, fluorescently labeled molecules on a total internal reflection fluorescence (TIRF) microscope. In this technique, a biotinylated, fluorescent bait-molecule is attached to a polyethylene glycol (PEG)/Biotin-PEG passivated glass microscope slide through a streptavidin-biotin sandwich. A solution containing a fluorescent prey-molecule (supplied by purified sample or cellular extract) is flowed in and binding (colocalization) with the bait molecule is monitored in real time. TIRF imaging only excites fluorescent molecules very close to the slide interface (approximately 100 nm), making it possible to use cellular extracts, which normally contribute a substantial level of background fluorescence (Crawford et al., 2008; Hoskins et al., 2011; Shcherbakova et al., 2013; Jain and Ha, 2012). Furthermore, one of the major advantages of the Gelles lab microscope design is the capability of monitoring three different colored fluorophores simultaneously so complex events can be monitored (Friedman et al., 2006; Hoskins et al., 2011).

In our version of this assay, we attach fluorescently-labeled exocyst complexes from yeast extract to the flow cell containing the Biotin-PEG/PEG surface. Depending on the immobilization method (to be discussed below), various controls are used to determine the specificity and identity of the immobilized particles, which appear as discrete, diffraction limited spots in the field of view. When the appropriate surface density of exocyst particles is achieved, the remaining extract is washed out of the flow cell. At this point, a solution containing fluorescently-labeled secretory vesicles is introduced to the flow cell and the colocalization of vesicles with exocyst spots can be

monitored in real time (Fig 3.1a). In future versions of this assay, we will take advantage of the 3-color detection system. Although we do not support a model where exocyst assembly occurs concurrently with tethering (Fig 3.1b), this experimental setup would allow this model to be tested. Furthermore, Förster resonance energy transfer (FRET), also known as fluorescence resonance energy transfer, can be used in combination with this method, to monitor putative conformational (Fig 3.1c) or assembly changes of exocyst in response to binding vesicles or other partners (Crawford et al., 2013; Ha, 2001).

First version of tethering assay:

Exocyst slide immobilization using antibodies:

Due to our success at purifying intact, functional, endogenous exocyst complexes from yeast extract using the IgG-Protein-A (PrA) approach (Chapter II), we decided to use this method for attaching exocyst complexes to slides. In order to do this, we also required biotinylated antibody for bridging the Biotin-PEG/streptavidin surface to the PrA-tagged exocyst complexes (Fig 3.2a). Since the rabbit antibody (Thermo Fisher Scientific 50177287) we use to generate the IgG-magnetic beads has an exceptionally tight affinity for the Protein-A tag (Richman et al., 1982; Oeffinger et al., 2007), this antibody was reacted with Sulfo-NHS-Biotin (Pierce) to generate biotinylated rabbit IgG (data not shown).

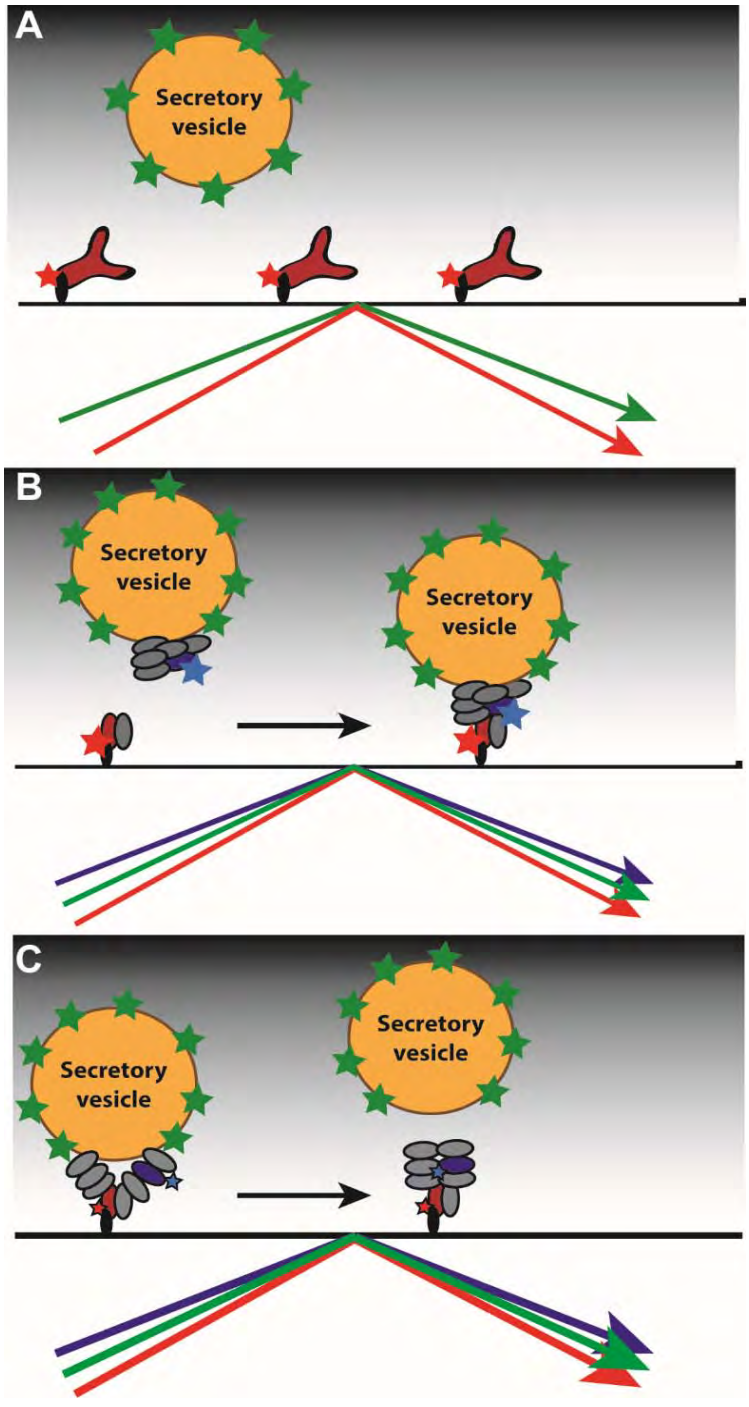

Figure 3.1 Schematics of CoSMoS assay for investigating vesicle tethering by exocyst complex. (**a**) 2-color vesicle tethering assay with fluorescent, immobilized exocyst complex and fluorescent, endogenous secretory vesicles. (**b**) 3-color experiment where putative exocyst subcomplexes are labeled with different colored fluorophores. The ordering of colocalization events can be monitored in real time. (**c**) Single molecule FRET to monitor exocyst conformational changes in concert with binding fluorescent vesicles (or other partners).

Fluorescent labeling of exocyst complexes:

The other requirement for the immobilized exocyst is that it be detectable with a fluorescent molecule. We decided to make use of genetically encoded SNAP-tags, which enable the incorporation of bright, photostable organic dyes into the subunits (Juillerat et al., 2005); these dyes avoid the poor photon output and blinking behavior of single fluorescent proteins (Dickson et al., 1997) (Fig 3.2b). The SNAP-tag is a 20 kDa mutant of the DNA repair protein O^6-alkylguanine-DNA alkyltransferase that reacts specifically and rapidly with benzylguanine (BG) derivatives leading to covalent labeling of the

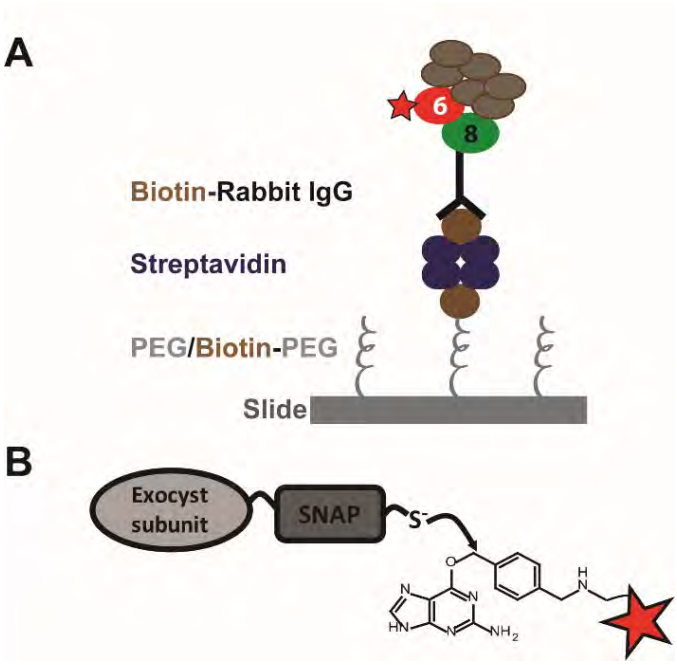

Figure 3.2 Schematic of exocyst immobilization and fluorescent visualization strategy. (**a**) Double-tagged exocyst complexes containing a SNAP-tagged subunit (red) and Protein-A-tagged subunit (PrA, green) are attached to PEG-biotin-streptavidin from yeast extract via biotinylated IgG. (**b**) C-terminal SNAP tag on exocyst subunit of interest is covalently labeled in yeast extract with a BG—conjugated organic dye (modified from Eric Anderson).

SNAP-tag with a synthetic substrate. The specificity of this reaction is sufficient that the SNAP-tagged protein of interest can be labeled in cell extract. Furthermore, we are making use of a more recently modified version of the SNAP tag called fast SNAP ($SNAP_f$ hereafter referred to as SNAP) with 10-fold faster labeling kinetics (Sun et al.,

2011). All exocyst subunits were functional with C-terminal SNAP tags, as none of the tagged proteins caused growth defects on YPD at the temperatures tested (Fig 3.3a)

Most of the exocyst subunit SNAP fusions were tested to determine which were least prone to proteolysis during the period of SNAP-tag labeling in yeast extract (prepared by cryogenic grinding lysis). Ultimately, Sec6-SNAP was decided upon for showing greater stability in extract both at room temperature and on ice, compared with other exocyst subunits (Fig 3.3b). DNA encoding the C-terminal SNAP tag was

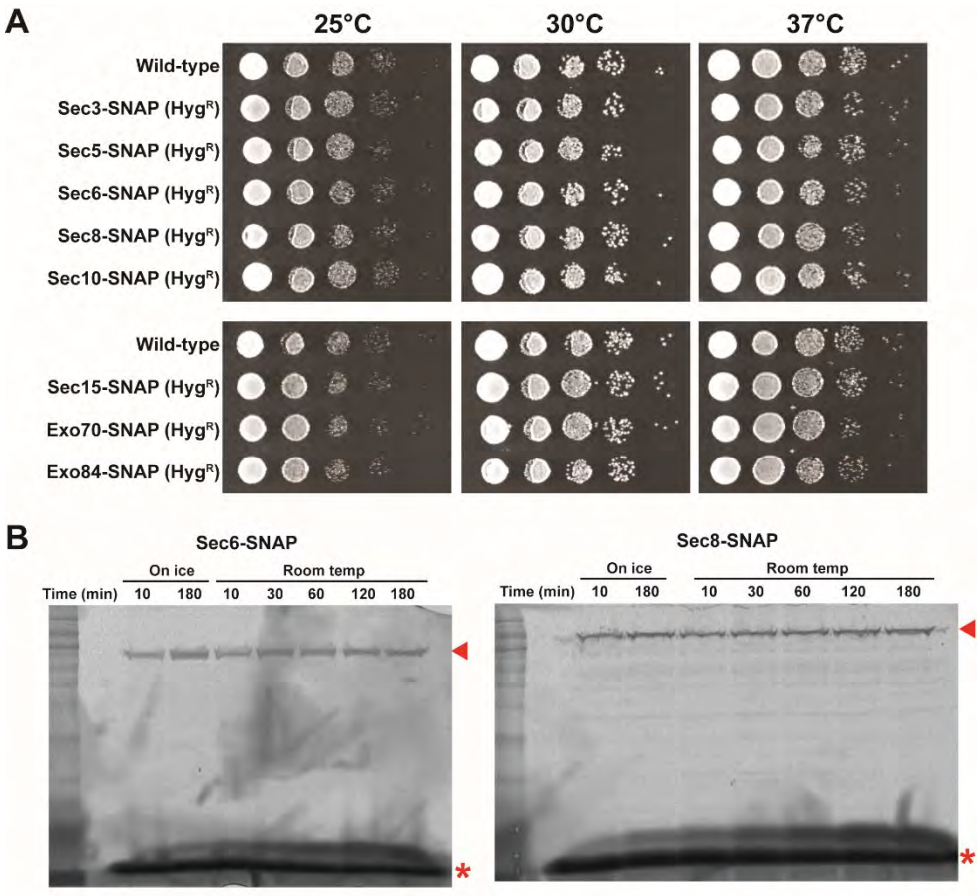

Figure 3.3 Use of the SNAP tag for labeling exocyst subunits. (**a**) Serial dilution growth assay on YPD plates confirm that all genomic, C-terminal exocyst SNAP-tag fusions are functional in yeast. (**b**) Extract labeling using BG-DY-649P1 was tested for all exocyst-SNAP strains (2 representative shown) and visualized by SDS-PAGE and Typhoon FLA9000 imaging. Red arrow=full-length protein, Red asterisks=unreacted dye substrate.

transformed and integrated at the genomic locus of Sec6 in a strain containing a C-terminal PrA tag on Sec8.

Although unreacted SNAP dye would primarily be washed out of the flow cell with unbound cell extract once exocyst complexes attach to the slide surface, unreacted dye does have some tendency for non-specific adsorption to the slide at high concentrations (≥50 nM) (Eric Anderson, unpublished data). In order to remove some of this residual dye substrate, labeled extracts were loaded on a NAP-5 buffer exchange column and fractions were collected from the column (Fig 3.4a). Although a substantial amount of unreacted dye remains, the total dye concentration in these fractions was sufficiently low to avoid concern for non-specific sticking (Fig 3.4b). Fractions 3 and 4 were used as

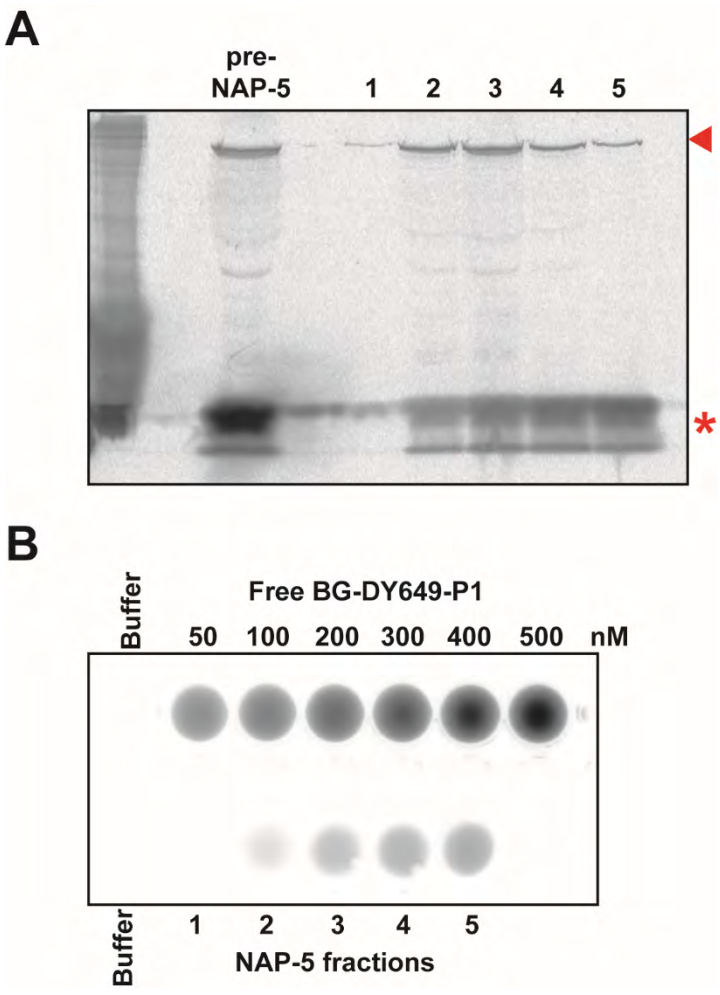

Figure 3.4 Use of NAP-5 desalting column to reduce unreacted substrate levels in labeled yeast extracts. (**a**) Samples of input (pre-NAP-5) and fractions from NAP-5 column run on SDS-PAGE and imaged on Typhoon FLA9000. Red arrow=full-length protein, Red asterisks=unreacted BG-DY649P1 substrate. (**b**) Total dye level in extract reduced to less than 50 nM. Plate reader assay on Typhoon FLA9000: top row=standard curve of BG-DY649P1 substrate, bottom row=labeled extract fractions from NAP-5 column.

the source of exocyst complexes for the slide surface in this first set of TIRF experiments described below.

Fluorescent secretory vesicles:

In order to maximize the functionality of the secretory vesicles used in the tethering assay, we opted to use endogenous post-Golgi vesicles purified from yeast extract rather than proteoliposomes. Endogenous vesicles will likely contain most of the functionally relevant lipid content and protein factors required for an optimal interaction with exocyst complexes. In future efforts, once the exocyst-vesicle interaction is better understood, we may be able to fully reconstitute tethering *in vitro* with liposomes.

Vesicle trafficking and fusion is normally a highly efficient process in eukaryotic cells. In a wild-type yeast cell, few vesicles can be seen in the cytosol by electron microscopy (Walworth and Novick, 1987). Therefore, in order to improve the yield of

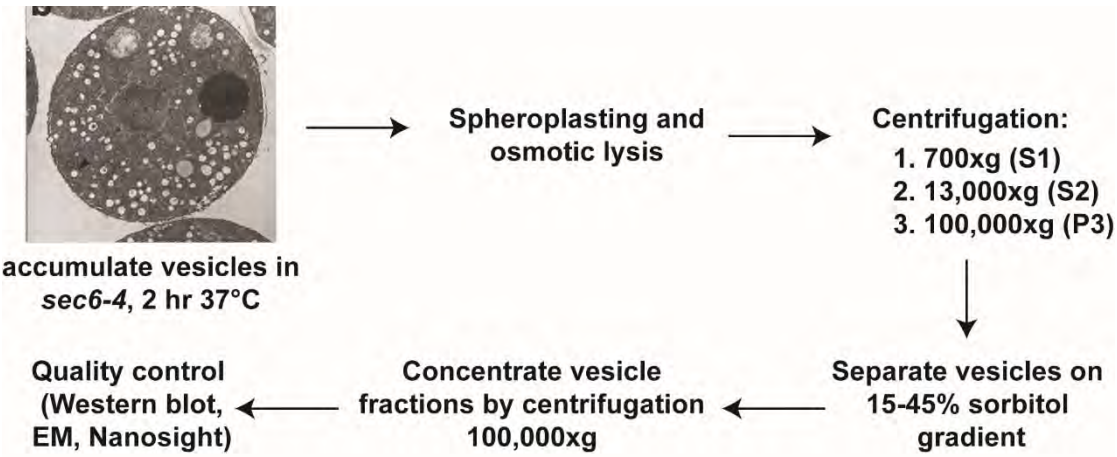

Figure 3.5 Purification scheme for post-Golgi vesicles. (S1) -- supernatant 1, (S2) -- supernatant 2, (P3) -- pellet 3. P3 is gently resuspended, layered onto sorbitol gradient, and centrifuged 71,000xg. Quality control involves western blotting for known vesicle marker proteins including membrane proteins (Snc, Sso, Sec4) and soluble cargo (Bgl2), negative stain electron microscopy (EM), Nanosight=Nanosight NTA single particle tracking and light scattering.

purified vesicles, temperature-sensitive post-Golgi secretory mutants are used to accumulate vesicles prior to purification. The purification scheme for secretory vesicles was modified from previous studies (Fig 3.5, Walworth and Novick, 1987; Forsmark et al., 2011; Rossi et al., 2015).

Several secretory mutants were tested: *sec6-4* (exocyst subunit), *sec9-7* (exocytic t-SNARE), and *sec9-4* and all resulted in sufficient vesicle yield for purification (Fig 3.6). In a previous proteomic study, *sec6-4* vesicles were analyzed by mass spectrometry for vesicle resident proteins and no exocyst subunits were detected, potentially because the exocyst is destabilized in this mutant or the exocyst interaction with vesicles is not stable enough to withstand the extensive vesicle purification protocol (Forsmark et al., 2011). Based upon this, we decided to move forward with *sec6-4* vesicles to ensure they were not pre-loaded with exocyst complexes that could inhibit the interaction with surface-immobilized complexes. However, even when vesicles were purified from mutants where the exocyst is not destabilized (*sec9-4* and *sec9-7*), exocyst subunits did

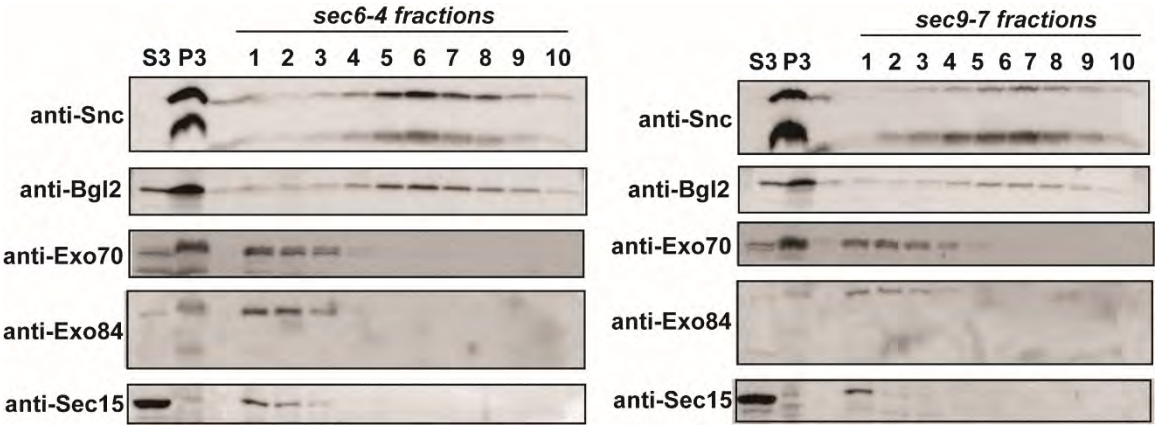

Figure 3.6 Purification of post-Golgi vesicles from different exocytic mutants. S3=supernatant 3, P3=pellet 3 (gradient input). Fractions (1-10) from top of sorbitol density gradient were western blotted for vesicle markers (v-SNARE, Snc, and cargo protein, Bgl2). Exocyst subunits (Exo70, Exo84, Sec15) did not co-migrate with vesicle markers in either mutant background, suggesting association with vesicles is not stable. Snc blots show both full-length (upper band) and proteolyzed Snc (lower band).

not co-purify with vesicle markers as detected by western blot, consistent with the idea that this interaction is lost during purification (Fig 3.6).

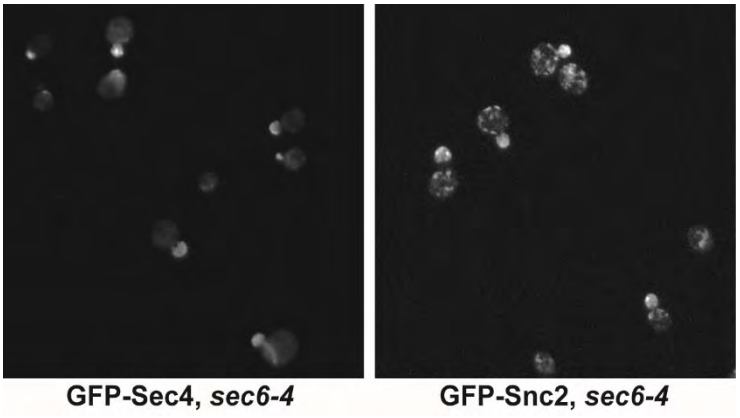

Figure 3.7 N-terminally GFP-tagged Sec4 and Snc2 localize to budding daughter cell in *sec6-4* strain background at permissive temperature (25°C). GFP tags were integrated at genomic locus with endogenous promoter.

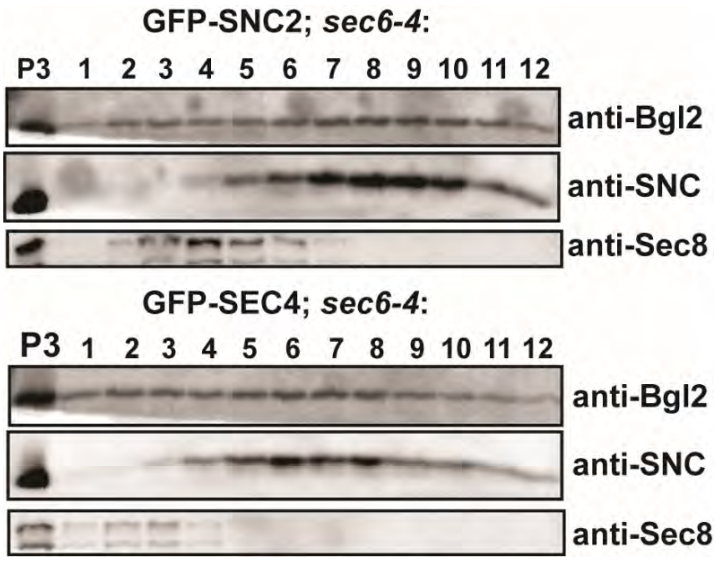

Figure 3.8 Purification of post-Golgi vesicles with GFP-tagged Snc2 or GFP-Sec4. Fractions (1-10 from the top) from sorbitol gradient were western blotted for vesicle markers (Snc and Bgl2) and Sec8. Molecular weight of Snc in top blots corresponds to GFP-tagged Snc.

We next sought a method for detecting purified secretory vesicles by TIRF microscopy. N-terminal GFP fusions of the Rab GTPase Sec4 and the vesicle SNARE Snc1/2 have been commonly used over the years as post-Golgi vesicle markers for microscopy (Donovan and Bretscher, 2012). We integrated N-terminal GFP tags at the genomic locus for Sec4 and Snc2 in the *sec6-4* strain background and the proteins localized properly to the budding daughter cell at the permissive temperature (Fig 3.7). GFP-tagged Snc2 co-migrated with vesicle marker proteins in density gradient fractions by western blotting, suggesting that the tagged protein is properly loaded into vesicles (Fig 3.8). The soluble vesicle cargo protein, Bgl2

(Adamo et al., 1999), co-migrated with the v-SNARE Snc suggesting these vesicles are intact. Negative stain electron microscopy and Nanosight NTA (single particle tracking/light scattering) confirmed the integrity and approximate 100-150 nm size of the post-Golgi vesicles (Fig 3.9).

Prior to testing the GFP-vesicles for capture by surface-immobilized exocyst

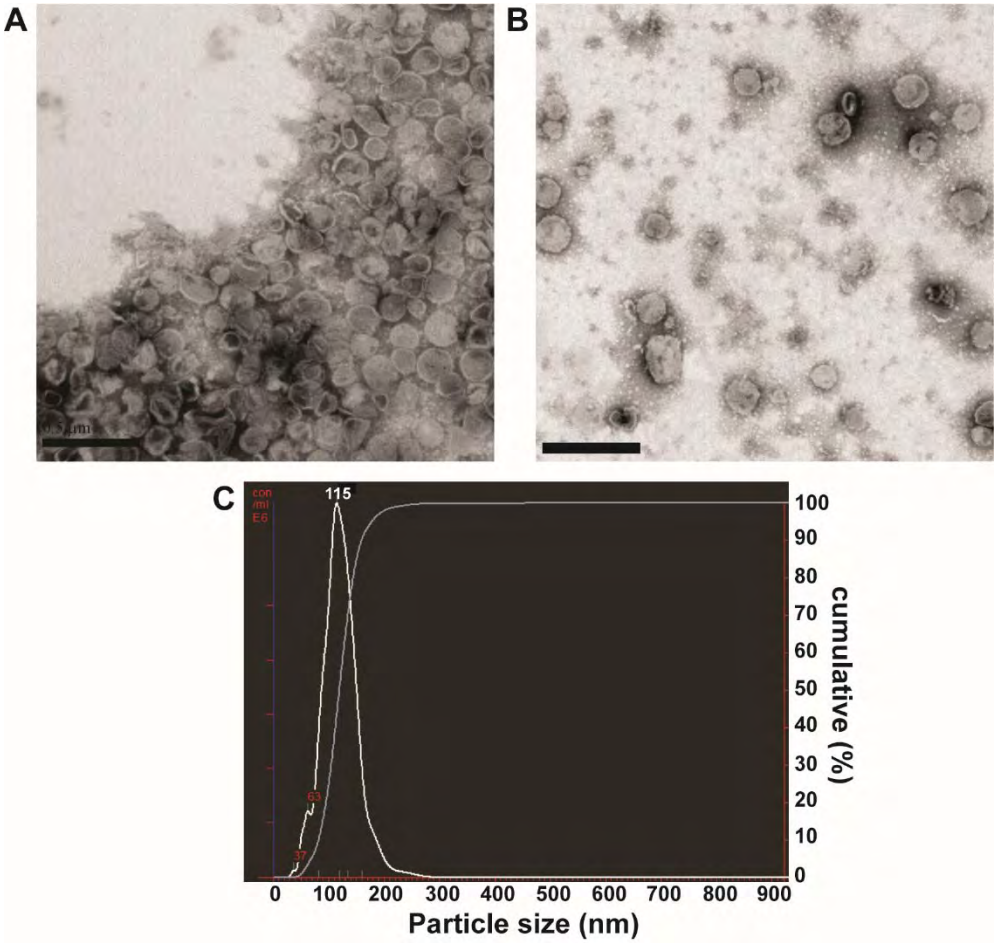

Figure 3.9 Purified GFP-Sec4, *sec6-4* vesicles are intact, homogenous, and properly sized. (**a**) Clustered negatively-stained purified vesicles imaged by transmission EM (TEM). Scale bar = 0.5 µm. (**b**) Spread out negatively-stained purified vesicles imaged by TEM. Scale bar = 0.5 µm. (**c**) Representative Nanosight NTA histogram for diameter of vesicle population. The population was homogenous and predominantly ~115 nm in diameter.

complexes, we evaluated the GFP-tagged vesicles on the TIRF microscope. Firstly, in order to detect the GFP-vesicles, we used a clean slide that was not coated in PEG in

order to stick vesicles to the slide surface, as the photostability of molecules in solution cannot be characterized by TIRF. Only the GFP-Sec4 vesicles were detectable in this experiment (not GFP-Snc2) (Fig 3.10). A buffer solution containing the glucose oxidase/catalase oxygen scavenging system (Crawford et al., 2008), was then added and the photostability of individual GFP-Sec4 vesicle spots was monitored over time (3.10b). This was compared to a second flow cell where the vesicle spots were incubated in buffer that lacked oxygen scavengers (Fig 3.10a). The total number of vesicle spots was counted in a single field of view from each flow cell and plotted versus frame number (with frame

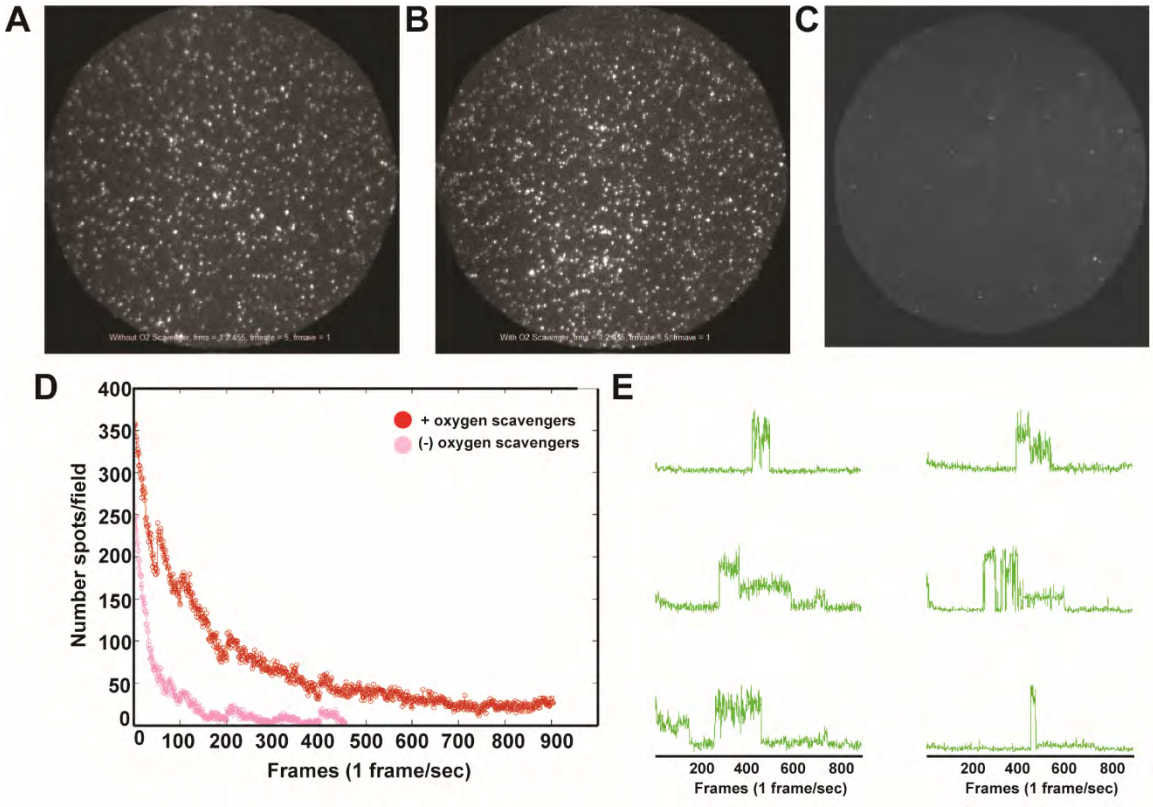

Figure 3.10 Evaluation of GFP-tagged vesicles for single molecule TIRF experiments. (**a**) GFP-Sec4 vesicles on clean slide surface in absence of oxygen scavenger system. (**b**) GFP-Sec4 vesicles on clean slide surfaces in presence of glucose oxidase/catalase oxygen scavenging system. (**c**) Few GFP-Sec4 vesicles stick non-specifically on PEG-passivated slide surface. (**d**) Total number of vesicle spots per field in (A, pink) versus (B, red) monitored over time for photobleaching. Acquisition rate=1 frame/s. (**e**) 6 representative fluorescence intensity traces (from >100) for single vesicle spots (from (B)) over time. Photobleaching steps and blinking behavior are apparent.

rate of 1 frame/sec) (Fig 3.10d). GFP-vesicles bleached in approximately 1 minute while oxygen scavengers prolonged the fluorescence for a few minutes longer. Over 100 vesicle spots were analyzed for fluorescence intensity over time. In the oxygen scavenger treated samples, many of these fluorescence traces revealed distinct photobleaching steps consistent with 2-3 GFP-Sec4 molecules per vesicle (Fig 3.10e). However, this is likely an underestimate due to the incomplete maturation of fluorescent proteins in the yeast cytosol (Iizuka et al., 2011; Ulbrich and Isacoff, 2007). The traces also revealed severe blinking properties for GFP-Sec4 molecules (Fig 3.10e). For stable interactions, blinking is not necessarily a significant limitation but for transient interactions, blinking events may be hard to distinguish from rapid binding and release events. Importantly, however, we confirmed that GFP-Sec4 vesicles did not non-specifically stick or accumulate on PEG-coated slides, which will be used for exocyst binding experiments (Fig 3.10c, and discussed below).

Fluorescent vesicle capture by immobilized exocyst complexes:

In order to test vesicle capture by immobilized exocyst, a number of control experiments were required. The slides and coverslips were cleaned by sonication in acid followed by 200 proof ethanol, passivated using PEG-Silane/Biotin-PEG-Silane, and stored at -80°C until ready for use (See experimental procedures). Just before beginning the experiment, vacuum grease was used to create 4 flow chambers. Streptavidin was added to each flow chamber one at a time when ready for use and washed out quickly before incubating with IgG-biotin. In all cases, when a field of view was being

monitored, the flow cell contained either buffer or purified vesicle solution, both containing oxygen scavengers. As tested previously, GFP-Sec4 vesicles were added to the first flow chamber and no non-specific accumulation of vesicles was observed in the green channel (no image acquired). In the second flow cell, streptavidin and IgG-biotin were once again added. After washing, undiluted yeast extract (Sec6-SNAP, Sec8-PrA labeled with BG-DY649P1) was added and, within 1 minute, a dense field of spots (carpet) was detected in the red channel (Fig 3.11a). In a third flow chamber, streptavidin was added but no IgG-biotin. The undiluted yeast extract was added to the slide. After several minutes, no spots accumulated in the red or green channels, suggesting that exocyst attachment to slides does require the antibody and no other fluorescent contaminants from the cell extract stuck to the slide surface (Fig 3.11b).

Although the carpet of exocyst in the second flow chamber was too dense for accurate colocalization experiments, we added undiluted GFP-Sec4 vesicles to determine whether the number of vesicle binding events was higher in the presence of exocyst (field (A)) than the absence (field (B)). Indeed, when 8 different fields of view were monitored, the number of green spots on the surface was always 4-6 times higher in the fields of view containing immobilized exocyst complexes (Fig 3.11c). It was also apparent that the GFP-vesicles bleached very rapidly in this experiment (Fig 3.11c). Although this result was promising, a number of questions arose. With the large number of exocyst particles on the surface, why were so few vesicle binding events observed? Are the vesicles or exocyst particles not fully functional? Is the orientation of the exocyst relative to the slide

surface obstructing vesicle binding sites? Are additional, soluble factors required to bridge this interaction?

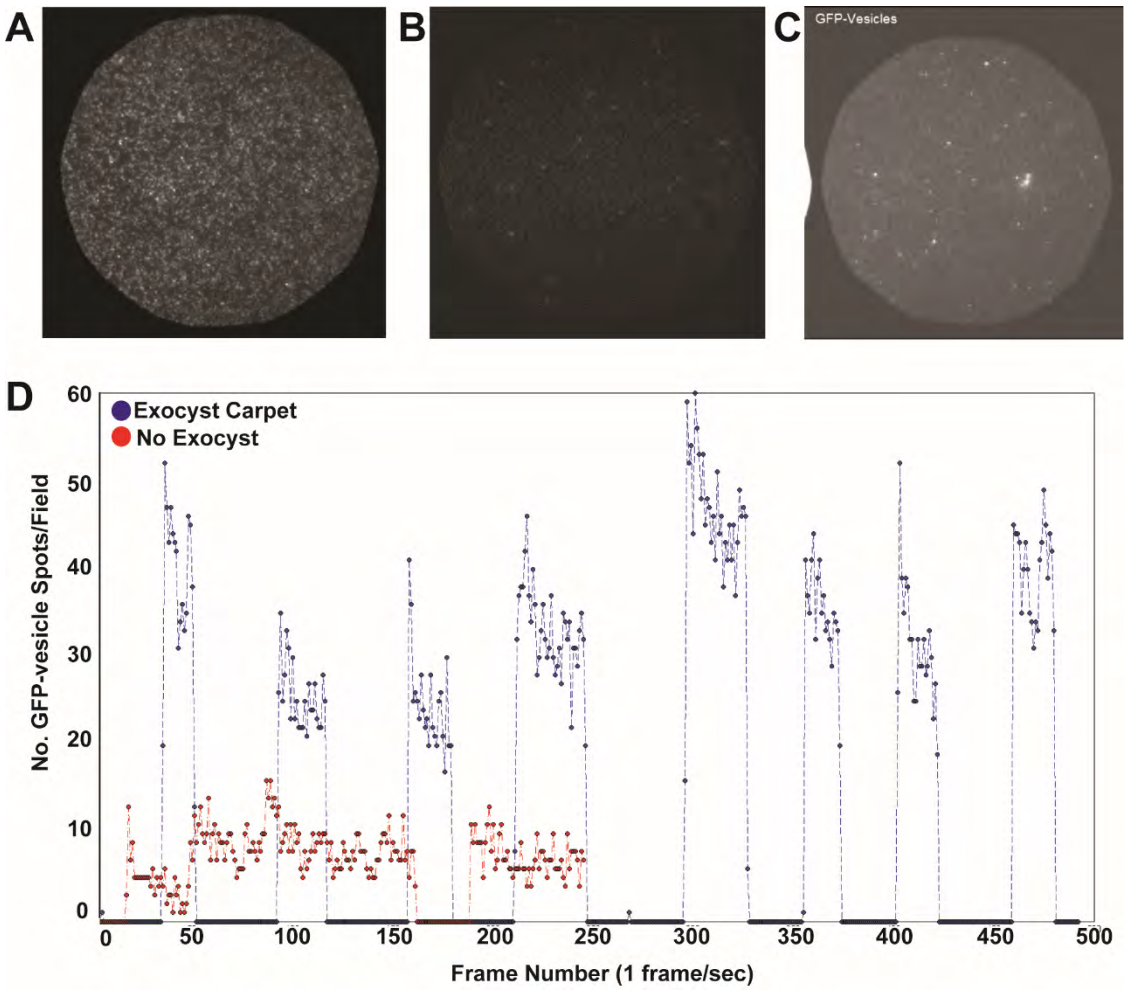

Figure 3.11 Protein-A exocyst and GFP-vesicle binding experiment by TIRFm. (**a**) Specific slide attachment of Sec8-PrA, Sec6-SNAP exocyst complexes from yeast extract using rabbit IgG-biotin. Sec6-SNAP is labeled with BG-DY649P1. The red channel is shown. (**b**) Sec8-PrA, Sec6-SNAP exocyst complexes did not attach to slides in the absence of IgG-biotin, indicating specificity of attachment. The red channel is shown. (**c**) Example field of captured GFP vesicles in green channel (frame 216). (**d**) GFP-Sec4 vesicles were added to fields A (exocyst carpet, blue) and B (no exocyst, red). Movies were acquired in the green channel (1 frame/sec) for approximately 20 seconds in 8 fields of view (exocyst carpet) and 2 fields of view (no exocyst). The total number of GFP-vesicles on the slide surface were quantified over 20 seconds. The gaps in the plot (e.g. between frame number 50 and 100) indicate moving to a new field of view and refocusing.

Ongoing optimization of tethering assay reagents

Sources of problems with exocyst complexes:

In addition to some of the concerns raised in the previous section regarding the functionality and orientation of surface-immobilized exocyst complexes, several other issues later became apparent. Firstly, in subsequent experiments, attachment of exocyst to slide surfaces using the PrA-IgG-Biotin approach proved to be unreliable. It was difficult to achieve a reproducible, sufficiently high level of exocyst spots on the slide surface and so an alternative attachment method was required. Secondly, despite using the cryogenic lysis method to generate exocyst extracts, which greatly reduces proteolysis during lysis, substantial proteolysis was still observed by western blot for some exocyst subunits in the SNAP-tagged extracts (Fig 3.12). This is likely due to the prolonged period of extract incubation required for SNAP tag labeling and dye removal. The assembly of the exocyst complex depends on the integrity of most of its subunits, so reducing this proteolysis is important for preserving structure and function. Ongoing efforts to optimize these different aspects of exocyst preparation will be discussed below.

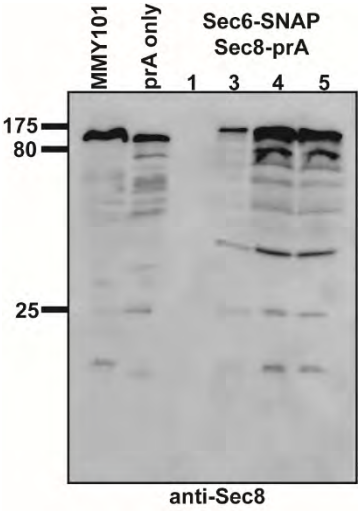

Figure 3.12 Proteolysis of exocyst subunit Sec8-PrA during SNAP-tag labeling and excess dye removal. Western blot for Sec8 revealed substantial proteolysis of Sec8-PrA in labeled, extract fractions from NAP-5 column (Fractions 1,3,4,5). Proteolysis is compared to untagged Sec8 in extract from strain expressing PrA-tag alone prepared by a similar method and to untagged Sec8 in MMY101 (Wild-type) lysate prepared by rapid NaOH/SDS lysis. No laddering is observed in NaOH/SDS sample indicating proteolysis occurs during the extended period of labeling and NAP-5 purification of extracts.

Optimization of exocyst immobilization method:

In order to improve the reproducibility of exocyst slide attachment, we next aimed to use the bifunctional SNAP substrate BG-PEG-Biotin-DY649 (Ivan Correa, New England Biolabs) as a means to both attach and visualize exocyst complexes on the slide surface (Fig 3.13). However, the major challenge with using this substrate is the need to remove the unreacted dye from yeast lysate since both unreacted dye and labeled, SNAP-tagged proteins will bind to streptavidin on the slide surface. The desalting columns used for the other SNAP substrates did not remove sufficient dye to make the bifunctional substrate useable.

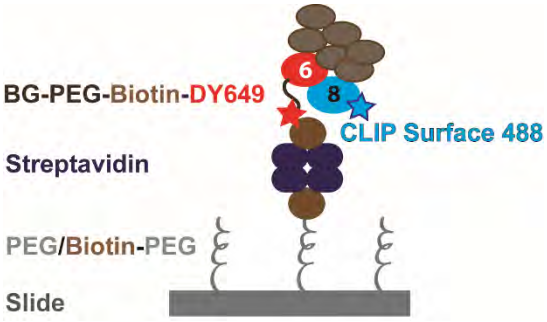

Figure 3.13 Slide attachment method using bifunctional SNAP substrate. Exocyst complexes with genomic $SNAP_f$ and $CLIP_f$ tags are immobilized from yeast extract and visualized using BG-PEG-Biotin-DY649. Complex assembly is confirmed by colocalization of DY649 and CLIP Surface 488.

The first approach tested for removing unreacted dye was to use our PrA/IgG purification approach. Sec6-SNAP, Sec8-PrA complexes were labeled with BG-PEG-Biotin-DY649 and then pulled out of yeast extract using Rabbit IgG magnetic beads. Although the double-tagged, labeled complexes were effectively pulled down, substantial proteolysis was apparent and complexes could not be efficiently eluted from the beads by PreScission Protease (PPX) digest (Fig 3.14).

Although the NAP-5 commercial desalting columns were not effective in removing unreacted BG-PEG-Biotin-DY649, we decided to test other gel filtration resins and columns. A number of gel filtration resins and column sizes were tested including

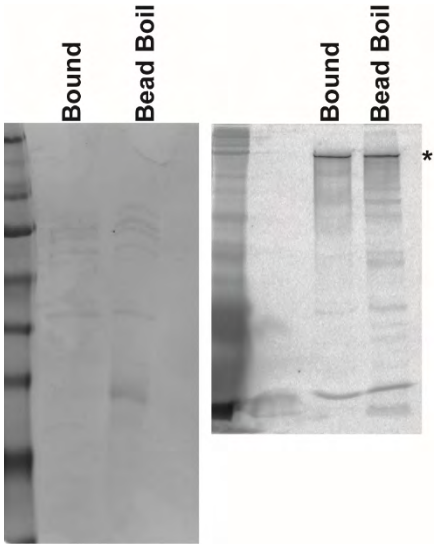

Figure 3.14 Purification of Sec8-PrA/Sec6-SNAP complexes labeled with BG-PEG-Biotin-DY649 to remove unreacted dye. Complexes were eluted from beads using PPX (Bound). Beads were boiled in SDS/DTT to elute remaining complexes. (Left) is Coomassie-stained SDS-PAGE and (right) is gel imaged on Typhoon, Alexa 647 fluor settings. 50% of each bound and bead boil loaded for each gel. Substantial proteolysis of Sec6-SNAP (marked *) is apparent (right).

GE Superdex 200 10/300, GE Superose 6 10/300, and a homemade Fine G-50 5/200 column. Only the Superose 6 column showed significant separation of labeled exocyst complexes from free dye when the fractions were run on SDS-PAGE and visualized on the Typhoon FLA9000 fluorescence reader. Increasing the salt concentration of the lysis buffer from 150 mM to 300 mM further reduced the level of unreacted dye that co-fractionated with exocyst complex on the Superose 6, presumably by disrupting weak, ionic interactions between the charged dye and other high molecular weight components in yeast extract. However, the level of free dye was still higher than that of labeled exocyst proteins by SDS-PAGE so additional steps were needed.

The most effective tool for removing the unreacted bifunctional substrate was using purified, recombinant $SNAP_f$ protein conjugated to agarose resin as a 'sponge'. Using the $SNAP_f$ resin alone greatly reduced the unreacted BG-PEG-Biotin-DY649 from yeast extract (Fig. 3.15, right gel, second lane). However, using a Superose 6 10/300 gel filtration column (GE) after $SNAP_f$ bead incubation resulted in labeled exocyst fractions with virtually no unreacted dye remaining. Exocyst-containing fractions were readily concentrated using 30 kDa molecular weight cutoff, centrifugal concentrators (Fig 3.15).

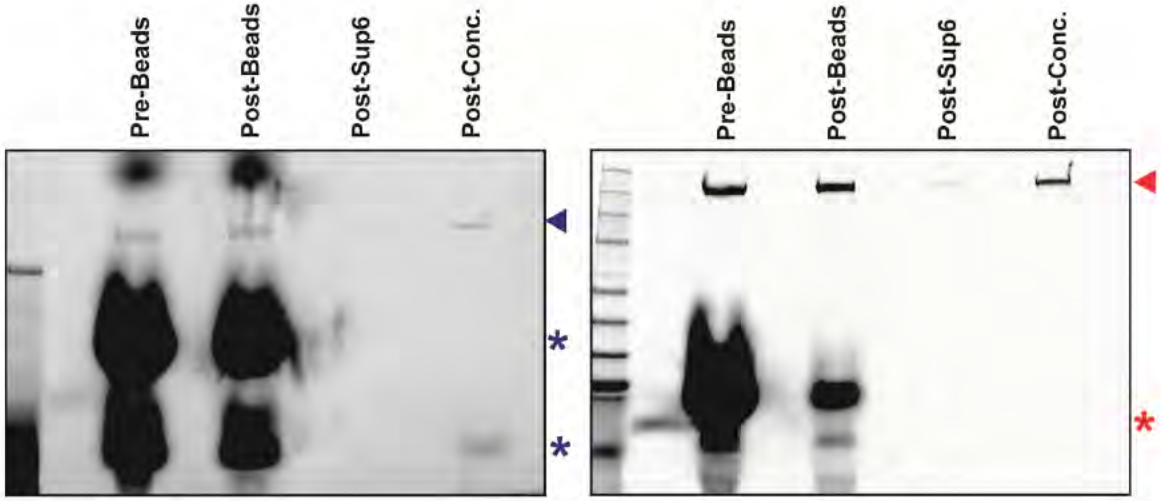

Figure 3.15 Stepwise method to remove unreacted SNAP and CLIP substrates. Sec3-SNAP, Sec10-CLIP was labeled with BG-PEG-Biotin-DY649 and CLIP Surface 488. The ratio of labeled protein to unreacted dye can be seen in the 'pre-beads' sample by SDS-PAGE imaged on Typhoon FLA9000. The extract was then incubated with SNAP resin (post-beads sample), loaded onto a Superose 6 10/300 column (post-Sup6), and then the exocyst-containing fractions were concentrated using 30 kDa molecular weight cutoff concentrators (Post-Conc.). Left panel is the gel imaged in the blue channel (blue arrow=labeled Sec10-CLIP, blue asterisks=free dye). Right panel is the gel imaged in the red channel (red arrow=labeled Sec3-SNAP, red asterisk=free dye).

Improving functionality of immobilized exocyst complexes:

During the course of these experiments, it became clear that using double-labeled exocyst complexes would be an ideal way to identify spots on the slide as exocyst as opposed to unreacted dye molecules. Furthermore, the presence of two labeled subunits would be a good readout for assembled exocyst. To this end, a number of strains were generated (Appendix Table 5.2) that contained a genomic SNAP tag on one exocyst subunit and genomic CLIP tag on another. CLIP tag is a point mutant of SNAP tag, which reacts specifically with Benzyl-cytosine (BC) substrates so these tags can be labeled orthogonally in yeast extract. The strains were generated in a protease-deficient strain background (MATa prc1-407 prb1-1122 pep4-3 leu2 trp1 ura3-52 gal2 (BJ2168)), which greatly reduced the proteolysis that occurred during extract labeling and dye removal, a factor that will likely favor assembled, functional exocyst complexes (Fig 2.1c).

Two considerations were important for making use of the CLIP tag. First, the kinetics of CLIP tag labeling are slower than that of SNAP tag (Ivan Correa, communication). Second, the SNAP tag reacts non-specifically at a low level with BC substrates (Eric Anderson, communication). To overcome this problem, SNAP labeling was done rapidly and to completion at room temperature followed by CLIP tag labeling on ice. Due to the protease-deficient strain background, performing labeling in sequence and at room temperature was not a problem and no cross-reactivity of the tags was detectable (Fig 3.16). Furthermore, the SNAP beads reacted at a low level with the unreacted CLIP substrate and the remainder was predominantly removed by Superose 6 gel filtration (Fig 3.15, left).

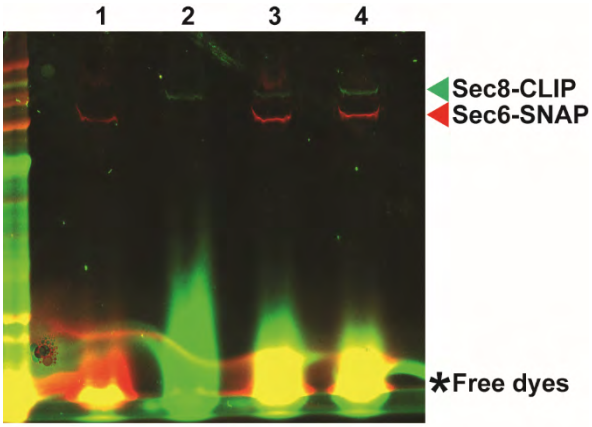

Figure 3.16 Orthogonal labeling of SNAP and CLIP tag in yeast extract. Extract samples were run on SDS-PAGE and imaged in red (for BG-PEG-Biotin-DY649) and green (for CLIP Surface 547) channels. Gel images were overlaid and pseudo-colored in Photoshop. (1) SNAP labeling to completion, (2) CLIP labeling to completion, (3,4) SNAP labeling followed by CLIP labeling. No reaction of SNAP tag with CLIP substrate was observed.

We next tested the attachment of Sec6-SNAP/Sec8-CLIP (labeled with BG-PEG-Biotin-DY649 and CLIP Surface 488) exocyst complexes on the TIRF microscope. In one lane, no streptavidin was added and undiluted labeled extract was flowed in. Very few spots were detected in both the red (3.17a, left) and blue channels (no image acquired). In a second lane, streptavidin was loaded before the undiluted exocyst samples and in this case a dense carpet of spots was detected in both the red and blue

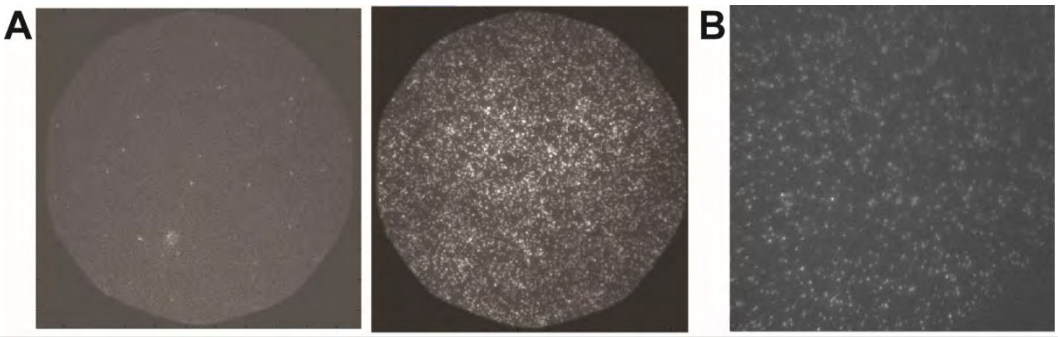

Figure 3.17 Specific attachment of SNAP-tagged exocyst complexes to slides using BG-PEG-Biotin-DY649. The yeast extract used (Sec6-SNAP, Sec8-CLIP) was also labeled with CLIP Surface 488. (**a**) Left: In the absence of streptavidin, no spots were observed in the red channel or blue (not shown). Right: In the presence of streptavidin, a carpet of spots was seen in both the red channel and the blue (not shown). (**b**) The number of exocyst spots on the surface can be fine-tuned by diluting the extract (10-fold here) and washing out extract when desired density was achieved. The red channel is shown.

channels (3.17a, right). The carpet was too dense to do accurate colocalization experiments, but given that the carpet was specific to lanes containing streptavidin and the signal was high in the blue channel as well, this is good indication that assembled exocyst complexes readily attached to the surface. In order to do vesicle binding experiments, the density of the exocyst on the slide surface must be optimized. In a recent experiment performed on the TIRF microscope at UMass, using a 10-fold dilution of exocyst sample did reduce the number of spots in the red channel, suggesting that sufficient dilution and rapid wash out will allow for fine-tuning of the surface density (Fig 3.17b).

Another variable to consider for these experiments is which exocyst subunits to tag as that will determine the face of the complex accessible for vesicle binding. In order to achieve different orientations of the exocyst complex relative to the slide, a number of different protease-deficient strains were made with different SNAP-tagged subunits. In these strains (Appendix Table 5.2), another subunit was CLIP-tagged. Our recent architectural studies informed the design of these strains in that we opted to fuse the two tags on subunits in different modules in order to avoid masking one module entirely (Fig

2.9, 2.11). Fig 3.15 shows one example of labeling these SNAP/CLIP double-tagged exocyst complexes in the protease-deficient yeast extract.

Sources of problems with fluorescent secretory vesicles:

The functionality of the purified vesicles depends on the integrity of vesicle resident proteins as well as the lipid composition. In order to maximize the potential for exocyst binding to vesicles, it is important to not disrupt any potential exocyst receptors. Although the required factors for exocyst binding vesicles are not known, Snc1/2 and Sec4 were previously shown to interact with Sec6 and Sec15 respectively (Shen et al., 2013; Guo et al., 1999a). Myo2, the vesicle transport motor protein in yeast, interacts with Sec15 (Jin et al., 2011). Western blot of purified vesicle fractions revealed substantial proteolysis of intrinsically disordered Snc1/2 during the course of the purification (Fig 3.6). Furthermore, GFP-Snc2 vesicles were not detectable by TIRF microscopy, which may be an outcome of the severe proteolysis. Myo2 does not co-migrate with vesicle markers suggesting that it is not stably associated with these vesicles (Fig 3.18). Finally, GFP-Sec4 vesicles, which were used in the preliminary vesicle binding experiments, are likely not fully functional due to the N-terminal GFP tag based on several lines of evidence. First, we

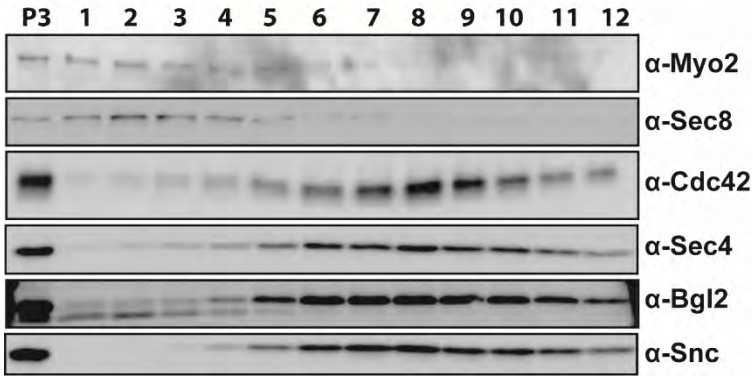

Figure 3.18 Myo2 does not stably associate with purified post-Golgi vesicles. Vesicle fractions from sorbitol gradient (1-12 from the top) were western blotted for Myo2, Sec8, and vesicle markers (Cdc42, Sec4, Bgl2, and Snc). P3=pellet of 100,000xg spin loaded onto gradient.

observed qualitatively that the GFP-Sec4, *sec6-4* strain grows more slowly than its *sec6-4* parent strain in liquid culture. Additionally, fusion of the smaller AID tag at the N-terminus of both Sec4 and Snc2 results in a severe vesicle accumulation phenotype (Fig. 2.12b,c) and strains expressing N-terminally SNAP-tagged of Sec4 are inviable (data not shown). In summary, in order to improve the function of these post-Golgi vesicles, it is preferable to tag proteins other than putative exocyst interacting partners and to reduce proteolysis during the purification as well.

Vesicle labeling with lipophilic dyes:

An alternative to protein tagging is to make use of lipophilic dyes. Many variations of such dyes exist, but they are often characterized by poor photon output and inconvenient excitation/emission properties for the established microscope setup (Jeff Gelles, communication). Consistent with this, the dye DilC12(3) was tested on *sec6-4* vesicles. Labeling with DilC12(3) was highly efficient and readily detectable by viewing the density gradient fractions on a fluorescence plate reader (Fig 3.19a). However, when tested on the TIRF microscope, spots and aggregates of dye or vesicles accumulated rapidly and non-specifically on PEG-passivated slides; these spots were also rapidly photobleached even in the presence of oxygen scavengers (Fig 3.19b,c). Another dye, FM4-64, efficiently labeled vesicles (Fig 3.20) and preliminary testing showed higher photostability for this dye. However, this dye has a large Stokes shift, which may not be compatible with multi-wavelength single molecule experiments.

Fluorescent labeling of vesicles using SNAP tagged vesicle proteins:

While optimizing the tagging of vesicle marker proteins, it was also prudent to switch from the GFP tag to the SNAP tag so that a bright, photostable dye could be used. SNAP-Cdc42 was tested in combination with *sec6-4*, as it is a known vesicle cargo protein and its interaction with exocyst is proposed to be required downstream of vesicle tethering

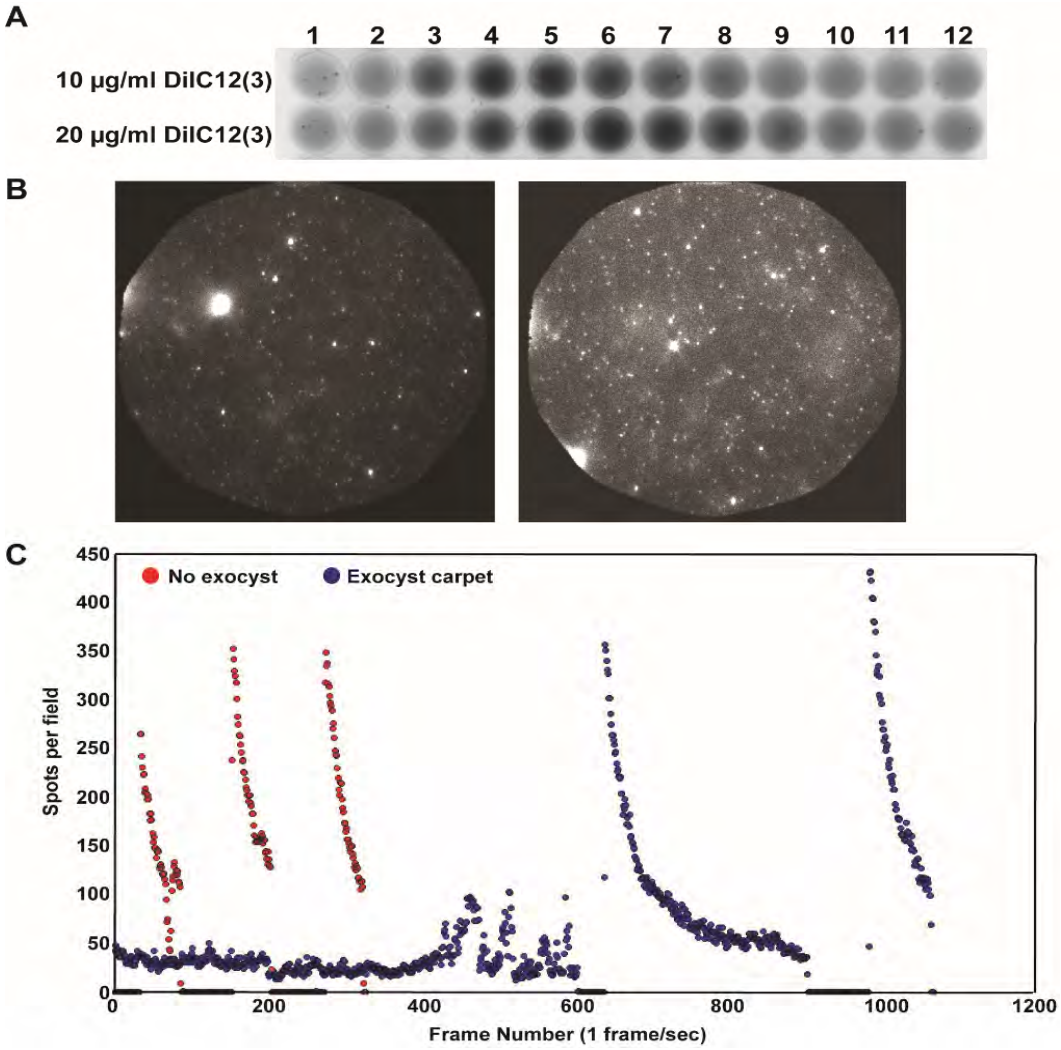

Figure 3.19 Fluorescent labeling of *sec6-4* vesicles using DilC12(3). (**a**) Vesicle fractions from sorbitol gradient (1-12 from the top) were imaged in the green channel on the Typhoon FLA9000 in a 96 well plate. Two different concentrations were tested for labeling. Signal corresponding to the dye co-migrated with vesicle-containing fractions. (**b**) (Left) Vesicle spots on surface in presence of exocyst carpet, (Right) vesicle spots on surface in absence of exocyst carpet. One representative field of view is shown for each. (**c**) Quantification of total number of vesicle spots on surface in presence (blue) or absence of exocyst carpet (red) over time for several fields of view (time gaps are due to moving to new field and re-focusing). Acquisition rate=1 frame/sec.

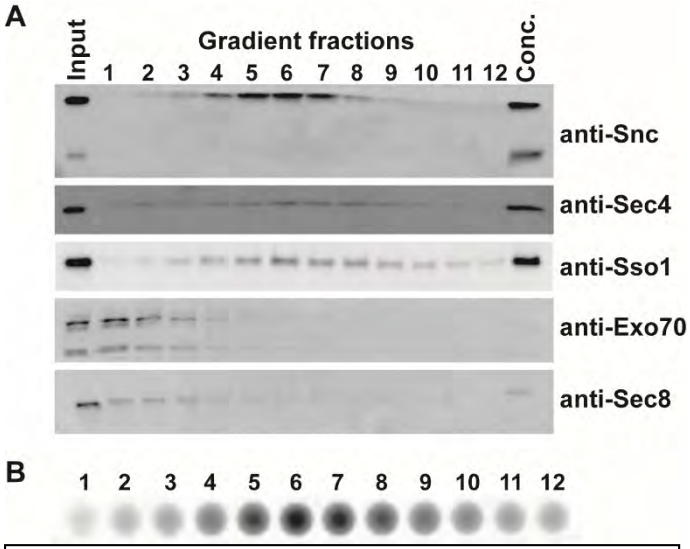

Figure 3.20 Purification of FM4-64-labeled vesicles. (**a**) Western blot of sorbitol gradient fractions (1-12 from the top), Input=100,000xg pellet loaded on gradient, Conc.=concentrated vesicle fractions. (**b**) Sorbitol gradient fractions imaged in 96 well plate on Typhoon FLA9000 in green channel. FM4-64 signal co-fractionates with vesicle markers (Snc, Sec4, Sso1).

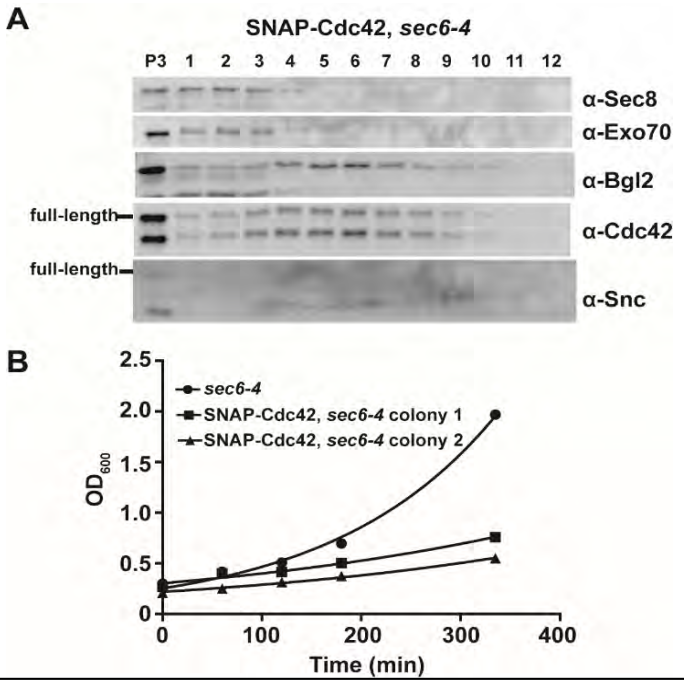

Figure 3.21 SNAP-tagged Cdc42 is proteolyzed during vesicle preparation. (**a**) Western blot of sorbitol gradient fractions (1-12 from top), P3=100,000xg pellet loaded on gradient. Cdc42 associates with vesicles but is substantially proteolyzed. (**b**) SNAP-Cdc42, *sec6-4* grew more slowly than its parent strain *sec6-4* in liquid culture at 25°C in YPD.

(Guo et al., 2001; Zhang et al., 2008; Hutagalung et al., 2009; Wu et al., 2010). However, labeled SNAP-Cdc42 was difficult to detect in purified vesicle fractions, was substantially degraded during purification (Fig. 3.21a), and the strain exhibited very slow growth in liquid culture (Fig. 3.21b). Consistent with this, previous reports using GFP-Cdc42 suggested that N-terminal tagging of this protein reduces its vesicle association (Watson et al., 2014). Alternatively, SNAP-Sso1 is another potential marker, as this plasma membrane SNARE is transported on vesicles as it is recycled and the exocyst is not known to interact with this SNARE on its own (Forsmark et al., 2011; Dubuke et al.,

2015). When SNAP-Sso1, *sec6-4* vesicles were labeled with SNAP-Surface 547 and purified, SNAP-Sso1 was detectable in the purified fractions by Western blot (Fig 3.22a)

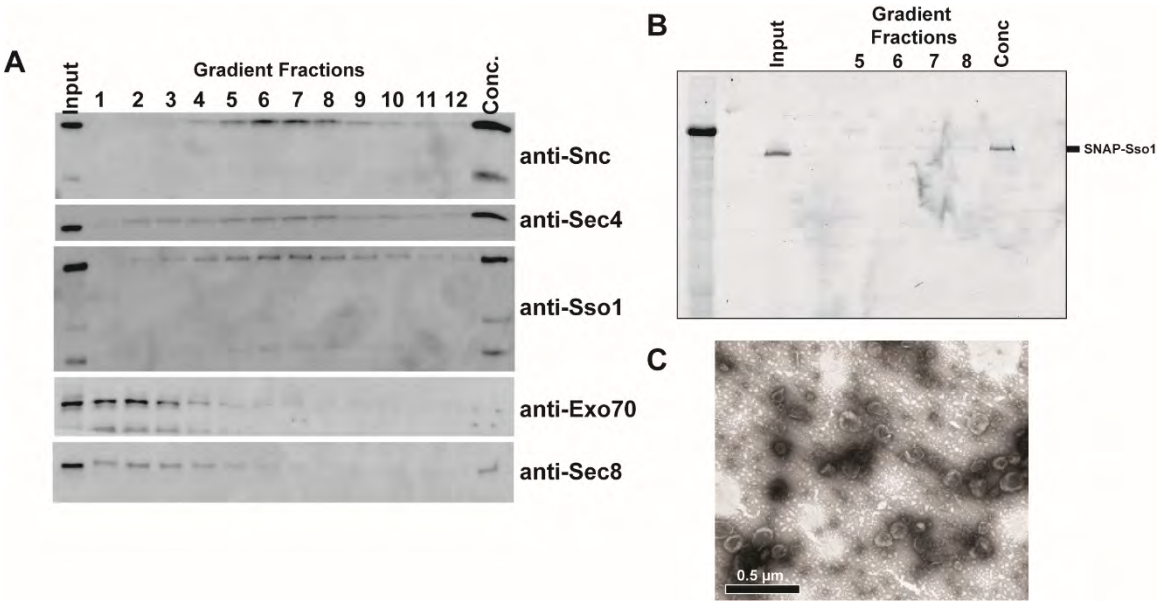

Figure 3.22 Purification of SNAP-Sso1, *sec6-4* vesicles labeled with SNAP-Surface 547 (**a**) Western blot of sorbitol gradient fractions (1-12 from top), input=100,000xg pellet loaded on gradient, Conc.=concentrated vesicle fractions. SNAP-Sso1 co-fractionates with other vesicle markers (Snc, Sec4). (**b**) Input, gradient fractions 5-8, and Conc. vesicle sample were run on SDS-PAGE and imaged on Typhoon FLA9000 in the green channel. Fluorescently-labeled SNAP-Sso1 is detectable. (**c**) Negative stain EM of purified, labeled SNAP-Sso1, *sec6-4* vesicles.

and Typhoon imaging (Fig 3.22b). Additionally these vesicles appeared to be of the correct size by negative stain EM (Fig 3.22c). Therefore, we will move forward with these vesicles for future single molecule TIRF experiments.

Optimization of vesicle purification method:

Lysis method is another variable that affects the integrity of the vesicle proteins. Established vesicle purification protocols use spheroplasting with the cell wall enzyme zymolyase (Walworth and Novick 1987; Forsmarck et al., 2011; Rossi et al., 2015). Spheroplasting is a relatively gentle lysis method that maintains the integrity of

membrane-bound organelles. However, it has long been known that commercially available zymolyase contains contaminating proteases, which may contribute to the significant proteolysis observed with the intrinsically disordered SNARE proteins. Cryogrinding lysis is a preferable method for reducing proteolysis, however, preliminary experiments suggest it may be too harsh for preserving vesicle integrity and other large membrane fragments contaminated the preparations as determined by Nanosight and negative stain EM. As an alternative, we expressed and generated recombinant oxalyticase enzyme in *E. coli* shock fluid as an alternative to zymolyase for spheroplasting. Oxalyticase lysed efficiently and a substantially higher level of full-length Snc, Sso1, and several exocyst subunits were recovered by this method (Fig 3.23).

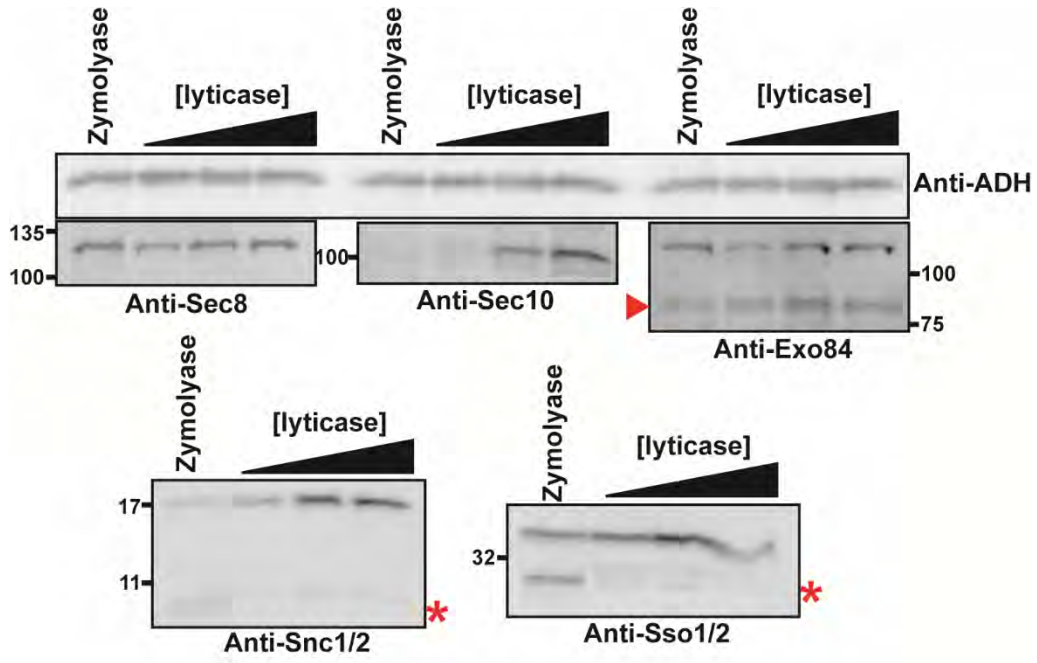

Figure 3.23 Yeast lysis with oxalyticase reduces proteolysis of SNAREs and some exocyst subunits. Yeast pellets of identical OD units were lysed either with zymolyase (0.5 mg/ml 20T) or increasing volume of lyticase shock fluid (100 µl, 500 µl, or 1 ml lyticase shock fluid per 30 ml spheroplasting buffer). Lysate samples were run on SDS-PAGE and imaged by Western blot. ADH was blotted as a total protein control and revealed that while lyticase did not substantially increase the lysis efficiency over zymolyase, it substantially improved the recovery of full-length Snc, Sso, and Sec10. The red arrowhead indicates Exo84 (the above band is due to nonspecific binding of the antibody). Red asterisks indicate SNARE degradation products.

Increasing the concentration of full-length vesicle proteins will improve the functionality of the vesicles and increase the number of fluorescent SNAP-Sso1 proteins per vesicle for better detection on the TIRF microscope.

Summary and next steps with the assay:

With these new reagents in hand, the next step is to test them on the TIRF microscope. SNAP-Sso1 vesicles labeled with SNAP-Surface 547 will be added to flow cells containing BG-PEG-Biotin-DY649-immobilized exocyst complexes with different orientations and different CLIP-488-labeled subunits. Minimizing proteolysis of both vesicular and exocyst components is likely to improve the functionality of all assay components. However, it remains to be seen whether vesicle capture depends upon additional soluble components lost during the purification, which could be supplied by yeast extract. Using the AID system or available temperature-sensitive mutants, we can eliminate vesicular and/or cytosolic components from yeast extract to determine the required factors for vesicle binding by exocyst. Additionally, we can generate exocyst subcomplexes using the exocyst AID strains, which would allow us to determine the minimal complex for stable vesicle binding. Using this single molecule approach, we have the capability of visualizing the kinetics and heterogeneity of vesicle binding events in real time. Furthermore, using the multi-wavelength capabilities of the Gelles' lab TIRF microscope, we can also monitor more complex events as well. An *in vitro* assay is necessary to definitively demonstrate the role of the exocyst complex as a vesicle tether during exocytosis and it is likely that a similar assay could be used to characterize this function with related MTCs.

Experimental procedures:

Yeast methods: The strains used in this study are listed in Appendix Table 5.2. Standard methods were used for yeast media and genetic manipulations. Cells were grown in YPD medium containing 1% Bacto-yeast extract (Fisher Scientific), 2% Bacto-peptone (Fisher Scientific), and 2% glucose (Sigma Aldrich). All protein-A (PrA) tags were integrated at the genomic loci in haploid yeast strains (BY4741 or BY4742) by integration of linear PCR products. PrA products were amplified from a plasmid (pProtAHIS5, Rout lab Rockefeller) encoding a PreScission Protease (PPX) site upstream of the PrA tag and a *S. pombe HIS5* selection marker (Oeffinger et al., 2007). Approximately 60 bp of homology to the 3' end of the coding sequence and 60 bp of homology to the 3' flanking sequence were used for homologous recombination. All exocyst PrA tags were added at the C-terminal ends. Linear PCR products of $SNAP_f$ and $CLIP_f$ tags, linker, and drug resistance marker were amplified from pFast-SNAP-Hyg^R and pFast-CLIP-Nat^R plasmids (Moore lab, UMass Medical School). Tags were integrated at the C-termini of exocyst subunits at the genomic locus in either the previously described PrA-tagged parent strains or protease-deficient yeast strains (BJ2168) using at least 55 bp of homology to the 3' end of the coding sequence and 55 bp of homology to the 3' flanking sequence. N-terminal GFP and SNAP tags were added to vesicle marker genes at the genomic locus of *sec6-4* (NY778, Novick et al., 1980) using the pRS306 integrating plasmid (Sikorski and Hieter, 1989). Inserts were amplified by overlap extension of PCR products to generate a product consisting of ~300-500 bp of 5' regulatory element, SNAP or GFP tag, linker, and homology to 5' end of the gene of interest, and this was then inserted into pRS306 using

NotI and XhoI restriction sites. The plasmids were linearized using a restriction enzyme specific to the 5' regulatory elements of each gene prior to yeast transformation.

SNAP and CLIP tag labeling in yeast extract: Yeast strains were grown at 30°C in YPD until OD_{600}=1.3, harvested in liquid nitrogen as frozen noodles, and lysed using cryogenic ball mill grinding (Retsch). For a single extract preparation, two tubes each with 200 mg of yeast extract powder were each resuspended in 450 µl of resuspension buffer (50 mM Hepes pH 7.4, 300 mM NaCl, 10% glycerol, 1 mM DTT, 1X cOmplete Mini EDTA-free protease inhibitor solution (Roche Life Science)) and resuspended by briefly vortexing and pipetting gently. Extracts were spun at 14,000xg for 15 minutes at 4°C and the supernatants were recovered. SNAP tag labeling was performed at room temperature, in the dark, for 20 minutes with 350 nM BG-substrate (either SNAP-Surface-549 (New England Biolabs S9112S) or BG-PEG-Biotin-DY649 (Ivan Correa, Material Transfer Agreement, New England Biolabs)). CLIP tag labeling was performed at room temperature, in the dark, for 30 minutes with 2 µM BC-substrate (either CLIP-Surface-547 (New England Biolabs S9233S) or CLIP-Surface-488 (New England Biolabs S9232S)). Labeled extracts were spun at 45,000 rpm for 40 min at 4°C in TLA100.4 ultracentrifuge rotor. The supernatant was recovered and added to pre-washed $SNAP_f$ agarose beads (approximately 100 µl bead volume) and incubated on ice under foil for 20 min and then in dark at room temperature for 30 minutes. Mix beads by pipetting (do not nutate to avoid beads on side of tube that could later be loaded on gel filtration column). Spin tubes in Galaxy mini centrifuge, inject 400 µl lysate supernatant

onto Superose 6 10/300 column (GE), and elute in same buffer as used for resuspension. Collect 0.5 ml fractions, pool fractions previously determined to contain exocyst complexes, and concentrate using 0.5 ml, 30 kDa molecular weight cutoff centrifugal concentrators (Amicon Ultra). Freeze 25 µl concentrated extract samples in liquid nitrogen and store at -80°C in dark. Fluorescently labeled exocyst complex samples were visualized by SDS-PAGE and a Typhoon FLA9000 fluorescence reader (GE).

Purification of secretory vesicles: Vesicle accumulating yeast strains were grown at 25°C to OD=0.8-1.0 in YPD and then shifted to pre-warmed YPD at 37°C for 2 hours. Cells were pelleted (~2000 ODs per 50 ml conical), washed with ice cold yeast wash buffer (20 mM Tris pH 8, 20 mM sodium azide, 20 mM sodium fluoride), flash frozen in liquid nitrogen, and stored at -80°C. A conical tube with 2000 ODs of yeast pellet was spheroplasted with buffer containing 0.1 M Tris-HCl pH 7.5, 1.4M sorbitol (add fresh: 10 mM sodium azide, 1 mM DTT, 1.5 ml oxalyticase shock fluid (oxalyticase expression construct from C. Stroupe, Univ. of Virginia Medical School) or 0.5 mg/ml 20T Zymolyase (MP Biomedicals)) at 37°C, 90 rpm, for 30 min in shaking incubator. Spheroplasts were pelleted at 2000xg and then resuspended in lysis buffer (0.8 M sorbitol, 20 mM triethanolamine pH 7.4, add fresh: 2 cOmplete Mini EDTA-free tablets (Roche Life Science), 1 mM EDTA, 1 mM DTT, 1 mM PMSF). Samples were spun at 700xg at 4°C and supernatant (S1) was saved. S1 was spun at 13,000xg at 4°C in SS34 rotor for 20 min and supernatant (S2) was saved. Depending on the experiment, S2 was either subjected to a 30,000xg, 4°C, 15 min spin in a Ti50.2 ultracentrifuge rotor or not,

and then a 100,000xg, 4°C, 60 min spin in a Ti50.2 rotor to generate pellet 3 (P3). P3 was gently resuspended in 200 µl lysis buffer and, if SNAP tag labeling was being performed, 1 µM final concentration of SNAP-Surface-549 (New England Biolabs S9112S) was added for 30 min on ice under foil. If FM4-64 (Thermo Fisher Scientific T-3166) labeling was being performed, FM4-64 (from 1 mg/ml stock solution in DMSO) was added to a final concentration of 1 µg/ml before the 100,000xg spin. To obtain a homogeneous population of post-Golgi vesicles, the resuspended 100,000xg pellet was subjected to an 11 ml 15– 45% sorbitol (in 20 mM triethanolamine pH 7.2) velocity gradient and spun for 1 hour at 71,000xg, 4°C, with slow acceleration and no braking. Fractions were collected from the top and analyzed by fluorescent plate reader (Typhoon FLA9000) to identify vesicle fractions. Vesicle fractions were pooled based on plate reader (and previous western blot experiments) and spun at 100,000xg in TLA100.4 ultracentrifuge rotor for 40 min at 4°C to generate pellet 4 (P4). P4 was gently resuspended in a sufficient volume of lysis buffer for 10-fold concentration, aliquoted into 25 µl tubes, flash frozen in liquid nitrogen, and stored in the dark at -80°C. Vesicle fractions were blotted using the same antibodies described in Chapter II experimental methods with the addition of our rabbit polyclonal antibody to Sso1 and rabbit polyclonal antibody to Bgl2 (P. Brennwald, UNC Chapel Hill). Vesicle integrity was validated using negative stain EM with uranyl acetate (performed as described in Rossi et al., 2015 by Anne Mirza) and Nanosight NTA single particle tracking analysis.

Single molecule total internal reflection fluorescence (TIRF) microscopy experiments and analysis: The slides and the coverslips for flow chambers were acid cleaned in coplin jars by water bath sonication in a series of solutions: 1) 200 proof ethanol, 2) 1:1 HCl:methanol, 3) H_2SO_4, 4) distilled water, 5) 200 proof ethanol. The slides and coverslips were treated with polyethylene glycol (PEG)/biotin-PEG (200:1) (Crawford et al., 2008) and stored at -80°C. Flow cells were constructed using vacuum grease just before TIRF experiments. Experiments were performed using custom-made micromirror TIRF microscopes (Friedman et al., 2006) with modifications (Hoskins et al., 2011) and data collection was performed using LabView (National Institutes, Austin, TX). The microscope fields of view ranged between 314 mm and 3,250 mm. Flow cells were washed with buffer containing 0.1 mg/ml BSA. Streptavidin was added to slides at 0.01 mg/ml concentration for 20 seconds before wash out. 25 µl exocyst and vesicle samples were added to flow cells without dilution but with added glucose oxidase/catalase oxygen scavenging system reagents (Crawford et al., 2008). Movies were acquired at 1 frame per second continuously for the indicated length of time in Fig. 3.10, 3.11, and 3.21. Data analysis was performed by Eric Anderson (Moore lab, UMass Medical School) using custom programs implemented in MATLAB (The Mathworks) as previously described (Hoskins et al., 2011; Shcherbakova et al., 2013; Friedman and Gelles, 2015).

.

CHAPTER IV: Discussion

Scientific Questions

Despite nearly two decades of study, many questions still remain regarding exocyst structure and function, primarily due to the inability to purify intact exocyst complexes as well as the generic secretory phenotype exhibited by exocyst mutants. A better understanding of the subunit topology and architecture of the exocyst is critical to making mechanistic predictions regarding its function in vesicle tethering and SNARE complex regulation. In a number of other MTCs, such structural studies revealed the spatial separation of subunits involved in interacting with opposing membranes. We sought to develop an improved exocyst purification method for characterizing the complex biochemically and structurally, which would allow us to propose a model for how the eight exocyst subunits are positioned for vesicle capture. Furthermore, we aimed to use this purification approach to identify putative exocyst subcomplexes, determine whether or not the exocyst complex undergoes regulated assembly/disassembly *in vivo*, and identify which factors may be required for stabilizing or regulating the assembly of the exocyst in the cell.

Although classified as an MTC, the exocyst has not been experimentally shown to possess an intrinsic vesicle tethering function. Over the years, numerous binding partners have been identified, which are consistent with such a function but do not conclusively show that exocyst itself is capable of functioning as a tether. We aimed to design an *in vitro* vesicle tethering assay for the exocyst complex, which would allow us to definitively test the exocyst's capacity to capture secretory vesicles and to systematically test the requirements for tethering activity. By selective elimination of exocyst subunits,

we could identify the minimal complex required for stable vesicle capture. An *in vitro* system would allow us to dissect the other required factors including vesicle receptor proteins and potentially other soluble factors present in the cytoplasm. It is possible that some of these known partners will not be required for vesicle tethering *in vitro*, which will lead to further interesting questions regarding the requirement for these interactions in the cell. The development of such an assay for the exocyst complex will pave the way for similar assays that test the tethering function of other putative MTCs.

Major results and implications:

Subunit connectivity, assembly determinants, and architecture of the yeast exocyst complex

In this study we used biochemical, genetic, and structural methods to dissect the architecture of the yeast exocyst complex and examined mechanisms for its assembly and function. We purified endogenous, intact exocyst complexes from *S. cerevisiae* (Fig. 2.2) and our biochemical and structural characterization demonstrated an intrinsically stable, intact, octameric complex (Fig. 2.5 and Fig. 2.15). Our results using the AID system indicated that the presence of most of the exocyst subunits are critical to complex integrity and stability (Fig. 2.10 and Fig. 2.11). Degradation of 6 out of the 7 AID-tagged subunits tested, except Sec3, triggered complete separation of the exocyst into two modules (Fig. 2.10 and Fig. 2.11). Each of these modules (Sec3–5–6–8 and Sec10–15–Exo70–Exo84) is assembled by several critical pairwise interactions (3–5, 6–8, 10–15) with weaker contributions from 5–6, 70–84, 84–10, and 8–10 or 8–15 (Fig. 2.5 and 2.12); furthermore, the disassembly of one module does not affect the integrity of the other. Consistent with this, our negative stain EM 2D class averages demonstrate a stable, homogenous, octameric complex (Fig. 2.15 and Fig. 2.16). The assembly and stability of the exocyst structure is independent of the known binding partners Sec4, Snc1/2, Myo2, Sec1, and Cdc42 (Fig. 2.14). These components are not stable, stoichiometric partners of the exocyst complex, nor is their binding necessary to assemble or stabilize the exocyst complex during vesicle transport, tethering or fusion. We propose that the role of these interactions is to modulate the function, rather than the assembly, of the exocyst complex.

Our results do not support previous hypotheses that suggested a requirement for polarized vesicle transport in driving the assembly of a subcomplex of exocyst subunits (e.g. Sec15–10–5–6–8–Exo84) on vesicles with a subgroup (Sec3 and Exo70) serving as a "landmark" on the plasma membrane; assembly of these two subgroups would subsequently drive vesicle tethering (Boyd et al., 2004). Under physiological conditions, we do not detect any stable subcomplexes in our pulldowns. It is possible that we detect only stoichiometric complexes because uncomplexed subunits or unstable subcomplexes are degraded during the purification; however, our biochemical and AID experiments argue against this possibility, as we can easily purify individual subunits and subcomplexes from yeast lysate with equal yield to assembled complexes (Fig. 2.5, 2.10, 2.11). Furthermore, under conditions where we have disrupted vesicle transport, cell polarity, and exocyst binding to vesicles, no subcomplexes are detectable (Fig. 2.14). We cannot rule out the presence of either low levels of subcomplexes or free pools of exocyst subunits below our level of detection (<5-10%), however, the majority of the exocyst exists in the fully assembled state. On the other hand, subcomplexes appear to be present in mammalian cells: the components identified thus far (Exo84–Sec10 and Sec5–Sec6 in opposing groups) are consistent with the modules identified here (Moskalenko et al., 2003; Bodemann et al., 2011). Similarly, differences in subunit localization patterns in the growing hyphae of *Neurospora crassa,* in *Arabidopsis thaliana,* and in different *Drosophila melanogaster* tissues suggest putative subgroups of exocyst subunits (Riquelme et al., 2014; Fendrych et al., 2013; Murthy et al., 2005). Regulated assembly and disassembly of the exocyst in different organisms may be an important mechanism

by which the exocyst complex participates in a diverse array of processes in a variety of cell types.

Negative stain EM revealed, for the first time, the ellipsoid-shaped structure of the yeast exocyst complex, with its distinct helical bundle-shaped "legs" packed together (Fig. 2.15, 2.16). Overall, the yeast exocyst structure is roughly similar to those of the mammalian exocyst complexes previously imaged using rotary shadowing EM (Hsu et al., 1998). However, unlike the individual Y-shape structures observed with glutaraldehyde-fixed mammalian exocyst particles, our yeast 2D averages do not appear to have the same short "arms." The arms may be too flexible or heterogeneous to be observed in our 2D averages, they may represent mammalian specific domains (e.g. Ral binding domains in Sec5 and Exo84), or perhaps the mammalian exocyst was partially disassembled during processing.

Members of the CATCHR family of MTCs, including exocyst, COG, GARP, and Dsl1, share functional similarity, as well as structural similarity at the individual subunit level. Thus, they might be expected to assemble into similar quaternary structures, although they contain different numbers of subunits (Yu and Hughson, 2010). Similar to the exocyst modules identified here, COG consists of two structurally and functionally distinct subassemblies with four subunits each (Lees et al., 2010; Ungar et al., 2005). However, in terms of their overall shapes, as determined by negative stain EM, the exocyst differs markedly from that of both COG and Dsl1. The COG and Dsl1 structures consist of ~3 nm wide legs emanating from a central flexible "joint" (Lees et al., 2010, Ren et al., 2009), whereas the exocyst's legs fold alongside each other to form a compact

ellipsoid structure. It is possible that the COG and Dsl1 complexes might adopt more compact structures with all their subunits present, or perhaps they represent a different, biologically relevant conformation that is not captured in the exocyst EM particles.

All putative tethering complexes interact with numerous partners that could allow them to bridge a vesicle at the appropriate target membrane. The recent COG, Dsl1, and HOPS structures demonstrate that known binding sites for factors on opposing membranes are spatially separated within each complex, suggesting a mechanism by which vesicle tethering and regulation of SNARE complex assembly might occur (Lees et al., 2010; Tripathi et al., 2009; Brocker et al., 2012). Consistent with this, Sec3 and Sec15, exocyst subunits that interact with the plasma membrane and vesicle respectively (Guo et al., 2001; Zhang et al., 2001; Baek et al., 2010; Yamashita et al., 2010; Guo et al., 1999), are found in opposing modules (Fig. 2.12). Exo70, which functions redundantly with Sec3 to interact with factors on the plasma membrane (Zhang et al., 2008; Hutagalung et al., 2009), associates most strongly with the module containing Sec15 but may be spatially separated within the 3D structure (Fig. 2.12). Additionally, Sec3 and Exo70's membrane-interacting domains may be on the same side of the complex despite being in different connectivity modules (Fig. 2.12). In the Dsl1 structure, the sites known to bind COPI vesicle coats and the ER are separated by about 30 nm (Tripathi et al., 2009; Ren et al., 2009). Similarly, in HOPS, one end of the structure contains the binding sites for the Rab GTPase Ypt7 and SNAREs, and the other end contains the second Ypt7 binding site (Brocker et al., 2012). It will be interesting to determine whether there is a conserved distance for vesicle capture by MTCs at the target membrane and whether all

MTCs undergo conformational changes to bring vesicles into closer proximity for SNARE assembly and vesicle fusion, as was previously suggested for the Dsl1 complex (Ren et al., 2009). Future efforts will require the use of higher resolution data and other strategies to uniquely identify each exocyst subunit within the structure.

We propose that, in contrast with models proposing that assembly of subcomplexes is required for exocyst function, the yeast exocyst complex functions as a stable, assembled octamer in the cell. The subunits pack together into an elongated structure. This structure could be a single conformation that functions through changing interactions with various partner proteins. Alternatively, the exocyst may undergo conformational changes in response to binding its protein or membrane partners. Defining the subunit positions and binding of partners at higher resolution is necessary for elucidating the mechanisms of vesicle tethering and SNARE complex regulation at the plasma membrane. This knowledge is also critical in determining whether the MTCs function by similar mechanisms, and how they are uniquely suited to specific trafficking pathways and cell types. Importantly, the ability to purify stable yeast exocyst complexes will now enable functional studies to obtain a detailed molecular understanding of its role in vesicle tethering and SNARE complex regulation.

A single molecule fluorescence microscopy assay to study vesicle tethering by the exocyst complex

We designed an *in vitro* assay for monitoring vesicle tethering by the exocyst complex, which makes use of single molecule TIRF microscopy. In order to maximize the functionality of the components used in this assay, we used endogenous yeast exocyst

complexes and endogenous, purified yeast post-Golgi vesicles. A number of approaches were tested for visualization of both exocyst complexes and vesicles as well as attachment of exocyst complexes to the glass slide surface. In the first version of this assay, we attached PrA-tagged exocyst complexes from yeast extract to a biotinylated slide using streptavidin and biotinylated IgG and monitored the capture of vesicles containing GFP-Sec4. In a good proof of principle, we observed 4-6 times more vesicle capture events at the slide surface in the presence of exocyst complexes compared to fields lacking exocyst complexes (Fig 3.11c). However, given the carpet of exocyst complexes on the slide surface (Fig. 3.11a), we expected to observe more tethering events and for ease of experiments, increasing the number of events in a single field of view is desirable. As a result, we sought to identify ways of improving the functionality of the exocyst complexes and vesicles used to optimize the assay.

Our biochemical and architectural studies on exocyst complex provided several critical insights for improving the functionality of the exocyst complexes used in the tethering assay. Substantial proteolysis of exocyst components occurred during extract preparation and SNAP-tag labeling (Fig. 3.3, 3.4, 3.12). Our biochemistry data suggested that loss of any one exocyst subunit is sufficient to disassemble the exocyst complex (Fig 2.9) and proteolysis resulted in reduced recovery of intact exocyst complexes (Fig 2.1c). In the initial single molecule studies we were only monitoring the association of Sec6 and Sec8 (Fig 3.11, 3.17), which are components of the same module (Fig 2.11), therefore, it is possible that some fraction of the exocyst complexes on the slide surface were only partially assembled. Furthermore, by attaching and visualizing exocyst complexes on

slides using Sec6 and Sec8 respectively, we were potentially obstructing vesicle access to the Sec3-Sec5-Sec6-Sec8 module with two large tags or the vesicle-interacting side of the complex facing toward the slide surface. Finally, the PrA/Biotin-IgG attachment method proved to be irreproducible and so we sought an alternative approach.

Our biochemical studies on exocyst complex also shed light on a number of potential considerations for improving the functionality of the purified post-Golgi vesicles. First, N-terminal AID tagging of Sec4 and Snc2 resulted in a severe vesicle accumulation phenotype (Fig. 2.12) indicating that these tags partially compromised the function of these proteins. Combining this information with the knowledge that GFP-Sec4, *sec6-4* showed a synthetic growth defect in liquid culture and that SNAP-Sec4 was inviable, we sought to tag alternative components that are not predicted to interact with exocyst complex. Second, substantial proteolysis was apparent in western blots of purified vesicle fractions, particularly for the intrinsically disordered SNARE proteins Snc and Sso (Fig 3.6 and 3.23). Since the vesicle SNARE, Snc, was previously shown to interact with exocyst complex (Shen et al., 2013), it may be an important binding partner for the exocyst on vesicles and so increasing the yield of full-length Snc (and potentially other vesicular proteins) is important.

We generated a number of new reagents in order to test the next version of the tethering assay. Several yeast extracts were generated from protease-deficient yeast strains, which contained a SNAP-tagged subunit labeled with BG-PEG-Biotin-DY649 for both attachment and visualization of exocyst complexes. A second subunit was CLIP-tagged and labeled with the fluorescent substrate CLIP-Surface-488, allowing for

unambiguous identification of exocyst spots on the slide surface as well as for confirming the assembly status of the complex. The SNAP- and CLIP-tagged subunits are found in different modules (Fig. 2.11), in an effort to avoid masking one group with double tags. Several different SNAP- and CLIP-tag combination strains were generated in order to determine which version was most functional (Appendix Table 5.2); testing different SNAP-tagged subunits may be important in particular as this will allow testing of different orientations of the complex relative to the slide surface. For fluorescent labeling of vesicles, we sought to avoid N-terminal tagging of potential exocyst partners on the vesicle. SNAP-Sso1 vesicles are the current focus, as Sso1 is a vesicular cargo and has not been shown to interact directly with the exocyst. Finally, spheroplasting lysis using purified, recombinant lyticase greatly improved the recovery of full-length SNARE proteins during vesicle purification so moving forward, this will be the lysis method for vesicle preparations.

Tethering activity by MTCs has been challenging to study due to the difficulty in purifying intact complexes and the predicted transient nature of such events. We now have the assay and reagents for monitoring vesicle tethering activity by the exocyst complex in real time, using endogenous components isolated directly from yeast extract. Over the course of developing this assay, we have identified and addressed many critical factors for preparing these reagents using the *S. cerevisiae* system. Since we are attaching complexes to slides using yeast extract, such an approach should be amenable to other yeast MTCs as long as the complexes tolerate the SNAP tag. Now with this assay in

place, we will be able to experimentally test the kinetics and requirements of exocytic vesicle tethering as well as potential exocyst complex dynamics during these events.

Future Directions:

Exocyst architecture and binding partners:

Our work predicts that the exocyst complex functions as a fully assembled octamer in yeast and that regulated assembly/disassembly does not take place as part of its function. However, given the complexity of the exocyst and its 8 subunits, we wondered whether the exocyst functions by binding and releasing a series of partners or by undergoing conformational changes. Due to the large size of the exocyst complex, it seems likely that the exocyst may have to shift conformation or be displaced in order to allow vesicles to approach the plasma membrane at a distance sufficient for SNARE complex assembly. Furthermore, the available structural information for the partial COG and Dsl1 complexes show a more 'open' conformation with legs extending from a central joint (Lees et al., 2010; Ren et al., 2009), while our exocyst EM structure is more compact and 'closed'. We wondered whether the structures we obtained represent a single conformation of the exocyst or if the COG and Dsl1 structures may more closely resemble that of the exocyst when fully assembled. Additionally, it is also important to note that our EM studies used native yeast complexes while the others were assembled *in vitro* using recombinantly expressed subunits of COG and Dsl1, which is another possible source of variation. Our biochemical and structural studies provide several tools to answer these questions.

Subcomplex structural studies:

In order to address the potential difference in fully-assembled versus partial complex structures, we can make use of the subcomplexes generated by the AID system (Fig. 2.9). These subcomplexes are stably assembled and using the different exocyst AID strains, a variety of exocyst subassemblies are available to be characterized structurally by EM. Of particular interest would be to test each of the 4-subunit modules to see if these structures can be placed into the overall negative stain structure we obtained and if our hypothesis is correct regarding the two faces of the complex (Fig. 2.14). Furthermore, it would be interesting to see whether the structure of either of these 4-subunit modules resemble that of the partial COG structure. COG also contains 8 subunits, which are also divided into two, functionally distinct, 4-subunit groups. This information, combined with the highly conserved CATCHR fold of COG and exocyst subunits, make these complexes the most likely to assume similar quaternary structures. A deeper understanding of the holocomplex structures of these and other CATCHR MTCs is critical to determining whether there is a common mechanism of function among them and if vesicle capture occurs at a conserved distance from the target membrane based on structural restrictions.

Structural studies with exocyst binding partners:

It is possible that the ‘closed’ structure we obtained for the octameric exocyst complex represents only one conformation and that the complex may adopt additional conformations during the course of its function in yeast. Since the complexes used for our EM studies are highly purified and contain only substoichiometric levels of known

binding partners, we wonder whether the presence of additional factors could modulate the structure we observe by EM. The small GTPases Cdc42 and Rho3 are of particular interest as they have a required but unclear function in exocytosis and interact with the exocyst subunits Exo70 and Sec3 (Robinson et al., 1999; Guo et al., 2001; Zhang et al., 2001; Adamo et al.,1999; Adamo et al., 2001; Wu et al., 2010). Interestingly, GTP-hydrolysis deficient mutants in Rho3 and Cdc42 rescue specifically exocytosis-defective mutants in these GTPases and it was proposed that the role of these interactions with exocyst is to locally 'activate' the polarized exocyst complex to increase vesicle fusion events at these sites (Roumanie et al., 2005). It is possible that this local activation is induced by a conformational change of the exocyst, which may impact either its role in vesicle tethering or SNARE complex regulation. Adding purified binding partners such as the Rho GTPases to our purified complexes may trigger conformational changes that we could detect by EM. Furthermore, we can purify additional binding partners including vesicles, SNAREs, Myo2, and Sec1, all of which can be tested in the context of exocyst binding by EM. These EM studies will also facilitate localizing the binding sites for these partners within the 3-dimensional exocyst structure.

Exocyst subunit positioning:

Making mechanistic predictions about exocyst function in vesicle tethering and SNARE regulation depends on a more detailed knowledge of subunit positions within the 3-dimensional structure. With this information and the extensive array of known exocyst binding partners, we can begin to build a model for how these interaction sites are spatially organized within the complex. We were unable to localize density associated

with the C-terminal GFP tag on Sec15 in our negative stain EM studies (Fig. 2.14); it is possible that the C-terminus of this protein is too flexible to be detected in our 2-dimensional averages. The C-termini of several of the other exocyst subunits are also predicted to be flexible and, consistent with this, preliminary subunit positioning studies using Exo70-GFP and Sec8-GFP were unsuccessful (Adam Frost, communication). N-terminal GFP tags may yield better results but we have not yet tested whether these GFP-fusions will be functional. An alternative approach for subunit positioning is to make use of some of the exocyst yeast strains generated for the single molecule tethering assay. For the first version of that assay, strains were generated that contained a C-terminal SNAP tag and a C-terminal PrA tag on different exocyst subunits. In collaboration with Dr. Gang Han's lab (UMass Medical School), we generated a SNAP tag substrate conjugated to a gold particle. We can purify exocyst complexes with the PrA tag, label the SNAP-tagged subunit specifically with gold particles, and elute the complexes from beads using protease digestion. It is also possible that we will not have success in positioning subunits using the negative stain EM approach and we are already working toward a higher resolution cryo-EM structure in our collaboration with the Frost lab. Finally, we are also collaborating with the Rout and Chait laboratories at Rockefeller to use *in vitro* chemical cross-linking and mass spectrometry to identify intra-exocyst interacting residues. The connectivity model we developed (Fig. 2.11) combined with any subunit interaction information gleaned from the cross-linking studies will provide critically important restraints for positioning subunits within the 3-dimensional structure determined by EM.

Single molecule vesicle tethering assay:

The clear next step for the single molecule vesicle tethering assay is to test the newly developed reagents on the TIRF microscope in a vesicle capture experiment. As previously discussed, we are confident that the exocyst complexes attached to slides from protease-deficient yeast extracts are predominantly fully assembled and functional. Furthermore, fluorescently labeled SNAP-Sso1 vesicles are more likely to be functional as tagging this protein is unlikely to obstruct tethering interactions and our new lysis and vesicle purification approach improves the integrity of vesicle-associated proteins. Using an appropriate density of exocyst complex at the slide surface, we will monitor vesicle capture events by colocalization of vesicles (green) with immobilized exocyst complexes (red and blue) in real time. It is possible that the orientation of exocyst complex may not be optimal when using Sec6-SNAP as the attachment point so we will systematically test differently tagged exocyst complexes of different orientations and determine whether we observe increased numbers of vesicle capture events with certain SNAP-tagged subunits.

Once the tethering assay has been effectively established, the next steps will involve using this assay to identify the required factors for stable vesicle capture by the exocyst. The AID system is an effective way to degrade several known vesicle proteins including Sec4 and Snc (Fig. 2.13). We can selectively eliminate vesicular components during the temperature shift of vesicle accumulating yeast strains, and purify vesicles that lack certain components. Furthermore, if we determine that cellular extract is required for the assay, we can also selectively degrade AID-tagged candidate components from the extract to identify the required factors. There are also a number of mutants available for

the Rab GTPase Sec4 including GDP-locked and GTP-locked versions. It has been proposed that the role of Rab GTPases in membrane trafficking is to mediate binding and release events of vesicular cargos, where binding is dependent on the active (GTP) conformation and release would occur upon GTP hydrolysis. We could test whether Sec4-GDP vesicles are capable of binding to exocyst complex and whether GTP-locked Sec4 vesicles exhibit slower release kinetics than wild-type. Finally, as a further test of specificity of vesicle capture by exocyst, transport vesicles from other intracellular trafficking pathways could be specifically accumulated and purified from other mutant strains. For example, temperature sensitive mutants in ER to Golgi SNAREs could be used as a source of 50 nm COPII vesicles (Kaiser and Schekman, 1990; Liu and Barlowe, 2002) and these vesicles could be tested as a putative negative control in the tethering assay.

Vesicle-interacting subunits are found in both 4-subunit modules of the exocyst complex. We could attach different modules of exocyst subunits using AID/SNAP double-tagged complexes and determine whether an individual module is capable of stable vesicle binding. It is possible that the combination of binding from two subunits (potentially Sec15 and Sec6) will be required. Additionally, it is possible that the overall 3-dimensional structure of the octamer is a critical determinant for vesicle capture.

As we now have several critical conditions established for studying exocyst complexes by single molecule TIRF microscopy, we could also make use of this setup to do single molecule FRET experiments. In the last decade, numerous studies have taken advantage of FRET for monitoring intramolecular conformational changes (Kahlscheuer

et al., 2015). We could use such experiments to monitor FRET efficiency changes between different regions of the exocyst complex during putative conformational changes upon binding partners, such as GTPases and secretory vesicles. However, such experiments are nontrivial to design and more structural information about the exocyst will be necessary to carefully select the positions of the FRET pairs. Furthermore, the conformational changes of the exocyst could be quite small, though recent technological and analysis improvements in the single molecule field allow for monitoring of subnanometer distance changes, given the positions of the FRET or quenching fluorophore pairs are positioned properly (Zhou et al., 2011). If exocyst binding to its partners triggers larger scale changes to a conformation that more closely resembles the 'open' structures seen previously for other MTCs (Ren et al., 2009; Lees et al., 2010), the changes in FRET signal would be less challenging to interpret. Such studies would be an excellent complement to the structural approach described previously, providing real-time measurements of the conformational changes as they occur.

Summary

These studies provide an important advance in both our understanding of exocyst architecture and assembly determinants as well as methodologies for addressing important, unanswered questions about exocyst function. We determined that the exocyst complex exists and functions as a fully assembled octamer in yeast and now it remains to be determined mechanistically how this large complex functions in exocytosis. Further biochemical and structural studies will elucidate the positions of subunits within the complex, which will be critical to forming hypotheses as to how exocyst tethers and regulates SNARE complexes. Additionally, since assembly and disassembly do not appear to be critical features of exocyst function, it will be interesting to determine whether conformational changes or other means of regulation modulate the function of this large complex. With our development of an *in vitro* vesicle tethering assay for exocyst, we are poised to start dissecting functional questions and developing new hypotheses about exocyst function that can be tested in *vivo*.

The exocyst is part of a larger family of factors called tethering factors. On the whole, tethering factors are some of the most poorly understood regulators of intracellular trafficking. However, advances in our knowledge and technologies are bringing to light a number of commonalities among the MTCs. Our studies provide an important foundation for understanding both the structure and function of the yeast exocyst complex and may provide a framework for understanding how all of these essential, complex multi-subunit tethering machines modulate the proper targeting and fusion of vesicles in their respective trafficking pathways.

CHAPTER V: APPENDICES

APPENDIX A: Exocyst purification yield quantification

For all experiments based on exocyst pull-downs (Chapter II), it was important to determine what fraction of the exocyst complex is pulled down from yeast extract. This is necessary for determining the extent to which our conclusions represented the state of total exocyst complex in yeast cells.We quantified the amount of PrA-tagged exocyst complexes that are pulled down, relative to the input levels, using western blot analyses (Fig. 5.1a). We determined that for each PrA-tagged exocyst subunit, approximately 60% of exocyst complexes are isolated (Fig. 5.1a,b) (noted in Chapter II methods). When we performed sequential pull-downs from the same input lysate and visualized them on SDS-PAGE with the sensitive fluorescent protein stain Krypton (concentration correlates linearly with fluorescence intensity (Thermo Fisher Scientific)), we found that the exocyst is eventually depleted (Fig. 5.1c). Therefore, less than 100% of the complexes are bound in each experiment because the IgG-beads are saturated, not because any particular pools of exocyst are inaccessible to pull-down. Additionally, exocyst stoichiometry is unchanged with sequential pull-down suggesting that fully assembled complexes are not pulled out preferentially (Fig. 5.1c). PrA-tagged subunits from each exocyst module were tested and no apparent subcomplexes or free pools were detectable in either case (Fig. 5.1c). In summary, our studies relying upon exocyst pull-downs represent a majority of exocyst complexes in the yeast cell and the pull-downs are not biased in sampling different pools of exocyst complexes such as those that are fully assembled (Fig. 5.1c) or cytosolic (Fig. 2.5b).

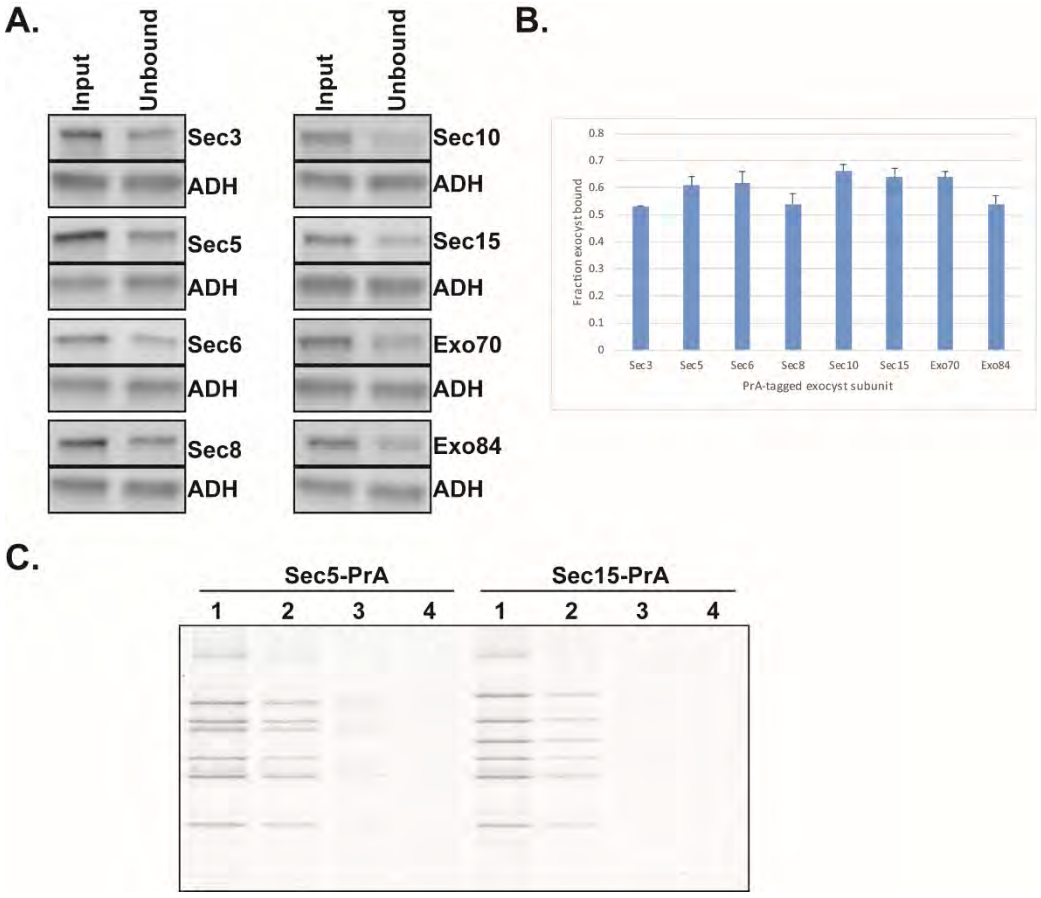

Figure 5.1 Yield quantification for exocyst PrA pull-downs. (**a**) Each PrA-tagged exocyst subunit was pulled down from yeast lysate using IgG magnetic beads and the unbound fraction was recovered. Levels of PrA-tagged exocyst subunits were compared by western blot for 0.3% input versus 0.3% unbound lysate samples and quantified using densitometry. (**b**) Densitometry quantification for western blots revealed that approximately 60% of exocyst complex from yeast lysate is bound in these purifications. Error bars indicate SEM (n=3). (**c**) Sequential exocyst pull-downs were performed from the same initial input lysate using fresh aliquots of IgG beads. Pull-downs were visualized by Krypton-stained SDS-PAGE. Exocyst yield decreased with sequential pull-down due to depletion of the PrA-tagged subunit from lysate but the stoichiometry was unchanged.

APPENDIX B: Exocyst subunit stoichiometry quantification

Our Krypton- and Coomassie-stained SDS-PAGE gels indicated that the exocyst subunits co-purify with equal stoichiometry. In order to show this as rigorously and quantitatively as possible, each PrA-tagged exocyst subunit was pulled down and the purified complexes were visualized on Krypton-stained SDS-PAGE gels (representative gel Fig. 2.2). Each PrA-tagged exocyst subunit was pulled down and the ratio of each co-purifying subunit band relative to the PrA purification handle was quantified using densitometry (Fig 2.3, Fig 5.2). If a free pool or subcomplex containing the PrA-tagged exocyst subunit existed, we would expect to see a higher ratio of that subunit or group of subunits relative to the remaining subunits of the complex. We saw no indication of such free pools, with the possible exception of Exo70, which also shows a small free pool by gel filtration of yeast extract (Fig. 5.5). However, this could also represent dissociation of Exo70 from the complex during the experiment as this subunit is likely less tightly associated. In all cases, the intensity of the Sec3 band was lower than that of the other subunits including in the experiments where Sec3-PrA was the purification handle. This is likely due to the smearing of phosphorylated Sec3 in the gel, which is more pronounced in these experiments as the gels were run long enough to sufficiently resolve all exocyst subunit bands for quantification. We conclude, therefore, that the exocyst complex exists predominantly as a fully assembled octamer with no detectable (<5-10%) free pools or subcomplexes, consistent with our EM structural studies as well (Fig. 2.14, 2.15).

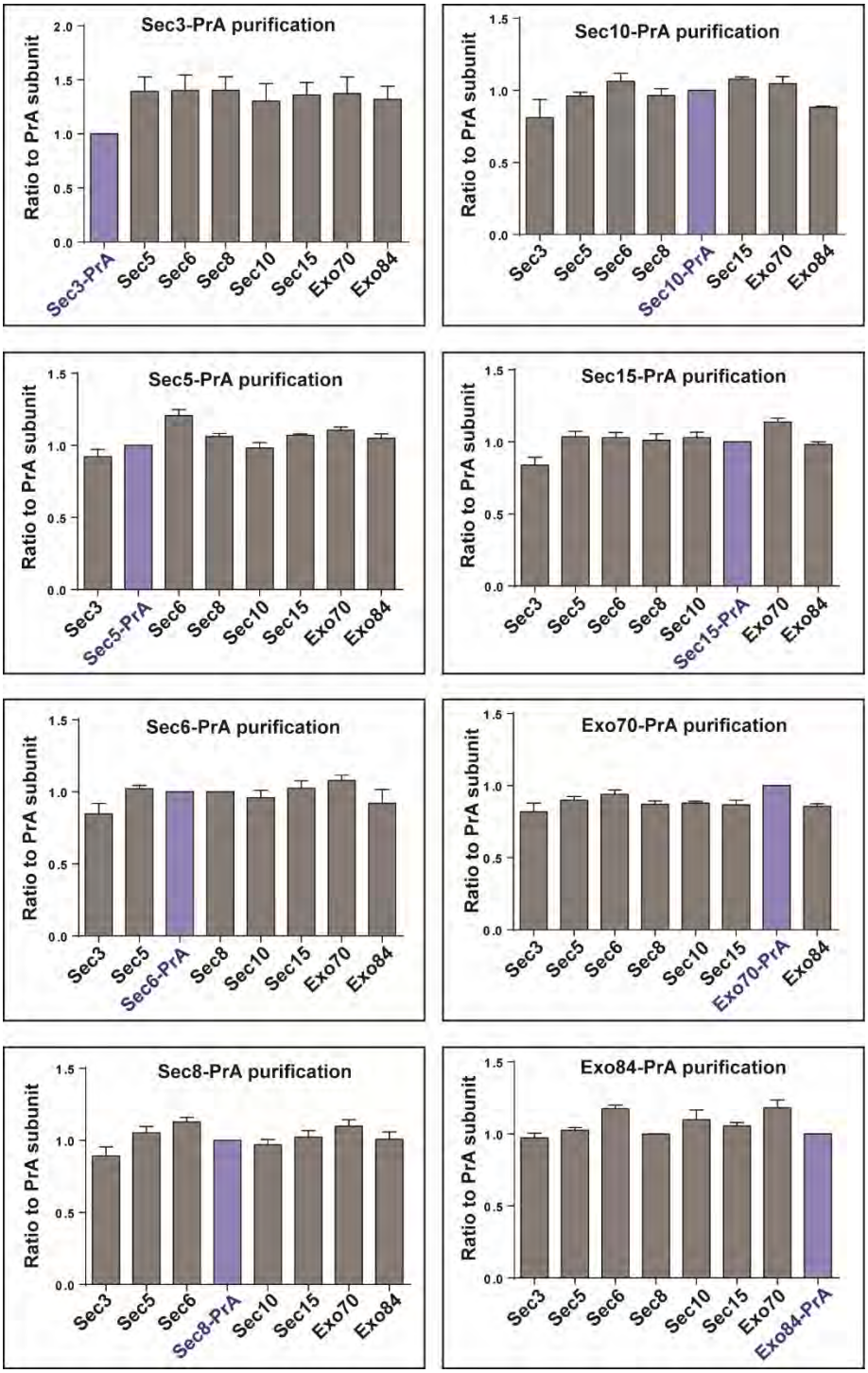

Figure 5.2 All exocyst subunits co-purify with equal stoichiometry. Exocyst complexes were purified with each subunit as PrA purification handle, run on SDS-PAGE, and stained with Krypton fluorescent protein stain. Densitometry analysis showed equal stoichiometry for all subunits with no excess of purification handle or subsets of subunits, suggesting there are no detectable free pools or subcomplexes for any subunits. Error bars indicate SEM (n=3-4 technical replicates).

APPENDIX C: Characterizing secretory defect in exocyst partner AID strains

We showed that yeast strains expressing either AID-tagged Snc2 (in *snc1Δ* background), Sec4, Myo2, Cdc42, or Sec1 were inviable or exhibited growth defects on IAA-containing YPD plates and that the proteins were depleted from cells grown in liquid culture after 1 hour treatment with IAA (Fig. 2.12). However, we needed to demonstrate that this depletion induced a secretory phenotype within the 1 hour of treatment in liquid culture in order to determine whether blocking post-Golgi vesicle trafficking affected exocyst assembly. We used a Bgl2 secretion assay to determine whether we were, in fact, disrupting exocytosis. In this experiment, yeast strains were monitored for the accumulation of a known post-Golgi vesicle cargo protein, Bgl2, in the cytosol upon depletion of each exocyst interacting partner. Using this assay we showed that all of the AID-tagged partners exhibited vesicle accumulation within 1 hour (Fig 2.12b) and validated this result with negative stain EM of yeast cells (Fig 2.12c). Here, a representative set of western blots used for densitometry quantification of Bgl2 accumulation is shown (Fig. 5.3).

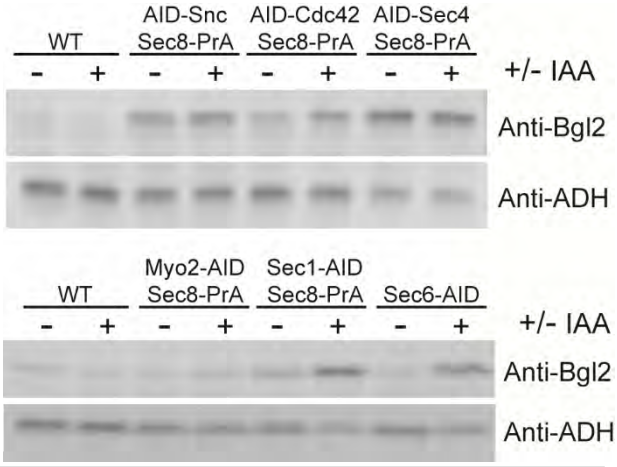

Figure 5.3 Depletion of exocyst binding partners using AID system results in accumulation of secretory vesicles. Western blots show increase of internal Bgl2 levels in AID-tagged partner strains over internal Bgl2 levels in the appropriate WT untreated control strain. Sec1-AID and Sec6-AID showed severe secretion defects, while Myo2-AID and AID-Cdc42 showed minor defects. AID-Snc and AID-Sec4 showed severe Bgl2 accumulation even before treatment, suggesting a partial loss of function due to the AID tag (quantified in Fig. 2.12b)

We went further to investigate whether each of these

secretion blocks affects exocyst localization by generating strains expressing Sec8-GFP at endogenous levels from its genomic locus in combination with each of these AID-tagged proteins. There is a clear effect on exocyst localization and cell morphology upon loss of Sec6, consistent with earlier studies (Fig 5.4) (Songer and Munson, 2009) and with exocyst complex disassembly (Figure 2.9). There is some mislocalization and increased cytosolic signal observed with Sec1-AID and Myo2-AID. Minor mislocalization was observed with AID-Sec4, minor spreading of the polarized exocyst signal in AID-Snc2 (consistent with Shen and Novick, 2013), and fewer budded cells but proper exocyst localization with AID-Cdc42. While these results are interesting, further investigation and careful quantification would be required to conclusively determine which of these factors are really required for polarized exocyst localization. Given that the exocyst complexes we purified from these strains are assembled, we believe that Sec8-GFP is a reliable readout for localization of the exocyst complex as a whole. In summary, consistent with the secretion assays (Fig 2.12), depletion of these proteins does have an effect on exocyst and the secretory pathway but does not disrupt the assembly or integrity of the complex (Figure 2.13).

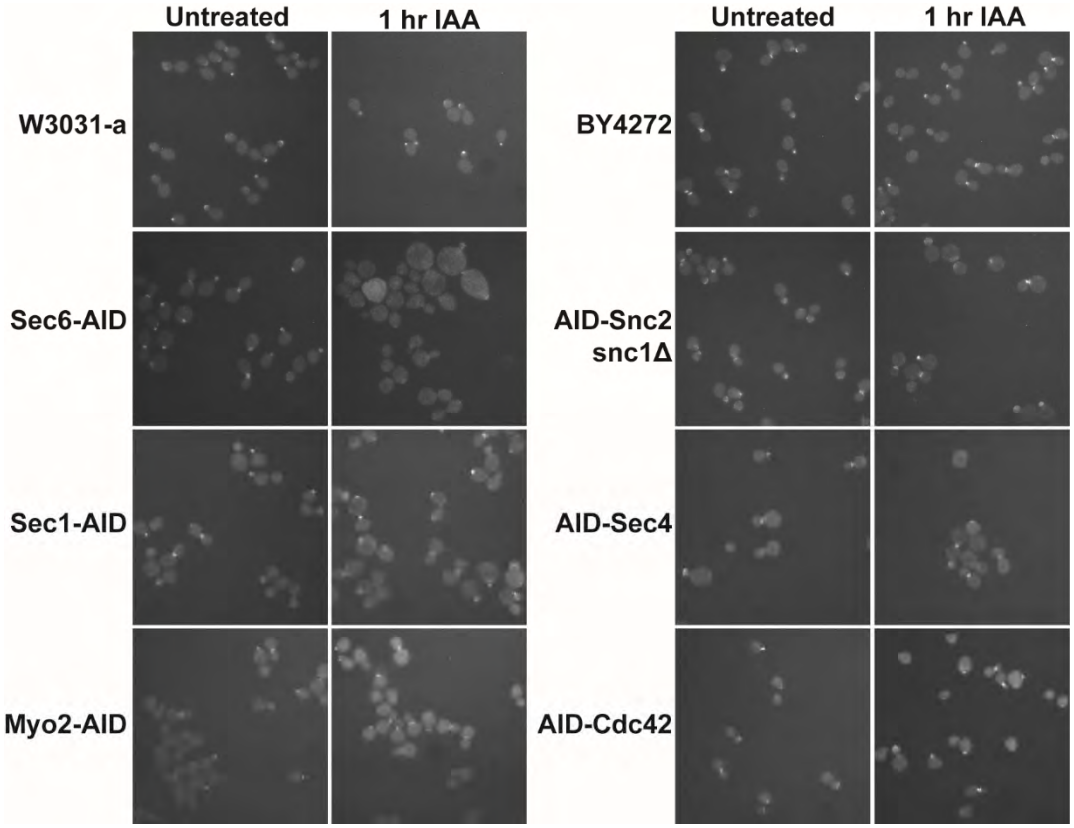

Figure 5.4 Exocyst localization is partially disrupted upon depletion of several exocyst binding partners. Sec8-GFP was monitored in all cases. The localization of Sec8-GFP was monitored in AID strains relative to Sec8-GFP in the appropriate wild-type strain background indicated at the top of each column. Yeast cells were treated for 1 hour with IAA, harvested in log-phase, fixed with methanol and then imaged on an Axioskop2 plus epifluorescent microscope (Zeiss, Thornwood, NY) fitted with a 100x Plan-NEOFLUAR (Zeiss 1.30 NA oil immersion) objective lens. Images were collected using a Diagnostic Instruments camera (Sterling Heights, MI; model 2.1.1) and 3rd Party Interface Advanced (ver. 3.5.4 for MacOS) software. Images were adjusted for total contrast in Adobe Photoshop. n>100 cells were imaged for each strain.

APPENDIX D: Fractionation of yeast lysate to identify exocyst subcomplexes

We showed that when any of the exocyst subunits was used as PrA purification handle, the stoichiometry of all subunits was equal (Fig 5.2). If free pools of subunits or subcomplexes existed, we would have expected to see an excess of the PrA handle with or without a subset of other subunits. However, we previously showed that when spheroplasted yeast lysates were fractionated on a Superose 6 gel filtration column, broad peaks for Sec6 and Sec8 corresponding to lower molecular weight species extended beyond the exocyst peak suggesting a possible cytosolic subcomplex (Morgera et al., 2012). Furthermore, a free pool corresponding to free Exo70 was also observed (Morgera et al., 2012). Since these results were largely inconsistent with the results from our new purification method and we showed that spheroplasting reduces the yield of intact exocyst complexes (Fig 2.1c), this experiment was repeated using lysate generated by cryogenic ball mill grinding. Furthermore, recent experiments also revealed that the Exo70 polyclonal antibody we used recognizes another protein that runs at approximately the same molecular weight as Exo70 by SDS-PAGE. In order to dissect the free pool peak contribution of this protein from Exo70, the lysate used for this study expressed Exo70-PrA. In this experiment, the exocyst subunits co-migrate in a single peak that correlates with the size of the intact complex (Fig. 5.5). A substantially smaller free pool of Exo70 was observed in this experiment compared to the previous one once the contribution from the non-specific 70 kDa band was eliminated. It is possible that a low level of free Exo70 does exist in the cell. Additionally, it is possible that since Exo70 is one of the more weakly associated subunits of the complex, some of this disassembles

from the complex during the course of the gel filtration fractionation experiment (Fig. 2.5). Given the varying sensitivity of the different exocyst antibodies for these dilute samples, the prolonged extract incubation time required for such experiments, and the resolution limitations of the gel filtration column, it is difficult to draw firm conclusions from such experiments. However, the gel filtration results are consistent our data from other assays, suggesting that the majority of exocyst subunits exist as part of the octameric complex.

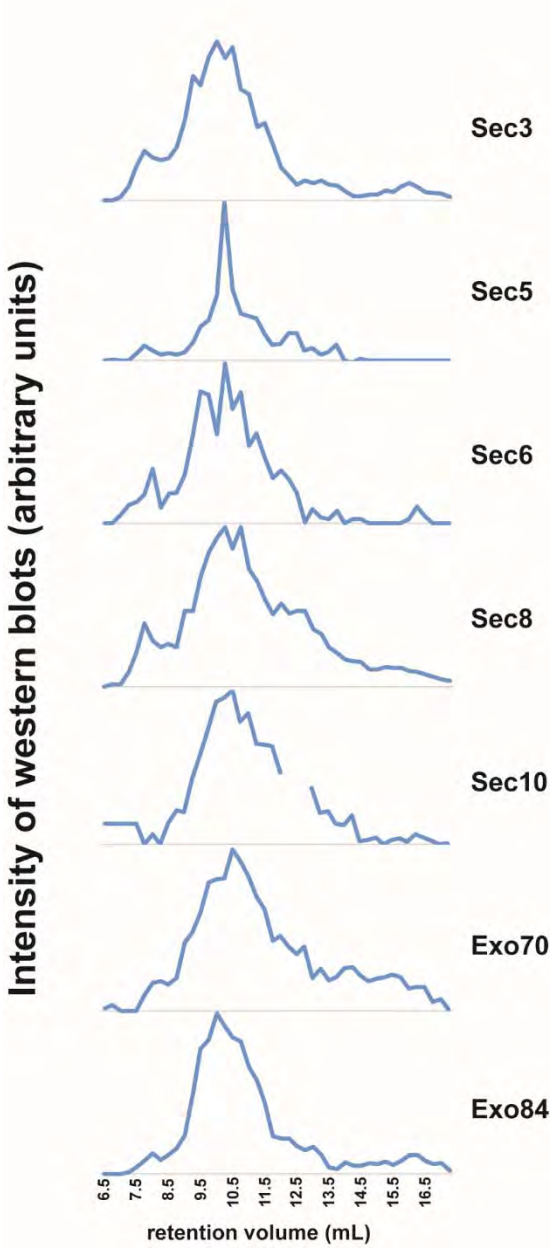

Figure 5.5 Fractionation of Exo70-PrA lysates on Superose 6 10/300 shows exocyst subunits are predominantly assembled in octameric complex. 0.25 ml fractions were analyzed by western blot using specific polyclonal antibodies. Band intensities were normalized to the most intense band visualized by ECL. Sec15 data not shown because antibody was not sensitive enough for dilute post-gel filtration lysate samples. 12 ml=670 kDa, 15 ml=158 kDa, 16 ml=44 kDa.

APPENDIX E: Strain table for Chapter II and Appendix C

Table 5.1

Yeast Strain	Genotype	Source
BY4741	*MATa his3Δ1 leu2Δ 0 met15Δ0 ura3Δ0*	Brachmann, 1998
BY4742	*MATα his3Δ1 leu2Δ0 lys2Δ0 ura3Δ0*	Brachmann, 1998
MMY1371	*MATa ura3-1::ADH1-OsTIR1-9Myc(URA3) ade2-1his3-11,15 leu2-3,112 trp1-1 can1-100*	from YGRC Japan
Exocyst PrA and GFP-PrA strain		
MMY1388	*MATa his3Δ1 leu2Δ 0 met15Δ0 ura3Δ0 LYS2::ADH1 promoter/GFP-PrA (HIS5)*	this study
MMY1183	*MATa his3Δ1 leu2Δ0 met15Δ0 ura3Δ0 SEC3::Sec3-PrA (HIS5)*	this study
MMY1316	*MATa his3Δ1 leu2Δ0 met15Δ0 ura3Δ0 SEC5::Sec5-PrA (HIS5)*	this study
MMY1074	*MATa his3Δ1 leu2Δ 0 met15Δ0 ura3Δ0 SEC6::Sec6-prA (HIS5)*	this study
MMY1185	*MATa his3Δ1 leu2Δ0 met15Δ0 ura3Δ0 SEC8::Sec8-PrA (HIS5)*	this study
MMY1186	*MATa his3Δ1 leu2Δ0 met15Δ0 ura3Δ0 SEC10::Sec10-PrA (HIS5)*	this study
MMY1075	*MATa his3Δ1 leu2Δ0 met15Δ0 ura3Δ0 SEC15::Sec15-PrA (HIS5)*	this study
MMY1187	*MATa his3Δ1 leu2Δ0 met15Δ0 ura3Δ0 EXO70::Exo70-PrA (HIS5)*	this study
MMY1188	*MATa his3Δ1 leu2Δ0 met15Δ0 ura3Δ0 EXO84::Exo84-PrA (HIS5)*	this study
MMY1175	*MATα his3Δ1 leu2Δ0 ura3Δ0 SEC6::SEC6-PrA HIS3 SEC15::SEC15-GFP (HIS5)*	this study
Exocyst AID strains		
MMY1372	*MATa ura3-1::ADH1-OsTIR1-9Myc(URA3) SEC3::Sec3-5xGA-IAA17 (kanMX) ade2-1his3-*	this study

	11,15 leu2-3,112 trp1-1 can1-100	
MMY1373	*MATa ura3-1::ADH1-OsTIR1-9Myc(URA3) SEC5::Sec5-5xGA-IAA17 (kanMX) ade2-1his3-11,15 leu2-3,112 trp1-1 can1-100*	this study
MMY1374	*MATa ura3-1::ADH1-OsTIR1-9Myc(URA3) SEC6::Sec6-5xGA-IAA17 (kanMX) ade2-1his3-11,15 leu2-3,112 trp1-1 can1-100*	this study
MMY1375	*MATa ura3-1::ADH1-OsTIR1-9Myc(URA3) SEC8::Sec8-5xGA-IAA17 (kanMX) ade2-1his3-11,15 leu2-3,112 trp1-1 can1-100*	this study
MMY1376	*MATa ura3-1::ADH1-OsTIR1-9Myc(URA3) SEC10::Sec10-5xGA-IAA17 (kanMX) ade2-1his3-11,15 leu2-3,112 trp1-1 can1-100*	this study
MMY1377	*MATa ura3-1::ADH1-OsTIR1-9Myc(URA3) SEC15::Sec15-5xGA-IAA17 (kanMX) ade2-1his3-11,15 leu2-3,112 trp1-1 can1-100*	this study
MMY1378	*MATa ura3-1::ADH1-OsTIR1-9Myc(URA3) EXO70::Exo70-5xGA-IAA17 (kanMX) ade2-1his3-11,15 leu2-3,112 trp1-1 can1-100*	this study
MMY1379	*MATa ura3-1::ADH1-OsTIR1-9Myc(URA3) EXO84::Exo84-5xGA-IAA17 (kanMX) ade2-1his3-11,15 leu2-3,112 trp1-1 can1-100*	this study
Exocyst AID/PrA strains		
MMY1380	*MATa ura3-1::ADH1-OsTIR1-9Myc(URA3) ade2-1his3-11,15 leu2-3,112 trp1-1can1-100; SEC6::Sec6-PrA (HIS5)*	this study
MMY1389	*MATa ura3-1::ADH1-OsTIR1-9Myc(URA3) ade2-1his3-11,15 leu2-3,112 trp1-*	this study

	1can1-100; SEC8::Sec8-PrA (HIS5)	
MMY1381	*MATa ura3-1::ADH1-OsTIR1-9Myc(URA3) ade2-1his3-11,15 leu2-3,112 trp1-1can1-100; SEC15::Sec15-PrA (HIS5)*	this study
MMY1393	*MATa ura3-1::ADH1-OsTIR1-9Myc(URA3) ade2-1his3-11,15 leu2-3,112 trp1-1can1-100; SEC3::Sec3-AID (kanMX); SEC8::Sec8-PrA (HIS5)*	this study
MMY1396	*MATa ura3-1::ADH1-OsTIR1-9Myc(URA3) ade2-1his3-11,15 leu2-3,112 trp1-1can1-100; SEC3::Sec3-AID (kanMX); SEC15::Sec15-PrA (HIS5)*	this study
MMY1402	*MATa ura3-1::ADH1-OsTIR1-9Myc(URA3) ade2-1his3-11,15 leu2-3,112 trp1-1can1-100; SEC5::Sec5-AID (kanMX); SEC8::Sec8-PrA (HIS5)*	this study
MMY1397	*MATa ura3-1::ADH1-OsTIR1-9Myc(URA3) ade2-1his3-11,15 leu2-3,112 trp1-1can1-100; SEC5::Sec5-AID (kanMX); SEC15::Sec15-PrA (HIS5)*	this study
MMY1392	*MATa ura3-1::ADH1-OsTIR1-9Myc(URA3) ade2-1his3-11,15 leu2-3,112 trp1-1can1-100; SEC6::Sec6-AID (kanMX); SEC8::Sec8-PrA (HIS5)*	this study
MMY1395	*MATa ura3-1::ADH1-OsTIR1-9Myc(URA3) ade2-1his3-11,15 leu2-3,112 trp1-1can1-100; SEC6::Sec6-AID (kanMX); SEC15::Sec15-PrA (HIS5)*	this study
MMY1401	*MATa ura3-1::ADH1-OsTIR1-9Myc(URA3) ade2-1his3-11,15 leu2-3,112 trp1-1can1-100; SEC8::Sec8-AID (kanMX); SEC6::Sec6-PrA (HIS5)*	this study
MMY1398	*MATa ura3-1::ADH1-OsTIR1-9Myc(URA3) ade2-1his3-11,15 leu2-3,112 trp1-1can1-100; SEC8::Sec8-AID (kanMX); SEC15::Sec15-PrA (HIS5)*	this study

MMY1403	*MATa ura3-1::ADH1-OsTIR1-9Myc(URA3) ade2-1his3-11,15 leu2-3,112 trp1-1can1-100; SEC10::Sec10-AID (kanMX); SEC8::Sec8-PrA (HIS5)*	this study
MMY1391	*MATa ura3-1::ADH1-OsTIR1-9Myc(URA3) ade2-1his3-11,15 leu2-3,112 trp1-1can1-100; SEC15::Sec15-AID (kanMX); SEC8::Sec8-PrA (HIS5)*	this study
MMY1390	*MATa ura3-1::ADH1-OsTIR1-9Myc(URA3) ade2-1his3-11,15 leu2-3,112 trp1-1can1-100; EXO70::Exo70-AID (kanMX); SEC8::Sec8-PrA (HIS5)*	this study
MMY1394	*MATa ura3-1::ADH1-OsTIR1-9Myc(URA3) ade2-1his3-11,15 leu2-3,112 trp1-1can1-100; EXO70::Exo70-AID (kanMX); SEC15::Sec15-PrA (HIS5)*	this study
MMY1404	*MATa ura3-1::ADH1-OsTIR1-9Myc(URA3) ade2-1his3-11,15 leu2-3,112 trp1-1can1-100; EXO84::Exo84-AID (kanMX); SEC8::Sec8-PrA (HIS5)*	this study
MMY1400	*MATa ura3-1::ADH1-OsTIR1-9Myc(URA3) ade2-1his3-11,15 leu2-3,112 trp1-1can1-100; EXO84::Exo84-AID (kanMX); SEC15::Sec15-PrA (HIS5)*	this study
Non-Exocyst AID/PrA strains		
MMY1411	*MATa ura3-1::ADH1-OsTIR1-9Myc(URA3) ade2-1his3-11,15 leu2-3,112 trp1-1can1-100; SEC1::Sec1-AID (kanMX); SEC8::Sec8-PrA (HIS5)*	this study
MMY1410	*MATa ura3-1::ADH1-OsTIR1-9Myc(URA3) ade2-1his3-11,15 leu2-3,112 trp1-1can1-100; MYO2::Myo2-AID (kanMX); SEC8::Sec8-PrA (HIS5)*	this study
MMY1433	*MATa his3Δ1 leu2Δ0 lys2Δ0 ura3Δ0 SNC2::AID-Snc2 MET15::OsTIR1-myc*	this study

	(URA3); SNC1::kanMX; SEC8::Sec8-PrA (HIS5)	
MMY1435	*MATa his3Δ1 leu2Δ0 lys2Δ0 ura3Δ0 SEC4::AID-Sec4 MET15::OsTIR1-myc (URA3); SEC8::Sec8-PrA (HIS5)*	this study
MMY1436	*MATα his3Δ1 leu2Δ0 lys2Δ0 ura3Δ0 CDC42::AID-Cdc42 MET15::OsTIR1-myc (URA3); SEC8::Sec8-PrA (HIS5)*	this study
AID/Sec8-GFP strains		
MMY1515	*MATa ura3-1::ADH1-OsTIR1-9Myc(URA3) ade2-1his3-11,15 leu2-3,112 trp1-1can1-100; SEC8::Sec8-GFP (HIS)*	this study
MMY1516	*MATa ura3-1::ADH1-OsTIR1-9Myc(URA3) ade2-1his3-11,15 leu2-3,112 trp1-1can1-100; SEC1::Sec1-AID (KANMX), SEC8::Sec8-GFP (HIS)*	this study
MMY1517	*MATα his3Δ1 leu2Δ0 lys2Δ0 ura3Δ0 CDC42::AID-Cdc42 MET15::OsTIR1-myc (URA3); SEC8::Sec8-GFP*	this study
MMY1487	*MATa ura3-1::ADH1-OsTIR1-9Myc(URA3) ade2-1his3-11,15 leu2-3,112 trp1-1can1-100; MYO2::Myo2-AID (KANMX); SEC8::Sec8-GFP (HIS)*	this study
MMY1508	*MATα his3Δ1 leu2Δ0 lys2Δ0 ura3Δ0 SNC2::AID-Snc2; MET15::OsTIR1-myc (URA3); SNC1::KANMX; SEC8::Sec8-GFP*	this study
MMY1513	*MATα his3Δ1 leu2Δ0 lys2Δ0 ura3Δ0 SEC4::AID-Sec4; MET15::OsTIR1-myc (URA3); SEC8::Sec8-GFP*	this study
MMY115	*MATa his3Δ1 leu2Δ 0 met15Δ0 ura3Δ0 Sec8-GFP(HIS3)*	Invitrogen

APPENDIX F: Strain table for CHAPTER III

Table 5.2

Yeast Strain	Genotype	Source
MMY1198	*MATa his3Δ1 leu2Δ 0 met15Δ0 ura3Δ0 SEC3::SEC3-SNAP-HygR*	this study
MMY1199	*MATa his3Δ1 leu2Δ 0 met15Δ0 ura3Δ0 SEC5::SEC5-SNAP-HygR*	this study
MMY1200	*MATa his3Δ1 leu2Δ 0 met15Δ0 ura3Δ0 SEC6::SEC6-SNAP-HygR*	this study
MMY1201	*MATa his3Δ1 leu2Δ 0 met15Δ0 ura3Δ0 SEC8::SEC8-SNAP-HygR*	this study
MMY1202	*MATa his3Δ1 leu2Δ 0 met15Δ0 ura3Δ0 SEC10::SEC10-SNAP-HygR*	this study
MMY1203	*MATa his3Δ1 leu2Δ 0 met15Δ0 ura3Δ0 SEC15::SEC15-SNAP-HygR*	this study
MMY1204	*MATa his3Δ1 leu2Δ 0 met15Δ0 ura3Δ0 EXO70::EXO70-SNAP-HygR*	this study
MMY1205	*MATa his3Δ1 leu2Δ 0 met15Δ0 ura3Δ0 EXO84::EXO84-SNAP-HygR*	this study
MMY1328	*MATa his3Δ1 leu2Δ0 met15Δ0 ura3Δ0 SEC8::Sec8prA (His3); SEC6::SEC6-fastSNAP (HygR)*	this study
MMY1353	*MATa his3Δ1 leu2Δ 0 met15Δ0 ura3Δ0; SEC6::Sec6-fastSNAP (HygR); EXO84::Exo84-prA (HIS)*	this study
MMY1354	*MATa his3Δ1 leu2Δ 0 met15Δ0 ura3Δ0; SEC8::Sec8-fastSNAP (HygR); EXO70::Exo70-prA (HIS)*	this study
MMY1355	*MATa his3Δ1 leu2Δ 0 met15Δ0 ura3Δ0; SEC15::Sec15-fastSNAP (HygR); EXO84::Exo84-prA (HIS)*	this study
MMY1356	*MATa his3Δ1 leu2Δ 0 met15Δ0 ura3Δ0; SEC6::Sec6-fastSNAP*	this study

	(HygR); SEC3::Sec3-prA (HIS)	
MMY1357	*MATa his3Δ1 leu2Δ 0 met15Δ0 ura3Δ0; EXO84::Exo84-fastSNAP (HygR); SEC3::Sec3-prA (HIS)*	this study
MMY1358	*MATa his3Δ1 leu2Δ 0 met15Δ0 ura3Δ0; EXO84::Exo84-fastSNAP (HygR); EXO70::Exo70-prA (HIS)*	this study
MMY1359	*MATa his3Δ1 leu2Δ 0 met15Δ0 ura3Δ0; SEC6::Sec6-fastSNAP (HygR); EXO70::Exo70-prA (HIS)*	this study
MMY1422	*MATa prc1-407 prb1-1122 pep4-3 leu2 trp1 ura3-52 gal2 SEC3::Sec3-SNAP (HygR)*	this study
MMY1423	*MATa prc1-407 prb1-1122 pep4-3 leu2 trp1 ura3-52 gal2 SEC5::Sec5-SNAP (HygR)*	this study
MMY1424	*MATa prc1-407 prb1-1122 pep4-3 leu2 trp1 ura3-52 gal2 SEC8::Sec8-SNAP (HygR)*	this study
MMY1425	*MATa prc1-407 prb1-1122 pep4-3 leu2 trp1 ura3-52 gal2 SEC10::Sec10-SNAP (HygR)*	this study
MMY1426	*MATa prc1-407 prb1-1122 pep4-3 leu2 trp1 ura3-52 gal2 SEC15::Sec15-SNAP (HygR)*	this study
MMY1427	*MATa prc1-407 prb1-1122 pep4-3 leu2 trp1 ura3-52 gal2 EXO70::Exo70-SNAP (HygR)*	this study
MMY1428	*MATa prc1-407 prb1-1122 pep4-3 leu2 trp1 ura3-52 gal2 EXO84::Exo84-SNAP (HygR)*	this study
MMY1479	*MATa prc1-407 prb1-1122 pep4-3 leu2 trp1 ura3-52 gal2 SEC3::Sec3-SNAP (HygR). SEC10::Sec10-CLIP (NatR)*	this study
MMY1480	*MATa prc1-407 prb1-1122 pep4-3 leu2 trp1 ura3-52 gal2 SEC3::Sec3-SNAP (HygR). EXO70::Exo70-CLIP (NatR)*	this study

MMY1481	*MATa prc1-407 prb1-1122 pep4-3 leu2 trp1 ura3-52 gal2 SEC5::Sec5-SNAP (HygR). SEC8::Sec8-CLIP (NatR)*	this study
MMY1482	*MATa prc1-407 prb1-1122 pep4-3 leu2 trp1 ura3-52 gal2 SEC5::Sec5-SNAP (HygR). EXO84::Exo84-CLIP (NatR)*	this study
MMY1483	*MATa prc1-407 prb1-1122 pep4-3 leu2 trp1 ura3-52 gal2 EXO70::Exo70-SNAP (HygR). SEC3::Sec3-CLIP (NatR)*	this study
MMY1484	*MATa prc1-407 prb1-1122 pep4-3 leu2 trp1 ura3-52 gal2 EXO70::Exo70-SNAP (HygR). SEC8::Sec8-CLIP (NatR)*	this study
MMY1485	*MATa prc1-407 prb1-1122 pep4-3 leu2 trp1 ura3-52 gal2 EXO84::Exo84-SNAP (HygR). SEC3::Sec3-CLIP (NatR)*	this study
MMY1486	*MATa prc1-407 prb1-1122 pep4-3 leu2 trp1 ura3-52 gal2 EXO70::Exo70-SNAP (HygR). SEC5::Sec5-CLIP (NatR)*	this study
MMY1505	*MATα leu2-3,112 ura3-52 sec6-4 SSO1::SNAP-Sso1*	this study
MMY1473	*MATa his3Δ1 leu2Δ 0 met15Δ0 ura3Δ0 CDC42::SNAP-Cdc42*	this study
MMY1474	*MATα leu2-3,112 ura3-52 sec6-4 CDC42::SNAP-Cdc42*	this study
MMY1349	*MATα his3Δ1 leu2Δ 0 met15Δ0 ura3Δ0 SNC2::SNAP-SNC2*	this study
MMY1350	*MATα leu2-3,112 ura3-52 sec6-4; SNC2::SNAP-Snc2*	this study
MMY1284	*SEC4::GFP-Sec4; MATa his3Δ1 leu2Δ 0 met15Δ0 ura3Δ0*	this study
MMY1303	*SEC4::GFP-Sec4; SEC6::sec6-4*	this study
MMY1277	*SNC2::GFP-Snc2 MATa his3Δ1 leu2Δ 0 met15Δ0 ura3Δ0*	this study
MMY1294	*SNC2::GFP-Snc2; SEC6::sec6-4*	this study
MMY1330	*sec9-4, SNC1::GFP-Snc1, SNC2::GFP-Snc2*	this study

APPENDIX G: Regulation of exocytosis by the exocyst subunit Sec6 and the SM protein Sec1

Morgera, F., **Sallah, M.R**., Dubuke, M.L., Gandhi, P., Brewer, D.N., Carr, C.M., and Munson, M. (2012). Regulation of exocytosis by the exocyst subunit Sec6 and the SM protein Sec1. Molecular Biology Of The Cell 23, 337-346.

Significant background and rationale (modified from Morgera et al., 2012):

The exocyst subunit Sec6 plays critical roles in several aspects of exocyst function. As with many of the exocyst subunits, Sec6 was originally discovered as a temperature-sensitive sec mutant of the secretory pathway (Novick et al., 1980). At the restrictive temperature, the *sec6-4* mutant strain shows a loss of exocyst stability, with defects in polarized growth and secretion (TerBush and Novick, 1995). Additional temperature-sensitive mutations in conserved residues on the surface of the Sec6 C-terminal domain (Sivaram et al., 2006) led to loss of localization of the exocyst without complex disassembly (Songer and Munson, 2009). These residues are proposed to maintain exocyst localization through interactions with anchoring factor(s) at sites of secretion. Sec6 also binds the reticulon Rtn1, implicating Sec6 in the organization of cortical endoplasmic reticulum structure (De Craene et al., 2006). Moreover, we previously showed that the yeast exocyst subunit Sec6 interacts with the plasma membrane t-SNARE Sec9, inhibiting the formation of Sec9-containing SNARE complexes *in vitro* (Sivaram et al., 2005). Because the loss of Sec6 function in *sec6-4* results in a block in SNARE assembly (Grote et al., 2000), the Sec6–Sec9 interaction we observe may be a critical intermediate in the assembly of SNARE complexes.

The SM protein family is essential for regulating SNARE proteins and SNARE-mediated membrane fusion. Although members of the SM family all bind individual

SNARE proteins and/or SNARE complexes, several distinct modes of interaction have been reported, raising the possibility that SM proteins have multiple functions via different mechanisms (Toonen and Verhage, 2003, 2007; Carr and Rizo, 2010). The best-characterized SM protein, Munc18-1 (neuronal Sec1), binds to 1) the "closed" inhibited conformation of the t-SNARE syntaxin-1a (Misura et al., 2000); 2) the N-terminus of syntaxin-1a (Burkhardt et al., 2008); and 3) ternary SNARE complexes containing syntaxin-1a (Dulubova et al., 2007; Shen et al., 2007; Rodkey et al., 2008; Xu et al., 2010). A similar constellation of binding interactions has been reported for the endosomal SM protein Vps45 (Carpp et al., 2006; Furgason et al., 2009). Other SM proteins such as Sly1 appear to bind only the N-terminus of the partner syntaxin (Bracher and Weissenhorn, 2002; Yamaguchi et al., 2002; Peng and Gallwitz, 2004; Arac et al., 2005). In contrast, the yeast Sec1 protein interacts predominantly with assembled ternary SNARE complexes and not with the syntaxin Sso1 (Carr et al., 1999; Togneri et al., 2006). Functionally, several SMs appear to have an inhibitory role in SNARE complex assembly, whereas other studies clearly identified a positive role for SM proteins in SNARE complex assembly and membrane fusion (Gallwitz and Jahn, 2003; Scott et al., 2004; Shen et al., 2007; Toonen and Verhage, 2007). Thus, the functions of SM proteins, the mechanism(s) underlying these functions, and the extent to which these functions are conserved all remain important and incompletely resolved questions.

Although our Sec6–Sec9 binding studies indicated that the exocyst may play a direct role in controlling SNARE complex assembly, the question remained: how is Sec6 inhibition of Sec9 released to promote SNARE complex assembly? Several studies

suggested that the exocyst might function with or through the SM protein Sec1 to regulate SNARE complex assembly (Finger and Novick, 2000; Grote et al., 2000;Wiederkehr et al., 2004; Hashizume et al., 2009), and the exocyst and Sec1 are specifically localized to sites of secretion in yeast. Although evidence pointed to a function for Sec1 after SNARE complex assembly by binding assembled SNARE complexes (Carr et al., 1999; Scott et al., 2004; Togneri et al., 2006) and promoting liposome fusion *in vitro* (Scott et al., 2004), a recent analysis of a large panel of Sec1 mutants demonstrated an additional functional requirement for Sec1 prior to SNARE complex assembly (Hashizume et al., 2009). Furthermore, overexpression of Sec1 resulted in increased levels of SNARE complexes (Wiederkehr et al., 2004). We hypothesized, therefore, that the exocyst and Sec1 work together to directly regulate the SNAREs and SNARE complex assembly. To understand the functional interplay among these proteins, we examined their relationships with one another both *in vitro* and *in vivo*.

Summary of results and implications (updated from Morgera et al., 2012):

Here we show that Sec6 binds Sec1 both *in vitro* (Morgera et al., Fig. 1) and *in vivo* (Appendix G Fig. 5.6 below, Morgera et al., Fig. 4b) and the Sec6–Sec1 interaction is exclusive of Sec6–Sec9 (Morgera et al., Fig. 3.5) but compatible with Sec6–exocyst assembly (Morgera et al., Fig. 5). These results are consistent with our exocyst pull-downs showing Sec1 co-purifies with Sec8-PrA and not solely Sec6 (Chapter II, Fig. 2.4c). In contrast, the Sec6–exocyst interaction is incompatible with Sec6–Sec9 (Morgera et al., Fig. 5). Consistent with the fact that Sec1 cannot outcompete Sec9 for binding to Sec6 (Morgera et al., Fig. 3), we observed that Sec1 could not relieve Sec6's inhibition of

SNARE complex assembly *in vitro* (Appendix G, Fig. 5.7 below, Morgera et al., Fig. 6). Therefore we proposed that, upon vesicle arrival, Sec6 releases Sec9 in favor of Sec6–exocyst assembly and simultaneously recruits Sec1 to sites of secretion for coordinated SNARE complex formation and membrane fusion.

Our recent results have led to a re-interpretation of this data, however. Firstly, we showed that the exocyst complex exists predominantly in the fully assembled state in yeast with all subunits at equal stoichiometry (Chapter II). Therefore, models proposing a role for a Sec6 dimer (Sivaram et al., 2005) outside of the exocyst as a regulator of SNARE complex assembly are unlikely. Additionally, our lab recently proposed that the physiological interaction of Sec6 with the SNAREs likely occurs through the assembled SNARE complex rather than Sec9 alone or Sec9-Sso1 binary SNARE complexes (Dubuke et al., 2015). Furthermore, Sec6 is not a negative regulator of binary SNARE complex assembly, as our previous native gel (Sivaram et al., 2005; Morgera et al., 2012) and gel filtration (Sivaram et al., 2005) SNARE assembly assays were misinterpreted (Dubuke et al., 2015). Therefore, it is likely that Sec6's interaction with SNARE complexes occurs in the context of the fully assembled exocyst and this interaction likely serves a positive regulatory role in SNARE complex assembly, consistent with that of other MTCs with their respective SNAREs (Dubuke et al., 2015; Hong and Lev, 2014). However, this role for exocyst in promoting SNARE complex assembly must be tested experimentally and it remains to be determined how exocyst binding to Sec1 fits into this process as well.

Figure contributions to Morgera et al., 2012:

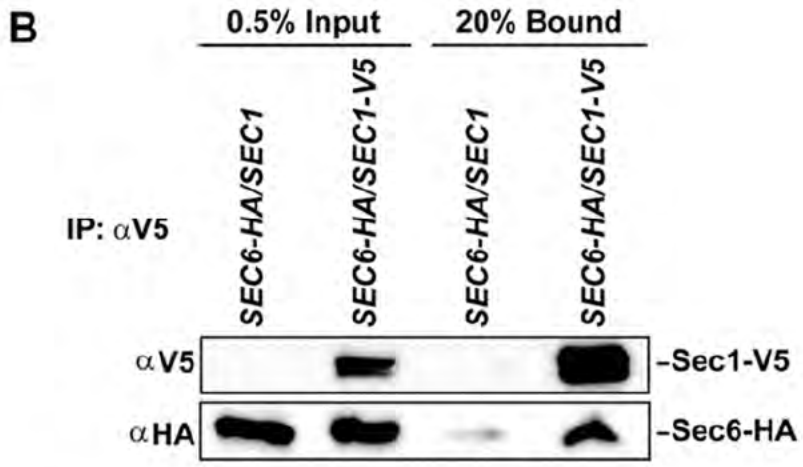

Figure 5.6 Sec6 interacts with Sec1 *in vivo*. Sec1-V5 immunoprecipitated from yeast lysates binds endogenously expressed Sec6-HA3. The input and bound samples were run on 8% SDS–PAGE and immunoblotted for V5 and HA epitope tags. The amount of Sec6 coimmunoprecipitated was consistently above background levels, although the amount bound was only a fraction (~1%) of the total Sec6 in the cell. This low percentage was similar to the amount that we observed for the Sec6–Sec9 interaction. In contrast, the other exocyst subunits readily coimmunoprecipitate with Sec6-HA3 (Songer and Munson, 2009). The Sec1–Sec6 data are consistent with previous results from the Novick lab, in which a comparable amount (~0.2–0.4%) of Sec1 bound to the exocyst complex, when coimmunoprecipitated with either Sec8-Myc or Sec10-Myc (Wiederkehr *et al.*, 2004).

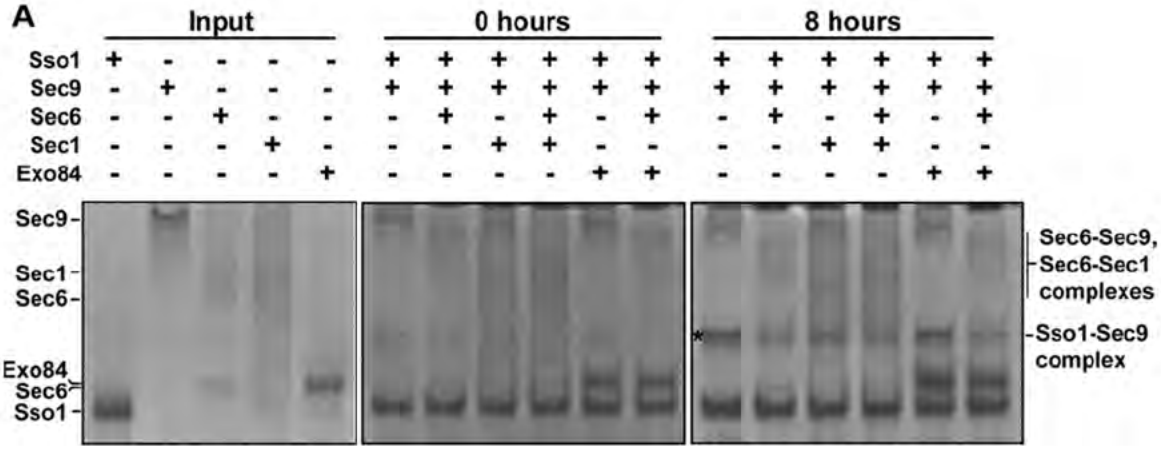

Figure 5.7 Sec6 inhibition of SNARE complex assembly. Sec6 inhibits Sec9–Sso1 formation; this is not relieved by addition of Sec1. Purified Sec6 ± Sec1 proteins were incubated at equimolar concentrations with Sso1 and Sec9 for 0 or 8 h at 18°C to allow SNARE complex assembly. Reactions were run on 6% native PAGE gels and stained with Coomassie blue. Representative gels (more than three experiments at four different time points were run) for the 0 h (middle) and 8 h (right) time points are shown; the uncomplexed proteins were run on a separate gel for comparison (left). Asterisk indicates the mobility of the Sso1–Sec9 complex.

APPENDIX H: Investigating the role of the exocyst subunit Sec6 in exocyst polarization using *sec6-49* and *sec6-54**

*These studies are based upon findings of Songer and Munson, 2009

Significant background and rationale (based on Songer and Munson, 2009):

Our lab previously identified a requirement for the exocyst subunit Sec6 in the proper localization of the exocyst complex. Two different patches of highly conserved residues on the surface of Sec6 were mutated to generate two temperature-sensitive (ts) *S. cerevisiae mutants*: *sec6-49* and *sec6-54*. Both mutants displayed severe growth and secretion defects at the non-permissive temperature and were inviable in YPD rich media. Additionally, at the non-permissive temperature, all of the exocyst subunits showed severe mislocalization while complex assembly was unaffected. Therefore, it was proposed that these mutants may be defective in binding to a partner that facilitates exocyst localization at polarized secretion sites on the plasma membrane. Purified Sec6-49p and Sec6-54p still bound to known partners including Sec9 and several exocyst subunits, so the unknown "anchor" factor remains to be identified. Furthermore, this study also revealed that exocyst assembly and localization are functionally separate events.

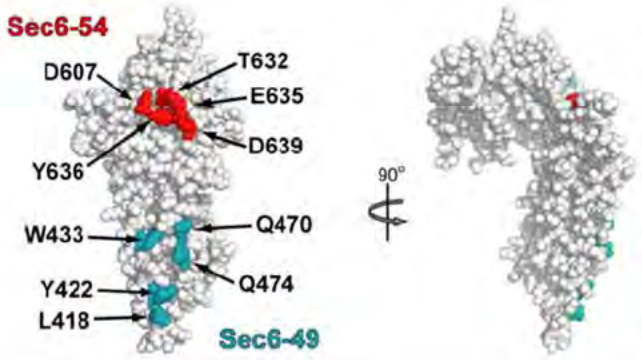

Figure 5.8 Mutations of highly conserved surface residues in yeast Sec6p. Structure of the C-terminal domain of Sec6p, showing the location of the conserved patch amino acids. The Patch-1 residues L418, Y422, W433, Q470, Q474, and V478 were mutated to Ala (*sec6-49*). In Patch-2, residues D607, T632, and Y636 were mutated to Ala, and residues E635 and D639 mutated to Arg, to create *sec6-54*. (Adapted from Songer and Munson, 2009).

These studies brought up several new questions, which I aimed to address. The exocyst complex no longer exhibits characteristic foci of localization at the bud tip. However, it is unclear whether the exocyst is still on the plasma membrane and unpolarized or if the complex has become cytosolic. Furthermore, it remains to be tested whether localization is the true defect in these mutants or if the loss of localization is an outcome of another defect such as a failure of exocyst complexes to disassemble for recycling after tethering events. Our recent results, which indicate that the exocyst complex remains assembled at all times, are not consistent with this possibility (Chapter II). Finally, the surface residues mutated are highly conserved and indicative of a putative protein-protein interaction site, so we predict that there is a Sec6 binding partner that remains to be identified. Once the partner is known, more information will be available for understanding the functional impact of this interaction.

Osh4 overexpression studies

The Beh lab (Simon Fraser University) proposed a potential interaction between Sec6 and the putative sterol transport factor Osh4. In their studies, they purified post-Golgi secretory vesicles and observed that Osh4 co-fractionation with vesicles was dependent on exocyst function because this interaction was lost in *sec6-4* and *sec6-49*. Furthermore, using co-immunoprecipitation they observed interactions between Osh4 and Cdc42, Rho1, Sec4, and Sec6. Since Osh4 association with vesicles was disrupted in *sec6-49*, a mutant where exocyst complexes remain assembled, they concluded that Osh4's direct binding partner may be Sec6 (Alfaro et al., 2011). However, since the co-immunoprecipitation studies were performed in extract, it is possible that this is not a

direct interaction and the loss of Osh4 on vesicles may be due to the loss of properly localized exocyst complex (or other function lost in the *sec6-49* mutant).

As part of a candidate-based approach to search for the putative "anchor" factor, we went on to characterize the potential role of this interaction using genetic interaction studies. Overexpression of a binding partner (such as by using a high copy 2µ plasmid) can sometimes rescue the phenotypic defects of a yeast strain mutated for binding that partner. A 2µ plasmid expressing OSH4 (or an empty vector) was transformed into yeast strains expressing either *SEC6*, *sec6-4, sec6-49*, or *sec6-54* as the sole copy of Sec6 on a *CEN LEU* plasmid. We did not observe rescue of *sec6* mutant growth by OSH4 overexpression (Fig. 5.9). However, a slight synthetic negative growth defect could be seen for *sec6-49* and *sec6-54* upon OSH4 overexpression even at permissive temperatures in some experiments (Fig. 5.9). As we did not observe a clear result from these studies, we did not further pursue the possible interaction between exocyst and Osh4.

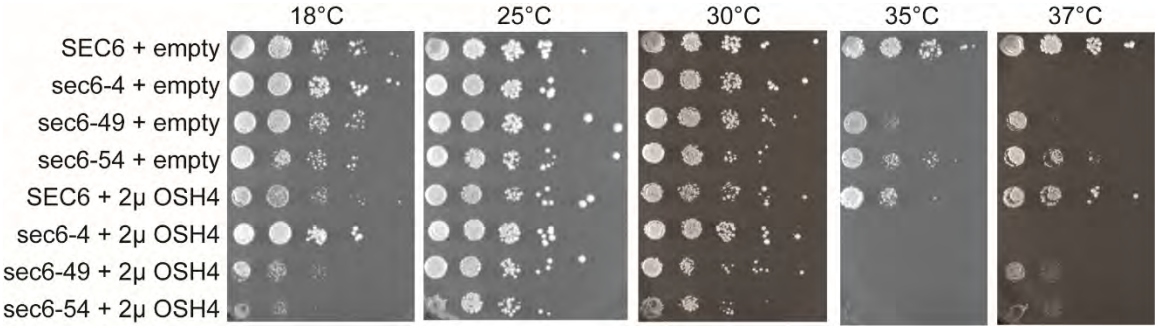

Figure 5.9 Investigating a potential genetic interaction between SEC6 and OSH4. OSH4 was overexpressed using a 2µ URA plasmid in strains expressing SEC6, *sec6-4, sec6-49*, or *sec6-54* as the sole copy of Sec6 on a CEN LEU plasmid. Synthetic genetic effects were assessed as a function of growth by serial dilution growth assay on SC-URA plates at the indicated temperatures.

Plasma membrane targeting

If the major deficiency in the *sec6-49* and *sec6-54* mutants is mislocalization, then the phenotype should be rescued by forcing Sec6-49p or Sec6-54p localization at polarized membrane sites. Many cytosolic proteins are targeted to the plasma membrane and polarized sites by distinct protein- or lipid-interacting domains. The Cdc42/Rac Interactive Binding (CRIB) domain has been identified in many effectors of Cdc42p and is required for binding to the GTP-bound form of Cdc42p (Zhang et al., 2008; Burbelo et al., 1995; Lamson et al., 2002; Orlando et al., 2008). Additionally, upstream polybasic (PB) motifs, such as the one found in the Cdc42 effector Gic2p, are proposed to enhance membrane association through interactions with negatively charged phospholipids (Zhang et al., 2008). Fusing the Gic2 CRIB domain/PB motif to the C-termini of Sec6-49p and Sec6-54p may be sufficient for re-polarizing the exocyst complex at the plasma membrane. Another possibility is to add a C-terminal polybasic sequence and CAAX motif to Sec6p, Sec6-49p and Sec6-54p. This is the target sequence for the addition of a lipid moiety that anchors proteins into membranes and is a required motif for the localization of Cdc42p (Johnson et al., 1999; Fairn et al., 2010). However, this motif is not sufficient for polarization and could lead to localization at other intracellular membranes as well (Richman et al., 2002), but it is possible that a sufficient amount of exocyst would be properly localized to rescue the exocytic defects of the mutants. Additionally, if properly localized, the CAAX motif/PB motif-tagged Sec6p could demonstrate if physical anchoring in the plasma membrane is detrimental for exocyst

function; for example, a growth defect may be observed if Sec6p needs to be recycled off the plasma membrane following a vesicle tethering and docking event.

Two different truncations of the wild-type Gic2 N-terminal region (aa 1-208 or aa 96-208) with a V5 epitope tag (for detection by western blot and immunofluorescence) were fused to the C-termini of either *SEC6 CEN LEU*, *sec6-49 CEN LEU*, or *sec6-54 CEN LEU*, under the control of the SEC6 promoter. Each of these tags contains the basic residues (PB motif) and CRIB motif found in Gic2, but Gic2(1-208) contains an additional functional domain that is predicted, but not yet confirmed, to be unnecessary for membrane targeting (Peter Pryciak, communication). As an alternative approach, the CCAAX motif from the yeast Ras2 protein with an upstream V5 epitope tag were also fused to wild-type and mutant Sec6 on *CEN* plasmids. To assay whether C-terminal tagging itself is detrimental to the Sec6 proteins, a mutated form of the CCAAX motif (SSAAX) that is not membrane-targeting was also tested. Each *CEN LEU* plasmid was plasmid shuffled into a strain expressing *SEC6 CEN URA* by counter-selection of URA3-expression on 5-FOA. Thus, each tagged protein could be tested for rescue of cellular growth as the sole copy of Sec6 (Fig. 5.10). None of the tags negatively impacted the growth of wild-type SEC6. Neither *sec6-49* or *sec6-54* was viable with the Gic2(1-208)-V5, V5-CCAAX, or V5-SSAAX tags consistent with previous studies suggesting these mutants were only viable with the short HA epitope tag at their C-termini (Songer and Munson, 2009). However, it is also possible that plasma membrane targeting was successful in these constructs and that the targeting itself had a negative functional consequence, perhaps by mis-targeting the few remaining functional exocyst complexes.

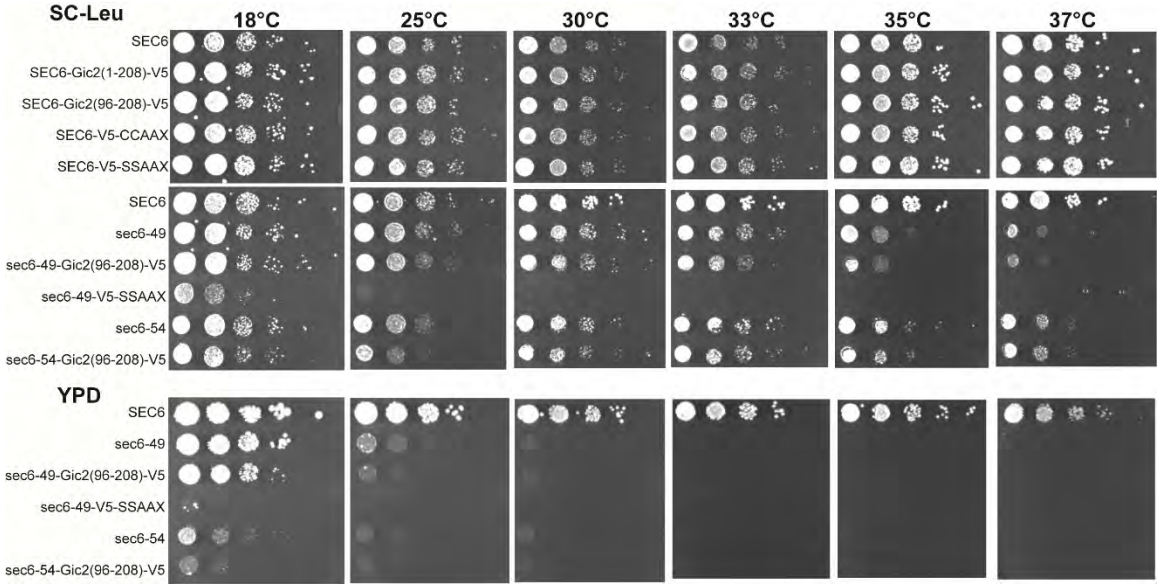

Figure 5.10 The growth defects of *sec6-49* and *sec6-54* are not rescued by C-terminal plasma membrane targeting sequences, assayed by serial dilution growth assay. SEC6, *sec6-49*, and *sec6-54* were fused at the C-terminus with the indicated tags, expressed at endogenous levels on CEN plasmids as the sole copy. SC-Leu=synthetic complete media without Leucine.

Neither *sec6-49* nor *sec6-54* growth was rescued by the Gic2(96-208)-V5 tag (Fig. 5.10). The expression of the fusion proteins was confirmed by Western blot in strains expressing wild-type *SEC6 CEN URA* plasmid in the presence of *SEC6 CEN LEU, sec6-49 CEN LEU*, or *sec6-54 CEN LEU* plasmids. All tagged proteins were the correct molecular weight and were expressed at similar levels to wild-type protein, with the exception of the Gic2(96-208)-V5 constructs, which ran smaller than expected by western blot (data not shown).

It is important to note that the endogenous Gic2 targeting sequence is found at its N-terminus and we wondered whether this might be required for targeting Sec6. Furthermore, it is possible that *sec6-49* and *sec6-54* might be more amenable to N-terminal tagging as C-terminal tagging was already shown to be problematic (Songer and Munson, 2009). However, before proceeding with generating these constructs, we sought

to investigate whether these targeting sequences were functioning as expected by fusing the same sequences to GFP protein alone. *CEN LEU* plasmids were cloned with Sec6 regulatory elements, GFP, and the C-terminal membrane-targeting tags (Gic2(1-208)-V5, Gic2(96-208)-V5, V5-CCAAX, V5-SSAAX) and transformed into wild-type yeast. The expression levels and localization patterns for each construct were highly variable, thus these experiments were inconclusive. Further testing with higher expression plasmids (2μ and *GAL CEN*) containing GFP fused with these targeting sequences revealed that the sequences are functional for targeting. Lower expression level constructs similar to the expression level of Sec6, such as Ste5, were more difficult to detect (Fig. 5.11, right). Therefore, the low copy number of exocyst subunits (Ghaemmaghami et al., 2003; Kulak et al., 2014; Chong et al., 2015) makes imaging a challenging approach for validating the efficiency of membrane targeting by these tags.

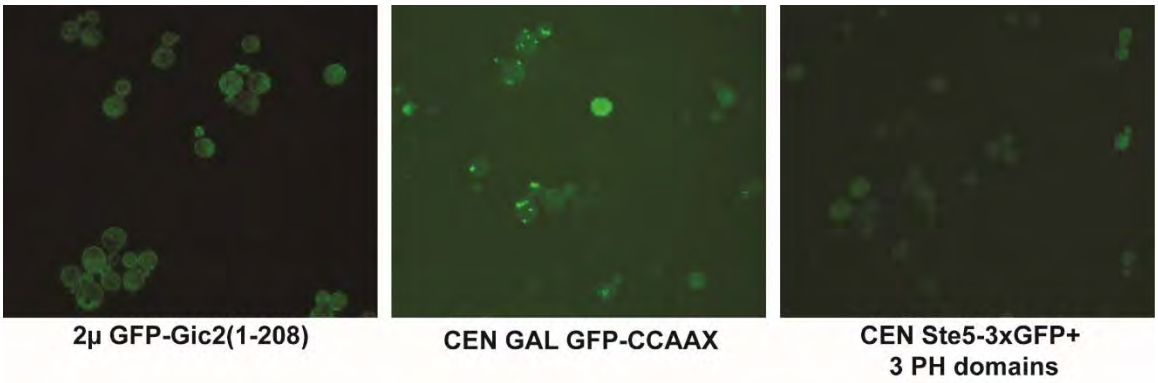

Figure 5.11 Visualizing plasma membrane targeting constructs of varied expression levels using wide-field fluorescence microscopy. (Left) GFP alone with indicated Gic2 sequence on 2μ overexpression plasmid was readily visualized at cell periphery. (Center) GFP with CCAAX motif was expressed under GAL promoter and readily visualized in punctate structures. (Right) GFP-tagged Ste5 protein expressed at endogenous levels was difficult to visualize due to low copy number in *S. cerevisiae*. Magnification=1000x.

N-terminal Gic2 sequences (1-208) and (96-208) were tested at the N-termini of SEC6, *sec6-49*, and *sec6-54* in *CEN LEU* plasmids under the control of the SEC6 promoter. These tags did not impact growth either positively or negatively for SEC6, *sec6-49*, or *sec6-54* (Fig. 5.12). It remains to be tested whether or not these tags are sufficient for targeting Sec6, but the low endogenous expression level and likely incomplete targeting of Sec6 made this challenging to resolve. It is possible that directing

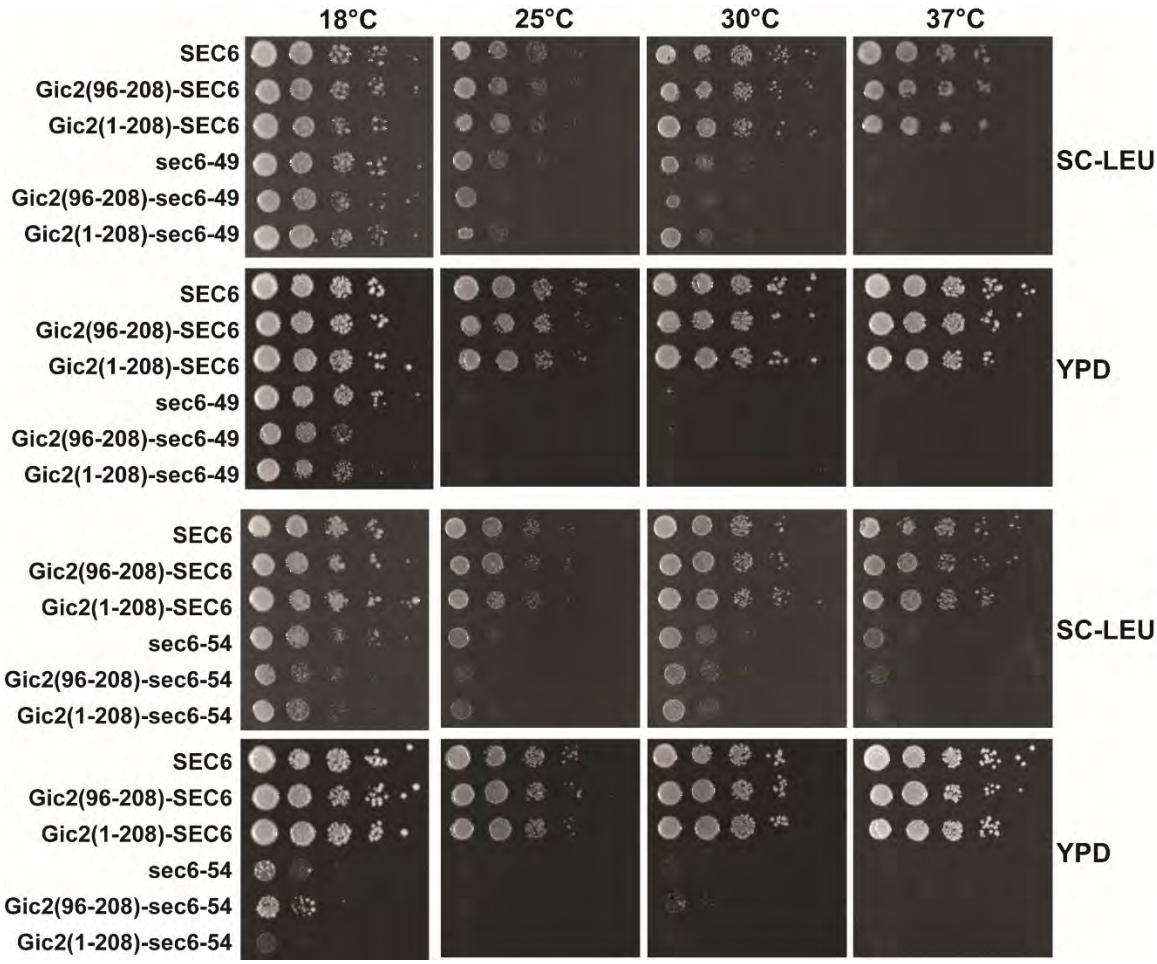

Figure 5.12 Investigating growth effects of targeting Sec6 and mutants to the plasma membrane using N-terminal tagging constructs. SEC6, *sec6-49*, and *sec6-54* were fused at the N-terminus with the indicated tags, expressed at endogenous levels on CEN plasmids as the sole copy, and assayed for growth by serial dilution assay. None of the targeting tags rescued growth of *sec6-49* and *sec6-54* but tagged mutant strains were viable in this case. SC-Leu=synthetic complete media without Leucine.

Sec6, Sec6-49p, and Sec6-54p to the plasma membrane does not occur in the context of the assembled exocyst complex due to masking of the CRIB motif. Additionally, it is possible that the complex is being properly targeted but re-localization is not sufficient to rescue the phenotype.

In order to obtain more consistent expression levels, the *sec6-49* (MMY1174) and *sec6-54* (MMY1281) alleles were integrated at the genomic locus. These strains exhibited

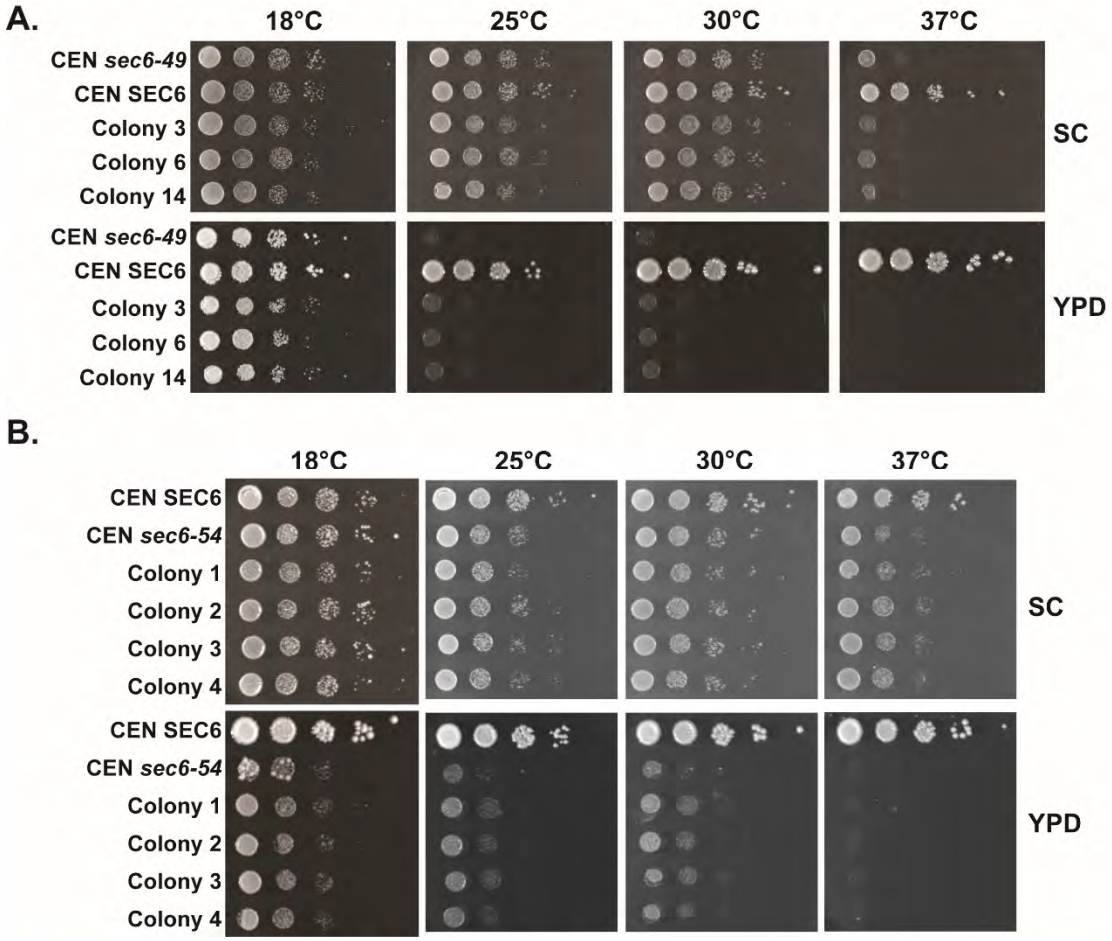

Figure 5.13 Genomic integration of *sec6-49* and *sec6-54.* Several colonies for each integrated strain were tested for growth compared to strains expressing the mutant or wild-type gene on a CEN plasmid. The genomic integration versions of the mutants displayed the same growth as plasmid-borne mutants by serial dilution growth assay. (A) *sec6-49* was integrated into BY4742 using a linear PCR product with a LYS2 marker. Transformants were validated by sequencing. (B) *sec6-54* was integrated into BY4743 using a linear PCR product with a URA3 marker. Diploids were sporulated and haploids were confirmed by temperature-sensitivity and sequencing.

similar growth patterns to the plasmid-borne copy strains, with severe growth defects on synthetic media at higher temperatures and no growth on rich media except at permissive temperatures (Fig 5.13). Preliminary examination of exocyst localization changes in the integrated *sec6-49* and *sec6-54* strains indicated mislocalization at the non-permissive temperature, as expected, but remains to be completed quantitatively.

In summary, it is not clear whether the plasma membrane targeting of Sec6 or the mutants is occurring properly and further experiments are required to draw firm conclusions. It is unlikely that further analyzing the C-terminally-tagged constructs will be fruitful, as none of them rescued growth and it is likely that the tags further exacerbate the loss of function in *sec6-49* and *sec6-54*. The next step will be to further characterize the Gic2(1-208) N-terminal tags to see whether targeting is properly occurring, in order to conclude whether re-localization of the exocyst can rescue the mutants. Since imaging approaches have proven challenging given the low signal of exocyst subunits by fluorescence microscopy and the likely incomplete targeting of these proteins, cell fractionation experiments may give clearer results.

Proteomics screen for Sec6 interacting partner

We decided to also use a proteomics approach to identify the disrupted interacting partner in *sec6-49* and *sec6-54*. To this end, we integrated a C-terminal Protein-A tag on Sec8 in the integrated *sec6-49* and *sec6-54* strains, in order to purify exocyst complexes and identify changes in associated binding partners. We purified Sec8-PrA tagged exocyst complexes from yeast strains expressing SEC6, *sec6-49*, or *sec6-54* that were

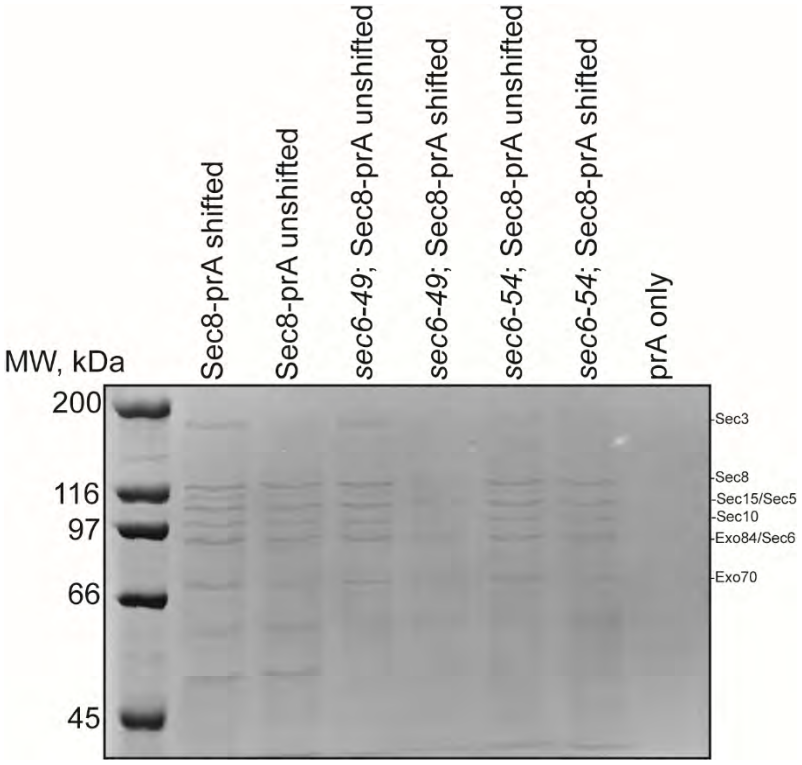

Figure 5.14 Purification of wild-type, *sec6-49*, and *sec6-54* exocyst complexes using Sec8-PrA. Purified complexes were visualized by SDS-PAGE and Coomassie staining. In all cases, particularly with *sec6-49*, exocyst yield was lower after the 3 hour temperature shift at 37°C in SC media.

either shifted for 3 hours at 37°C or unshifted. We used a lower salt condition (150 mM NaCl) in order to increase the level of binding of weaker partners and PPX native digestion from the beads to reduce non-specific partners associated with the beads in our samples (Fig. 5.14). The levels of recovered exocyst complex were lower in temperature-shifted samples consistent with previous studies (Songer and Munson, 2009) but may be sufficient for mass spectrometry studies. The stoichiometry of exocyst subunits does not appear to be different, as expected from previous studies (Songer and Munson, 2009), but this remains to be tested quantitatively.

These experiments serve as a good proof of principle that we will be able to purify sufficient levels of the mutant exocyst complexes for proteomic studies. Further optimization is required for increasing the recovery of digested complexes from the IgG beads, particularly in lower salt conditions. Additionally, as a membrane-anchored or membrane-associated factor is the most likely candidate for the exocyst anchoring factor,

purification buffer containing different detergents will also need to be tested for solubilization of these factors during lysis. The next stage will be to send these samples for mass spectrometry and determine the differences in binding partner profiles for SEC6 versus *sec6-49* and *sec6-54*, as well as temperature-shifted versus unshifted samples.

REFERENCES

Aalto, M.K., Ronne, H., and Keränen, S. (1993). Yeast syntaxins Sso1p and Sso2p belong to a family of related membrane proteins that function in vesicular transport. The EMBO Journal 12, 4095-104.

Abenza, J.F., Galindo, A., Pinar, M., Pantazopoulou, A., de Rios, V.L., and Penalva, M.A. (2012). Endosomal maturation by Rab conversion in Aspergillus nidulans is coupled to dynein-mediated basipetal movement. Molecular Biology Of The Cell 23, 1889-1901.

Abenza, J.F., Galindo, A., Pantazopoulou, A., Gil, C., de Ríos, V.L., and Peñalva, M.A. (2010). Aspergillus RabB Rab5 integrates acquisition of degradative identity with the long distance movement of early endosomes. Molecular Biology Of The Cell 21, 2756-69.

Adamo, J.E., Rossi, G., and Brennwald, P. (1999). The Rho GTPase Rho3 has a direct role in exocytosis that is distinct from its role in actin polarity. Molecular Biology Of The Cell 10, 4121-33.

Adamo, J.E., Moskow, J.J., Gladfelter, A.S., Viterbo, D., Lew, D.J., and Brennwald, P.J. (2001). Yeast Cdc42 functions at a late step in exocytosis, specifically during polarized growth of the emerging bud. The Journal Of Cell Biology 155, 581-92.

Aggarwal, V., and Ha, T. (2014). Single-molecule pull-down (SiMPull) for new-age biochemistry: methodology and biochemical applications of single-molecule pull-down (SiMPull) for probing biomolecular interactions in crude cell extracts. Bioessays: News And Reviews In Molecular, Cellular And Developmental Biology 36, 1109-19.

Alfaro, G., Johansen, J., Dighe, S.A., Duamel, G., Kozminski, K.G., and Beh, C.T. (2011). The sterol-binding protein Kes1/Osh4p is a regulator of polarized exocytosis. Traffic 12, 1521-36.

Araç, D., Dulubova, I., Pei, J., Huryeva, I., Grishin, N.V., and Rizo, J. (2005). Three-dimensional structure of the rSly1 N-terminal domain reveals a conformational change induced by binding to syntaxin 5. Journal Of Molecular Biology 346, 589-601.

Baek, K., Knödler, A., Lee, S.H., Zhang, X., Orl, K., Orlando, K., o, Zhang, J., Foskett, T.J., Guo, W., et al. (2010). Structure-function study of the N-terminal domain of exocyst subunit Sec3. The Journal Of Biological Chemistry 285, 10424-33.

Balderhaar, H.J.K., and Ungermann, C. (2013). CORVET and HOPS tethering complexes - coordinators of endosome and lysosome fusion. Journal Of Cell Science 126, 1307-16.

Balderhaar, H.J.K., Lachmann, J., Yavavli, E., Bröcker, C., Lürick, A., and Ungermann, C. (2013). The CORVET complex promotes tethering and fusion of Rab5/Vps21-positive membranes. Proceedings Of The National Academy Of Sciences Of The United States Of America 110, 3823-8.

Barlowe, C. (1997). Coupled ER to Golgi transport reconstituted with purified cytosolic proteins. The Journal Of Cell Biology 139, 1097-108.

Barrowman, J., Bhandari, D., Reinisch, K., and Ferro-Novick, S. (2010). TRAPP complexes in membrane traffic: convergence through a common Rab. Nature Reviews. Molecular Cell Biology 11, 759-63.

Bendezú, F.O., and Martin, S.G. (2011). Actin cables and the exocyst form two independent morphogenesis pathways in the fission yeast. Molecular Biology Of The Cell 22, 44-53.

Bielinski, D.F., Pyun, H.Y., Linko-Stentz, K., Macara, I.G., and Fine, R.E. (1993). Ral and Rab3a are major GTP-binding proteins of axonal rapid transport and synaptic vesicles and do not redistribute following depolarization stimulated synaptosomal exocytosis. Biochimica Et Biophysica Acta 1151, 246-56.

Bodemann, B.O., Orvedahl, A., Cheng, T., Ram, R.R., Ou, Y., Formstecher, E., Maiti, M., Hazelett, C.C., Wauson, E.M., Balakireva, M., et al. (2011). RalB and the exocyst mediate the cellular starvation response by direct activation of autophagosome assembly. Cell 144, 253-67.

Bonifacino, J.S., and Glick, B.S. (2004). The mechanisms of vesicle budding and fusion. Cell 116, 153-66.

Bonifacino, J.S., and Hierro, A. (2011). Transport according to GARP: receiving retrograde cargo at the trans-Golgi network. Trends In Cell Biology 21, 159-67.

Bowser, R., and Novick, P. (1991). Sec15 protein, an essential component of the exocytotic apparatus, is associated with the plasma membrane and with a soluble 19.5S particle. The Journal Of Cell Biology 112, 1117-31.

Bowser, R., Müller, H., Govindan, B., and Novick, P. (1992). Sec8p and Sec15p are components of a plasma membrane-associated 19.5S particle that may function downstream of Sec4p to control exocytosis. The Journal Of Cell Biology 118, 1041-56.

Boyd, C., Hughes, T., Pypaert, M., and Novick, P. (2004). Vesicles carry most exocyst subunits to exocytic sites marked by the remaining two subunits, Sec3p and Exo70p. The Journal Of Cell Biology 167, 889-901.

Bracher, A., and Weissenhorn, W. (2002). Structural basis for the Golgi membrane recruitment of Sly1p by Sed5p. The EMBO Journal 21, 6114-24.

Brachmann, C.B., Davies, A., Cost, G.J., Caputo, E., Li, J., Hieter, P., and Boeke, J.D. (1998). Designer deletion strains derived from Saccharomyces cerevisiae S288C: a useful set of strains and plasmids for PCR-mediated gene disruption and other applications. Yeast 14, 115-32.

Brennwald, P., Kearns, B., Champion, K., Keränen, S., Bankaitis, V., and Novick, P. (1994). Sec9 is a SNAP-25-like component of a yeast SNARE complex that may be the effector of Sec4 function in exocytosis. Cell 79, 245-58.

Brunet, S., and Sacher, M. (2014). Are all multisubunit tethering complexes bona fide tethers? Traffic 15, 1282-7.

Burbelo, P.D., Drechsel, D., and Hall, A. (1995). A conserved binding motif defines numerous candidate target proteins for both Cdc42 and Rac GTPases. The Journal Of Biological Chemistry 270, 29071-4.

Burkhardt, P., Hattendorf, D.A., Weis, W.I., and Fasshauer, D. (2008). Munc18a controls SNARE assembly through its interaction with the syntaxin N-peptide. The EMBO Journal 27, 923-33.

Cai, H., Reinisch, K., and Ferro-Novick, S. (2007). Coats, tethers, Rabs, and SNAREs work together to mediate the intracellular destination of a transport vesicle. Developmental Cell 12, 671-82.

Cai, H., Yu, S., Menon, S., Cai, Y., Lazarova, D., Fu, C., Reinisch, K., Hay, J.C., and Ferro-Novick, S. (2007). TRAPPI tethers COPII vesicles by binding the coat subunit Sec23. Nature 445, 941-4.

Camonis, J.H., and White, M.A. (2005). Ral GTPases: corrupting the exocyst in cancer cells. Trends In Cell Biology 15, 327-32.

Cao, X., Ballew, N., and Barlowe, C. (1998). Initial docking of ER-derived vesicles requires Uso1p and Ypt1p but is independent of SNARE proteins. The EMBO Journal 17, 2156-65.

Carpp, L.N., Ciufo, L.F., Shanks, S.G., Boyd, A., and Bryant, N.J. (2006). The Sec1p/Munc18 protein Vps45p binds its cognate SNARE proteins via two distinct modes. The Journal Of Cell Biology 173, 927-36.

Carr, C.M., Grote, E., Munson, M., Hughson, F.M., and Novick, P.J. (1999). Sec1p binds to SNARE complexes and concentrates at sites of secretion. The Journal Of Cell Biology 146, 333-44.

Carr, C.M., and Rizo, J. (2010). At the junction of SNARE and SM protein function. Current Opinion In Cell Biology 22, 488-95.

Cavanaugh, L.F., Chen, X., Richardson, B.C., Ungar, D., Pelczer, I., Rizo, J., and Hughson, F.M. (2007). Structural analysis of conserved oligomeric Golgi complex subunit 2. The Journal Of Biological Chemistry 282, 23418-26.

Chen, X., Inoue, M., Hsu, S.C., and Saltiel, A.R. (2006). RalA-exocyst-dependent recycling endosome trafficking is required for the completion of cytokinesis. The Journal Of Biological Chemistry 281, 38609-16.

Chen, X., Leto, D., Xiao, J., Goss, J., Wang, Q., Shavit, J.A., Xiong, T., Yu, G., Ginsburg, D., Toomre, D., et al. (2011). Exocyst function is regulated by effector phosphorylation. Nature Cell Biology 13, 580-8.

Cheung, P.P., Limouse, C., Mabuchi, H., and Pfeffer, S.R. (2015). Protein flexibility is required for vesicle tethering at the Golgi. Elife 4.

Chien, Y., Kim, S., Bumeister, R., Loo, Y., Kwon, S.W., Johnson, C.L., Balakireva, M.G., Romeo, Y., Kopelovich, L., Gale, M., Jr, et al. (2006). RalB GTPase-mediated activation of the IkappaB family kinase TBK1 couples innate immune signaling to tumor cell survival. Cell 127, 157-70.

Chong, Y.T., Chong, A.T., Koh, J.L.Y., Friesen, H., Duffy, S.K., Duffy, K., Cox, M.J., Moses, A., Moffat, J., Boone, C., et al. (2015). Yeast Proteome Dynamics from Single Cell Imaging and Automated Analysis. Cell 161, 1413-24.

Conibear, E., and Stevens, T.H. (2000). Vps52p, Vps53p, and Vps54p form a novel multisubunit complex required for protein sorting at the yeast late Golgi. Molecular Biology Of The Cell 11, 305-23.

Conibear, E., Cleck, J.N., and Stevens, T.H. (2003). Vps51p mediates the association of the GARP (Vps52/53/54) complex with the late Golgi t-SNARE Tlg1p. Molecular Biology Of The Cell 14, 1610-23.

Crawford, D.J., Hoskins, A.A., Friedman, L.J., Gelles, J., and Moore, M.J. (2008). Visualizing the splicing of single pre-mRNA molecules in whole cell extract. RNA 14, 170-9.

Croteau, N.J., Schultz, P.G., Anderson, J.C., and Munson, M. (2009). Conservation of helical bundle structure between the exocyst subunits. Plos One 4, e4443.

Cvrčková, F., Grunt, M., Bezvoda, R., Hála, M., Kulich, I., Rawat, A., and Žárský, V. (2012). Evolution of the Land Plant Exocyst Complexes. Frontiers In Plant Science 3.

Amlan, das, and Guo, W. (2011). Rabs and the exocyst in ciliogenesis, tubulogenesis and beyond. Trends In Cell Biology 21, 383-6.

de Craene, J., Coleman, J., de Martin, P.E., Pypaert, M., Anderson, S., 3rd, J.R.Y., Ferro-Novick, S., and Novick, P. (2006). Rtn1p is involved in structuring the cortical endoplasmic reticulum. Molecular Biology Of The Cell 17, 3009-20.

Derby, M.C., Lieu, Z.Z., Brown, D., Stow, J.L., Goud, B., and Gleeson, P.A. (2007). The trans-Golgi network golgin, GCC185, is required for endosome-to-Golgi transport and maintenance of Golgi structure. Traffic 8, 758-73.

Dickson, R.M., Cubitt, A.B., Tsien, R.Y., and Moerner, W.E. (1997). On/off blinking and switching behaviour of single molecules of green fluorescent protein. Nature 388, 355-8.

Dong, G., Hutagalung, A.H., Fu, C., Novick, P., and Reinisch, K.M. (2005). The structures of exocyst subunit Exo70p and the Exo84p C-terminal domains reveal a common motif. Nature Structural & Molecular Biology 12, 1094-100.

Donovan, K.W., and Bretscher, A. (2015). Tracking individual secretory vesicles during exocytosis reveals an ordered and regulated process. The Journal Of Cell Biology 210, 181-189.

Donovan, K.W., and Bretscher, A. (2012). Myosin-V is activated by binding secretory cargo and released in coordination with Rab/exocyst function. Developmental Cell 23, 769-81.

Dubuke, M.L., Maniatis, S., Shaffer, S.A., and Munson, M. (2015). The Exocyst Subunit Sec6 Interacts with Assembled Exocytic SNARE Complexes. The Journal Of Biological Chemistry 290, 28245-56.

Dulubova, I., Yamaguchi, T., Wang, Y., Südhof, T.C., and Rizo, J. (2001). Vam3p structure reveals conserved and divergent properties of syntaxins. Nature Structural Biology 8, 258-64.

Dulubova, I., Zhu, H., Houry, W.A., Huryeva, I., Südhof, T.C., and Rizo, J. (2007). Munc18-1 binds directly to the neuronal SNARE complex. Proceedings Of The National Academy Of Sciences Of The United States Of America 104, 2697-702.

Fairn, G.D., Hermansson, M., Somerharju, P., and Grinstein, S. (2011). Phosphatidylserine is polarized and required for proper Cdc42 localization and for development of cell polarity. Nature Cell Biology 13, 1424-1430.

Fasshauer, D., Antonin, W., Margittai, M., Pabst, S., and Jahn, R. (1999). Mixed and non-cognate SNARE complexes. Characterization of assembly and biophysical properties. The Journal Of Biological Chemistry 274, 15440-6.

Fendrych, M., Synek, L., Pecenkova, T., Toupalova, H., Cole, R., Drdova, E., Nebesarova, J., Sedinova, M., Hala, M., Fowler, J.E., et al. (2010). The Arabidopsis Exocyst Complex Is Involved in Cytokinesis and Cell Plate Maturation. The Plant Cell 22, 3053-3065.

Finger, F.P., and Novick, P. (1997). Sec3p is involved in secretion and morphogenesis in Saccharomyces cerevisiae. Molecular Biology Of The Cell 8, 647-62.

Finger, F.P., Hughes, T.E., and Novick, P. (1998). Sec3p is a spatial landmark for polarized secretion in budding yeast. Cell 92, 559-71.

Forsmark, A., Rossi, G., Wadskog, I., Brennwald, P., Warringer, J., and Adler, L. (2011). Quantitative proteomics of yeast post-Golgi vesicles reveals a discriminating role for Sro7p in protein secretion. Traffic 12, 740-53.

Friedman, L.J., Chung, J., and Gelles, J. (2006). Viewing dynamic assembly of molecular complexes by multi-wavelength single-molecule fluorescence. Biophysical Journal 91, 1023-31.

Friedman, L.J., and Gelles, J. (2015). Multi-wavelength single-molecule fluorescence analysis of transcription mechanisms. Methods 86, 27-36.

Friedrich, G.A., Hildebr, J.D., Hildebrand, J.D., and Soriano, P. (1997). The secretory protein Sec8 is required for paraxial mesoderm formation in the mouse. Developmental Biology 192, 364-74.

Fukai, S., Matern, H.T., Jagath, J.R., Scheller, R.H., and Brunger, A.T. (2003). Structural basis of the interaction between RalA and Sec5, a subunit of the sec6/8 complex. The EMBO Journal 22, 3267-78.

Furgason, M.L.M., MacDonald, C., Shanks, S.G., Ryder, S.P., Bryant, N.J., and Munson, M. (2009). The N-terminal peptide of the syntaxin Tlg2p modulates binding of its closed conformation to Vps45p. Proceedings Of The National Academy Of Sciences Of The United States Of America 106, 14303-8.

Gallwitz, D., and Jahn, R. (2003). The riddle of the Sec1/Munc-18 proteins - new twists added to their interactions with SNAREs. Trends In Biochemical Sciences 28, 113-6.

Garcia, E.P., McPherson, P.S., Chilcote, T.J., Takei, K., and de Camilli, P. (1995). rbSec1A and B colocalize with syntaxin 1 and SNAP-25 throughout the axon, but are not in a stable complex with syntaxin. The Journal Of Cell Biology 129, 105-20.

Gerst, J.E., Rodgers, L., Riggs, M., and Wigler, M. (1992). SNC1, a yeast homolog of the synaptic vesicle-associated membrane protein/synaptobrevin gene family: genetic interactions with the RAS and CAP genes. Proceedings Of The National Academy Of Sciences Of The United States Of America 89, 4338-42.

Ghaemmaghami, S., Huh, W., Bower, K., Howson, R.W., Belle, A., Dephoure, N., O'Shea, E.K., and Weissman, J.S. (2003). Global analysis of protein expression in yeast. Nature 425, 737-41.

Giansanti, M.G., E., T., erleest, Jewett, C.E., Sechi, S., Frappaolo, A., Fabian, L., Robinett, C.C., Brill, J.A., Loerke, D., et al. (2015). Exocyst-Dependent Membrane Addition Is Required for Anaphase Cell Elongation and Cytokinesis in Drosophila. PLOS Genetics 11, e1005632.

Gillingham, A.K., and Munro, S. (2003). Long coiled-coil proteins and membrane traffic. Biochimica Et Biophysica Acta 1641, 71-85.

Goud, B., Salminen, A., Walworth, N.C., and Novick, P.J. (1988). A GTP-binding protein required for secretion rapidly associates with secretory vesicles and the plasma membrane in yeast. Cell 53, 753-68.

Goud, B., and Gleeson, P.A. (2010). TGN golgins, Rabs and cytoskeleton: regulating the Golgi trafficking highways. Trends In Cell Biology 20, 329-36.

Govindan, B., Bowser, R., and Novick, P. (1995). The role of Myo2, a yeast class V myosin, in vesicular transport. The Journal Of Cell Biology 128, 1055-68.

Grindstaff, K.K., Yeaman, C., An, N., Anandasabapathy, N., asabapathy, Hsu, S.C., Rodriguez-Boulan, E., Scheller, R.H., and Nelson, W.J. (1998). Sec6/8 complex is recruited to cell-cell contacts and specifies transport vesicle delivery to the basal-lateral membrane in epithelial cells. Cell 93, 731-40.

Gromley, A., Yeaman, C., Rosa, J., Redick, S., Chen, C., Mirabelle, S., Guha, M., Sillibourne, J., and Doxsey, S.J. (2005). Centriolin anchoring of exocyst and SNARE complexes at the midbody is required for secretory-vesicle-mediated abscission. Cell 123, 75-87.

Grosshans, B.L., Andreeva, A., Gangar, A., Niessen, S., 3rd, J.R.Y., Brennwald, P., and Novick, P. (2006). The yeast lgl family member Sro7p is an effector of the secretory Rab GTPase Sec4p. The Journal Of Cell Biology 172, 55-66.

Grote, E., Carr, C.M., and Novick, P.J. (2000). Ordering the final events in yeast exocytosis. The Journal Of Cell Biology 151, 439-52.

Guermonprez, H., Smertenko, A., Crosnier, M.-., Durandet, M., Vrielynck, N., Guerche, P., Hussey, P.J., Satiat-Jeunemaitre, B., and Bonhomme, S. (2008). The POK/AtVPS52 protein localizes to several distinct post-Golgi compartments in sporophytic and gametophytic cells. Journal Of Experimental Botany 59, 3087-3098.

Guichard, A., Nizet, V., and Bier, E. (2014). RAB11-mediated trafficking in host–pathogen interactions. Nature Reviews Microbiology 12, 624-634.

Guo, W., Roth, D., Walch-Solimena, C., and Novick, P. (1999). The exocyst is an effector for Sec4p, targeting secretory vesicles to sites of exocytosis. The EMBO Journal 18, 1071-80.

Guo, W., Grant, A., and Novick, P. (1999). Exo84p is an exocyst protein essential for secretion. The Journal Of Biological Chemistry 274, 23558-64.

Guo, W., Tamanoi, F., and Novick, P. (2001). Spatial regulation of the exocyst complex by Rho1 GTPase. Nature Cell Biology 3, 353-60.

Haarer, B.K., Corbett, A., Kweon, Y., Petzold, A.S., Silver, P., and Brown, S.S. (1996). SEC3 mutations are synthetically lethal with profilin mutations and cause defects in diploid-specific bud-site selection. Genetics 144, 495-510.

Hakhverdyan, Z., Domanski, M., Hough, L.E., Oroskar, A.A., Oroskar, A.R., Keegan, S., Dilworth, D.J., Molloy, K.R., Sherman, V., Aitchison, J.D., et al. (2015). Rapid, optimized interactomic screening. Nature Methods 12, 553-60.

Hamburger, Z.A., Hamburger, A.E., West, A.P., Jr, and Weis, W.I. (2006). Crystal structure of the S.cerevisiae exocyst component Exo70p. Journal Of Molecular Biology 356, 9-21.

Hashizume, K., Cheng, Y., Hutton, J.L., Chiu, C., and Carr, C.M. (2009). Yeast Sec1p functions before and after vesicle docking. Molecular Biology Of The Cell 20, 4673-85.

Hayashi, T., Yamasaki, S., Nauenburg, S., Binz, T., and Niemann, H. (1995). Disassembly of the reconstituted synaptic vesicle membrane fusion complex in vitro. The EMBO Journal 14, 2317-25.

Hazelett, C.C., Sheff, D., and Yeaman, C. (2011). RalA and RalB differentially regulate development of epithelial tight junctions. Molecular Biology Of The Cell 22, 4787-800.

Hazuka, C.D., Foletti, D.L., Hsu, S.C., Kee, Y., Hopf, F.W., and Scheller, R.H. (1999). The sec6/8 complex is located at neurite outgrowth and axonal synapse-assembly domains. The Journal Of Neuroscience 19, 1324-34.

He, B., Xi, F., Zhang, X., Zhang, J., and Guo, W. (2007). Exo70 interacts with phospholipids and mediates the targeting of the exocyst to the plasma membrane. The EMBO Journal 26, 4053-65.

He, B., Xi, F., Zhang, J., TerBush, D., Zhang, X., and Guo, W. (2007). Exo70p mediates the secretion of specific exocytic vesicles at early stages of the cell cycle for polarized cell growth. The Journal Of Cell Biology 176, 771-7.

He, B., and Guo, W. (2009). The exocyst complex in polarized exocytosis. Current Opinion In Cell Biology 21, 537-42.

Heider, M.R., and Munson, M. (2012). Exorcising the exocyst complex. Traffic 13, 898-907.

Hertzog, M., and Chavrier, P. (2011). Cell polarity during motile processes: keeping on track with the exocyst complex. The Biochemical Journal 433, 403-9.

Hohenstein, A.C., and Roche, P.A. (2001). SNAP-29 is a promiscuous syntaxin-binding SNARE. Biochemical And Biophysical Research Communications 285, 167-71.

Hong, W., and Lev, S. (2014). Tethering the assembly of SNARE complexes. Trends In Cell Biology 24, 35-43.

Hoskins, A.A., Friedman, L.J., Gallagher, S.S., Crawford, D.J., Anderson, E.G., Wombacher, R., Ramirez, N., Cornish, V.W., Gelles, J., and Moore, M.J. (2011). Ordered and dynamic assembly of single spliceosomes. Science 331, 1289-95.

Hsu, S.C., Ting, A.E., Hazuka, C.D., Davanger, S., Kenny, J.W., Kee, Y., and Scheller, R.H. (1996). The mammalian brain rsec6/8 complex. Neuron 17, 1209-19.

Hsu, S.C., Hazuka, C.D., Roth, R., Foletti, D.L., Heuser, J., and Scheller, R.H. (1998). Subunit composition, protein interactions, and structures of the mammalian brain sec6/8 complex and septin filaments. Neuron 20, 1111-22.

Hutagalung, A.H., Coleman, J., Pypaert, M., and Novick, P.J. (2009). An internal domain of Exo70p is required for actin-independent localization and mediates assembly of specific exocyst components. Molecular Biology Of The Cell 20, 153-63.

Iizuka, R., Yamagishi-Shirasaki, M., and Funatsu, T. (2011). Kinetic study of de novo chromophore maturation of fluorescent proteins. 1-6.

Inoue, M., Chang, L., Hwang, J., Chiang, S., and Saltiel, A.R. (2003). The exocyst complex is required for targeting of Glut4 to the plasma membrane by insulin. Nature 422, 629-33.

Ishikawa, H., Ma, Z., and Barber, G.N. (2009). STING regulates intracellular DNA-mediated, type I interferon-dependent innate immunity. Nature 461, 788-92.

Izawa, R., Onoue, T., Furukawa, N., and Mima, J. (2012). Distinct Contributions of Vacuolar Qabc- and R-SNARE Proteins to Membrane Fusion Specificity. Journal Of Biological Chemistry 287, 3445-3453.

Jafar-Nejad, H., Andrews, H.K., Acar, M., Bayat, V., Wirtz-Peitz, F., Mehta, S.Q., Knoblich, J.A., and Bellen, H.J. (2005). Sec15, a component of the exocyst, promotes notch signaling during the asymmetric division of Drosophila sensory organ precursors. Developmental Cell 9, 351-63.

Jahn, R., and Scheller, R.H. (2006). SNAREs--engines for membrane fusion. Nature Reviews. Molecular Cell Biology 7, 631-43.

Jain, A., Liu, R., Xiang, Y.K., and Ha, T. (2012). Single-molecule pull-down for studying protein interactions. Nature Protocols 7, 445-452.

Jin, R., Junutula, J.R., Matern, H.T., Ervin, K.E., Scheller, R.H., and Brunger, A.T. (2005). Exo84 and Sec5 are competitive regulatory Sec6/8 effectors to the RalA GTPase. The EMBO Journal 24, 2064-74.

Jin, Y., Sultana, A., G, P., Gandhi, P., hi, Franklin, E., Hamamoto, S., Khan, A.R., Munson, M., Schekman, R., et al. (2011). Myosin V transports secretory vesicles via a Rab GTPase cascade and interaction with the exocyst complex. Developmental Cell 21, 1156-70.

Johnson, D.I. (1999). Cdc42: An essential Rho-type GTPase controlling eukaryotic cell polarity. Microbiology And Molecular Biology Reviews 63, 54-105.

Jones, S., Jedd, G., Kahn, R.A., Franzusoff, A., Bartolini, F., and Segev, N. (1999). Genetic interactions in yeast between Ypt GTPases and Arf guanine nucleotide exchangers. Genetics 152, 1543-56.

Jones, S., Newman, C., Liu, F., and Segev, N. (2000). The TRAPP complex is a nucleotide exchanger for Ypt1 and Ypt31/32. Molecular Biology Of The Cell 11, 4403-11.

Jose, M., Tollis, S., Nair, D., Mitteau, R., Velours, C., Massoni-Laporte, A., Royou, A., Sibarita, J.-., and McCusker, D. (2015). A quantitative imaging-based screen reveals the exocyst as a network hub connecting endocytosis and exocytosis. Molecular Biology Of The Cell 26, 2519-2534.

Juillerat, A., Juillerat, R., Heinis, C., Sielaff, I., Barnikow, J., Jaccard, H., Kunz, B., Terskikh, A., and Johnsson, K. (2005). Engineering substrate specificity of O6-alkylguanine-DNA alkyltransferase for specific protein labeling in living cells. Chembiochem : A European Journal Of Chemical Biology 6, 1263-9.

Kahlscheuer, M.L., Widom, J., and Walter, N.G. (2015). Single-Molecule Pull-Down FRET to Dissect the Mechanisms of Biomolecular Machines. Methods In Enzymology 558, 539-70.

Kaiser, C.A., and Schekman, R. (1990). Distinct sets of SEC genes govern transport vesicle formation and fusion early in the secretory pathway. Cell 61, 723-33.

Kamena, F., and Spang, A. (2004). Tip20p prohibits back-fusion of COPII vesicles with the endoplasmic reticulum. Science 304, 286-9.

Katoh, Y., Nozaki, S., Hartanto, D., Miyano, R., and Nakayama, K. (2015). Architectures of multisubunit complexes revealed by a visible immunoprecipitation assay using fluorescent fusion proteins. Journal Of Cell Science 128, 2351-2362.

Kim, Y., Raunser, S., Munger, C., Wagner, J., Song, Y., Cygler, M., Walz, T., Oh, B., and Sacher, M. (2006). The architecture of the multisubunit TRAPP I complex suggests a model for vesicle tethering. Cell 127, 817-30.

Koumandou, V.L., Dacks, J.B., Coulson, R.M.R., and Field, M.C. (2007). Control systems for membrane fusion in the ancestral eukaryote; evolution of tethering complexes and SM proteins. BMC Evolutionary Biology 7, 29.

Kramer, L., and Ungermann, C. (2011). HOPS drives vacuole fusion by binding the vacuolar SNARE complex and the Vam7 PX domain via two distinct sites. Molecular Biology Of The Cell 22, 2601-2611.

Kraynack, B.A., Chan, A., Rosenthal, E., Essid, M., Umansky, B., Waters, M.G., and Schmitt, H.D. (2005). Dsl1p, Tip20p, and the novel Dsl3(Sec39) protein are required for the stability of the Q/t-SNARE complex at the endoplasmic reticulum in yeast. Molecular Biology Of The Cell 16, 3963-77.

Kulak, N.A., Pichler, G., Paron, I., Nagaraj, N., and Mann, M. (2014). Minimal, encapsulated proteomic-sample processing applied to copy-number estimation in eukaryotic cells. Nature Methods 11, 319-24.

Kulich, I., Pečenková, T., Sekereš, J., Smetana, O., Fendrych, M., Foissner, I., Höftberger, M., and Zárský, V. (2013). Arabidopsis exocyst subcomplex containing subunit EXO70B1 is involved in autophagy-related transport to the vacuole. Traffic 14, 1155-65.

Kweon, Y., Rothe, A., Conibear, E., and Stevens, T.H. (2003). Ykt6p is a multifunctional yeast R-SNARE that is required for multiple membrane transport pathways to the vacuole. Molecular Biology Of The Cell 14, 1868-81.

Laage, R., and Ungermann, C. (2001). The N-terminal domain of the t-SNARE Vam3p coordinates priming and docking in yeast vacuole fusion. Molecular Biology Of The Cell 12, 3375-85.

Lalli, G., and Hall, A. (2005). Ral GTPases regulate neurite branching through GAP-43 and the exocyst complex. The Journal Of Cell Biology 171, 857-69.

Lamson, R.E., Winters, M.J., and Pryciak, P.M. (2002). Cdc42 Regulation of Kinase Activity and Signaling by the Yeast p21-Activated Kinase Ste20. Molecular And Cellular Biology 22, 2939-2951.

Lees, J.A., Yip, C.K., Walz, T., and Hughson, F.M. (2010). Molecular organization of the COG vesicle tethering complex. Nature Structural & Molecular Biology 17, 1292-1297.

Lehman, K., Rossi, G., Adamo, J.E., and Brennwald, P. (1999). Yeast homologues of tomosyn and lethal giant larvae function in exocytosis and are associated with the plasma membrane SNARE, Sec9. The Journal Of Cell Biology 146, 125-40.

Lieu, Z.Z., and Gleeson, P.A. (2010). Identification of different itineraries and retromer components for endosome-to-Golgi transport of TGN38 and Shiga toxin. European Journal Of Cell Biology 89, 379-93.

Lieu, Z.Z., Derby, M.C., Teasdale, R.D., Hart, C., Gunn, P., and Gleeson, P.A. (2007). The golgin GCC88 is required for efficient retrograde transport of cargo from the early endosomes to the trans-Golgi network. Molecular Biology Of The Cell 18, 4979-91.

Lipatova, Z., and Segev, N. (2014). Ypt/Rab GTPases regulate two intersections of the secretory and the endosomal/lysosomal pathways. Cellular Logistics 4, e954870.

Lipatova, Z., Tokarev, A.A., Jin, Y., Mulholl, J., Mulholland, J., Weisman, L.S., and Segev, N. (2008). Direct interaction between a myosin V motor and the Rab GTPases Ypt31/32 is required for polarized secretion. Molecular Biology Of The Cell 19, 4177-87.

Liu, J., Yue, P., Artym, V.V., Mueller, S.C., and Guo, W. (2009). The role of the exocyst in matrix metalloproteinase secretion and actin dynamics during tumor cell invadopodia formation. Molecular Biology Of The Cell 20, 3763-71.

Liu, J., Zuo, X., Yue, P., and Guo, W. (2007). Phosphatidylinositol 4,5-bisphosphate mediates the targeting of the exocyst to the plasma membrane for exocytosis in mammalian cells. Molecular Biology Of The Cell 18, 4483-92.

Liu, J., and Guo, W. (2012). The exocyst complex in exocytosis and cell migration. Protoplasma 249, 587-97.

Liu, J., Zhao, Y., Sun, Y., He, B., Yang, C., Svitkina, T., Goldman, Y.E., and Guo, W. (2012). Exo70 stimulates the Arp2/3 complex for lamellipodia formation and directional cell migration. Current Biology 22, 1510-5.

Liu, Y., and Barlowe, C. (2002). Analysis of Sec22p in endoplasmic reticulum/Golgi transport reveals cellular redundancy in SNARE protein function. Molecular Biology Of The Cell 13, 3314-24.

Lo, S., Brett, C.L., Plemel, R.L., Vignali, M., Fields, S., Gonen, T., and Merz, A.J. (2011). Intrinsic tethering activity of endosomal Rab proteins. Nature Structural & Molecular Biology 19, 40-47.

Lobingier, B.T., and Merz, A.J. (2012). Sec1/Munc18 protein Vps33 binds to SNARE domains and the quaternary SNARE complex. Molecular Biology Of The Cell 23, 4611-4622.

Lobstein, E., Guyon, A., Férault, M., Twell, D., Pelletier, G., S, Bonhomme, S., and Bonhomme, R. (2004). The putative Arabidopsis homolog of yeast vps52p is required for pollen tube elongation, localizes to Golgi, and might be involved in vesicle trafficking. Plant Physiology 135, 1480-90.

Lu, H., Liu, J., Liu, S., Zeng, J., Ding, D., Carstens, R., Cong, Y., Xu, X., and Guo, W. (2013). Exo70 Isoform Switching upon Epithelial-Mesenchymal Transition Mediates Cancer Cell Invasion. 1-14.

Ludtke, S.J., Baldwin, P.R., and Chiu, W. (1999). EMAN: semiautomated software for high-resolution single-particle reconstructions. Journal Of Structural Biology 128, 82-97.

Luo, G., Zhang, J., Luca, F.C., and Guo, W. (2013). Mitotic phosphorylation of Exo84 disrupts exocyst assembly and arrests cell growth. The Journal Of Cell Biology 202, 97-111.

Luo, G., Zhang, J., and Guo, W. (2014). The role of Sec3p in secretory vesicle targeting and exocyst complex assembly. Molecular Biology Of The Cell 25, 3813-3822.

Mathieson, E.M., Suda, Y., Nickas, M., Snydsman, B., Davis, T.N., Muller, E.G.D., and Neiman, A.M. (2010). Vesicle docking to the spindle pole body is necessary to recruit the exocyst during membrane formation in Saccharomyces cerevisiae. Molecular Biology Of The Cell 21, 3693-707.

McDonold, C.M., and Fromme, J.C. (2014). Four GTPases differentially regulate the Sec7 Arf-GEF to direct traffic at the trans-golgi network. Developmental Cell 30, 759-67.

McNew, J.A., Parlati, F., Fukuda, R., Johnston, R.J., Paz, K., Paumet, F., Söllner, T.H., and Rothman, J.E. (2000). Compartmental specificity of cellular membrane fusion encoded in SNARE proteins. Nature 407, 153-9.

Medkova, M., France, Y.E., Coleman, J., and Novick, P. (2006). The Rab exchange factor Sec2p reversibly associates with the exocyst. Molecular Biology Of The Cell 17, 2757-69.

Mehta, S.Q., Hiesinger, P.R., Beronja, S., Zhai, R.G., Schulze, K.L., Verstreken, P., Cao, Y., Zhou, Y., Tepass, U., Crair, M.C., et al. (2005). Mutations in Drosophila Sec15 reveal a function in neuronal targeting for a subset of exocyst components. Neuron 46, 219-32.

Miller, V.J., and Ungar, D. (2012). Re“COG”nition at the Golgi. Traffic 13, 891-7.

Mima, J., Hickey, C.M., Xu, H., Jun, Y., and Wickner, W. (2008). Reconstituted membrane fusion requires regulatory lipids, SNAREs and synergistic SNARE chaperones. The EMBO Journal 27, 2031-42.

Mindell, J.A., and Grigorieff, N. (2003). Accurate determination of local defocus and specimen tilt in electron microscopy. Journal Of Structural Biology 142, 334-47.

Misura, K.M., Scheller, R.H., and Weis, W.I. (2000). Three-dimensional structure of the neuronal-Sec1-syntaxin 1a complex. Nature 404, 355-62.

Mizuno-Yamasaki, E., Medkova, M., Coleman, J., and Novick, P. (2010). Phosphatidylinositol 4-phosphate controls both membrane recruitment and a regulatory switch of the Rab GEF Sec2p. Developmental Cell 18, 828-40.

Moore, B.A., Robinson, H.H., and Xu, Z. (2007). The crystal structure of mouse Exo70 reveals unique features of the mammalian exocyst. Journal Of Molecular Biology 371, 410-21.

Morgera, F., Sallah, M.R., Dubuke, M.L., Gandhi, P., Brewer, D.N., Carr, C.M., and Munson, M. (2012). Regulation of exocytosis by the exocyst subunit Sec6 and the SM protein Sec1. Molecular Biology Of The Cell 23, 337-346.

Morozova, N., Liang, Y., Tokarev, A.A., Chen, S.H., R, Cox, R., Cox, al, Andrejic, J., Lipatova, Z., Sciorra, V.A., et al. (2006). TRAPPII subunits are required for the specificity switch of a Ypt-Rab GEF. Nature Cell Biology 8, 1263-9.

Moskalenko, S., Henry, D.O., Rosse, C., Mirey, G., Camonis, J.H., and White, M.A. (2002). The exocyst is a Ral effector complex. Nature Cell Biology 4, 66-72.

Moskalenko, S., Tong, C., Rosse, C., Mirey, G., Formstecher, E., Daviet, L., Camonis, J., and White, M.A. (2003). Ral GTPases regulate exocyst assembly through dual subunit interactions. The Journal Of Biological Chemistry 278, 51743-8.

Mott, H.R., Nietlispach, D., Hopkins, L.J., Mirey, G., Camonis, J.H., and Owen, D. (2003). Structure of the GTPase-binding domain of Sec5 and elucidation of its Ral binding site. The Journal Of Biological Chemistry 278, 17053-9.

Munson, M. (2009). Tip20p reaches out to Dsl1p to tether membranes. Nature Structural & Molecular Biology 16, 100-2.

Munson, M., and Novick, P. (2006). The exocyst defrocked, a framework of rods revealed. Nature Structural & Molecular Biology 13, 577-81.

Murthy, M., Teodoro, R.O., Miller, T.P., and Schwarz, T.L. (2010). Sec5, a member of the exocyst complex, mediates Drosophila embryo cellularization. Development 137, 2773-83.

Murthy, M., Ranjan, R., Denef, N., Higashi, M.E.L., Schupbach, T., and Schwarz, T.L. (2005). Sec6 mutations and the Drosophila exocyst complex. Journal Of Cell Science 118, 1139-50.

Murthy, M., and Schwarz, T.L. (2004). The exocyst component Sec5 is required for membrane traffic and polarity in the Drosophila ovary. Development 131, 377-88.

Murthy, M., Garza, D., Scheller, R.H., and Schwarz, T.L. (2003). Mutations in the exocyst component Sec5 disrupt neuronal membrane traffic, but neurotransmitter release persists. Neuron 37, 433-47.

Neiman, A.M. (1998). Prospore membrane formation defines a developmentally regulated branch of the secretory pathway in yeast. The Journal Of Cell Biology 140, 29-37.

Neto, H., Balmer, G., and Gould, G. (2013). Exocyst proteins in cytokinesis: Regulation by Rab11. Communicative & Integrative Biology 6, e27635.

Nichols, C.D., and Casanova, J.E. (2010). Salmonella-directed recruitment of new membrane to invasion foci via the host exocyst complex. Current Biology 20, 1316-20.

Nickerson, D.P., Brett, C.L., and Merz, A.J. (2009). Vps-C complexes: gatekeepers of endolysosomal traffic. Current Opinion In Cell Biology 21, 543-51.

Nie, C., and Chen, X. (2015). Recycling of the insulin-responsive glucose transporter Glut4 regulated by the small GTPase RalA and the exocyst complex.

Nishimura, K., Fukagawa, T., Takisawa, H., Kakimoto, T., and Kanemaki, M. (2009). An auxin-based degron system for the rapid depletion of proteins in nonplant cells. Nature Methods 6, 917-922.

Nishimura, K., and Kanemaki, M.T. (2014). Rapid Depletion of Budding Yeast Proteins via the Fusion of an Auxin-Inducible Degron (AID). Current Protocols In Cell Biology 64, 20.9.1-20.9.16.

Nooren, I.M.A., and Thornton, J.M. (2003). Structural characterisation and functional significance of transient protein-protein interactions. Journal Of Molecular Biology 325, 991-1018.

Nooren, I.M.A., and Thornton, J.M. (2003). Diversity of protein-protein interactions. The EMBO Journal 22, 3486-92.

Novick, P., and Schekman, R. (1979). Secretion and cell-surface growth are blocked in a temperature-sensitive mutant of Saccharomyces cerevisiae. Proceedings Of The National Academy Of Sciences Of The United States Of America 76, 1858-62.

Novick, P., Field, C., and Schekman, R. (1980). Identification of 23 complementation groups required for post-translational events in the yeast secretory pathway. Cell 21, 205-15.

Oeffinger, M., Wei, K.E., Rogers, R., DeGrasse, J.A., Chait, B.T., Aitchison, J.D., and Rout, M.P. (2007). Comprehensive analysis of diverse ribonucleoprotein complexes. Nature Methods 4, 951-6.

Ohya, T., Miaczynska, M., Coskun, Ü., Lommer, B., Runge, A., Drechsel, D., Kalaidzidis, Y., and Zerial, M. (2009). Reconstitution of Rab- and SNARE-dependent membrane fusion by synthetic endosomes. Nature 459, 1091-1097.

Oka, T., and Krieger, M. (2005). Multi-component protein complexes and Golgi membrane trafficking. Journal Of Biochemistry 137, 109-14.

Oka, T., Ungar, D., Hughson, F.M., and Krieger, M. (2004). The COG and COPI complexes interact to control the abundance of GEARs, a subset of Golgi integral membrane proteins. Molecular Biology Of The Cell 15, 2423-35.

Orlando, K., o, Zhang, J., Zhang, X., Yue, P., Chiang, T., Bi, E., and Guo, W. (2008). Regulation of Gic2 localization and function by phosphatidylinositol 4,5-bisphosphate during the establishment of cell polarity in budding yeast. The Journal Of Biological Chemistry 283, 14205-12.

Ortiz, D., Medkova, M., Walch-Solimena, C., and Novick, P. (2002). Ypt32 recruits the Sec4p guanine nucleotide exchange factor, Sec2p, to secretory vesicles; evidence for a Rab cascade in yeast. The Journal Of Cell Biology 157, 1005-15.

Ostrowicz, C.W., Bröcker, C., Ahnert, F., Nordmann, M., Lachmann, J., Peplowska, K., Perz, A., Auffarth, K., Engelbrecht-V, S., Engelbrecht-Vandré, S., et al. (2010). Defined subunit arrangement and rab interactions are required for functionality of the HOPS tethering complex. Traffic11, 1334-46.

Paczkowski, J.E., Richardson, B.C., and Fromme, J.C. (2015). Cargo adaptors: structures illuminate mechanisms regulating vesicle biogenesis. Trends In Cell Biology 25, 408-16.

Panic, B., Whyte, J.R.C., and Munro, S. (2003). The ARF-like GTPases Arl1p and Arl3p act in a pathway that interacts with vesicle-tethering factors at the Golgi apparatus. Current Biology 13, 405-10.

Panic, B., Perisic, O., Veprintsev, D.B., Williams, R.L., and Munro, S. (2003). Structural basis for Arl1-dependent targeting of homodimeric GRIP domains to the Golgi apparatus. Molecular Cell 12, 863-74.

Pashkova, N., Jin, Y., Ramaswamy, S., and Weisman, L.S. (2006). Structural basis for myosin V discrimination between distinct cargoes. The EMBO Journal 25, 693-700.

Peng, R., and Gallwitz, D. (2004). Multiple SNARE interactions of an SM protein: Sed5p/Sly1p binding is dispensable for transport. The EMBO Journal 23, 3939-49.

Peplowska, K., Markgraf, D.F., Ostrowicz, C.W., Bange, G., and Ungermann, C. (2007). The CORVET tethering complex interacts with the yeast Rab5 homolog Vps21 and is involved in endo-lysosomal biogenesis. Developmental Cell 12, 739-50.

Pérez-Victoria, F.J., Abascal-Palacios, G., Tascón, I., Kajava, A., Magadán, J.G., Pioro, E.P., Bonifacino, J.S., and Hierro, A. (2010). Structural basis for the wobbler mouse neurodegenerative disorder caused by mutation in the Vps54 subunit of the GARP complex. Proceedings Of The National Academy Of Sciences Of The United States Of America 107, 12860-5.

Pérez-Victoria, F.J., Schindler, C., Magadán, J.G., Mardones, G.A., Delevoye, C., Romao, M., Raposo, G., and Bonifacino, J.S. (2010). Ang2/fat-free is a conserved subunit of the Golgi-associated retrograde protein complex. Molecular Biology Of The Cell 21, 3386-95.

Perez-Victoria, F.J., Mardones, G.A., and Bonifacino, J.S. (2008). Requirement of the Human GARP Complex for Mannose 6-phosphate-receptor-dependent Sorting of Cathepsin D to Lysosomes. Molecular Biology Of The Cell 19, 2350-2362.

Perez-Victoria, F.J., and Bonifacino, J.S. (2009). Dual Roles of the Mammalian GARP Complex in Tethering and SNARE Complex Assembly at the trans-Golgi Network. Molecular And Cellular Biology 29, 5251-5263.

Pfeffer, S.R. (1996). Transport vesicle docking: SNAREs and associates. Annual Review Of Cell And Developmental Biology 12, 441-61.

Plemel, R.L., Lobingier, B.T., Brett, C.L., Angers, C.G., Nickerson, D.P., Paulsel, A., Sprague, D., and Merz, A.J. (2011). Subunit organization and Rab interactions of Vps-C protein complexes that control endolysosomal membrane traffic. Molecular Biology Of The Cell 22, 1353-1363.

Pleskot, R., Cwiklik, L., Jungwirth, P., Žárský, V., and Potocký, M. (2015). Membrane targeting of the yeast exocyst complex. Biochimica Et Biophysica Acta 1848, 1481-9.

Pollard, T.D., and Borisy, G.G. (2003). Cellular motility driven by assembly and disassembly of actin filaments. Cell 112, 453-65.

Price, A., Seals, D., Wickner, W., and Ungermann, C. (2000). The docking stage of yeast vacuole fusion requires the transfer of proteins from a cis-SNARE complex to a Rab/Ypt protein. The Journal Of Cell Biology 148, 1231-8.

Ram, R.J., Li, B., and Kaiser, C.A. (2002). Identification of Sec36p, Sec37p, and Sec38p: components of yeast complex that contains Sec34p and Sec35p. Molecular Biology Of The Cell 13, 1484-500.

Reddy, J.V., Burguete, A.S., Sridevi, K., Ganley, I.G., Nottingham, R.M., and Pfeffer, S.R. (2006). A functional role for the GCC185 golgin in mannose 6-phosphate receptor recycling. Molecular Biology Of The Cell 17, 4353-63.

Reilly, B.A., Kraynack, B.A., VanRheenen, S.M., and Waters, M.G. (2001). Golgi-to-endoplasmic reticulum (ER) retrograde traffic in yeast requires Dsl1p, a component of the ER target site that interacts with a COPI coat subunit. Molecular Biology Of The Cell 12, 3783-96.

Ren, J., and Guo, W. (2012). ERK1/2 regulate exocytosis through direct phosphorylation of the exocyst component Exo70. Developmental Cell 22, 967-78.

Ren, Y., Yip, C.K., Tripathi, A., Huie, D., Jeffrey, P.D., Walz, T., and Hughson, F.M. (2009). A structure-based mechanism for vesicle capture by the multisubunit tethering complex Dsl1. Cell 139, 1119-29.

Ren, Y., Yip, C.K., Tripathi, A., Huie, D., Jeffrey, P.D., Walz, T., and Hughson, F.M. (2009). A structure-based mechanism for vesicle capture by the multisubunit tethering complex Dsl1. Cell 139, 1119-29.

Richardson, B.C., Smith, R.D., Ungar, D., Nakamura, A., Jeffrey, P.D., Lupashin, V.V., and Hughson, F.M. (2009). Structural basis for a human glycosylation disorder caused by mutation of the COG4 gene. Proceedings Of The National Academy Of Sciences Of The United States Of America 106, 13329-34.

Richman, D.D., Clevel, P.H., Cleveland, P.H., Oxman, M.N., and Johnson, K.M. (1982). The binding of staphylococcal protein A by the sera of different animal species. Journal Of Immunology 128, 2300-5.

Richman, T.J., Sawyer, M.M., and Johnson, D.I. (2002). Saccharomyces cerevisiae Cdc42p Localizes to Cellular Membranes and Clusters at Sites of Polarized Growth. Eukaryotic Cell 1, 458-468.

Ridley, A.J., Schwartz, M.A., Burridge, K., Firtel, R.A., Ginsberg, M.H., Borisy, G., Parsons, J.T., and Horwitz, A.R. (2003). Cell migration: integrating signals from front to back. Science (New York, N.Y.) 302, 1704-9.

Riezman, H. (1985). Endocytosis in yeast: several of the yeast secretory mutants are defective in endocytosis. Cell 40, 1001-9.

Riquelme, M., Bredeweg, E.L., Callejas-Negrete, O., Roberson, R.W., Ludwig, S., Beltrán-Aguilar, A., Seiler, S., Novick, P., and Freitag, M. (2014). The Neurospora crassa exocyst complex tethers Spitzenkörper vesicles to the apical plasma membrane during polarized growth. Molecular Biology Of The Cell 25, 1312-26.

Robinson, N.G., Guo, L., Imai, J., Toh-E, A., Matsui, Y., and Tamanoi, F. (1999). Rho3 of Saccharomyces cerevisiae, which regulates the actin cytoskeleton and exocytosis, is a GTPase which interacts with Myo2 and Exo70. Molecular And Cellular Biology 19, 3580-7.

Rodkey, T.L., Liu, S., Barry, M., and McNew, J.A. (2008). Munc18a scaffolds SNARE assembly to promote membrane fusion. Molecular Biology Of The Cell 19, 5422-34.

Rossi, G., Watson, K., Demonch, M., Temple, B., and Brennwald, P. (2015). In vitro reconstitution of Rab GTPase-dependent vesicle clustering by the yeast lethal giant larvae/tomosyn homolog, Sro7. The Journal Of Biological Chemistry 290, 612-24.

Roth, D., Guo, W., and Novick, P. (1998). Dominant negative alleles of SEC10 reveal distinct domains involved in secretion and morphogenesis in yeast. Molecular Biology Of The Cell 9, 1725-39.

Roumanie, O., Wu, H., Molk, J.N., Rossi, G., Bloom, K., and Brennwald, P. (2005). Rho GTPase regulation of exocytosis in yeast is independent of GTP hydrolysis and polarization of the exocyst complex. The Journal Of Cell Biology 170, 583-94.

Rybak, K., Alex, Steiner, A., Steiner, E., Synek, L., Klaeger, S., Kulich, I., Facher, E., Wanner, G., Kuster, B., et al. (2014). Plant cytokinesis is orchestrated by the sequential action of the TRAPPII and exocyst tethering complexes. Developmental Cell 29, 607-20.

Sacher, M., Jiang, Y., Barrowman, J., Scarpa, A., Burston, J., Zhang, L., Schieltz, D., 3rd, J.R.Y., Abeliovich, H., and Ferro-Novick, S. (1998). TRAPP, a highly conserved novel complex on the cis-Golgi that mediates vesicle docking and fusion. The EMBO Journal 17, 2494-503.

Sacher, M., Barrowman, J., Wang, W., Horecka, J., Zhang, Y., Pypaert, M., and Ferro-Novick, S. (2001). TRAPP I implicated in the specificity of tethering in ER-to-Golgi transport. Molecular Cell 7, 433-42.

Sakurai-Yageta, M., Recchi, C., Le Dez, G., Sibarita, J., Daviet, L., Camonis, J., D'Souza-Schorey, C., and Chavrier, P. (2008). The interaction of IQGAP1 with the exocyst complex is required for tumor cell invasion downstream of Cdc42 and RhoA. The Journal Of Cell Biology 181, 985-98.

Sano, H., Peck, G.R., Blachon, S., and Lienhard, G.E. (2015). A potential link between insulin signaling and GLUT4 translocation: Association of Rab10-GTP with the exocyst subunit Exoc6/6b. Biochemical And Biophysical Research Communications 465, 601-5.

Sato, T.K., Rehling, P., Peterson, M.R., and Emr, S.D. (2000). Class C Vps protein complex regulates vacuolar SNARE pairing and is required for vesicle docking/fusion. Molecular Cell 6, 661-71.

Scheres, S.H.W. (2012). RELION: implementation of a Bayesian approach to cryo-EM structure determination. Journal Of Structural Biology 180, 519-30.

Schindler, C., Chen, Y., Pu, J., Guo, X., and Bonifacino, J.S. (2015). EARP is a multisubunit tethering complex involved in endocytic recycling. Nature Cell Biology 17, 639-650.

Schmitt-John, T., Drepper, C., Mußmann, A., Hahn, P., Kuhlmann, M., Thiel, C., Hafner, M., Lengeling, A., Heimann, P., Jones, J.M., et al. (2005). Mutation of Vps54 causes motor neuron disease and defective spermiogenesis in the wobbler mouse. Nature Genetics 37, 1213-1215.

Scott, B.L., van Komen, J.S., Irshad, H., Liu, S., Wilson, K.A., and McNew, J.A. (2004). Sec1p directly stimulates SNARE-mediated membrane fusion in vitro. The Journal Of Cell Biology 167, 75-85.

Seals, D.F., Eitzen, G., Margolis, N., Wickner, W.T., and Price, A. (2000). A Ypt/Rab effector complex containing the Sec1 homolog Vps33p is required for homotypic vacuole fusion. Proceedings Of The National Academy Of Sciences Of The United States Of America 97, 9402-7.

Shcherbakova, I., Hoskins, A.A., Friedman, L.J., Serebrov, V., Corrêa, I.R., Jr, Xu, M., Gelles, J., and Moore, M.J. (2013). Alternative spliceosome assembly pathways revealed by single-molecule fluorescence microscopy. Cell Reports 5, 151-65.

Shen, D., Yuan, H., Hutagalung, A., Verma, A., Kummel, D., Wu, X., Reinisch, K., McNew, J.A., and Novick, P. (2013). The synaptobrevin homologue Snc2p recruits the exocyst to secretory vesicles by binding to Sec6p. The Journal Of Cell Biology 202, 509-526.

Shen, J., Tareste, D.C., Paumet, F., Rothman, J.E., and Melia, T.J. (2007). Selective activation of cognate SNAREpins by Sec1/Munc18 proteins. Cell 128, 183-95.

Shestakova, A., Suvorova, E., Oleks, Pavliv, O., Pavliv, R., Khaidakova, G., and Lupashin, V. (2007). Interaction of the conserved oligomeric Golgi complex with t-SNARE Syntaxin5a/Sed5 enhances intra-Golgi SNARE complex stability. The Journal Of Cell Biology 179, 1179-92.

Sikorski, R.S., and Hieter, P. (1989). A system of shuttle vectors and yeast host strains designed for efficient manipulation of DNA in Saccharomyces cerevisiae. Genetics 122, 19-27.

Siniossoglou, S., and Pelham, H.R. (2001). An effector of Ypt6p binds the SNARE Tlg1p and mediates selective fusion of vesicles with late Golgi membranes. The EMBO Journal 20, 5991-8.

Sivaram, M.V.S., Furgason, M.L.M., Brewer, D.N., and Munson, M. (2006). The structure of the exocyst subunit Sec6p defines a conserved architecture with diverse roles. Nature Structural & Molecular Biology 13, 555-6.

Sivaram, M.S.V., Saporita, J.A., Furgason, M.L.M., Boettcher, A.J., and Munson, M. (2005). Dimerization of the Exocyst Protein Sec6p and Its Interaction with the t-SNARE Sec9p. Biochemistry 44, 6302-6311.

Sohda, M., Misumi, Y., Yamamoto, A., Nakamura, N., Ogata, S., Sakisaka, S., Hirose, S., Ikehara, Y., and Oda, K. (2010). Interaction of Golgin-84 with the COG complex mediates the intra-Golgi retrograde transport. Traffic 11, 1552-66.

Sohda, M., Misumi, Y., Yoshimura, S., Nakamura, N., Fusano, T., Ogata, S., Sakisaka, S., and Ikehara, Y. (2007). The interaction of two tethering factors, p115 and COG complex, is required for Golgi integrity. Traffic 8, 270-84.

Söllner, T., Bennett, M.K., Whiteheart, S.W., Scheller, R.H., and Rothman, J.E. (1993). A protein assembly-disassembly pathway in vitro that may correspond to sequential steps of synaptic vesicle docking, activation, and fusion. Cell 75, 409-18.

Söllner, T., Whiteheart, S.W., Brunner, M., Erdjument-Bromage, H., Geromanos, S., Tempst, P., and Rothman, J.E. (1993). SNAP receptors implicated in vesicle targeting and fusion. Nature 362, 318-24.

Sommer, B., Oprins, A., Rabouille, C., and Munro, S. (2005). The exocyst component Sec5 is present on endocytic vesicles in the oocyte of Drosophila melanogaster. The Journal Of Cell Biology 169, 953-63.

Songer, J.A., and Munson, M. (2009). Sec6p anchors the assembled exocyst complex at sites of secretion. Molecular Biology Of The Cell 20, 973-82.

Spang, A. (2012). The DSL1 complex: the smallest but not the least CATCHR. Traffic 13, 908-13.

Starai, V.J., Hickey, C.M., and Wickner, W. (2008). HOPS proofreads the trans-SNARE complex for yeast vacuole fusion. Molecular Biology Of The Cell 19, 2500-8.

Stegmann, M., Anderson, R.G., Westphal, L., Rosahl, S., McDowell, J.M., and Trujillo, M. (2013). The exocyst subunit Exo70B1 is involved in the immune response of Arabidopsis thaliana to different pathogens and cell death. Plant Signaling & Behavior 8, e27421.

Stenmark, H., Vitale, G., Ullrich, O., and Zerial, M. (1995). Rabaptin-5 is a direct effector of the small GTPase Rab5 in endocytic membrane fusion. Cell 83, 423-32.

Stroupe, C. (2012). The yeast vacuolar Rab GTPase Ypt7p has an activity beyond membrane recruitment of the homotypic fusion and protein sorting–Class C Vps complex. Biochemical Journal 443, 205-211.

Stroupe, C., Hickey, C.M., Mima, J., Burfeind, A.S., and Wickner, W. (2009). Minimal membrane docking requirements revealed by reconstitution of Rab GTPase-dependent membrane fusion from purified components. Proceedings Of The National Academy Of Sciences Of The United States Of America 106, 17626-33.

Sun, X., Zhang, A., Baker, B., Sun, L., Howard, A., Buswell, J., Maurel, D., Masharina, A., Johnsson, K., Noren, C.J., et al. (2011). Development of SNAP-tag fluorogenic probes for wash-free fluorescence imaging. Chembiochem : A European Journal Of Chemical Biology 12, 2217-26.

Takamori, S., Holt, M., Stenius, K., Lemke, E.A., Grønborg, M., Riedel, D., Urlaub, H., Schenck, S., Brügger, B., Ringler, P., et al. (2006). Molecular anatomy of a trafficking organelle. Cell 127, 831-46.

Terbush, D.R., Guo, W., Dunkelbarger, S., and Novick, P. (2001). Purification and characterization of yeast exocyst complex. Methods In Enzymology 329, 100-10.

TerBush, D.R., Maurice, T., Roth, D., and Novick, P. (1996). The Exocyst is a multiprotein complex required for exocytosis in Saccharomyces cerevisiae. The EMBO Journal 15, 6483-94.

TerBush, D.R., and Novick, P. (1995). Sec6, Sec8, and Sec15 are components of a multisubunit complex which localizes to small bud tips in Saccharomyces cerevisiae. The Journal Of Cell Biology 130, 299-312.

Thapa, N., Sun, Y., Schramp, M., Choi, S., Ling, K., and Anderson, R.A. (2012). Phosphoinositide signaling regulates the exocyst complex and polarized integrin trafficking in directionally migrating cells. Developmental Cell 22, 116-30.

Togneri, J., Cheng, Y., Munson, M., Hughson, F.M., and Carr, C.M. (2006). Specific SNARE complex binding mode of the Sec1/Munc-18 protein, Sec1p. Proceedings Of The National Academy Of Sciences Of The United States Of America 103, 17730-5.

Toonen, R.F.G., and Verhage, M. (2003). Vesicle trafficking: pleasure and pain from SM genes. Trends In Cell Biology 13, 177-86.

Toonen, R.F.G., and Verhage, M. (2007). Munc18-1 in secretion: lonely Munc joins SNARE team and takes control. Trends In Neurosciences 30, 564-72.

Tripathi, A., Ren, Y., Jeffrey, P.D., and Hughson, F.M. (2009). Structural characterization of Tip20p and Dsl1p, subunits of the Dsl1p vesicle tethering complex. Nature Structural & Molecular Biology 16, 114-23.

Ulbrich, M.H., and Isacoff, E.Y. (2007). Subunit counting in membrane-bound proteins. Nature Methods 4, 319-21.

Ungar, D., Oka, T., Brittle, E.E., Vasile, E., Lupashin, V.V., Chatterton, J.E., Heuser, J.E., Krieger, M., and Waters, M.G. (2002). Characterization of a mammalian Golgi-localized protein complex, COG, that is required for normal Golgi morphology and function. The Journal Of Cell Biology 157, 405-15.

Vanrheenen, S.M., Reilly, B.A., Chamberlain, S.J., and Waters, M.G. (2001). Dsl1p, an essential protein required for membrane traffic at the endoplasmic reticulum/Golgi interface in yeast. Traffic 2, 212-31.

VanRheenen, S.M., Cao, X., Lupashin, V.V., Barlowe, C., and Waters, M.G. (1998). Sec35p, a novel peripheral membrane protein, is required for ER to Golgi vesicle docking. The Journal Of Cell Biology 141, 1107-19.

Vasan, N., Hutagalung, A., Novick, P., and Reinisch, K.M. (2010). Structure of a C-terminal fragment of its Vps53 subunit suggests similarity of Golgi-associated retrograde

protein (GARP) complex to a family of tethering complexes. Proceedings Of The National Academy Of Sciences Of The United States Of America 107, 14176-81.

Mollard, von, G.F., Nothwehr, S.F., and Stevens, T.H. (1997). The yeast v-SNARE Vti1p mediates two vesicle transport pathways through interactions with the t-SNAREs Sed5p and Pep12p. The Journal Of Cell Biology 137, 1511-24.

Walter, D.M., Paul, K.S., and Waters, M.G. (1998). Purification and characterization of a novel 13 S hetero-oligomeric protein complex that stimulates in vitro Golgi transport. The Journal Of Biological Chemistry 273, 29565-76.

Walworth, N.C., and Novick, P.J. (1987). Purification and characterization of constitutive secretory vesicles from yeast. The Journal Of Cell Biology 105, 163-74.

Wang, H. (2002). The Multiprotein Exocyst Complex Is Essential for Cell Separation in Schizosaccharomyces pombe. Molecular Biology Of The Cell 13, 515-529.

Wang, H., Tang, X., and Balasubramanian, M.K. (2003). Rho3p regulates cell separation by modulating exocyst function in Schizosaccharomyces pombe. Genetics 164, 1323-31.

Wang, J., Ding, Y., Wang, J., Hillmer, S., Miao, Y., Lo, S.W., Wang, X., Robinson, D.G., and Jiang, L. (2010). EXPO, an exocyst-positive organelle distinct from multivesicular endosomes and autophagosomes, mediates cytosol to cell wall exocytosis in Arabidopsis and tobacco cells. The Plant Cell 22, 4009-30.

Wang, S., and Hsu, S.C. (2006). The molecular mechanisms of the mammalian exocyst complex in exocytosis. Biochemical Society Transactions 34, 687-90.

Wang, W., Sacher, M., and Ferro-Novick, S. (2000). TRAPP stimulates guanine nucleotide exchange on Ypt1p. The Journal Of Cell Biology 151, 289-96.

Watson, L.J., Rossi, G., and Brennwald, P. (2014). Quantitative analysis of membrane trafficking in regulation of Cdc42 polarity. Traffic 15, 1330-43.

Weber, T., Zemelman, B.V., McNew, J.A., Westermann, B., Gmachl, M., Parlati, F., Söllner, T.H., and Rothman, J.E. (1998). SNAREpins: minimal machinery for membrane fusion. Cell 92, 759-72.

Whyte, J.R., and Munro, S. (2001). The Sec34/35 Golgi transport complex is related to the exocyst, defining a family of complexes involved in multiple steps of membrane traffic. Developmental Cell 1, 527-37.

Wiederkehr, A., Yunrui, du, Pypaert, M., Ferro-Novick, S., and Novick, P. (2003). Sec3p is needed for the spatial regulation of secretion and for the inheritance of the cortical endoplasmic reticulum. Molecular Biology Of The Cell 14, 4770-82.

Wiederkehr, A., de Craene, J., Ferro-Novick, S., and Novick, P. (2004). Functional specialization within a vesicle tethering complex: bypass of a subset of exocyst deletion mutants by Sec1p or Sec4p. The Journal Of Cell Biology 167, 875-87.

Willett, R., Kudlyk, T., Pokrovskaya, I., Sch&ouml, R., Sch, R., ouml, nherr, Ungar, D., Duden, R., Lupashin, V., et al. (2013). COG complexes form spatial landmarks for distinct SNARE complexes. Nature Communications 4, 1553.

Willett, R., Ungar, D., and Lupashin, V. (2013). The Golgi puppet master: COG complex at center stage of membrane trafficking interactions. Histochemistry And Cell Biology 140, 271-283.

Wilson, G.M., Fielding, A.B., Simon, G.C., Yu, X., Andrews, P.D., Hames, R.S., Frey, A.M., Peden, A.A., Gould, G.W., and Prekeris, R. (2005). The FIP3-Rab11 protein complex regulates recycling endosome targeting to the cleavage furrow during late cytokinesis. Molecular Biology Of The Cell 16, 849-60.

Wong, M., and Munro, S. (2014). The specificity of vesicle traffic to the Golgi is encoded in the golgin coiled-coil proteins. Science 346, 1256898-1256898.

Wu, H., Turner, C., Gardner, J., Temple, B., and Brennwald, P. (2010). The Exo70 subunit of the exocyst is an effector for both Cdc42 and Rho3 function in polarized exocytosis. Molecular Biology Of The Cell 21, 430-42.

Wu, H., Rossi, G., and Brennwald, P. (2008). The ghost in the machine: small GTPases as spatial regulators of exocytosis. Trends In Cell Biology 18, 397-404.

Wu, S., Mehta, S.Q., Pichaud, F., Bellen, H.J., and Quiocho, F.A. (2005). Sec15 interacts with Rab11 via a novel domain and affects Rab11 localization in vivo. Nature Structural & Molecular Biology 12, 879-85.

Wurmser, A.E., Sato, T.K., and Emr, S.D. (2000). New component of the vacuolar class C-Vps complex couples nucleotide exchange on the Ypt7 GTPase to SNARE-dependent docking and fusion. The Journal Of Cell Biology 151, 551-62.

Xu, Y., Su, L., and Rizo, J. (2010). Binding of Munc18-1 to synaptobrevin and to the SNARE four-helix bundle. Biochemistry 49, 1568-76.

Yamaguchi, T., Dulubova, I., Min, S., Chen, X., Rizo, J., and Südhof, T.C. (2002). Sly1 binds to Golgi and ER syntaxins via a conserved N-terminal peptide motif. Developmental Cell 2, 295-305.

Yamamoto, A., Kasamatsu, A., Ishige, S., Koike, K., Saito, K., Kouzu, Y., Koike, H., Sakamoto, Y., Ogawara, K., Shiiba, M., et al. (2013). Exocyst complex component Sec8: a presumed component in the progression of human oral squamous-cell carcinoma by secretion of matrix metalloproteinases. Journal Of Cancer Research And Clinical Oncology 139, 533-42.

Yamashita, M., Kurokawa, K., Sato, Y., Yamagata, A., Mimura, H., Yoshikawa, A., Sato, K., Nakano, A., and Fukai, S. (2010). Structural basis for the Rho- and phosphoinositide-dependent localization of the exocyst subunit Sec3. Nature Structural & Molecular Biology 17, 180-6.

Yang, B., Gonzalez, L., Jr, Prekeris, R., Steegmaier, M., Advani, R.J., and Scheller, R.H. (1999). SNARE interactions are not selective. Implications for membrane fusion specificity. The Journal Of Biological Chemistry 274, 5649-53.

Yip, C.K., Berscheminski, J., and Walz, T. (2010). Molecular architecture of the TRAPPII complex and implications for vesicle tethering. Nature Structural & Molecular Biology 17, 1298-304.

Yu, I., and Hughson, F.M. (2010). Tethering factors as organizers of intracellular vesicular traffic. Annual Review Of Cell And Developmental Biology 26, 137-56.

Zárský, V., Kulich, I., Fendrych, M., and Pečenková, T. (2013). Exocyst complexes multiple functions in plant cells secretory pathways. Current Opinion In Plant Biology 16, 726-33.

Zárský, V., Cvrcková, F., Potocký, M., and Hála, M. (2009). Exocytosis and cell polarity in plants - exocyst and recycling domains. The New Phytologist 183, 255-72.

Zhang, X., Bi, E., Novick, P., L, du, Kozminski, K.G., Lipschutz, J.H., and Guo, W. (2001). Cdc42 interacts with the exocyst and regulates polarized secretion. The Journal Of Biological Chemistry 276, 46745-50.

Zhang, X., Ellis, S., Sriratana, A., Mitchell, C.A., and Rowe, T. (2004). Sec15 is an effector for the Rab11 GTPase in mammalian cells. The Journal Of Biological Chemistry 279, 43027-34.

Zhang, X., Zajac, A., Zhang, J., Wang, P., Li, M., Murray, J., TerBush, D., and Guo, W. (2005). The critical role of Exo84p in the organization and polarized localization of the exocyst complex. The Journal Of Biological Chemistry 280, 20356-64.

Zhang, X., Wang, P., Gangar, A., Zhang, J., Brennwald, P., TerBush, D., and Guo, W. (2005). Lethal giant larvae proteins interact with the exocyst complex and are involved in polarized exocytosis. The Journal Of Cell Biology 170, 273-83.

Zhang, X., Orl, K., Orlando, K., o, He, B., Xi, F., Zhang, J., Zajac, A., and Guo, W. (2008). Membrane association and functional regulation of Sec3 by phospholipids and Cdc42. The Journal Of Cell Biology 180, 145-58.

Zhang, Y., Liu, C., Emons, A.C., and Ketelaar, T. (2010). The plant exocyst. Journal Of Integrative Plant Biology 52, 138-46.

Zick, M., and Wickner, W.T. (2014). A distinct tethering step is vital for vacuole membrane fusion. Elife 3, e03251.

Zink, S., Wenzel, D., Wurm, C.A., and Schmitt, H.D. (2009). A link between ER tethering and COP-I vesicle uncoating. Developmental Cell 17, 403-16.

Zolov, S.N., and Lupashin, V.V. (2005). Cog3p depletion blocks vesicle-mediated Golgi retrograde trafficking in HeLa cells. The Journal Of Cell Biology 168, 747-59.

Zucchi, P.C., and Zick, M. (2011). Membrane fusion catalyzed by a Rab, SNAREs, and SNARE chaperones is accompanied by enhanced permeability to small molecules and by lysis. Molecular Biology Of The Cell 22, 4635-4646.

Zuo, X., Zhang, J., Zhang, Y., Hsu, S., Zhou, D., and Guo, W. (2006). Exo70 interacts with the Arp2/3 complex and regulates cell migration. Nature Cell Biology 8, 1383-8.